COASTAL SANDS OF NORTHEASTERN TASMANIA: GEOMORPHOLOGY AND GROUNDWATER HYDROLOGY

Adrian R. Bowden, B.Sc. (Hons.)

Submitted to the Faculty of Science in fulfilment of the requirements for the degree of Doctor of Philosophy

UNIVERSITY OF TASMANIA
HOBART
1981

STATEMENT OF AUTHOR

Except as stated herein this thesis contains no material which has been accepted for the award of any other degree or diploma in any university and to the best of my knowledge and belief, the thesis contains no copy or paraphrase of material previously published or written by another person, except when due reference is made in the text of the thesis.

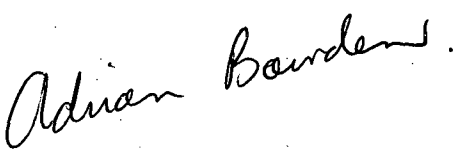

Adrian R. Bowden

TABLE OF CONTENTS

PART II

Section 1 LATE QUATERNARY MARINE SEQUENCES: SYMPTOMS OF TECTONIC ACTIVITY

List of Figures

List of Plates

List of Tables

Acknowledgements

The author gratefully acknowledges the stimulation, advice and criticism of Mr. Albert Goede and Dr. Eric Colhoun, who were joint supervisors. Invaluable time, support and encouragement were consistently provided by Dr. Manuel Nunez and Dr. Trevor Lee. Drs. Jamie Kirkpatrick and Les Wood frequently filled the role of sounding board.

Denis Charlesworth cheerfully provided the bulk of the laboratory and field assistance. Field assistance from Barry Cox, Adrian Cuthbertson, Bob Cotgrove, Graham, Jim and Amanda Bowden was highly valued. Kate Morris did some of the drafting and Pam Bowden typed the first draft. The excellent job of typing, and some editing, was performed by Terese Hughes.

The University of Tasmania, particularly the Geography Department, provided funds for which the author is most grateful. The Australian Water Resources Council funded the research for two years and a significant contribution was made by the AWRC reference panel which consisted of Professor Bruce Thom, Dr. Eric. Colhoun, Mr. Peter Stevenson and Mr. Don Woolley. Professor Thom and Dr. Jim Bowler provided stimulating discussions during field visits. The Tasmanian Department of Mines provided advice, equipment, analyses and field assistance which was invaluable. Help was also received from the CSIRO, SRWSC and

the HEC. Mr. and Mrs. Stewart Campbell of Tomahawk contributed greatly by supplying meteorologic records and regularly attending the groundwater level recorders.

This thesis would not have been possible without the assistance of the above people and organizations.

Abstract

A regional study of the Quaternary geomorphology of coastal northeastern Tasmania defined landforms and deposits which offer good groundwater development potential, and also pointed to geomorphic problems worthy of more detailed research. Marine transgression and regression appear to have been a main feature of landform development in coastal northeastern Tasmania since Late Tertiary times. The present landscape is dominated by low, sandy plains created during the Last Interglacial marine transgression and by aeolian landforms which were formed during the succeeding glacial stage. The immediate coastal areas are backed by marine and aeolian landforms deposited during and since the marine transgression.

The regional study revealed that deposits of possible marine origin and interglacial age, occur to an elevation of approximately 32 m. This is ~ 10 m above the upper limits of similar deposits elsewhere in Tasmania and is ~ 26 m higher than equivalent features in stable areas of mainland Australia. These relationships indicated that tectonic uplift in Tasmania may have occurred during the late Quaternary. Further research indicated that the sea level in northeastern Tasmania most likely attained an elevation of ~ 32 m during the Last Interglacial Stage, and that the area has experienced a moderate uplift rate of approximately 0.2 m/ka. The stratigraphic relationships between Quaternary marine deposits also indicate that older,

probably of Oxygen Isotope Stages 7 and 9 age, marine deposits occur to 49 and 71 m respectively, thus indicating that uplift in Tasmania has been occurring over at least 300,000 years.

Mapping and examination of the extensive longitudinal dunes and lunettes during initial stages of the programme indicated that they are products of environmental conditions substantially different from those of today. Dune morphology and grainsize characteristics suggest that zonal westerly air flows appear to have been stronger and from a slightly more northerly direction during the Last Glacial Stage than air flows which occur today. Stratigraphic studies infer that the temperature was markedly lower during formation of the longitudinal dunes. Evidence from fossil groundwater podzols indicates that precipitation during the Last Glacial Stage may have been only approximately one half of the present rainfall. Lunette stratigraphy and morphology reveal shifts in the relative importance of key components to the hydrologic cycle, such as precipitation, evapotranspiration and surface run-off, both during and since the late Last Glacial Stage.

The coastal plains of interglacial marine sand form extensive unconfined aquifers and contain abundant and accessible groundwater supplies. Computer and graphical simulations are applied to pumping test and drilling results, water table maps and continuous water level records to assess the groundwater system. Groundwater dynamics are controlled principally by precipitation and evapotranspiration. The system is renewable and moderate rates of groundwater withdrawal may even be beneficial.

INTRODUCTION

This research represents the first examination of the Quaternary history and shallow groundwater potential of northeastern Tasmania. The Australian Water Resources Council (AWRC) wholly funded this study for two years from April 1975 to 1977. The initial aim of the project (AWRC Research Project 75/84) was to study geohydrologic processes in coastal areas of eastern Tasmania and to classify coastal sediment bodies as potential aquifers on the basis of their form, stratigraphy, sedimentary and physical characteristics insofar as these properties can be related to the storage, transfer and yield of groundwater. These characteristics had previously been difficult to assess because too little was known of the distribution and origin of the coastal sand bodies and of their relationships with other surficial deposits. It was also hoped that the findings could be applied to other areas of similar environment. Initial field work showed that most landform types which occur in eastern Tasmania also occur on the northeast coast and were better represented there than on the east coast. The study area was therefore reduced to include only coastal northeastern Tasmania.

The reduced study area extends eastward from Bridport to Eddystone Point (Figure 1) and covers the northeastern coastal plain of

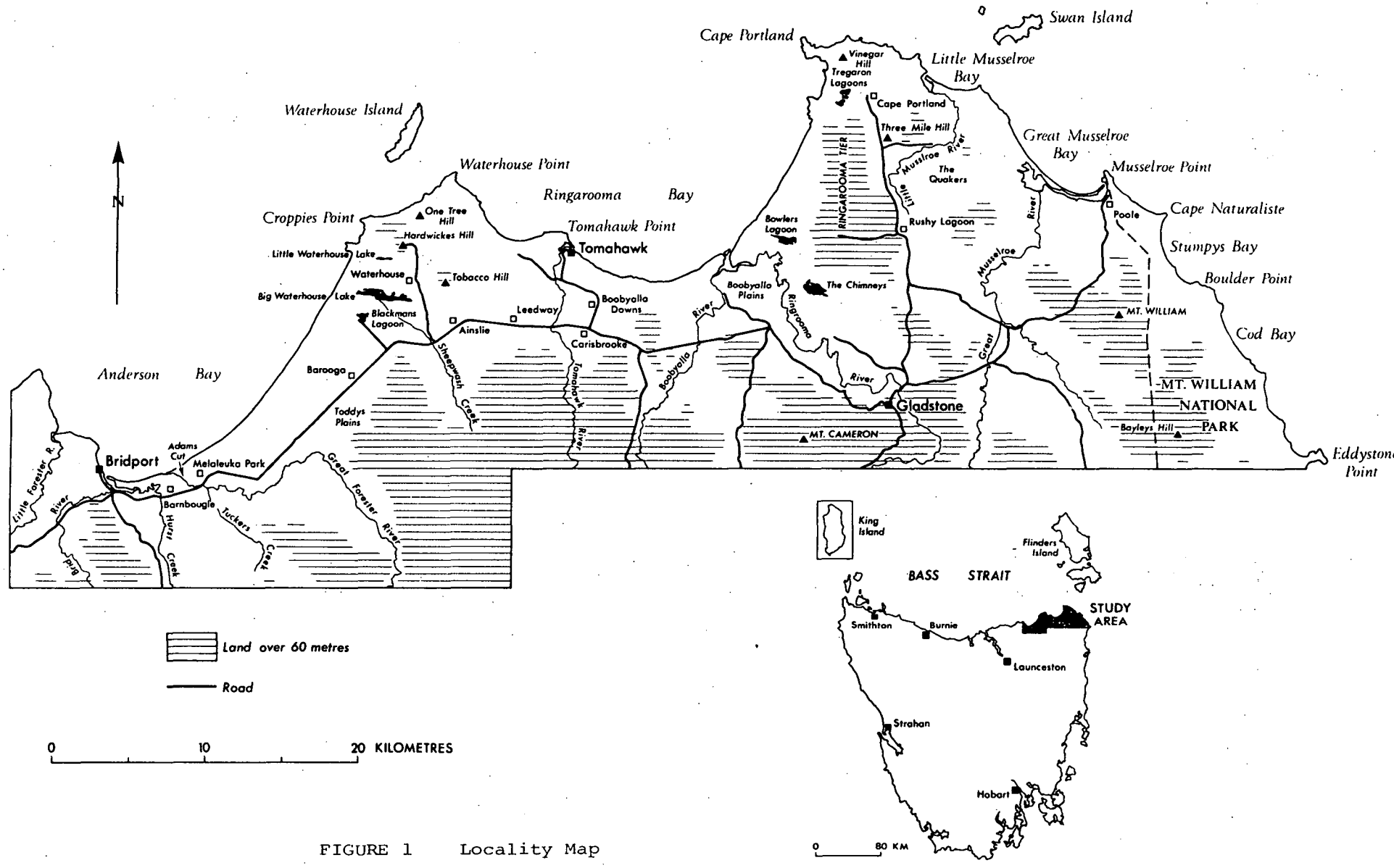

FIGURE 1 Locality Map

Tasmania. It includes marine plains, terrestrial and coastal dunes, lake floors and alluvial terraces. Thus the surface of the area consists largely of low lying, unconsolidated sands and associated sediments of Late Quaternary age.

This study began as an applied groundwater project, but examination of the regional Quaternary geomorphology, an essential preliminary, not only provided a framework for the applied project, but also raised questions of a broader geomorphic nature which stimulated comparison of northeastern Tasmania with other regions.

Consequently this thesis is an expansion of the AWRC research project and has three principal aims. One aim is to obtain a general understanding of the Quaternary geomorphology of coastal northeastern Tasmania, thus providing a framework which forms a starting point for the remaining two goals. The second objective is to examine two key aspects of Quaternary geomorphology and to determine how far specific events and conditions related to these aspects in northeastern Tasmania conform with those from elsewhere. The third aim is to understand the shallow groundwater dynamics and to evaluate the groundwater potential of aquifers formed by Quaternary deposits of northeastern Tasmania.

Each of the problems selected for detailed appraisal may well be considered as a thesis topic in its own right, if studied over a wider area. In such cases it is much easier to ignore, or miss, problems which concern the relationships of the study unit to its various surroundings, than it is with the present approach. It is therefore hoped that any loss of detail may be compensated for by a broader range of conclusions and deeper understanding of origins and inter-relationships between the various elements of the landscape.

Part I defines the general regional geomorphology. Parts II and III emanate from the findings of the regional geomorphic study. Part II deals with the pure geomorphic aspects while Part III covers the applied groundwater hydrology. Part IV summarises the conclusions of the study.

PART I

REGIONAL GEOMORPHOLOGY

1. INTRODUCTION

The principal aim of this section is to differentiate, classify and map the landforms and deposits of coastal northeastern Tasmania, and to establish the general sequence of events and conditions which formed the existing landscape. This approach leads to the identification of several problems worthy of more detailed research. It also differentiates the various aquifers and points to the most suitable aquifer for a detailed study of groundwater dynamics.

Formation names in the text follow the Australian Code of Stratigraphic Nomenclature (1964) and have been reserved by the Stratigraphic Nomenclature Subcommittee. These differ from the names published by Bowden (1978) because some names were either unavailable or did not strictly adhere to the Code.

2. TERTIARY DEPOSITS

The Tertiary record is very fragmented and poorly understood due to post depositional dissection, and because the fluvial gravels which dominate the sediments have not been intensively studied.

Alluvial quartzitic gravels of probable Tertiary age (Figure 2) occur in the Mount Cameron-Ringarooma River area and have been extensively mined for tin. Isolated ridges of quartz gravels occur throughout northeastern Tasmania. For example, a road cutting through a low ridge near Barooga revealed a V-shaped channel filled with river gravels which was cut in slates of Mathinna Beds (Plate 1). Other ridges of gravel are common in this area, and also occur near the Boobyalla River-Little Boobyalla River junction.

A sequence of unconsolidated marine sands, gravels and some peat was penetrated by a Tasmanian Department of Mines bore hole before basalt bedrock was reached at a depth of 72 m. This bore was located 2 km NNE of Three Mile Hill, near Cape Portland at an approximate elevation of 30 m. Mr. W.R. Moore kindly provided split samples which were taken at 1.5 metre intervals. The reverse circulation method of sample recovery that was used may have resulted in sample contamination from higher levels. The upper 20 m of the drill samples are probably marine sands of Last Interglacial age (Late Quaternary). Nearly all of the sand samples below 20 m depth contained abundant Bryozoa. Some shell fragments and echinoid spines also occurred in several samples, and confirm a marine origin of the sands.

Three approximately equally spaced samples which covered the range below 20 m were sent to Dr. R.E. Wass, Department of Geology, University of Sydney, for identification of the Bryozoans so that an estimate of age and environment of deposition could be attempted. Dr. Wass reported that identification of the specimens was difficult because of the large amount of secondary calcification and the small fragments. However, the Bryozoa were virtually the

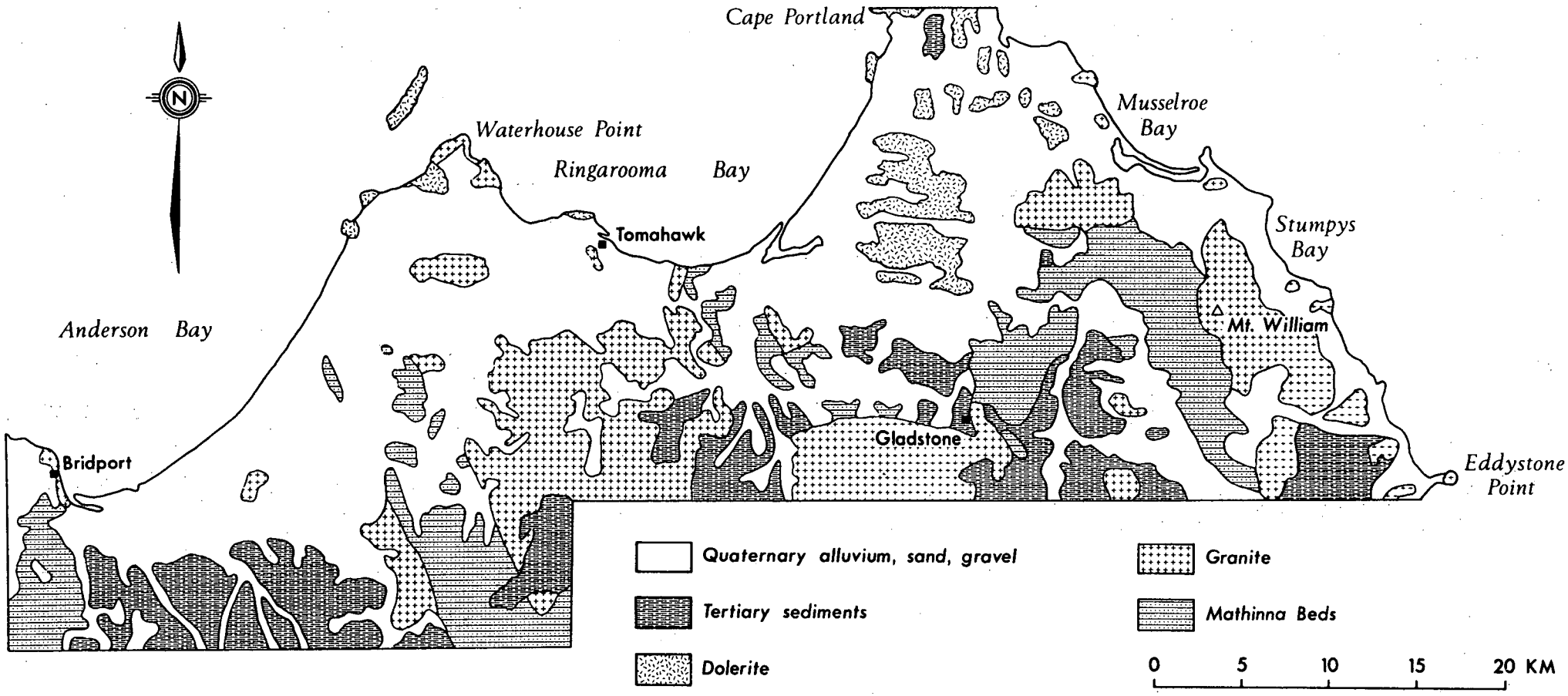

FIGURE 2 Generalized Geology: Northeastern Tasmania
(After Geol. Surv. Tasm. 1974)

PLATE 1 Tertiary age river gravels incised into Mathinna Beds slates near Barooga.

same from each sample and show a definite association with the Tertiary of Victoria. Some of the genera tentatively identified are not known later than the Miocene, but he stressed that Bryozoa have not been used extensively for age dating in the Victorian sequence. The dominant genera found were *Cellaria*, *Tubitrabecularia*, *Didymosella* and *Celleporaria*, and the zoarial forms noted were cellariform, adeoniform, reteporiform and celleporiform.

Lagaaij and Gautier (1965) provide the basis for an estimate of the palaeoecology of the various zoarial forms. According to these workers cellariform zoaria prefer shallow inner-neritic (less than 40 m water depth) environments where there is no active transport and resedimentation of sand. Adeoniform zoaria are found in sandy environments at 40-50 metres depth. Reteporiform zoaria inhabit sub-littoral regions where wave action and currents are strong. The celleporiform form is very sensitive to a moderate supply of fine sediment, is adapted to the littoral zone, and can tolerate wave action.

The Bryozoans therefore indicate that the marine sands penetrated by this bore are Tertiary in age, probably of Miocene age or older, and were deposited in a shallow, moderate to high energy, marine environment.

Mr. S. Forsyth (Tasmanian Department of Mines) examined two pollen samples from peat which contained the freshwater algae *Botryococcus*. Both samples contained typical Middle Tertiary assemblages with most of the common species represented. Pollen from the sample at 30.48 m depth was close to the boundary of the *Proteacidites tuberculatus* and *Triporopollenites bellus* pollen zones of Stover and Partridge (1973) and therefore is of Early to Middle

Miocene age. The sample from 68.5 m yielded an assemblage from the *Proteacidites tuberculatus* pollen zone which is of Late Oligocene to Early Miocene age.

This close association of shallow marine deposits and freshwater peats probably indicates that several marine transgressions occurred during the Late Oligocene to Middle Miocene. Marine transgression during this period has been previously recognised in northeastern Tasmania (Quilty, 1971), Cape Barren Island (Crespin, 1945), King Island (Jennings, 1959) and northwestern Tasmania (Spry and Banks, 1962). Pliocene marine deposits occur on Flinders Island (Sutherland and Kershaw, 1971). It appears from the above evidence that marine deposition has occurred in areas close to Bass Strait since Late Oligocene-Early Miocene time.

The interval from the Middle Miocene to the Late Quaternary represents a considerable gap in the sedimentary record of northeastern Tasmania about which there is little information.

3. LATE QUATERNARY MARINE DEPOSITS

3.1 Last Interglacial Marine Deposits

Coastal sand plains, which occupy former large coastal embayments, are widely distributed in northeastern Tasmania, as shown by Figure 3. The main areas are at Stumpys Bay, Boobyalla Plains, Tomahawk, Toddys Plain and east of Bridport in the Tuckers Creek area (Figure 1). In most cases the inland boundary of the plain is well defined by a break of slope at an altitude of approximately 32 m above HWM (High Water Mark). The plains have a relatively even surface and slope towards the sea. Sand thickness of the plains averages approximately 6 m as shown in Figure 4 but

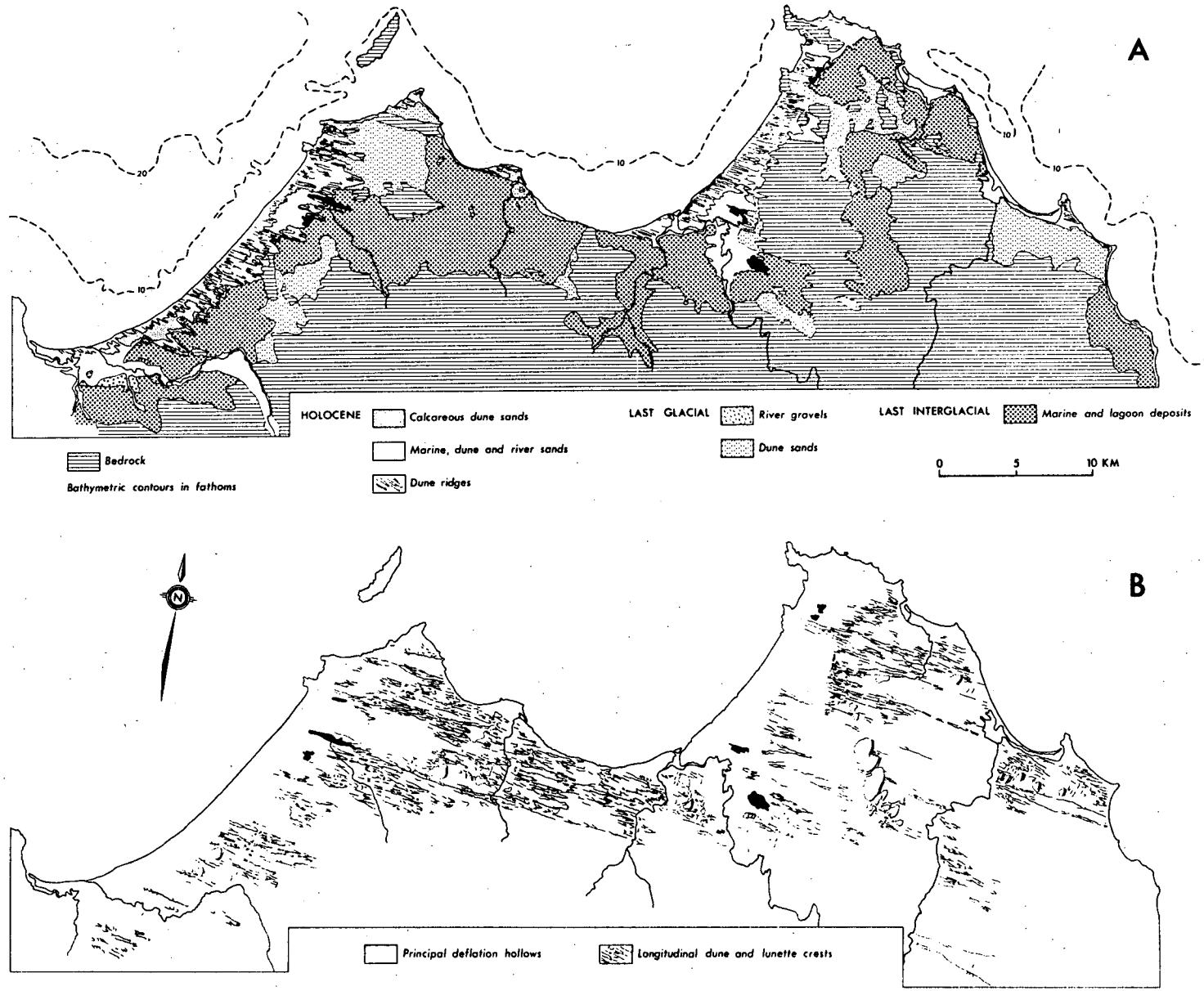

FIGURE 3 Landforms and Deposits: Coastal Northeastern Tasmania.
(a) Quaternary deposits (b) Terrestrial dunes

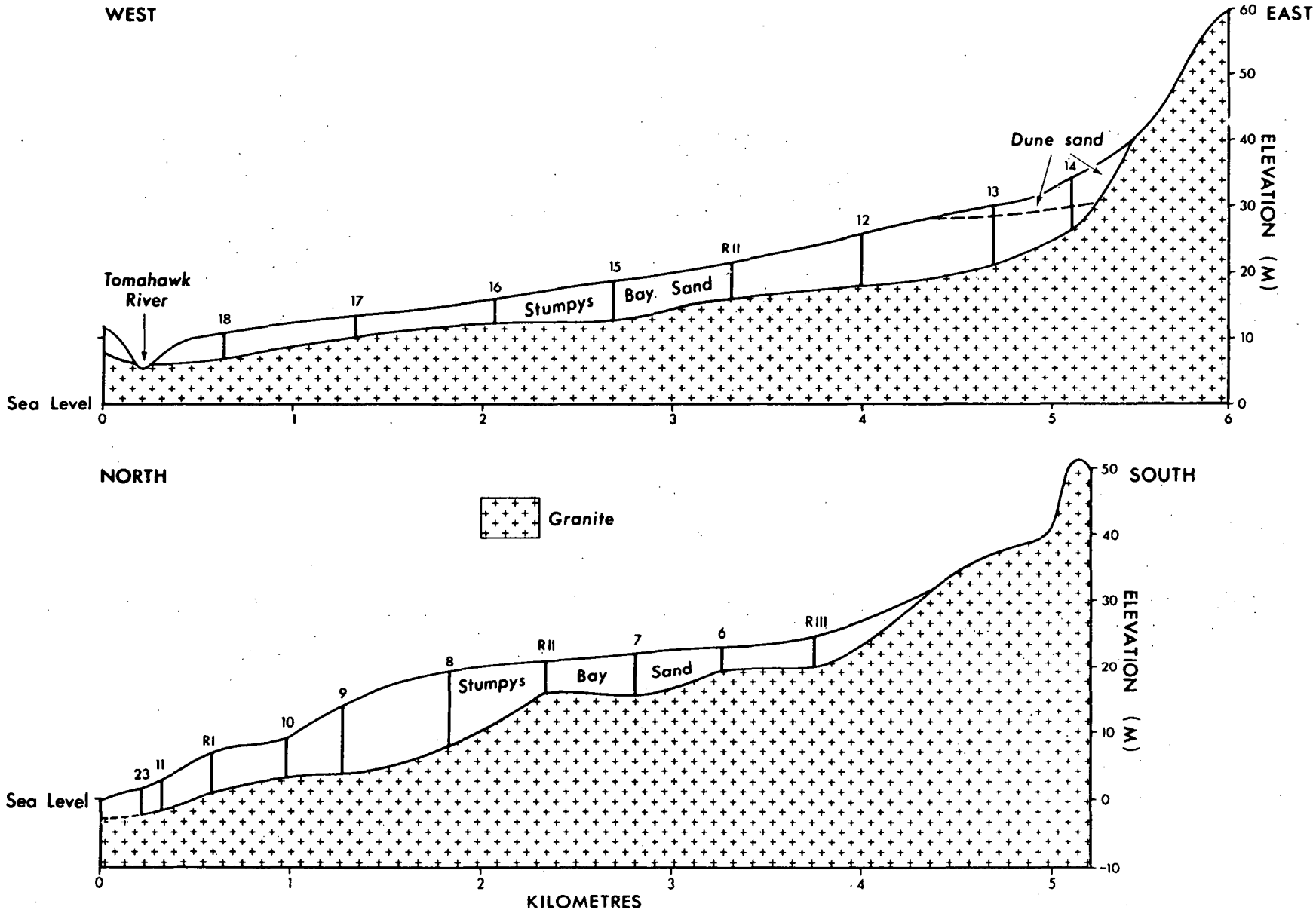

FIGURE 4 Cross sections of Stumpys Bay Sand at East Tomahawk.
See Figure 16 for locations. VE = 23x

depths of up to 12 m are common. The sands overlie Devonian granite, Siluro-Devonian Mathinna Beds, and Tertiary clays. The sands which form the body of the plains are readily mapped as a formation and are termed the Stumpys Bay Sand.

The internal composition of the Stumpys Bay Sand consists predominantly of moderately rounded quartz sand. It is medium to fine grained (average grainsize is 1.89 ± 0.65 ϕ) and moderately sorted, with an average sorting coefficient of 0.98 ± 0.40 ϕ. Sediments outside the sand size range, such as gravel and silt are rare.

Rounded quartz pebbles, derived from Tertiary gravels, from vein quartz within the Mathinna Beds, and possibly from granite, often occur between the base of the formation and bedrock. The cobbles are probably lag material derived from weathered bedrock or from surficial deposits that occurred on the land surface prior to the marine transgression which was responsible for deposition of the Stumpys Bay Sand.

Discontinuous peat layers of very limited extent occur near the margins of the sand embayment in the Tomahawk area, and form beds up to 20 cm thick. At Barooga (Figure 1) a bed of peat 80 cm thick is exposed in the base of a drainage ditch. Augering through the peat showed that it overlies the basal, thin sand and cobble bed which rests directly on weathered Mathinna Beds. A bore hole drilled 30 m west of this exposure did not encounter the peat but the basal gravel was present.

The Stumpys Bay Sand is often well bedded with extensive, low angle cross-beds which frequently dip seawards. Plate 2 demonstrates bedding within the formation. Biotic structures have not been observed in any field sections.

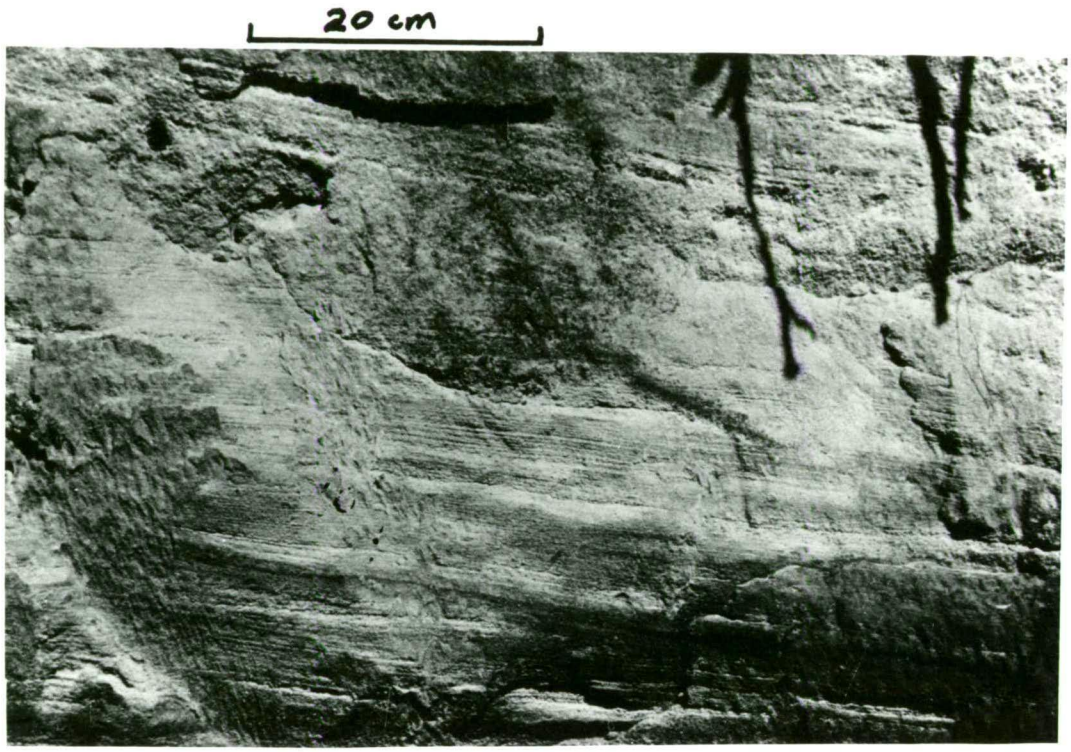

PLATE 2 Bedding of Stumpys Bay Sand.

The photograph, taken at East Tomahawk, shows the well bedded sands and low angle cross-beds which dip seawards (north).

Groundwater podzolization has been the dominant soil forming process and has controlled the nature of the soil profiles within the sands. An undisturbed soil profile usually displays an A_1 horizon 20-30 cm thick, a well developed, leached A_2 horizon 120-140 cm thick, and an enriched $B_{2h,ir}$ horizon 30-150 cm thick (Plate 3). Below the $B_{2h,ir}$ horizon the greyish-olive coloured Cg horizon indicates the zone of permanent saturation.

Field evidence indicates that the Stumpys Bay Sand is primarily of marine origin, although fluvial or lacustrine processes are capable of producing large plains of unconsolidated sand (pages 84-94).

The morphology of the sand plains is similar to that of large marine embayments. Each embayment is bounded to landward by a well defined break of slope which resembles an old shoreline. In addition, the seaward slope of the plains is a feature which is consistent with a marine origin. The Stumpys Bay area contains well preserved linear ridges, which are composed of well rounded, coarse sand (mean grainsize = 0.5 ϕ), that are oriented sub-parallel to the contours of the plain and to the present shore. These landforms are interpreted as beach ridges.

The internal composition of the sands provides firm evidence of their origin. Marked uniformity of the sands on older surficial deposits and bedrock over wide areas, moderate rounding of the particles and the presence of low angle, regular cross-bedding point to a marine origin. However fossil evidence provides the key to their environment of deposition. Two forms of siliceous sponge spicules have been found at all depths. The megascleres have a marine origin (Dr. M.R. Banks, pers. comm.) and although the origin of the microscleres is not as readily ascertained, their

PLATE 3 Groundwater podzol within the Stumpys Bay Sand at Barooga.

The leached A_2 horizon is approximately 1.2 m thick with a sharp lower contact with the $B_{2h,ir}$ horizon.

association with the megascleres indicates that they are likely to be of marine or brackish water origin.

As yet the Stumpys Bay Sand has not been dated but it is clearly of interglacial age as it extends to well above present sea level. This poses the problem of ascertaining in which particular interglacial stage the Stumpys Bay Sand was deposited.

Peat and wood occur within the Stumpys Bay Sand but even if the sands are as young as their minimum possible age, the Last Interglacial, the material is beyond the range of the ^{14}C dating method. No material was found in the deposits which could be assayed by any other absolute dating method. Evidence of age must therefore be a relative determination derived from geomorphic and stratigraphic relationships established for this area and from comparison of these with similar landforms and stratigraphic sequences described from elsewhere in Australia.

The well preserved shoreline feature at around 30-32 m above HWM supports a Last Interglacial age for the marine sands, rather than an older age, as it is preserved in readily erodable weathered granite and chemically decomposed Mathinna Beds. Morpho-stratigraphic evidence also indicates that the Stumpys Bay Sand is unlikely to be older than Last Interglacial in age. The system of longitudinal dunes which traverses the sand plains shows no evidence of more than one period of dune formation or soil development. If the Stumpys Bay Sand was older in age than the Last Interglacial then it is possible that it would have acted as a source of sand for aeolian deflation during more than one glacial cycle.

On the central and northern coast of New South Wales, which is considered to be a tectonically stable region, there is

apparently clear evidence that the highest sea level during the Last Interglacial was 4-6 metres above present sea level (Marshall & Thom, 1976). In northeastern Tasmania the Stumpys Bay Sand extends unbroken from below sea level to around 32 m, with no development of a pronounced shoreline at 4-6 m, a feature to be expected if northeastern Tasmania had been tectonically stable and if this formation was older in age than the Last Interglacial.

3.2 Older Interglacial Marine Deposits

Two suites of marine deposits older than the Last Interglacial in age have been partially preserved at Rockbank (Figure 1). The marine deposits of this area are relatively well protected from deflation by Ringarooma Tier (Figure 1), a north-south trending dolerite ridge which rises to around 140 m.

The lower suite of marine deposits consists of medium grained beach sands (1.75 ± 0.42 ϕ mean grainsize) which are moderately sorted (0.84 ϕ mean coefficient of sorting) and contain abundant un-reworked sponge spicules. These sands wedge-out sharply at an elevation of ~ 49 m above HWM against the higher suite of lagoonal sandy silts and silty sands. The two suites are separated by ~ 30 cm of freshwater peat which probably formed during a substantial period of terrestrial swamp conditions that occurred during an intervening interval of lower sea levels. The higher deposits at Rockbank terminate at a moderately preserved break of slope at ~ 71 m above HWM and also contain marine sponge spicules.

At the Star Hill Mine (Figure 1) tin mining operations have exposed higher, leached sand beneath younger alluvial gravels. The sands display cross-bedding which is consistent with a beach

environment of deposition, and also contain very poorly preserved sponge spicules. The elevation of the sands at Star Hill Mine has not been surveyed, but map contours show that the sands extend to ~ 90 m above present sea level.

Any interpretation of the age of these suites of deposits must naturally be speculative in the absence of material which can be dated radiometrically. However, the lower Rockbank deposits are higher and older than the Stumpys Bay Sand, which is probably of Last Interglacial age, and therefore the least possible age of these deposits is second Last Interglacial, or Stage 7 of the oxygen isotope curve from which older interglacial sea levels are inferred by Shackleton & Opdyke (1973). Similarly, the higher deposits at Rockbank probably represent a full interglacial stage and can therefore be no younger than the third Last Interglacial (Stage 9). The minimum age of the Star Hill Mine deposits would be Stage 11, but their age could be considerably older as stratigraphic control is extremely poor and any correlation with isotope stages cannot be more than a suggested relative sequence.

4. LAST GLACIAL AGE TERRESTRIAL DEPOSITS

4.1 Introduction

The Last Glacial Stage is well documented and occurred between 75,000 and 10,000 years ago as a consequence of a worldwide lowering of temperature (Emiliani, 1966; Emiliani & Shackleton, 1974; Ericson & Wollin, 1968). During this period the ocean levels were probably 100-120 m below their present level due to the extraction of ocean water for the nourishment of huge masses of glacier ice (Flint, 1965; Jennings, 1971). This degree of sea level

lowering would have produced a markedly different shoreline location in the Tasmanian region. Figure 5 shows the minimum position of the shoreline at this stage, with Tasmania being linked to mainland Australia by a land bridge. Thus, the coastal northeastern portion of Tasmania today would have formed the southern fringe of a large, probably sandy plain of low relief which is now the floor of Bass Strait. Consequently, landform development at this time would largely be controlled by continental, rather than coastal, processes.

4.2 Longitudinal Sand Dunes

An extensive system of presently stable sand dunes occurs over a large proportion of coastal northeastern Tasmania. The dunes are aligned in a WNW-ESE direction (~ 280°-100°) and are spaced approximately 400 metres apart. The sand ridges are narrow, relatively straight, up to 20 km long, 60 m wide, and 10 m high. Some dunes join to form V-shaped junctions which point mainly towards the east. Plate 4 shows the form of the longitudinal dunes. The southern flanks of the dunes are invariably steeper than the northern flanks. In some places, for example at Croppies (Figure 3), the dunes occur as undulating sand sheets, rather than as discrete dune ridges.

The longitudinal dunes occur mainly on the plains formed by the Stumpys Bay Sand, from which they were derived, but in some cases they are closely related to river beds and floodplains which in the past have supplied abundant sand for dune formation. The dunes are mappable as a landform unit, have a uniform lithology and disconformably overlie the Stumpys Bay Sand. Therefore they have been classed as a separate formation termed the Ainslie Sand.

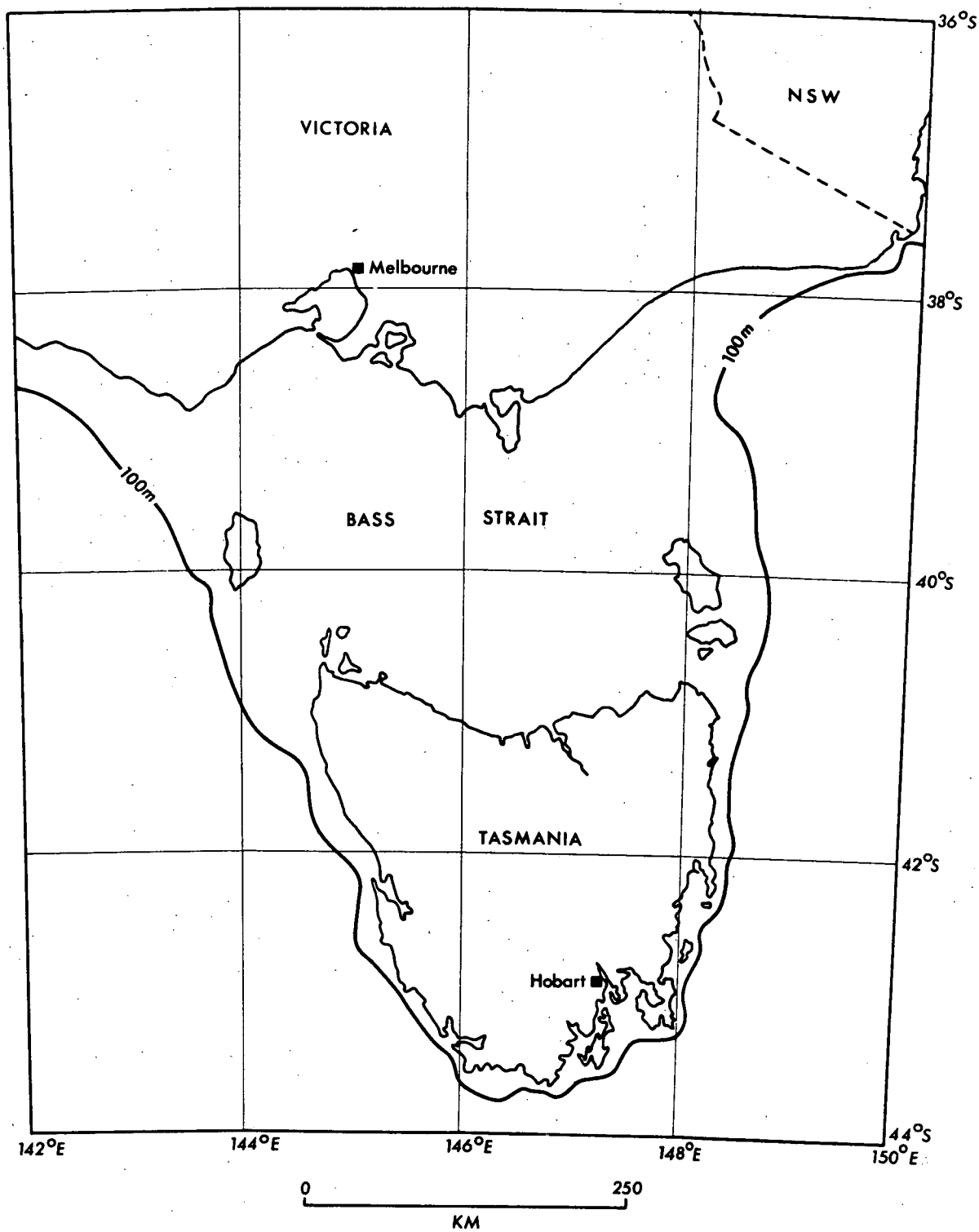

FIGURE 5 The coastline of Tasmania during the maximum of the Last Glacial Stage.
The location of the 100 metre isobath in the Tasmanian region approximates the minimum lowering of sea level during the Last Glacial Stage.

PLATE 4 Aerial view of the longitudinal dunes on the sand plain at East Tomahawk. The view looks towards the northeast.

The Ainslie Sand is composed of moderately well sorted (mean sorting coefficient 0.68 ± 0.16 ϕ), fine grained (mean grainsize 2.08 ± 0.38 ϕ), unconsolidated quartz sand. Steeply angled cross-beds were observed in some sections of the dunes but the dunes vary only slightly in grainsize between beds, and therefore any bedding is difficult to discern. Many aboriginal artefacts lie on the surface of the sand sheet in the Croppies area, which indicates that aboriginal occupation occurred in the area mainly, if not solely, after the formation of the dunes.

In sections and auger holes the dunes consistently display a well developed podzol profile (Plate 5) with the leached A_2 horizon up to 40 cm thick and the $B_{2h,ir}$ horizon up to 60 cm thick. The $B_{2h,ir}$ horizon is weakly to moderately indurated with some of the darker coloured zones being heavily indurated. The C horizon consists of pale yellow sand.

The interpretation of an aeolian environment of deposition for the sand ridges in northeastern Tasmania is well supported by the morphology of the landforms and their sedimentary characteristics. The ridges are all oriented in a sub-parallel pattern shown in Figure 3, and display a very similar form to the longitudinal dunes of the Simpson Desert described by Twidale (1968, 1972). Longitudinal dunes are characteristic of arid and semi-arid regions (Mabbutt, 1968; Twidale, 1972; Bowler, 1976; Wyrwoll & Milton, 1976) and the fact that the dunes are not being formed in the region today implies the occurrence of markedly different past climatic conditions. In order to get the widespread sand mobilization needed to form the large dune system which occurs throughout coastal northeastern Tasmania, the vegetation cover would have to be reduced considerably compared with today. Increased aridity associated with reduced temperatures are the most likely factors capable of reducing the vegetation to

PLATE 5 Podzol profile developed on longitudinal dune. The leached A_2 horizon forms a sharp, but irregular contact with the dark coloured $B_{2h,ir}$ horizon below.

such a marked extent. At Little Waterhouse Lake and Cape Portland (Figure 1), slope deposits produced by physical weathering on dolerite slopes are interbedded with the Ainslie Sand. Physical weathering and slope instability are known to have been widespread in Tasmania during the Last Glacial Stage (Colhoun, 1975) even at low elevations. This evidence lends support to the hypothesis of a significant temperature decrease during the period of formation of the longitudinal dunes.

Dune alignment in a WNW-ESE orientation indicates that the predominant wind direction was along that axis. Strong evidence that the sense of the wind direction was from the westerly quarter is provided by the dune convergences which are open to the west. King (1960) and Mabbutt (1968) consider that dune convergences are always open to windward and point to leeward. Some of the dunes in the study area extend up the western flanks of hills and terminate as the environment becomes more exposed, which also indicates the dominant role of westerly winds in their evolution. This is further emphasized by the location of eddy patterns created by dune ridges on the eastern side of Ringarooma Tier, and the subsequent reformation of linear dune ridges to the east of the eddies.

An absolute age determination of the period of longitudinal dune formation is not possible at this stage as no carbonaceous material has been found in close association with the dunes. Therefore, estimates of age can only be formed on a relative basis using indirect evidence such as the stratigraphy of the deposits, the morphology of the landforms and the degree of soil development.

Stratigraphic evidence of contemporaneous deposition of probable cold climate slope deposits and longitudinal dune formation has been described above, and indicates that the dunes are

probably of glacial age. A Last Glacial age is supported by the fact that there is only one period of slope mantle instability evident in the Waterhouse Lake and Cape Portland sections, and by the fact that the dolerite slope deposits are not greatly weathered. Nowhere in the study area is there stratigraphic evidence of more than one period of dune formation. If the longitudinal dunes are in fact older than the Last Glacial Stage then the sand plains and the dunes themselves would probably have been subject to further deflation during the Last Glacial Stage, providing evidence of dune reworking.

The morphology of the dunes suggests that they were formed during the Last Glacial Stage, rather than during an earlier glacial stage. Although the dunes are not in a perfect state of preservation, they retain many of the characteristics of fresh longitudinal dunes. For instance, many of the dune crests are sharp and well defined. If the dunes were older than the Last Glacial Stage they must have survived at least one interglacial/glacial cycle when it could be expected that they would have been at least partly re-mobilized and degraded.

Edaphic evidence also suggests that there has been only one period of longitudinal dune formation. Everywhere in the area the dunes have a moderately well developed podzol profile which shows very little variation. Palaeosols are totally absent. The high degree of podzol development on the dunes when compared with the weakly developed A-C soil profiles of the Holocene parabolic dunes (page 40) provides a clear indication that the longitudinal dunes are at least older than the Holocene in age.

4.3 Lunettes

Lunettes are crescent-shaped dunes found on the lee shores of lakes (Hills, 1940; Twidale, 1968). Lunettes are widespread in coastal northeastern Tasmania (Figure 3) and comprise the Rushy Lagoon Sand because they are also a mappable and discrete landform unit, have a fairly consistent internal composition, and disconformably overlie the Stumpys Bay Sand. They are associated with deflation hollows which either formerly contained lakes or are presently flooded in wet periods.

The largest lunettes occur at Rushy Lagoon (Figure 1) where they attain heights of up to 10 m above the old lake floor. Plate 6 shows the lagoon edge of the lunette at Rushy Lagoon. One lunette at Rushy Lagoon is approximately 2.5 km long. The presence of double lunette ridges in most areas, and a smaller third ridge in some cases, suggests that three periods of lunette formation probably occurred.

The composition of the lunettes displays some variation. At Rushy Lagoon some lunette ridges are composed of sand, and others of sand with interbedded sand and clay. The clay beds vary from a few cm to 30 cm in thickness. Alternation from sand to clay bedding indicates that the lakes were subject to dry periods when clay and sandy clay was blown from the dry lake floor to the leeward lake shore (Bowler, 1976). During lake full conditions the sand formed a beach on the lee shore from which sand was blown to form a dune immediately behind the beach (Twidale, 1968). The clay on the floor of the Rushy Lagoon lake was most probably derived from the lagoonal clayey silt deposits of interglacial age, which underlie the lake bed. The presence of the lagoonal clayey silt also explains the development of such large lunette lakes in this

PLATE 6 Rushy Lagoon Lunette.

The old, flat lake floor occurs to the left of the west-facing flank of the Rushy Lagoon Lunette.

area as the lagoonal sediments are much less permeable than the beach facies of the marine deposits.

At Leedway (Figure 1) there are two lunettes. A drainage ditch cut through one lunette and augering through the crest of each lunette showed that both dunes are composed entirely of sand. There is little or no clay available in the Leedway area to form a fine grained lake floor deposit. Drilling of the lake floor indicated that the lake was formed in a depression in the Stumpys Bay Sand and that weathered granite is within 10 cm of the surface at the centre of the lake floor.

The lakes which are associated with the lunettes in the study area most likely originated as deflation hollows in the marine sands, the maximum amount of aeolian scouring being determined by the lowest level of the water table. The depressions so formed would fill with water during periods of higher water table but might be dry during drier climatic phases or extended droughts.

Most of the lakes were very shallow, and a water table decline of 1-2 m would dry out the lake floor and make a large proportion of it available for deflation. Today, the water table fluctuates between 1-2 m each year, and the alternate sand and clay bedding of the lunettes are likely to have been associated with similar annual cycles as well as with longer term variations in lake level. The age of the lunettes will be discussed further on pages 193-197.

It is sufficient at present to note that a piece of wood from peaty sands associated with the innermost and third lunette at Rushy Lagoon was assayed by ^{14}C at ~ 8,500 BP and may predate the formation of this lunette. However, as determination of the extent

and degree of disturbance of the primary peaty sand deposit was difficult without extensive trenching that was not available to the author it is difficult to draw a firm conclusion on the age of the third lunette. Although the assay almost certainly implies that the outer two lunettes are of Pleistocene age it presents the possibility that the inner lunette is of Holocene age and that the lunette series spans late Last Glacial and Holocene times.

4.4 Alluvial Terraces

A well defined terrace occurs near the mouth of the Great Forester River and covers approximately 4 km^2. Prior to deposition of the terrace sediments the river became incised into a higher surface underlain by the marine Stumpys Bay Sand. This alluvial deposition was followed by a marine transgression during the Holocene which produced an inset fill of marine deposits - the Barnbougle Sand. Figure 6 shows the morphologic relationships and stratigraphic interpretation of limited bore log data. The level of the terrace is about 4 m above the Holocene marine Barnbougle Sand (page 36) and about 8 m below the plain of the Stumpys Bay Sand. Bore logs and field sections show that the sediments of the terrace are up to 10 m thick and are composed of poorly sorted, moderately-well rounded, coarse sands and gravels. Cross-bedding is marked in all field sections. The above evidence indicates a fluvial origin for the terraces. The fluvial terrace is a landform unit which has been used as a basis for field mapping. The associated sediments show a high degree of internal lithologic consistency and appear to have accumulated during a single aggradational phase. They are referred to as the Forester Gravel.

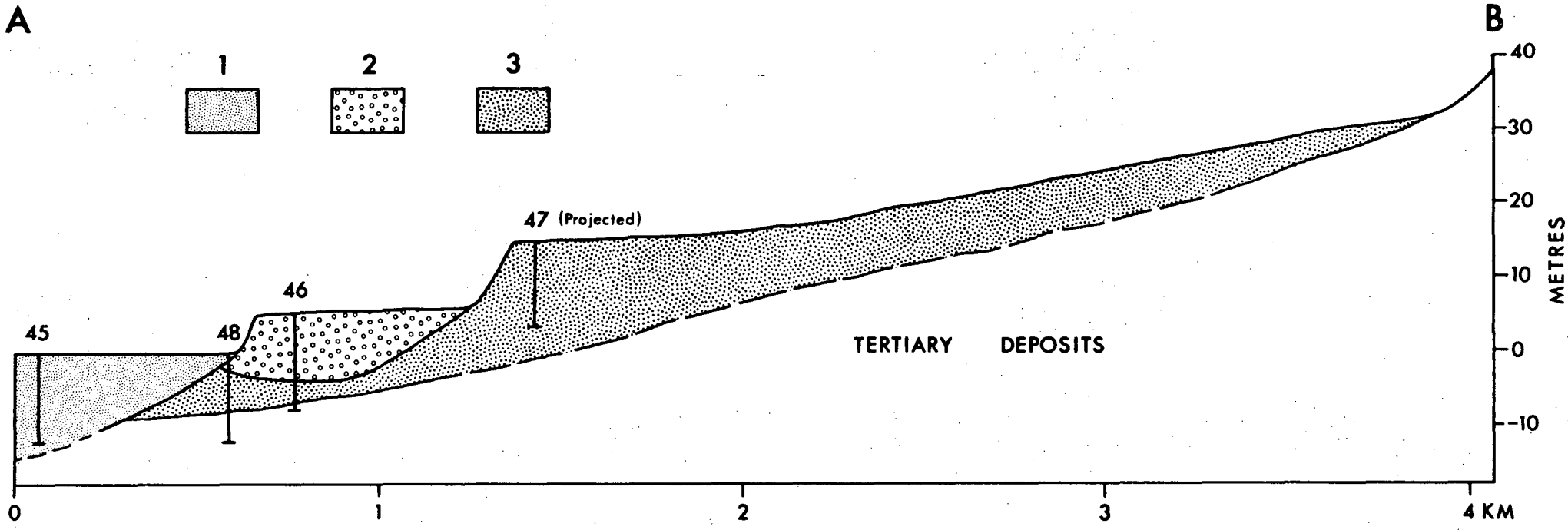

FIGURE 6 Profile showing the relationships between the Barnbougle Sand, the Forester Gravel and the Quaternary marine deposits: Tuckers Creek area. The location of the transect is shown on Figure 7. Elevation is above High Water Mark. VE = 20x

1 = Barnbougle Sand (marine)
2 = Forester Gravel (alluvial)
3 = Stumpys Bay Sand underlain by older Quaternary marine deposits

The terrace sediments are probably of similar age to the Ainslie Sand because the well developed podzol profile on the terraces is similar to the degree of podzol development on the longitudinal dunes. Also, several well indurated, organic/iron rich zones occur at a depth of around 1 m. Morphostratigraphic relationships also indicate that the Forester Gravel and the Ainslie Sand are of similar age. The surface of the alluvial terraces is not traversed by the longitudinal dunes, whereas the surface of the Stumpys Bay Sand plain to the rear of the alluvial terraces is crossed by the dunes (Figure 7). This could only occur if either the terraces post-dated the longitudinal dunes or were of the same age, as intermittent inundation of the floodplain could have precluded aeolian deposition. Thus the Forester Gravel is equivalent or of younger age to the Ainslie Sand and is therefore likely to be mainly of Last Glacial age.

Since the break of slope at the base of the fluvial terraces represents the limit of the Barnbougle Sand (page 36) the terrace deposits must predate the time of attainment of the upper marine limit by the Holocene transgression. Therefore their age is presumed to be greater than 6000 years (page 36).

The transportation and deposition of heavy bed loads during the Last Glacial Stage probably reflects slope instability, due to cold climate mass movement and weathering processes, in the upper reaches of the Great Forester River valley

4.5 Lacustrine Deposits

In the Waterhouse area (Figure 1) a small outcrop of fossiliferous marl and sandy marl occurs approximately 1 km east of One Tree Hill. The exposure is 1 to 2 m thick and is overlain by

FIGURE 7 Quaternary Deposits in the Tuckers Creek Area.

1 = Holocene parabolic and transverse dunes
2 = Holocene marine sands (Barnbougle Sand)
3 = Forester Gravel
4 = Stumpys Bay Sand
5 = Tertiary clays
6 = Longitudinal dune ridges
7 = Terrace edge

The numbered dots indicate bore hole locations.
AB is the transect shown in Figure 6.

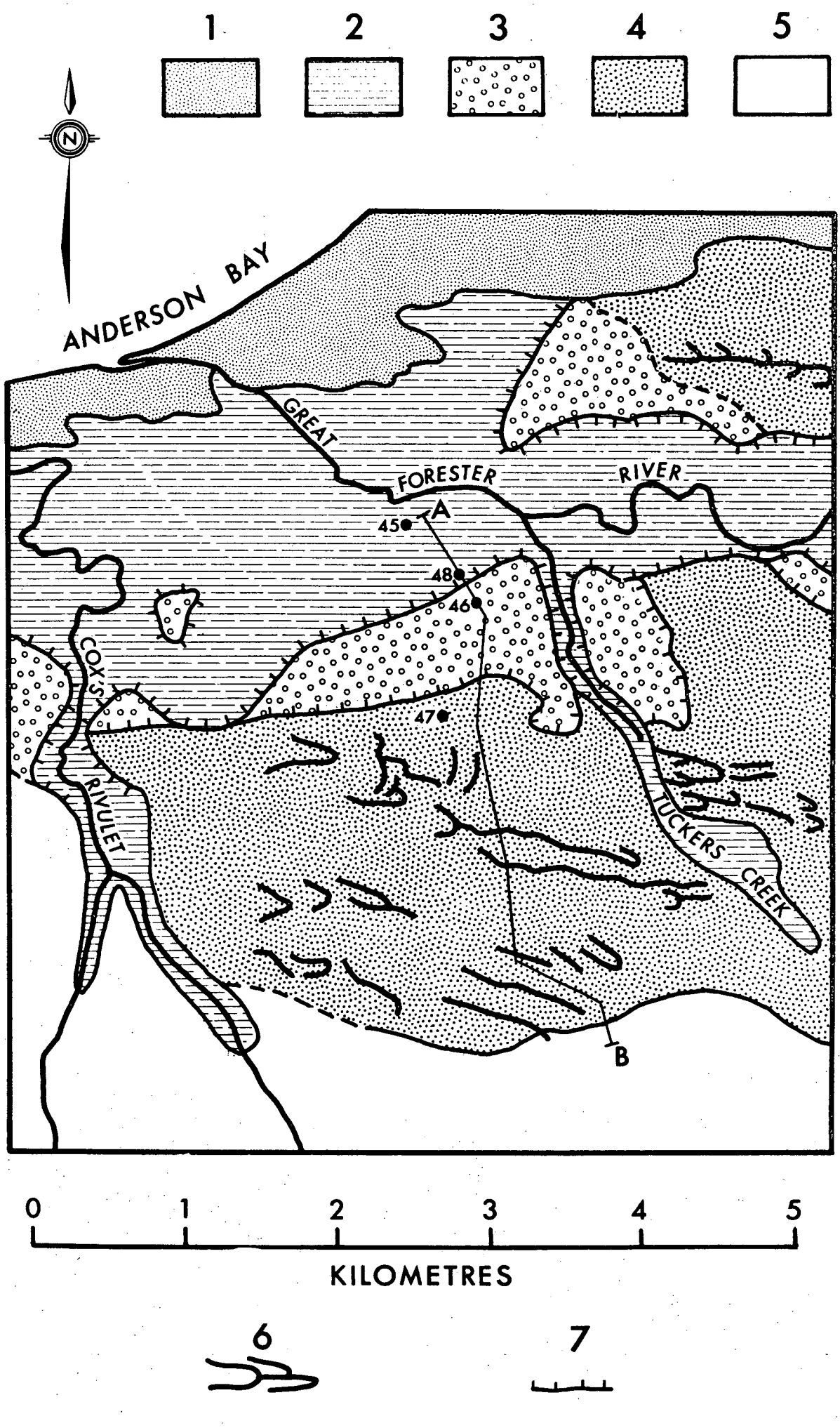
1
2
3
4
5
N
ANDERSON BAY
GREAT
FORESTER
RIVER
45
A
48
46
47
COX'S
RIVULET
TUCKERS
CREEK
B
0
1
2
3
4
5
KILOMETRES

6

7

a high, longitudinal sand dune composed of the Ainslie Sand. The marl is pictured cropping out beneath the dune in Plate 7. A bore through the flanks of the dune intersected lake deposits and the Stumpys Bay Sand and showed that the former overlies the latter. The marls observed in the outcrop were not penetrated by the bore but clay, sandy clay, and peat were encountered at the same level and are considered to be stratigraphically equivalent to the marl. This formation is hereinafter referred to as the Croppies Marl.

The Croppies Marl contains shells of freshwater Gastropods, including *Planorbis*, which is common in inland lakes, several types of Ostracods and a Charophyte oogonium, very common in lagoons and saline environments (Dr. C. Burrett, University of Tasmania, Geology Department, pers. comm.). The complete absence of foraminifera indicates a non-marine origin. The fossil evidence demonstrates a lacustrine origin of the beds.

The stratigraphic position of the lake deposits between the Stumpys Bay Sand and the Ainslie Sand fixes their age as being younger than the Last Interglacial and older than the late Last Glacial Stage. They may be of early to middle Last Glacial age. Unfortunately, the associated peaty sediments did not contain enough organic matter and were too disturbed by the auger method to be suitable for ^{14}C dating.

5. COASTAL DEPOSITS OF HOLOCENE AGE

5.1 Introduction

The period following the Last Glacial Stage was characterized by a rise in sea level as a result of deglaciation. In Australia, the Holocene marine transgression terminated around 6000 years ago

PLATE 7 Croppies Marl cropping out below dune of Ainslie Sand.

The marl bed extends from the figure standing in the middle ground to the viewer.

when sea level was within ± 1 m of its present position (Thom & Chappell, 1975). Many sectors of the coast of northeastern Tasmania are fringed by landforms and deposits that were formed subsequently under coastal conditions created by this marine transgression.

5.2 Marine Deposits

Young marine sediments form flat, generally level, swampy plains up to 3 km wide in the Ringarooma Bay and Anderson Bay areas, which have an exposed west-northwesterly aspect. Marine deposits also occur in the more sheltered eastern bays, such as Little Musselroe Bay and Great Musselroe Bay as a longshore barrier system partially enclosing a backshore lagoon. Narrow beach ridge plains lie landward of frontal dunes at Tomahawk and behind the east coast beaches in the Mount William National Park area. All of these marine deposits constitute the Barnbougle Sand.

The Barnbougle Sand has been drilled and sampled at Barnbougle (see Figure 7 for location). The upper layer of fine to medium fine sand occurs to a depth of ~ 1.5 m and is possibly a lagoonal, backshore deposit. This unit overlies approximately 6.5 m of medium to medium coarse shelly beach sand. Beneath the beach deposit fine to medium fine sand at least 3 m thick, contains some shells and probably represents a backshore facies. Figure 8 is a grainsize log of the bore samples. Although the bore did not reach the base of the deposits, the sequence suggests that a transgressive phase was followed by a regressive phase.

The Barnbougle Sand is of Holocene age and was deposited during the post-glacial transgression. This is indicated by its occurrence at elevations up to present sea level and its close

45

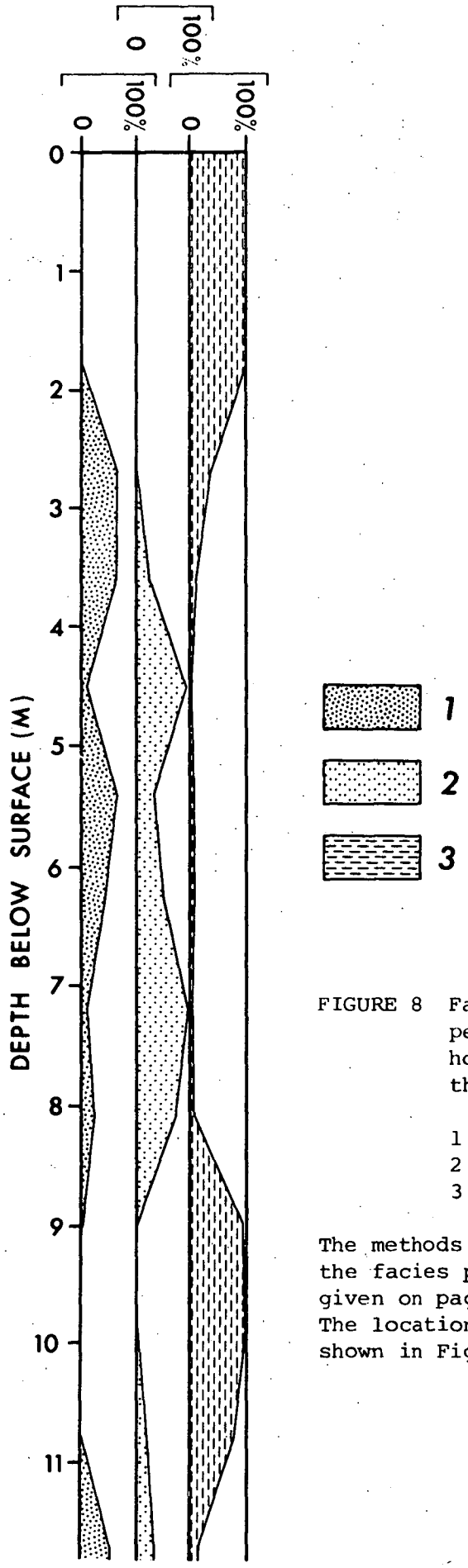

FIGURE 8 Facies proportions penetrated by a bore hole (Number 45) in the Barnbougle Sand.

1 = Beach facies
2 = Dune facies
3 = Lagoonal facies

The methods of determination of the facies proportions are given on pages 59 to 70. The location of the hole is shown in Figure 7.

association with the present coast and with large systems of very young parabolic dunes.

Progradation of the Holocene shore has not been accompanied by a perceptible change in relative sea level since the sea attained its present level about 6000 years ago. This is suggested by a levelling traverse from the base of the cliffed foredune of the present beach to a very well defined break of slope 3 cm higher which marks the upper limit of marine cliffing of the unconsolidated alluvial Forester Gravel. Plate 8 is an aerial photograph which shows clearly the cliffed Forester Gravel and upper limit of the Barnbougle Sand.

In a comprehensive study of Holocene barrier systems in New South Wales by Thom, Polach & Bowman (1978) there is strong evidence that the bulk of the sand of the barrier systems on the east coast of the mainland was deposited in the period 6000-3000 years BP and that since this period barrier modification involving aeolian reworking, rather than seaward growth, has occurred. Similar events appear to have occurred in northeastern Tasmania, but the events have not been dated. At Adams Cut the surface formed by the Holocene marine sands has been transgressed by siliceous, parabolic dunes that are now stable and is presently being transgressed by calcareous transverse dunes. These relationships of the Holocene dunes to the Barnbougle Sand are shown in Plate 9.

The differences in morphology between the Holocene marine deposits on coasts of northwesterly and easterly aspects are related to the degree of exposure. The coasts of Ringarooma Bay and Anderson Bay, where the Holocene marine plains are best developed, are exposed to strong, prevailing westerly winds. During coastal progradation the shores were probably subject to a powerful overbarrier wash, which produced the extensive back barrier sand flats. On the other hand,

PLATE 8 Aerial view of landward boundary of Holocene marine deposits in the Barnbougle area.

The terraces in the middle ground are formed by Forester Gravel.

PLATE 9 Aerial view of Adams Cut showing the fringe of Holocene coastal dunes which extend over the Barnbougle Sand. The view looks towards the north.

the deposits of the more protected coasts of Tomahawk and of the east coast, were laid down under a lower wave energy regime which would have favoured the development of the narrow beach ridge systems now present.

5.3 Parabolic Dunes

A series of long, narrow, siliceous parabolic dunes form a coastal fringe 2 to 3 km wide in the Anderson Bay and Ringarooma Bay areas (Figure 3). The dunes are here collectively referred to as the Waterhouse Sand. Areas of occurrence are exposed to the maximum fetch of westerly winds, except for a minor occurrence at Musselroe Point, the site of which has a westerly fetch over water of approximately 3 km.

The parabolic dunes are up to 2 km long, 30 m wide, 8 m high with an average spacing of approximately 100 m (11 per km). Measurement of the orientation of 86 dune ridges showed that the mean orientation is in a WNW-ESE direction (278 to 098 ± 5°) from True North. The dune ridges are extremely well defined in most cases with sharp crests and tight hairpins at the distal ends. The soil on the dunes is very poorly developed and consists of a uniform grey-brown A-C profile, but some dunes show a very weakly developed, irregular, podzol profile with an incipient B_2 horizon and a very shallow A_2 horizon. Seven samples were taken from the dunes for granulometric analysis and the component sand grains are moderately sorted (mean sorting = 0.51 ϕ) and medium to fine grained (mean grainsize = 2.15 ϕ).

These siliceous, parabolic dunes were derived by deflation of the beach sand by the prevailing onshore westerly winds. This is indicated by their position directly inland of the coast, and by

their orientation. At some localities the dunes rise over bedrock hills and form a blanket of dune sand. The dunes are not forming now and have been colonized by vegetation. In many cases the parabolic dunes are presently being deflated, due principally to destruction of the dune binding vegetation by fire. Lag deposits occur in areas where the dunes have been subject to deflation. This material consists of a concentrate of various aboriginal artefacts. At Musselroe Point as shown in Plates 10 and 11, extensive layered aboriginal middens, which contain abundant edible shellfish remains, artefacts, and charcoal, are interbedded with the dune sand thus demonstrating contemporaneity of origin and occupancy. Buried occupation layers which contain charcoal commonly occur within the Waterhouse Sand and reflect the close interrelationship of frequent firing and the presence of aboriginal man.

The immature soil profile developed on the Waterhouse Sand and its stratigraphic position above the Barnbougle Sand (page 38) indicates that the dunes are young, at least younger than 6000 years. Most of the dunes were probably formed during the last 3000 years. However, they are not being formed today because they are fully vegetated by Boobyalla. Although the fresher morphology of the parabolic dunes is a good indicator for separating them in age from the longitudinal dunes of the Ainslie Sand, the difference in soil profile development provides the most conclusive evidence.

5.4 Transverse Dunes

Masses of active sand with shell fragments are forming large transverse dunes in some coastal areas. They attain elevations of up to 25 m and cover areas of 2-3 km^2 (Figure 3), and form the Bowlers Lagoon Sand.

PLATE 10 Aboriginal Midden deposits at Musselroe Point.

PLATE 11 Shells and charcoal within the midden at Musselroe Point.

Steep, unstable, leeward slip faces which are shown in Plate 12 are common, and 14 measurements taken in the Barnbougle area, near Bridport, showed that the mean slip face angle is 32°20' and that the slip faces are oriented approximately normal to the direction of the prevailing wind. Aeolian cross-bedding is evident in many cases, particularly where old slip face beds are being deflated and intersect the surface of the low angle windward slopes. The surface of the dunes and the truncated slip face beds are shown in Plate 13.

The transverse dunes are moving inland by the continued action of sand removal from their windward flanks and re-deposition on the leeward slip faces. The sand and shell particles are derived from the present beaches and from some deflation of the parabolic dunes. Much of the present activity is confined to distinct corridors of active dune sand which lead inland from the beaches. The furthest inland occurrence of these dunes is on the eastern flanks of the northern end of Ringarooma Tier where the mobile calcareous sand occurs approximately 4.5 km from the coast. Although some of this dune sand is derived from the present beaches, as indicated by the presence of shell fragments, a large proportion is probably derived by deflation due to firing, causing reworking of much older dune sand which occurs on the crest of Ringarooma Tier.

6. GEOMORPHIC HISTORY OF COASTAL NORTHEASTERN TASMANIA

Table 1 summarizes the Quaternary stratigraphy. During Tertiary times (probably early to middle Miocene) several marine transgressions and regressions occurred. Fluvial gravels were also

PLATE 12 Steep leeward slip faces of Holocene transverse dune near Barnbougle.

PLATE 13 Surface of the transverse dunes (Bowlers Lagoon Sand) showing the truncated slip face beds.

TABLE 1 Stratigraphic Sequence of Coastal Northeastern Tasmania

Age	Formation	Landform and Origin	Extent
Holocene	Bowlers Lagoon Sand	Transverse calcareous sand dunes	Coastal margins of Anderson and Ringarooma Bays
	Waterhouse Sand	Parabolic sand dunes	Coastal margins of Anderson and Ringarooma Bays Musselroe Point
	Barnbougle Sand	Marine sand plains and beach ridges	All depositional coasts of northeastern Tasmania
Last Glacial	Forester Gravel	Fluvial terraces	Great Forester River
	Rushy Lagoon Sand	Terrestrial lunettes (? Holocene in part)	Widespread northeastern Tasmania
	Ainslie Sand	Terrestrial longitudinal sand dunes	Widespread northeastern Tasmania
	Croppies Marl	Inland lake deposits	5 km east of Croppies Point
Last Interglacial? (Isotope Stage 5)	Stumpys Bay Sand	Marine plains and beach ridges	Broad, coastal sand embayments: to +32 m
Second Last Interglacial? (Isotope Stage 7?)		Marine sands	Rockbank: to +49 m
Third Last Interglacial? (Isotope Stage 9?)		Marine sands	Rockbank: to +71 m
Older than Third Last Interglacial		Possibly marine sands	Star Hill Mine: to ~ 90 m
Middle Tertiary		Marine sands and freshwater peats	Bore 6 km SE of Cape Portland
Tertiary		Alluvial gravels	Widespread northeastern Tasmania

deposited in many areas during the Tertiary Period. No deposits have been found which can be assigned to the Late Tertiary or Early Quaternary period. During the Late Quaternary, eustatic sea level changes, probably coupled with tectonic uplift, produced marine deposits during several interglacial stages. Marine sands deposited in large embayments during the Last Interglacial Stage are now up to 32 m above present sea level.

During the Last Glacial Stage, when sea level was between 100 to 125 m below present level, the plains of marine sand provided the source material for an extensive system of longitudinal sand dunes. The decreased temperature and precipitation which probably prevailed caused a reduction in vegetation cover which allowed aeolian mobilization of the sand plains. During this period of longitudinal dune formation winter freeze-thaw action and associated processes may have been responsible for slope instability on steep, poorly vegetated hillsides. This slope instability was probably largely responsible for increased sediment load in the major river catchments of the region, and resulted in the deposition of alluvial terraces above the present river floodplains. At this time, or slightly later, deflation hollows were excavated in the plains of marine sand. Where the deflation hollows were excavated to the water table lakes were created and lunettes formed on their leeward margins. Lunette formation probably mainly terminated at the close of the Last Glacial Stage when the vegetation stabilized the surfaces from which the sands were derived but the dated evidence from Rushy Lagoon suggests the possibility that a few lunettes may be of Holocene age.

Marine sands were deposited on the coast as a result of the Holocene marine transgression and now form plains up to 3 km wide, narrow beach ridge systems and barrier beaches. Siliceous,

parabolic dunes derived from exposed beaches are closely associated with the marine deposits, but are now essentially stabilized by vegetation. Large, mobile, transverse dunes also occur in coastal areas and are derived from the present beaches and from erosion of the parabolic dunes.

7. POTENTIAL PROBLEMS FOR FURTHER RESEARCH

The preceding description of the regional geomorphologic framework has revealed several problems which can be examined in more detail. These include:

1) The Late Quaternary marine sequences of northeastern Tasmania should contain evidence for the recent tectonic history of Tasmania because a major discrepancy appears to exist between their present altitude and most of the documented sea level curves for stable coasts. The problem is to define the extent, mode of deposition, and age of these sequences in order to separate one suite of forms and deposits from another and interpret the Late Quaternary sea level and tectonic framework.

2) The presence of the longitudinal dune system and the lunettes implies that the climate during the Last Glacial Stage was markedly different to that of the present. Close examination of the longitudinal dunes should provide evidence of the wind regimes during deposition and the history of lunette formation should yield clues regarding the changing hydrologic balance at that time.

3) The Holocene sea level rise and sedimentation is not well documented or dated in Tasmania. Abundant shell material occurs within the Holocene marine deposits, which extend to a depth of at least 11 m, and a comprehensive drilling and dating programme similar to

that carried out by Thom, Polach & Bowman (1978) would provide information for comparison with mainland events. In addition, more work could be carried out on the Holocene dune sequence to establish the chronology and causes of dune mobilization and stabilization.

4) Contemporary coastal processes operating in northeastern Tasmania would be a productive field for further study, particularly with respect to the impact of Man on what is often regarded as a fragile environment. In addition, the establishment of the relationship between climatic variables and beach and dune formation should be of use when reconstructing the environmental conditions which produced inherited coastal landforms.

5) Water is an important resource and many of the deposits previously discussed contain groundwater at shallow depth under open water table conditions. A detailed appraisal of water table fluctuations and their relationship to inputs and outputs would allow assessment of the magnitude and sustainability of the water resources. Understanding of present water table conditions may also aid interpretation of climatic parameters where indications of past water table levels are obtainable.

6) Quaternary deposits containing pollen are sparsely distributed in northeastern Tasmania and preservation of a long pollen record is unlikely. However, comprehensive pollen analysis should provide fragmentary information on the history of local vegetation and environment which, when coupled with stratigraphic considerations, might be placed within a framework derived from elsewhere.

The remainder of the thesis follows up in more detail some of the questions which have become evident from the preceding analysis of the regional geomorphology. Part II examines two purely geomorphic problems. Section 1 of Part II examines the Quaternary marine sequences as evidence for tectonic activity in Tasmania. This problem has been chosen because it questions assumptions that Tasmania is tectonically stable, and if instability can be demonstrated, comparison can be made with other tectonically unstable regions. Such comparisons, when considered in the light of current tectonic models, may provide an indication of possible mechanisms for Tasmanian tectonic instability. Section 2 of Part II examines terrestrial dunes and associated features as evidence of past climatic change in northeastern Tasmania. This study looks at the evidence for changing hydrologic conditions during the Last Glacial Stage, the relationship between dune formation and wind conditions, and compares the findings with events and circulation patterns which have been tabled from elsewhere in southeastern Australia.

Part III is concerned with water table dynamics in unconfined aquifers with special reference to the groundwater of the Stumpys Bay Sand. Northeastern Tasmania is one of the driest areas of the island and is subject to summer drought and severe soil water deficits. Many coastal areas of Australia are fringed by plains of unconsolidated sand, which should contain groundwater, and the study therefore has potentially wider application.

Two of the three remaining problems are currently being examined elsewhere in Tasmania. A long pollen record has been obtained from northwestern Tasmania (Colhoun & van de Geer, pers. comm.) and is still under study. Drilling and sampling of several

Tasmanian Holocene barrier systems has been completed and radiocarbon dating is now in progress (Thom, pers. comm.). No further study of these topics will be made in this dissertation.

PART II

Section 1

LATE QUATERNARY MARINE SEQUENCES: SYMPTOMS OF TECTONIC ACTIVITY

1. INTRODUCTION

The aim of this section is to describe the occurrence and character of each of the major bodies of sediment which comprise the Stumpys Bay Sand in order to provide a firmer interpretation of the mode of origin and environmental conditions during its deposition. The lines of evidence which indicate that the Stumpys Bay Sand is of Last Interglacial age are then examined. The further inferences of tectonic uplift rely heavily on this interpretation of age, and on the estimates of the upper limits of marine activity. A similar approach is adopted for the older Quaternary marine deposits.

The evidence for uplift and the nature of uplift in northeastern Tasmania is assessed by comparing upper marine limits with eustatic sea level curves derived from stable areas and the deep sea oxygen isotope record. Finally, this section briefly considers the possible cause of Tasmanian tectonic instability and compares it with evidence from adjacent parts of mainland Australia.

2. STUMPYS BAY SAND

The Stumpys Bay Sand occurs in three distinct morphologic settings. Where the sand plains have been exposed to large scale aeolian reworking during the Last Glacial Stage (pages 20-26) the Stumpys Bay Sand is traversed by an extensive system of longitudinal sand dunes and the original surface morphology has been largely destroyed. This setting is mainly found in the western and northern portions of the study area. Conversely, the tracts of Stumpys Bay Sand that occur on the eastern coast of the study area have been largely protected from deflation by the shelter provided by the granite hills to windward. Thus the original morphology of the sand plains is preserved intact and low ridges sub-parallel to the coast characterize the surface configuration. The third setting occurs in the Little Musselroe River area where the Stumpys Bay Sand occupies a partially enclosed, flat-floored topographic depression with only few natural outlets to the coast.

2.1 Eastern Embayments

2.1.1 *Stumpys Bay*

2.1.1.1 Extent

In the type locality at Stumpys Bay, in the Mount William National Park, the Stumpys Bay Sand forms a narrow plain 2 to 3 km wide and 6 km long, which is wedged between the sea to the east and the prominent rise of Mount William to the west. The western boundary of the formation is marked by a fairly well defined break of slope at an altitude of 32.47 m above HWM. Drilling demonstrates that the formation has a maximum thickness of 8 m and is underlain by

granite. The cross profile (Figure 9) from the sea to the upper limit of the Stumpys Bay Sand shows that the formation wedges out at the break of slope on its landward margins and that it has been truncated by Holocene coastal deposits at the seaward margin. An important feature of the plain is that some original beach ridges lie sub-parallel to the coast (Plate 14) and remain in a good state of preservation. Several small streams originate in the Mount William area and traverse the plain but the plain is largely devoid of natural surface drainage.

2.1.1.2 Environment of deposition

The composition of a sediment is determined by the characteristics of the available material, the conditions of sedimentation, and the post depositional diagenesis. The environment of deposition is therefore usually potentially capable of being determined by study of the composition and characteristics of a sediment. This includes study of the mineral and fossil content, the grainsize, and the sedimentary structures. Environmental changes through time may be reflected in compositional variation through a depositional sequence. Composition is the principal line of evidence used for the interpretation of depositional environments throughout the study, but surface morphology is taken into account as an additional means of interpretation.

The morphology of the Stumpys Bay plain strongly resembles a marine embayment. It has a low, seaward sloping surface, with a gradient of approximately 12.5 m/km towards the NE and is backed by a more elevated, dissected landscape developed on granite. The possibility that the plain could have been formed by concentration of locally derived colluvial material from the granite hinterland can be discounted as the high degree of rounding of the quartz

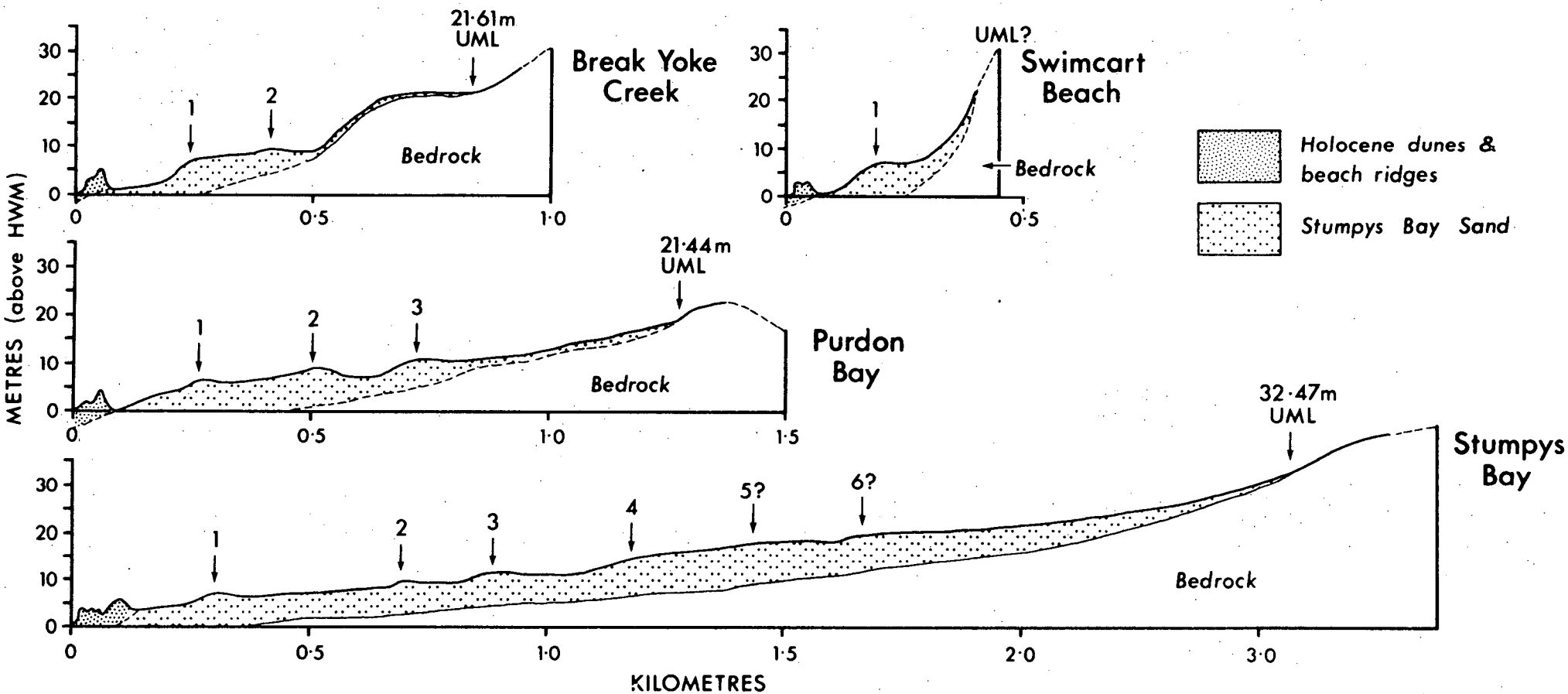

FIGURE 9 Cross profiles of the eastern embayments of Stumpys Bay Sand.
VE = 10x

PLATE 14 Vertical Aerial Photograph of Stumpys Bay Area.

The light areas are beach ridge crests which lie sub-parellel to the coast.

particles which comprise the sand plain is not consistent with such an interpretation. Colluvial mantles in the granite hinterland contain highly angular quartz particles which retain many of the primary crystal surfaces as well as numerous angular feldspar fragments.

The presence of low rounded ridges that can only be interpreted as beach ridges provide the most convincing evidence for a marine origin of the plain at Stumpys Bay. The ridges are well drained, elongate, sandy rises which commence with a noticeable break of slope on the seaward, steeper flank. The landward flanks form a wide, very low angle surface. The swales between the ridges are very poorly drained and often contain small lagoons. Jennings & McShane (1971) also interpreted these features as beach berms.

Six ridges occur in the profile of Stumpys Bay (Figure 9) over a horizontal distance of around 2 km. The top 40-80 cm of the ridges consist of coarse, very well rounded, quartz sand which is characteristic of a beach origin. The fossil content also indicates a marine origin for the sands. Samples from drill holes at Stumpys Bay contain many sponge spicules (Plate 16). This form of megasclere (triaenes) cannot belong to the Spongillids (freshwater sponges) and are therefore of marine origin (Dr. M. Banks, University of Tasmania, Geology Department, pers. comm.). In addition the spicules are of the same type as those which occur in the Holocene marine sands (Plate 15). The spicules are in a very good state of preservation, considering their delicate structure, and it seems highly unlikely that they have been reworked from some other sediment. The above evidence clearly demonstrates a marine mode of deposition for the sand plain at Stumpys Bay. Three auger holes were drilled

PLATE 15 Sponge Spicule (megasclere) from Holocene marine sands. (Bore 45, 2.72 m depth).

PLATE 16 Sponge Spicule (megasclere) from Stumpys Bay Sand at Stumpys Bay. (Bore 91, 6.94 m depth).

PLATE 17 Sponge Spicule (megasclere) from Stumpys Bay Sand at East Tomahawk. (Bore 8, 9.05 m depth).

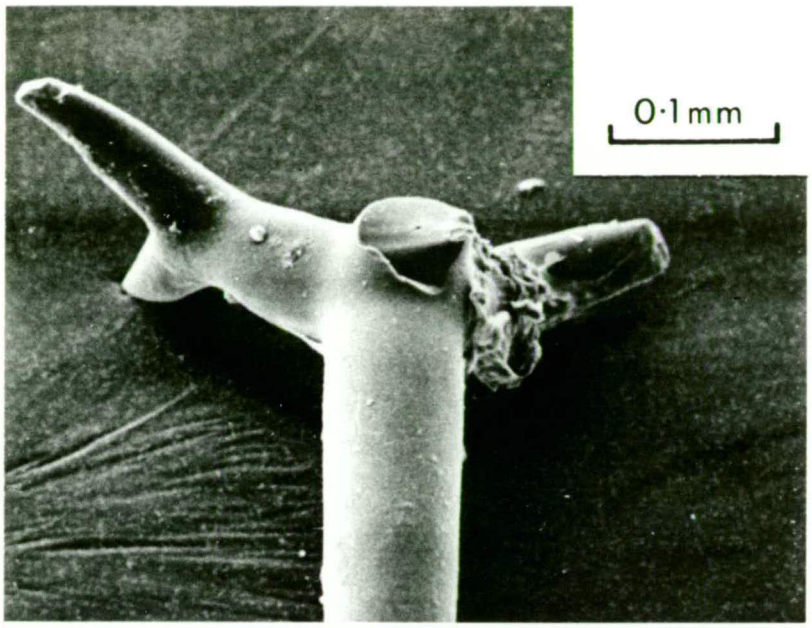
0·1 mm

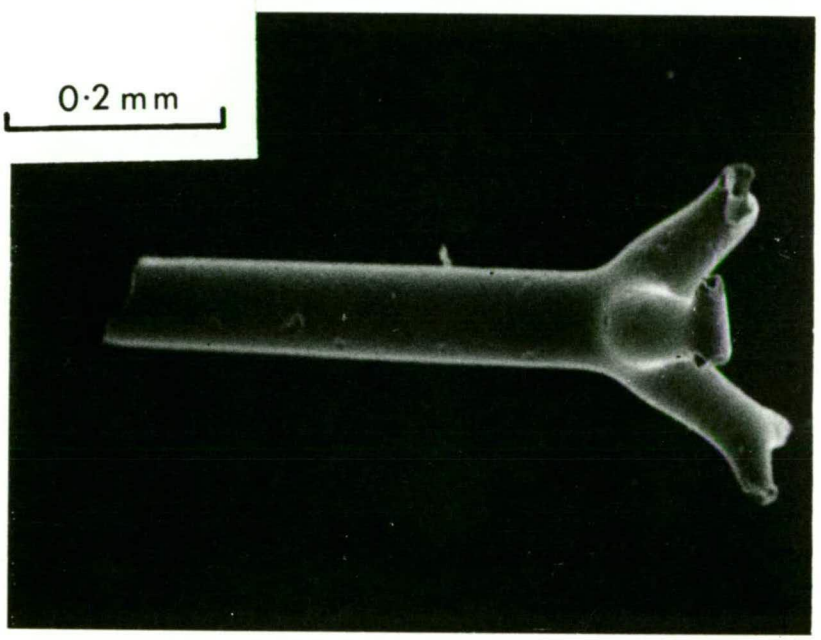
0·2 mm

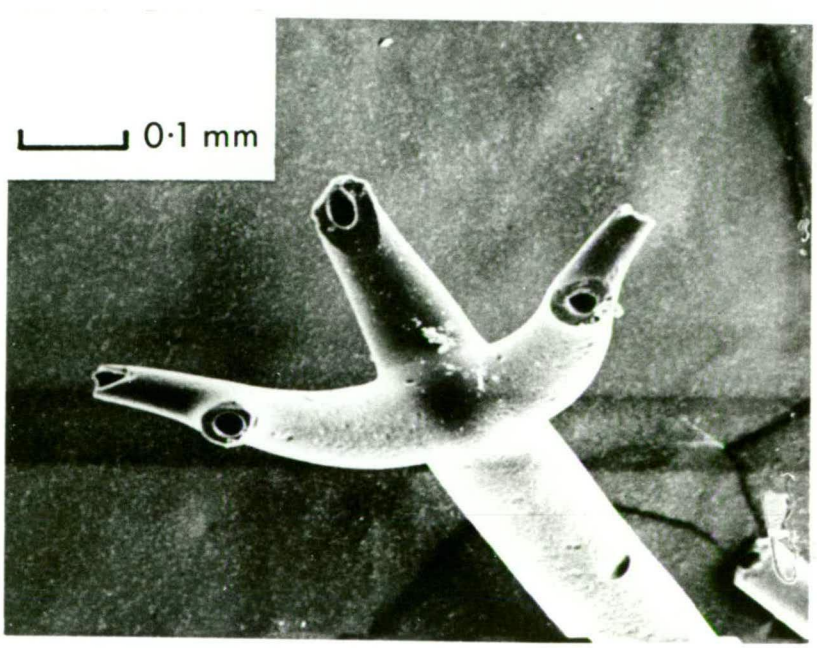
0·1 mm

in the plain to determine the sequence of deposition and to ascertain whether the sands were deposited during a single interglacial cycle.

Interpretation of facies change throughout a depositional sequence is frequently highly dependent on the analysis of grainsize characteristics and their relationship to depositional environment. This is shown by the work of Folk & Ward (1957), Passega (1957), Mason & Folk (1958), Friedman (1961), Bull (1962), Folk (1966). However, these relationships vary from one region to another, depending on the relative importance of the various physical processes in operation and on the type and availability of source material. Before proceeding with the analysis of the drilling results at Stumpys Bay it is therefore necessary to define and support the assumptions and arguments which are used throughout this study to determine the relationships between sediment size parameters and environments of deposition for the region.

Two similar, but basic problems emerge when attempting to analyze grainsize parameters from drilling samples. The first problem is caused by the fact that many sediments are the product of more than one agent of deposition. For example, coastal lagoons often have considerable quantities of aeolian sand blown into them by deflation from the beach and foredune zones. The sediment deposited in the lagoons therefore will contain elements of both sub-aqueous lagoonal sedimentation and aeolian sedimentation, and hence show a degree of bimodality. The second problem is related to the drilling method used and the level of resolution attainable on samples which have been derived from a depth interval, rather than from one specific sedimentary bed. In this study the drilling samples were taken from within 30-40 cm of the auger bit, and almost certainly at times produced samples which were derived

from vertically adjacent beds of different origin. In this manner, for example, it would be possible to sample from a bed of beach origin and one of aeolian origin which would produce a sediment sample which also showed a bimodal distribution. Given these two problems the analysis of grainsize parameters is dependent on the determination of the probable constitution of samples from single environments of deposition. If this can be achieved estimates of the sample proportions which are derived from different environments of deposition can be made through the analysis of polymodal sediments. Samples which are from areas such as the near shore marine zone, where a range of depositional processes operate in close juxtaposition, are often bimodal or polymodal as are samples derived from the above drilling method. Conventional statistical parameter estimates such as the mean and median grainsize, and the coefficient of sorting can be calculated for polymodal sediments but have very little applied significance. This is exemplified by Figure 10 which shows a histogram of the grainsize distribution of a hypothetical bimodal sample. Inspection of the frequency curve shows that the sample is composed of two approximately normally distributed sediment components. The coarser sediment peaks in the 0.00 to 0.25 ϕ range and the finer sediment in the 0.75 to 3.00 ϕ range. The calculated mean for the sample is 1.20 ϕ - a medium sand (Folk, 1965) but in Figure 10 only 1% of the sample falls within the 1.00 to 1.25 ϕ class, which contains the calculated mean. Obviously the calculated mean for this example is not representative of the bulk of sediment and cannot be used as a meaningful basis for environmental interpretation. The best approach is to assume that the sample is composed of two separate populations and to calculate the mean grainsize of each

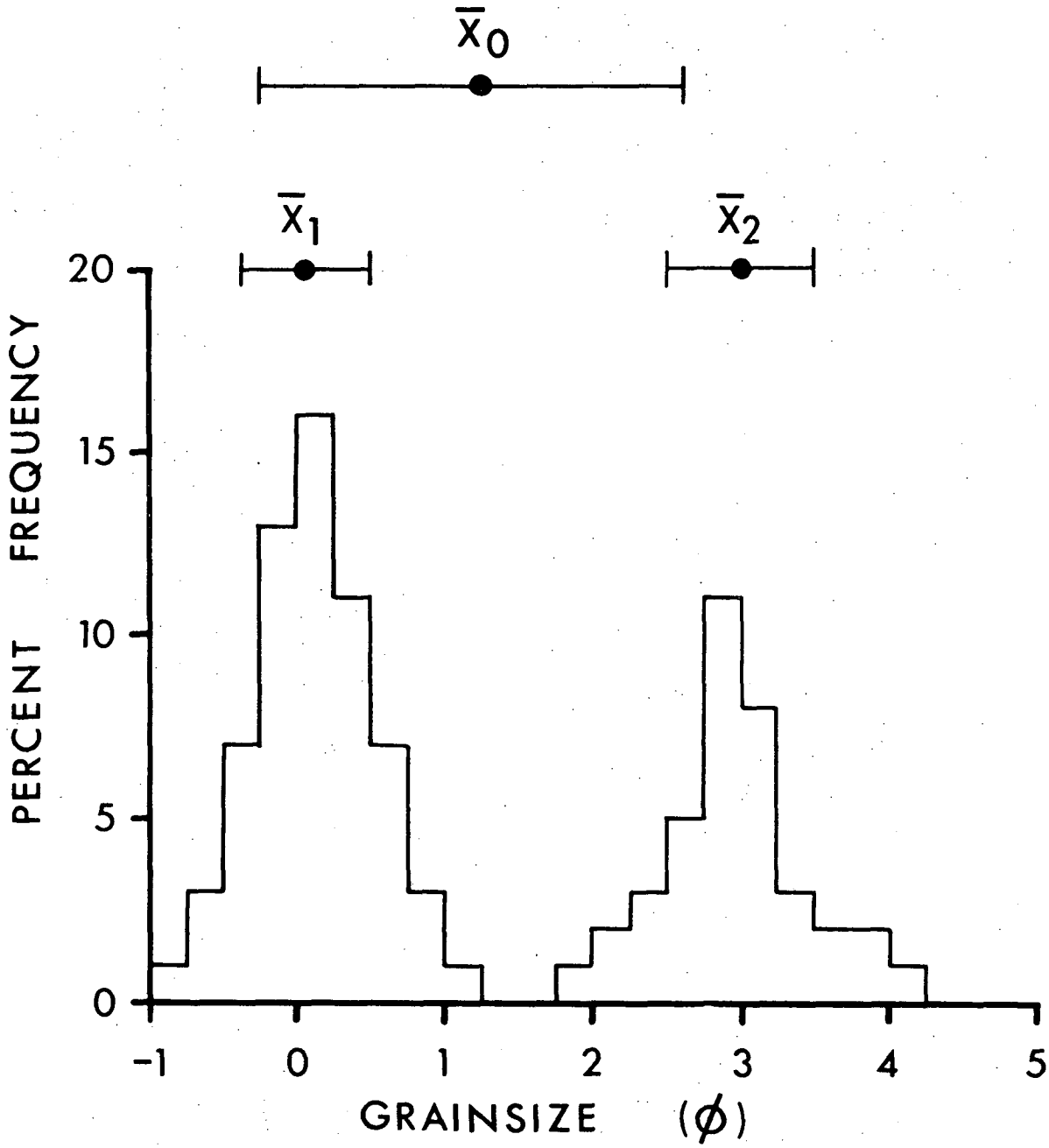

FIGURE 10 Hypothetical bimodal grainsize distribution.

$\bar{X}_0$ is the mean size of the total sample

$\bar{X}_1$ is the mean size of the coarse sample

$\bar{X}_2$ is the mean size of the fine sample

The horizontal bars represent one standard deviation (the sorting coefficient) on either side of the mean.

distribution. In this case the sample consists of two sediment components, a coarse sand with a mean grainsize of 0.12 ϕ and a fine sand with a mean grainsize of 2.97 ϕ. Furthermore, it would be possible to determine the relative proportion each sub-population contributed to the sample. Hence the coarser sub-population, which is probably the product of a higher energy environment forms 62% of the sample and the finer, lower energy sub-population comprises 38% of the sample. This calculation allows an estimate of the relative importance of the contributing depositional forces. The same argument can be used against the calculation of the median grainsize, which is also a measure of central tendency, on similar logical grounds.

The coefficient of sorting (the standard deviation) of bimodal and polymodal samples is not as useful a parameter as in unimodal samples. With unimodal distributions the standard deviation is a measure of dispersion from the mean and therefore is a good indicator of uniformity of grainsize within a sample. The large standard deviations which are derived from polymodal distributions reflect the diversity of grainsize within the sample but tend to mask the occurrence of well sorted sub-populations within the sample. Returning to the hypothetical example in Figure 10 the sorting coefficient of the entire population is $\pm$ 1.45 ϕ, poorly sorted (Folk, 1965) but the coarser sub-population is well sorted ($\pm$ 0.50 ϕ). Without taking the sub-populations into account the poorly sorted sample could be considered to be the product of one depositional process operating at different intensities. However when the sample is broken down into its sub-populations it is evident that a more likely interpretation is that two different

depositional processes were in operation but that each operated at a relatively consistent energy level.

The above example only considers the value of calculation of mean and sorting parameters for bimodal and polymodal samples but on the same grounds other standard statistical parameters such as skewness and kurtosis are also much less applicable than in unimodal populations. The most useful conclusion to be drawn from the above examples is that inspection of the frequency distribution curve is a necessary prerequisite to assessment of grainsize characteristics. Such inspection indicates the degree of validity and usefulness of the calculated parameters for interpretive purposes.

Probably the most hazardous, and potentially the most subjective, process in the interpretation of depositional environment from grainsize characteristics is the determination of the ideal grainsize distribution for each perceived environment of deposition. This step must be formulated according to the peculiarities of the region under study.

The coastal sand embayment at Stumpys Bay is of marine origin and these deposits are not likely to have been laid down in an offshore marine environment because of the thin wedge of sand present (up to 8 m), the proximity of the granite hinterland, and the development of the beach ridge topography. All the indications, therefore, are that the sands were deposited in an environment closely associated with shore processes. Contemporary barrier systems in northeastern Tasmania, such as occurs at Little Musselroe Bay (Figure 1), consist of barrier beach and foredune systems backed by lagoons, and these three depositional environments are considered here to be the principal environments controlling sedimentation of the coastal sand plains.

Identification of the facies type for each of these processes is necessary for the interpretation of the depositional sequences of the embayments. In terms of energy levels of deposition the beach zone is the highest energy zone and therefore one would expect the coarsest sands to be of beach origin. At the other end of the scale the lagoonal environment is one of relatively quiet water deposition resulting in the settling out of the finer available particles. Hence sediments from these two zones should be readily distinguishable and mutually exclusive in terms of particle size. The third zone however, controlled by aeolian processes, is of an intermediate energy level and therefore the grainsize characteristics of purely aeolian sands in the area need to be determined in order to define the facies composition of a mixed sample.

Seven samples from 500 m intervals along the crest of a Holocene parabolic coastal dune at Waterhouse possess extremely similar grainsize distributions. Sieving,using a 0.50 ϕ screen interval, showed that without exception the sands peak in the 2.00 to 2.50 ϕ range with the mean grainsize being 2.15 ϕ on average (fine sand), and their mean sorting coefficient is 0.51 ϕ. They are coarse-skewed with 98% of the grains lying in the range from 0.50 ϕ to 3.00 ϕ. All samples from bores were sieved at an interval of 0.25 ϕ. Figure 11(1) shows the grainsize distribution of the sample from Bore 2 (Tomahawk) at a depth of 1.81 m which is interpreted as being entirely of dune origin on the basis of the criteria outlined above (mean size = 2.17 ϕ, sorting = 0.52 ϕ).

A typical sample of beach origin is the sample from a depth of 0.92 m (Figure 11(2)) below the crest of a beach ridge at Stumpys Bay (Bore 91) which is of known beach origin. The mean

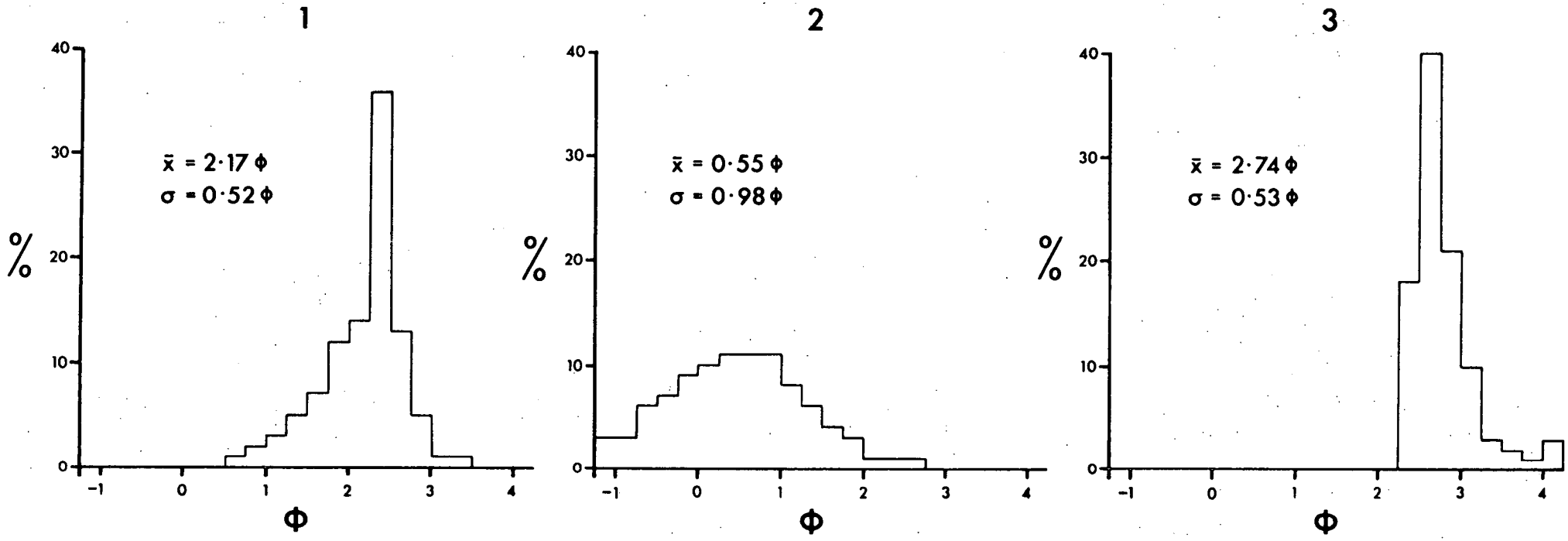

FIGURE 11 Grainsize frequency histograms for typical facies types.

1. Grainsize histogram for a typical dune sample from Bore 2, at a depth of 1.81 m.
2. Grainsize histogram for a typical beach sample from Bore 91, at a depth of 0.92 m.
3. Grainsize histogram for a typical lagoonal sample from Bore 11, at a depth of 3.62 m.

grainsize of this slightly coarse-skewed sample is 0.55 ϕ with a much higher sorting coefficient (0.98 ϕ) than the dune sands. For interpretive purposes, the key feature of beach sands is that the sediments are largely outside the size range of dune sand. Problems of interpretation arise when a fine grained beach sand is mixed with dune sand but the severity of the problem depends on the degree of accuracy required in the interpretation.

Sediments which largely fall beyond the fine range of dune sands are considered to have been deposited in a lagoonal environment. Some of the bore samples which consisted only of fine to very fine sand such as the sample from a depth of 3.62 m in Bore 11 at Tomahawk, showed a pronounced peak in the 2.50 to 2.75 ϕ range, which is too fine for dune sand, and were fine-skewed compared with the coarse-skewed dune sands. Figure 11(3) shows the percent frequency histogram of this sample which is considered to consist entirely of deposits of lagoonal origin. Probably the only limit to the fine end of the scale for lagoonal sediments is determined by the amount of silt and clay in the runoff water which enters the lagoon, because depositional energy levels in lagoonal environments are very low.

Taking the above three sediment distributions as a basis for interpretation of nearshore sediments it should be possible to inspect a frequency histogram and determine approximately the proportion of the sample which is composed of each facies. This is a useful technique because it is possible to detect sequential changes from predominantly lagoonal through dune, to beach facies that would indicate a transgressive phase of sedimentation. Figure 12(a) is an idealized diagram which shows the relative position of each facies type in the nearshore environment. A

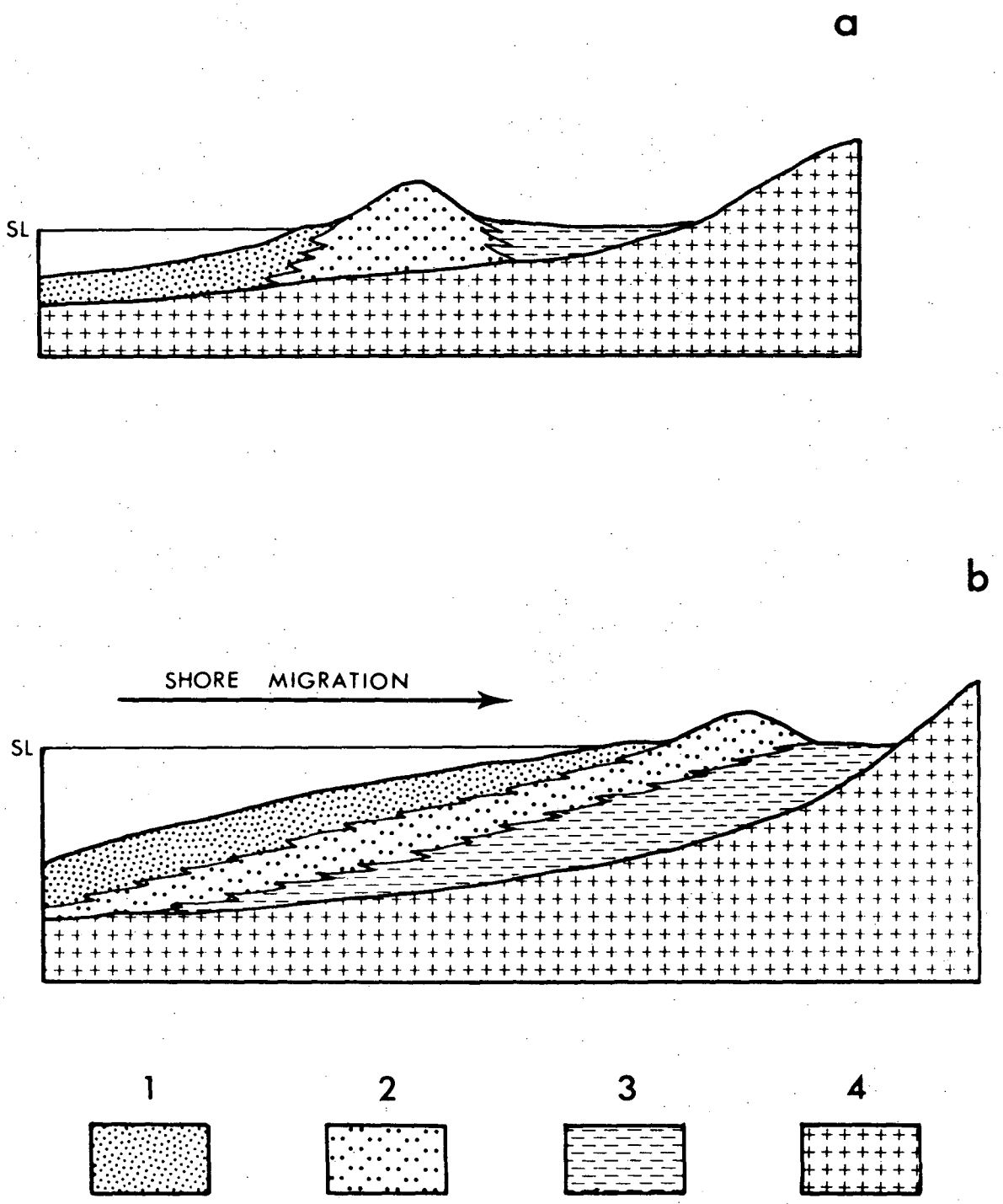

FIGURE 12 Schematic diagram of coastal facies relationships

(a) Near shore relationships of facies types at one point in time.

(b) Superimposition of facies types as a consequence of rising sea level and shoreline transgression.

1 = beach facies
2 = dune facies
3 = lagoonal facies
4 = bedrock

transgressive phase would produce lagoonal facies over-ridden by dune and then beach facies if viewed in section such as Figure 12(b).

The method which has been used to estimate the relative proportions of each facies type is demonstrated below utilizing an example from Bore 10 (Figure 16) at a depth of 4.57 m. The technique is based on the determination of the frequency distribution for dune sand, and once determined, the residue consists of beach and lagoon facies materials.

The grainsize distribution of the above sample from Bore 10 is presented in Figure 13 and contains a fairly low proportion of the coarser beach sand, and about equal proportions of dune and lagoon sand. Separation of the dune and lagoon facies is done by inspection, creating two distributions, one which is necessarily coarse-skewed with a peak in the 2.25-2.50 ϕ class, and one fine-skewed with a peak in the 2.50-2.75 ϕ class. The estimated frequency of the 2.25-2.50 ϕ dune sand modal class is determined by assuming that it is between 2.2 and 2.5 times greater than the frequency of the class before it (2.00-2.25 ϕ), which is poorly represented in the "standard" lagoon sample. Once these two size classes are estimated the remaining proportions in each class are estimated by inspection to conform approximately with the characteristics of the dune "standard". The mean grainsize and sorting coefficient of the resulting dune sand component are 2.16 ϕ and $\pm$ 0.49 ϕ, which agrees closely with the parameters 2.17 ϕ and $\pm$ 0.52 ϕ of the "standard". The frequency distribution of the remaining lagoonal facies is close to that of the "standard", fine-skewed with the mode lying in the 2.50 ϕ to 2.75 ϕ class.

It is possible to alter the frequency distribution by about $\pm$ 5 to 10% and retain a grainsize distribution for dune sand

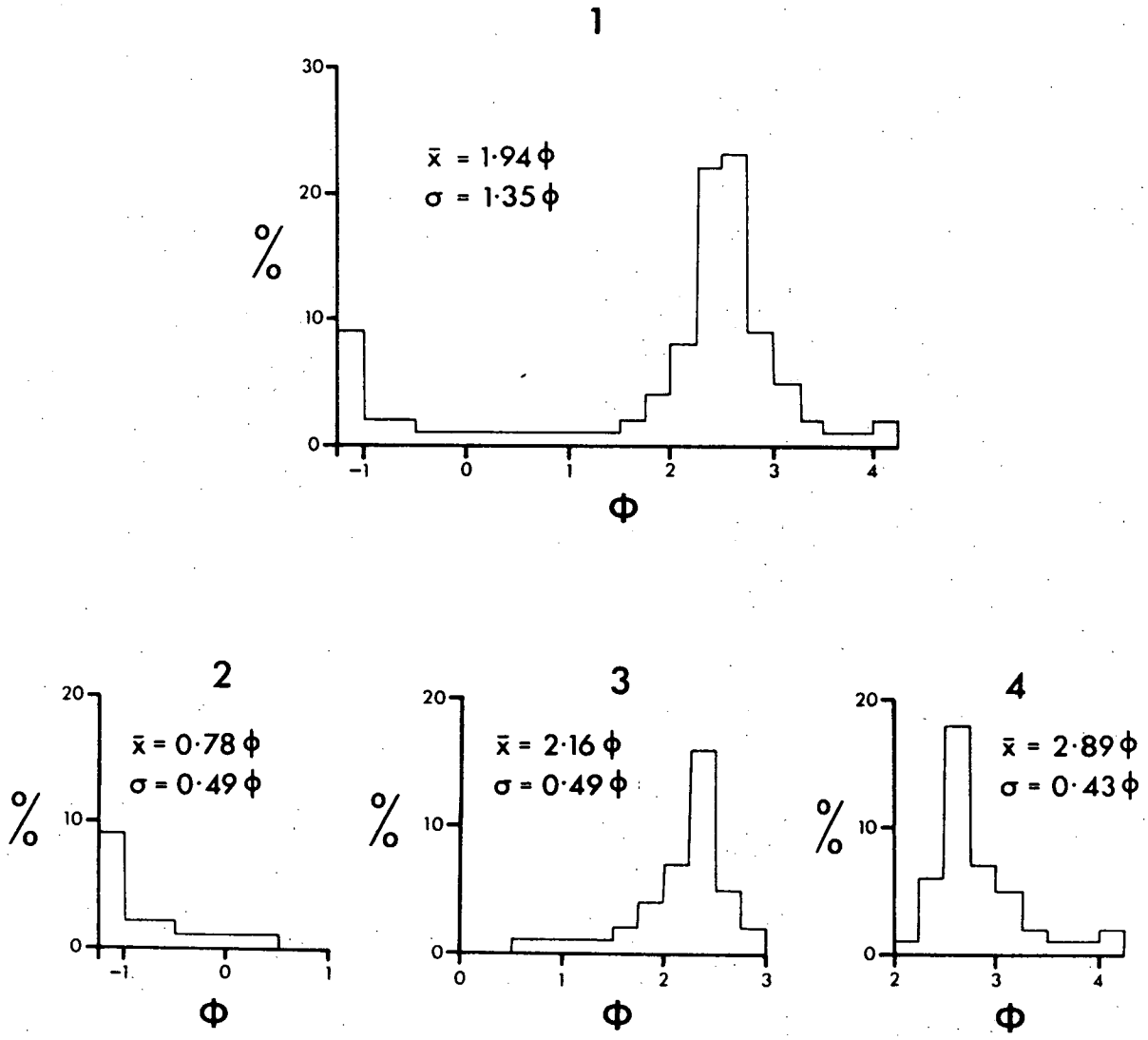

FIGURE 13 Separation of facies types from an example sample. The sample is from a depth of 4.57 m in Bore 10.

1. Grainsize distribution of total sample.
2. Interpreted grainsize distribution of the beach facies component.
3. Interpreted grainsize distribution of the dune facies component.
4. Interpreted grainsize distribution of the lagoonal facies component.

which is similar to the "standard" facies distribution. However, since the purpose of the sample division is to gain an approximation of the facies proportions present this level of accuracy is sufficient. The example above considers one of the most complex facies combinations which arose in this study and many of the samples which have only two facies present or predominantly one facies type can be more confidently assessed. The principal advantage of the technique is that, by its use, it is possible to plot the relative abundance of each facies down the bore log.

As the method of bore sample interpretation has now been defined it will be applied to the drilling results of the bore at Stumpys Bay in an attempt to determine the sequence of marine deposition.

Figure 14 is a depth plot of the percentage of the total sample which comprised each facies type in Bore 91. This hole was located on the crest of the most seaward beach ridge at an elevation of 6.1 m, and approximately 300 m inland from the present beach at Stumpys Bay. The bore reached weathered granite at a depth of 7.62 m. The sediments of the ridge have suffered negligible erosion since the near surface sands were deposited, because the beach ridge surface remains well preserved. This bore therefore should contain the most complete depositional sequence at Stumpys Bay.

The most pronounced feature of this bore log is the sequential shift from an initial lagoon environment, through a predominantly dune facies to a beach environment. The lagoon facies makes up about 96% of the basal sample at 7.01 and declines steadily upwards until it is not represented at 4.27 m depth. The dune sand facies first occurs in the section at 6.10 m where it comprises about 21% of the sample and increases up the bore section to 4.27 m which is entirely dune sand. From this point the proportion of

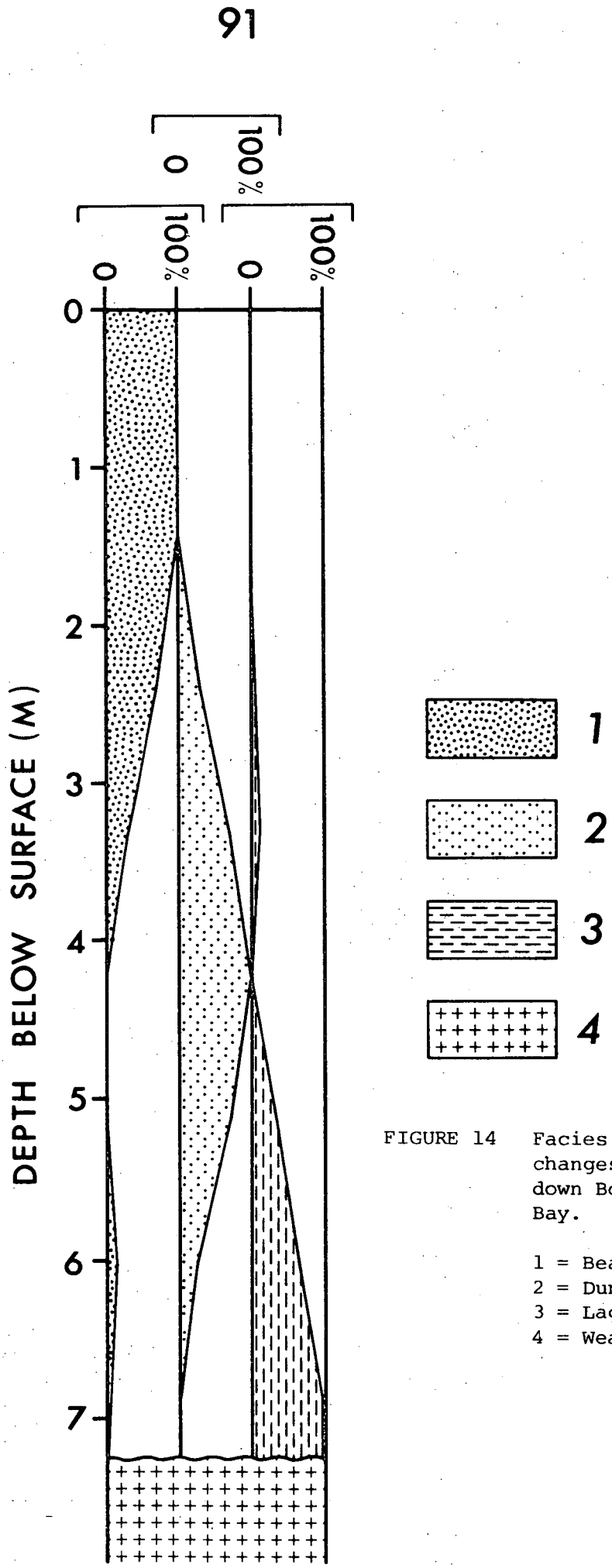

FIGURE 14 Facies proportion changes with depth down Bore 91, Stumpys Bay.

1 = Beach facies
2 = Dune facies
3 = Lagoonal facies
4 = Weathered granite

dune sand declines steadily and is substituted by beach facies to a depth of 1.52 m from which point the section consists entirely of beach sands. The sequence provides strong evidence of a marine transgression that involved landward migration of a foredune and barrier beach system which was backed by a lagoon. This is analogous to the conditions of formation of many barrier/lagoon systems in eastern Australia which are the product of the Holocene marine transgression (Bird, 1961, 1973; Thom *et al.*, 1978). The subsequent regression, which is probably represented by the top 1.5 m or so of beach sand, did not involve a beach and lagoon environment but consisted of beach ridge construction at decreasing elevations as the regression proceeded. As the sands are continuous from sea level to an elevation of 32.47 m the sequence was therefore deposited during a transgression to ≅ 32 m and subsequent regression to below present sea level. No evidence of peat layers or fossil soil horizons, which could indicate subaerial weathering, was encountered during drilling at Stumpys Bay. This indicates that only one interglacial cycle of marine transgression is represented.

2.1.1.3 Age

No material which can be dated radiometrically, has been found in the marine sequence at Stumpys Bay. However, it has already been suggested on several indirect lines of evidence that the entire sequence at Stumpys Bay is of Last Interglacial age (pages 17 and 18).

The sands at Stumpys Bay were deposited during a single major marine transgression representing a sequence of events related to a single interglacial. They extend from about 32 m to below

present sea level indicating that regression was fairly continuous within this range. The surface is characterized by beach ridges at successively lower levels indicating that this regressive sequence was interrupted by occasional periods of sea level stability.

Shackleton and Opdyke (1973) have shown that the deep sea oxygen isotope record indicates that interglacial sea levels on stable coasts over the last 800,000 years or so were within ± 10 metres of the present sea level. The Stumpys Bay Sands are less than 800,000 years old as indicated by the fact that the beach ridges, although composed of unconsolidated sand, are well preserved and are characterized by a relatively low degree of soil profile development. Since the sediments reach up to 32 m above present sea level the area has clearly experienced uplift since the sands were deposited. If any high interglacial sea levels had occurred since the deposition of the Stumpys Bay Sand, one might reasonably have expected to have found either erosional or depositional evidence of such occurrences at Stumpys Bay. The sediments are clearly not a product of a Holocene marine transgression because of their vertical extent, and their truncation by marine sands and dunes of Holocene age (pages 36 and 43). Thus it is highly probable that the Stumpys Bay Sand is of Last Interglacial age.

2.1.2 *Other Embayments*

The smaller embayments of sand with beach ridge topographies to the south of Stumpys Bay have been covered by levelling traverses and examined by shallow hand augering. They are very similar to Stumpys Bay in their geographic setting and sediment composition and all are regarded as the product of marine transgression during the Last Interglacial Stage. However, a prominent feature of the

embayments is that the bedrock coast, and the bedrock hinterland backing the embayments, becomes steeper with increasing distance southwards from Stumpys Bay. A further feature is that the elevation of the beach ridge plain/hinterland boundary is lower in the smaller embayments.

Purdon Bay, 9 km south of Stumpys Bay, is backed by a small beach ridge plain which is 2.5 km long, 1.4 km wide, and has a seaward surface slope of approximately 16.5 m/km. Augering in the area demonstrated that the plain is composed of medium grained to coarse grained well rounded beach sands near the surface. Three broad crested beach ridges lie sub-parallel to the coast, as shown by the profile of Figure 9. The sand wedges out at an indistinct break of slope at 21.4 metres above HWM.

At Break Yoke Creek, which is approximately 29 km south of Stumpys Bay, the beach ridge sand plain is 0.8 km wide, about 1 km long, and has a surface gradient of around 27 m/km towards the east. The surficial deposits of the plain consist of well rounded, coarse grained sand. The single beach ridge is wider than beach ridges in the previous embayments, but possesses a double crest (Figure 9). This suggests that the ridge at Break Yoke Creek is a composite ridge formed by superimposition of a younger, lower ridge on a previous beach ridge. The rounded beach sands wedge out sharply at a pronounced break of slope at an elevation of 21.61 m above HWM.

Swimcart Beach is 11 km south of Break Yoke Creek and is backed by a narrow sand plain 0.4 km wide, 1 km long, and with a surface slope of approximately 33.3 m/km (Figure 9). Only one beach ridge is present here and the upper marine limit of the sand plain has not been determined, because sands which are probably predominantly aeolian are banked against the steep flank of the confining landward hill.

2.1.3 *Comparison of the Eastern Embayments*

Table 2 is a comparison of the elevations of the upper marine limit, the beach ridge elevations and the approximate surface gradient for each of the eastern beach ridge plains. The beach ridges are numbered from lowest to highest as they occur in each area.

TABLE 2 Eastern Beach Ridge Plains - comparison of ridge elevations

		Area					
		Stumpys Bay	Purdon Bay	Break Yoke Creek	Swimcart Beach	Mean	SD
Beach ridge elevation (m above HWM)	1	7.2	6.5	7.6	7.1	7.1	± 0.39
	2	9.5	9.2	9.4	Absent	9.4	± 0.12
	3	11.5	11.2	Absent	"	11.4	N.A.
	4	15.0	Absent	"	"		N.A.
	5	18.7	"	"	"		N.A.
	6	20.0	"	"	"		N.A.
Upper limit of beach sand (m above HWM)		32.47	21.44	21.61	Not obtainable		
Surface gradient (m/km)		12.5	16.5	27.0	33.3		
Distance south from Stumpys Bay (km)		0	9	29	40		

N.A. = Not applicable

The three main features of this table are:

1) The striking similarity in elevation of the three lowest beach ridges.

2) The discordant upper marine limit elevations between Stumpys Bay and the remaining two areas.

3) The increasing surface slope in a southward direction.

Although the datum for each of the levelling transects is high water mark level and therefore could be ± 0.3 m in error, the strong elevation correlation of the three lowest beach ridges over a distance of 40 km indicates that the shorelines which they represent have not been appreciably warped since deposition of the beach ridges. However, taking the elevational differences of the upper marine limits into account, there would appear to be some tectonic warping along the coast. This apparent paradox can be explained by consideration of coastline sensitivity to modification by marine processes.

Two principal factors govern coastline sensitivity in northeastern Tasmania. The first is the amount of weathered granite mantle which is available for modification by a transgressive sea. Steeper surface slopes are less likely to develop a thick weathered layer than gentler slopes due to the more rapid removal of weathering products on steep surfaces. Thus, coastal erosional processes such as wave trimming, will have a greater effect on the unconsolidated weathered mantle than on bare rock or thinly mantled surfaces.

The second factor is the gradient of the surface which is being transgressed by the sea. Depositional features, particularly those which are the product of short term oscillations, such as beach ridges, are less likely to be evident on a high gradient coast

than on a low gradient coast. Horizontal "compression" of shore location on a steeply sloping coast during transgression and subsequent regression would not show the effects of short period variations in shore location as well as on a low gradient coast where minor sea level fluctuations result in larger horizontal displacements of the shore.

With respect to both weathering mantle thickness and surface gradient the embayments to the south of Stumpys Bay are increasingly less sensitive to coastal modification. Thus, of the six beach ridges which are recognizable at Stumpys Bay, only three occur at Purdon Bay, and the two which are present at Break Yoke Creek occur in close horizontal juxtaposition. However, the principal conclusion which can be drawn is that the different elevations of the apparent limits of marine deposition in these embayments are partly due to the increasing steepness of the surface, which has resulted in very little preservation of features during the maximum transgression to 32 metres.

An additional factor which could partly explain the upper limit elevation differences may be the nature of the transgression oscillations. The apparent upper marine limits at Purdon Bay and Break Yoke Creek are very similar, 21.4 m and 21.6 m respectively. Also, at Stumpys Bay there is a subtle, but definite, break of slope at 21.3 to 21.6 m above HWM. This is a very pronounced level and it may be that during the Last Interglacial the sea level for a substantial portion of the transgression/regression was at or below 21-22 m and that a short period of transgression to 32 m only left evidence on coasts which were very sensitive to marine modification. The beach ridge sequence at Stumpys Bay is therefore the most complete and indicates that the transgression to $\cong$ 32 m may have

been brief and was followed by beach ridge construction below 21-22 m during the subsequent regression.

2.2 Western Embayments

Coastal plains up to 40 km^2 in area occur in the western portion of the study area. These plains commonly slope from approximately 32 m at their inland margins to sea level, over horizontal distances of up to 5 km with surface slopes as low as 6-7 m/km. The western plains do not show the beach ridge topography which is so conspicuous on the eastern embayments. This appears to be due to post depositional aeolian deflation on the one hand, and their partial burial by the extensive system of longitudinal dunes on the other. The principal sand plain areas are at Tuckers Creek, Toddys Plain, Barooga, Tomahawk, and Boobyalla Plains (Figure 1). The Tomahawk plain has been the most closely bored and studied and the conclusions relating to the composition, environment of deposition and age of the Stumpys Bay Sand at Tomahawk are used as a basis for comparison with the other western plains which have been studied in less detail.

2.2.1 *Tomahawk*

2.2.1.1 Extent

At Tomahawk the plain has an area of approximately 60 km^2 and the Stumpys Bay Sand varies in thickness from 2 to 12 m, with an average thickness of approximately 7 m. The formation is underlain by highly weathered Devonian granite, which consists of angular fragments of feldspar, quartz, and some mica. Plate 18 shows the

PLATE 18 Weathered granite at Tomahawk.

The weathered granite contains large crystals of feldspar, quartz and some mica, in a clay matrix. The contact of the weathered granite with fresh granite occurs to the lower left.

contact of weathered granite with the underlying fresh granite. The sand plain is bounded to the south and east by granite hills and by the sea to the north. The western boundary is not well defined but the formation thins out considerably in the Ainslie Homestead area and wedges out on the eastern flanks of Tobacco Hill. Apart from the Tomahawk River, which flows from south to north and roughly bisects the plain, there are no natural surface drainage channels.

The portion of the embayment to the east of the Tomahawk River is approximately 26 km^2, and has been extensively drilled. Figure 15 is an isopach map of the Stumpys Bay Sand at East Tomahawk; (for bore hole location see Figure 16) and shows that the sands reach a maximum thickness of 12 m near the centre of the embayment. As shown in Figure 15 the formation wedges out at the margins of the embayment and thins towards the Tomahawk River which has become incised through the sand to the granite basement. The upper limit of the Stumpys Bay Sand occurs at a well defined break of slope at Carisbrooke at an elevation of 32.1 m above HWM. The surface geology of the East Tomahawk area is portrayed by Figure 17 and shows several features which are:

1) Small, isolated granite outcrops which protrude through the Stumpys Bay Sand and appear as "islands" on the sand plain. These were formed as irregularities in the granite bedrock surface and are the result of differential sub-surface weathering of granite and consequent variable weathering mantle thickness. Subsequent stripping of the mantle has exposed the protrusions of fresh granite.

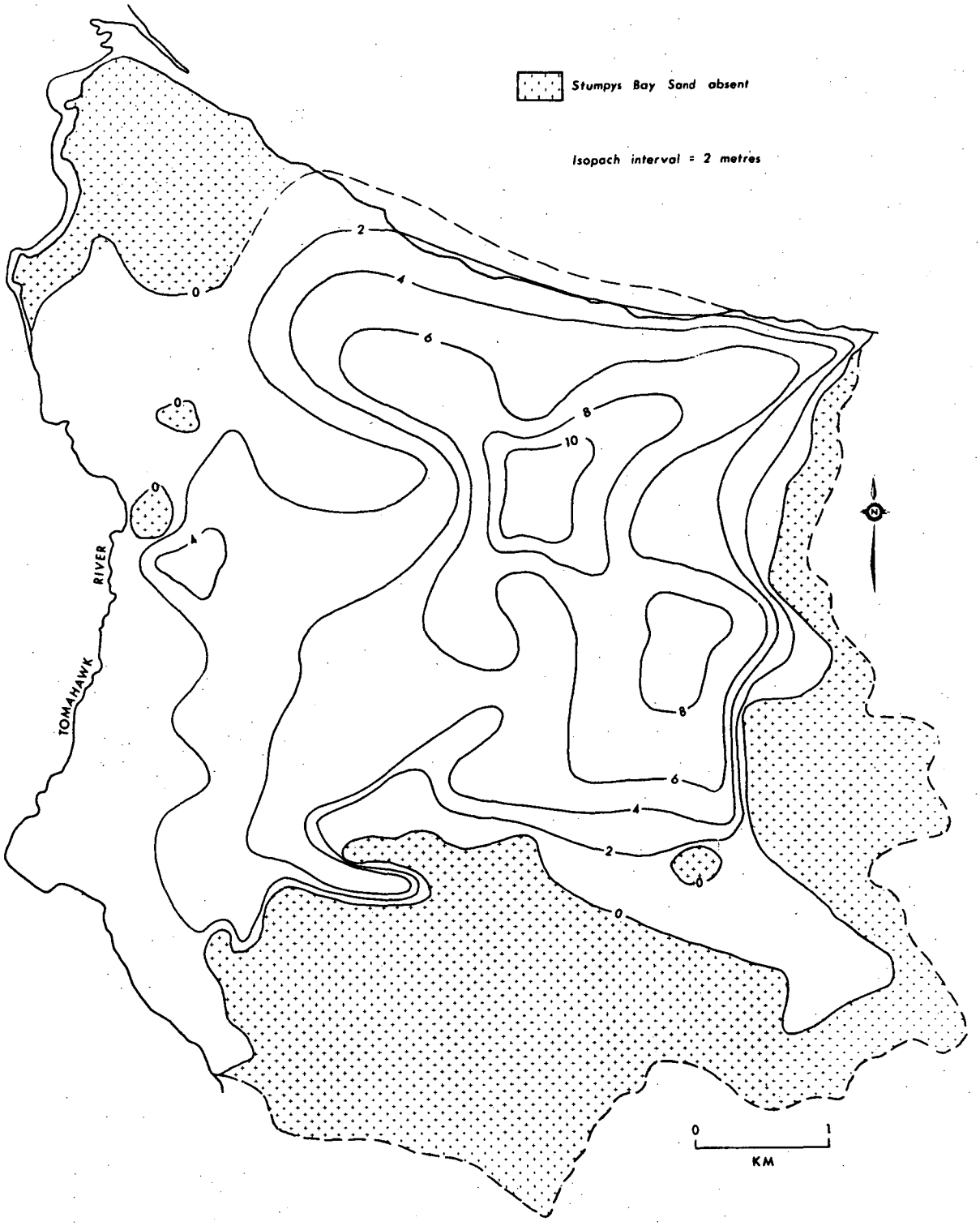

FIGURE 15 Stumpys Bay Sand Isopach - East Tomahawk.

The smaller granite outcrops and the narrow exposure of bedrock in the Tomahawk River bed are not shown.

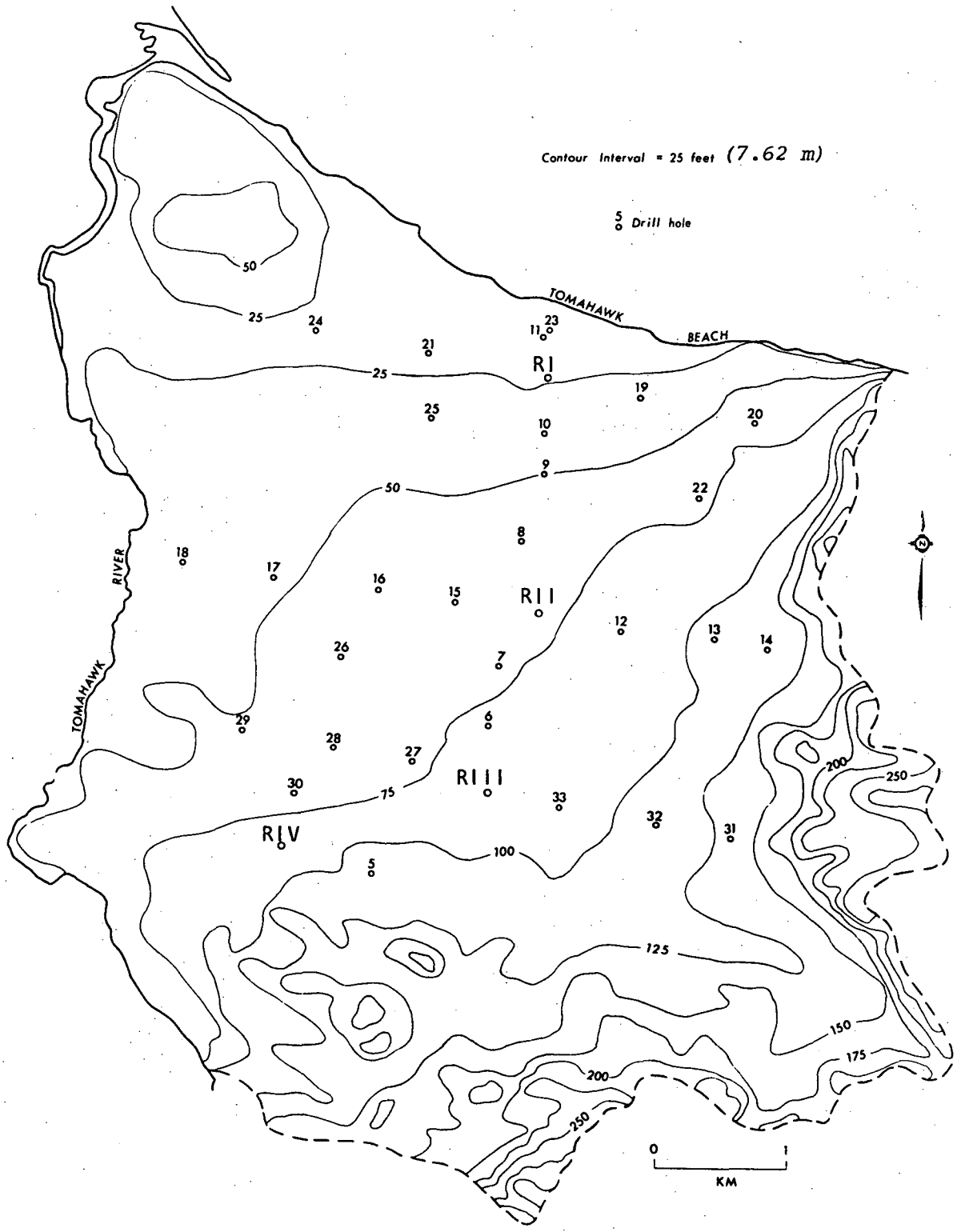

FIGURE 16 Bore Hole Location - East Tomahawk.

Roman numerals depict the location of each water level recorder.

Topographic Contours generalized from Tomahawk Sheet 8416-II-S, *Tasmanian Topographic Series*, 1:31,680.

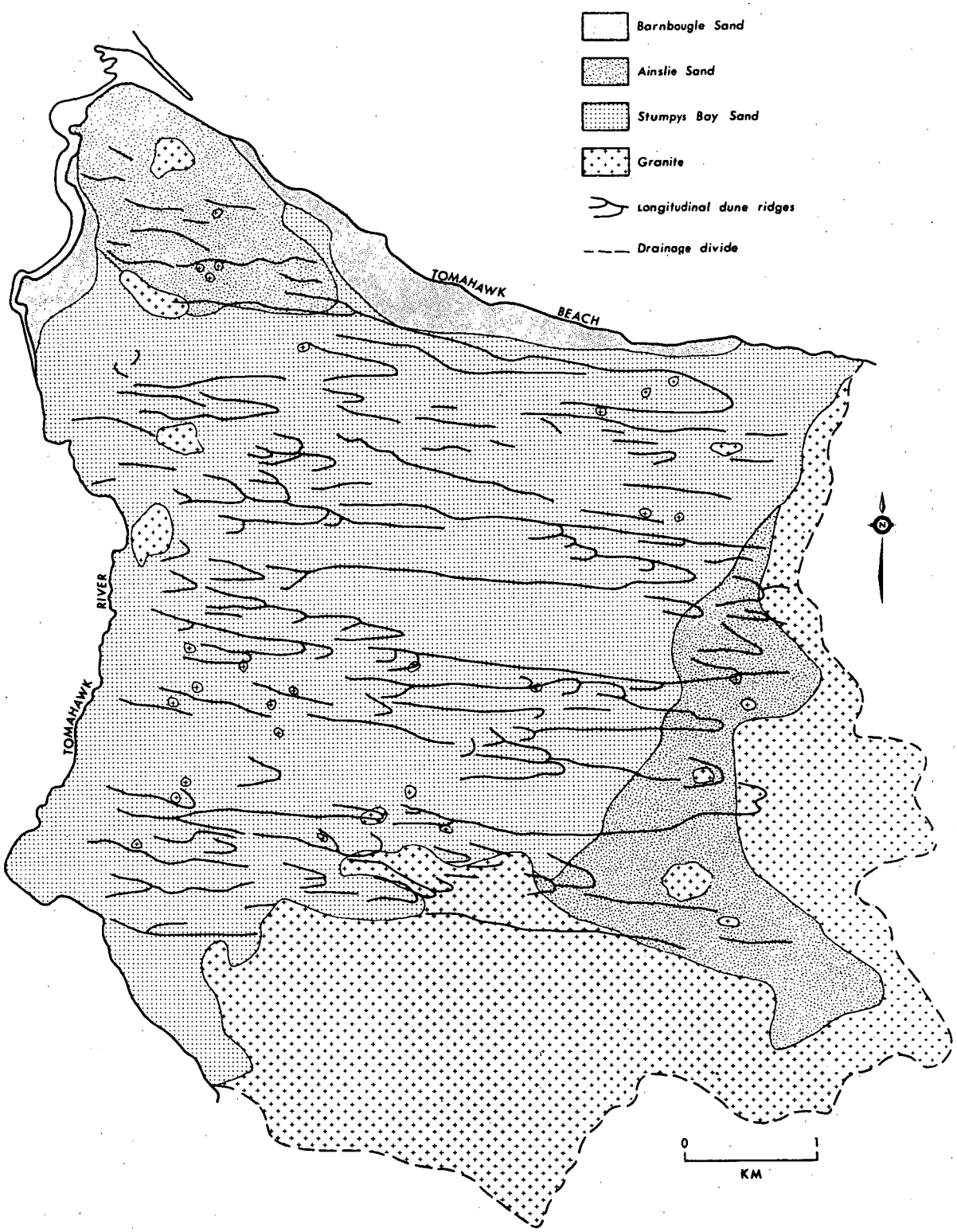

FIGURE 17 Geology - East Tomahawk Area

2) The transgression of the sand plain surface by the longitudinal dune system of the Ainslie Sand and the occurrence of two sand sheet areas of Ainslie Sand. One sand sheet occurs near the mouth of the Tomahawk River and has partially enveloped an outcrop of granite. The other sand sheet occurs on the eastern boundary of the sand plain and has banked against the granite hills. This sand sheet is up to 4 m thick and has been incorporated in the isopach map (Figure 15) above. The presence of the longitudinal dunes and sand sheets on the surface of the plain indicate the degree to which aeolian activity has remodelled the topography of the initial sand plain surface.

3) The effect of Holocene marine truncation of the Stumpys Bay Sand is shown at the coast. The Stumpys Bay Sand has been cliffed by the sea on the eastern shore of East Tomahawk but has also been truncated and overlain by a small set of linear beach ridges and frontal dunes of the Barnbougle Sand for the remainder of its coastline length.

2.2.1.2 Environment of Deposition

Discrimination of the environment of deposition of the sand plain at East Tomahawk is essential to the development of later arguments which analyze the significance of the deposits at a much broader level. Therefore alternative explanations of mode of origin will be discussed in some detail to establish the strength of the final interpretation.

Several modes of origin can be postulated for the deposition of the sand plain and each is examined to determine its validity.

Fluvial, lacustrine, aeolian and marine processes are all potentially capable of forming sand deposits similar to those which form the core of the plain at East Tomahawk.

Alluvial fill commonly forms relatively flat floors to valleys and often terminates at the valley sides with a pronounced break of slope. Morphologically therefore, the East Tomahawk plain resembles a fluvial deposit. However, the grainsize composition of the plain is not consistent with such an interpretation. The grainsize of the Stumpys Bay Sand at Tomahawk does not show the large grainsize variation which is typical of many alluvial deposits. Alluvial deposits commonly contain irregular lenses of channel derived gravels and of overbank clays and silts. The drilling programme did not encounter sediments which showed this degree of variability and no buried channels, high angle cross-bedding, or well rounded gravels were found in field sections. The sediments of the plain, although showing some degree of grainsize variation, are notable for their general uniformity of grainsize, mostly having a mean grainsize from 1.50 to 2.50 ϕ.

Another major detraction from the hypothesis of a fluvial origin for the plain is the apparent lack of a river source for the material. The Tomahawk River valley does not have the catchment size or the degree of incision in its reaches upstream from the Tomahawk plain to deposit such a large volume of sediment on the plain. Also, the margin of the plain occurs at right-angles to the entrance of the Tomahawk River Valley onto the plain. If the Tomahawk River was the primary source of the sediments in the plain then the flat-floored plain would extend with diminishing width some distance up the river valley. Other morphological evidence of fluvial deposition, such as meander scars in the confining granite hills do not occur. The absence of fluvial features such

as abandoned channels, levées, and meander scrolls on the plain surface also points to a non-fluvial origin for the plain, but it could also be argued that the post-depositional aeolian activity which has occurred would have erased or buried such features.

There is no positive evidence which supports a fluvial origin for the plain and the hypothesis has therefore been rejected.

An alternative hypothesis is that the sand plain could have been formed by lacustrine sedimentation. Material laid down in large lakes of the size indicated by the areal extent of the sand plain, might have grainsize and sorting characteristics similar to the existing sands. This would be particularly true of the beach environment near the lake shores. Two main objections, however, preclude a lacustrine origin. The first is that the sand plain slopes seaward and if the plain was the site of an old lake it would possess a sub-horizontal surface. The second objection is that the shoreline of the lake must at some time have been at an elevation of approximately 32 m. This is the upper limit of the sand plain and the elevation of the break of slope, which would have been a lake shoreline. At Tomahawk it is not possible to enclose a terrestrial water body at this elevation because there is no topographic barrier to the north or southwest to create lake closure. It is therefore clear that the plain is not of lacustrine origin.

The plain is traversed by longitudinal dunes and aeolian sand sheets occur on its surface which could indicate that the plain is underlain entirely by aeolian sands. Grainsize analysis does not support a dune origin for most of the sands within the plain. The longitudinal dune sands (Ainslie Sand) and the Holocene dune sands (Waterhouse Sand) in northeastern Tasmania are all moderately to well sorted, unimodal sands with a peak in the 2.0 to 2.5 ϕ size class, and are coarse-skewed. Other studies, for example Folk (1971),

also shows strong peaks in the 2.0-2.5 ϕ class for dune sands. The sands from beneath the plain often show bimodality or polymodality, are frequently fine-skewed, and are often poorly sorted. Study of the sedimentary structures from field sections also does not support an hypothesis of an entirely aeolian origin. The bedding is often sub-horizontal with low angle cross-bedding. Dune bedding is characteristically dominated by low angle beds dipping to windward which have been truncated by high angle beds deposited on the slip-off face (Bagnold, 1941). These features were not observed in any field sections. The grainsize and bedding characteristics therefore do not support an aeolian genesis.

Each of the three previous hypotheses for possible modes of origin of the sand plain at East Tomahawk has been rejected because they are not compatible with the observed characteristics.

The evidence for a marine mode of origin is presented below and is followed by a reconstruction of the conditions and sequence of sedimentation within the embayment.

The plain at Tomahawk possesses two morphologic characteristics which suggest that it is a former marine embayment. The surface of the plain has a fairly consistent seaward slope towards the NNE of approximately 7-8 m/km. This slope is attributed to deposition during a general regression from 32 m, the upper limit of the sand deposits, to below present sea level. Also, the pronounced break of slope at approximately 32 m occurs at the eastern and southern margins of the embayment and marks the limit of sand deposition. This feature, which can be traced for more than 20 km in the area, strongly resembles a former shoreline and defines the landward limit of a probable marine transgression.

Marine processes are most likely to be responsible for the bedding and grainsize characteristics of the sands. As discussed on

page 13, the low angle cross-bedding and sub-horizontal bedding, which often dips seaward, are similar to beach structures described by Lahee (1961). Also, the particle size of the sands is very similar to the marine sands at Stumpys Bay. At Tomahawk they are moderately rounded, moderately to poorly sorted, and fall in the fine sand to coarse sand size ranges. There is a marked lack of clay at the finer end of the scale or gravel at the coarser end. All of the deposits found at Tomahawk could have been deposited therefore in a nearshore marine environment.

As at Stumpys Bay the presence of siliceous sponge spicules at Tomahawk provides very strong evidence for marine deposition. Sponge spicules are very common in the sands. All of the samples at 0.91 m intervals from 18 bores were examined under the binocular microscope and 81 out of the 111 samples (73%) contained either megascleres, microscleres, or both (Plates 19, 20 and 21). The combined evidence of their good degree of preservation and their abundance points to the spicules being of primary origin. The sponge spicules are marine (page 57) and therefore a marine origin of the sands is strongly suggested.

Several other fossils within the sands at Tomahawk also indicate a marine origin but their occurrence is very rare. One specimen of a cheilostome polyzoan, from Bore 2 at a depth of 5.43 m, was found with a mineralized skeleton and was identified by Dr. M.R. Banks. It is of marine or brackish water origin. A very poorly preserved calcareous foraminifera fragment and a small shell fragment (Plates 22 and 23) were found at a depth of 4.57 m in Bore 2. These also suggest a marine origin. Shell fragments are extremely rare in the sands which could be due to two factors. The first is that there may not have been a high mollusc population in the waters of the area at the time of deposition. The second

PLATE 19

Sponge spicules (megascleres) from Tomahawk (Bore 8, 9.05 m depth).

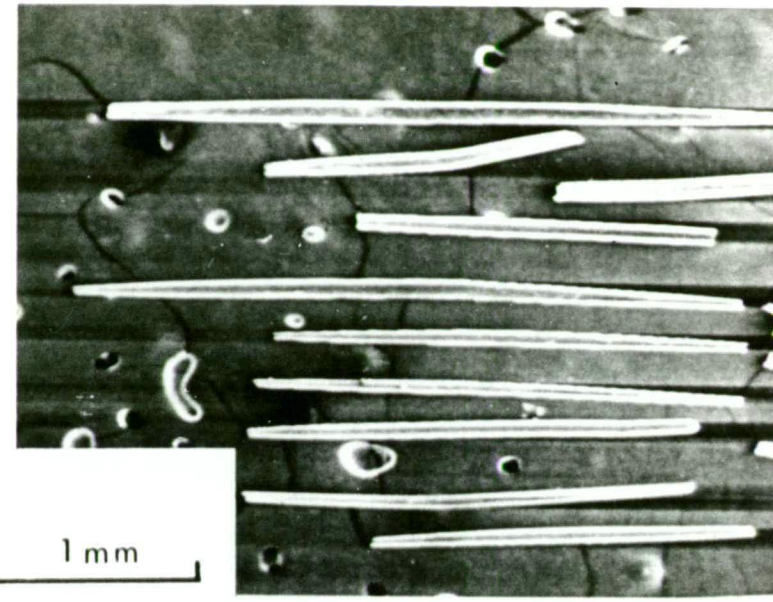

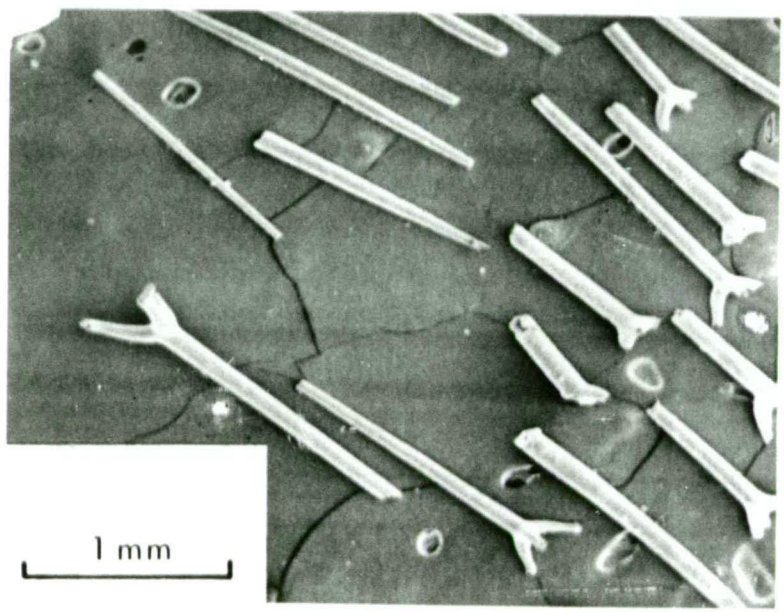

PLATE 20

Sponge spicules (megascleres, triaenes) from Tomahawk (Bore 8, 9.05 m depth).

PLATE 21

Sponge spicules (microscleres) from Tomahawk (Bore 2, 4.53 m depth).

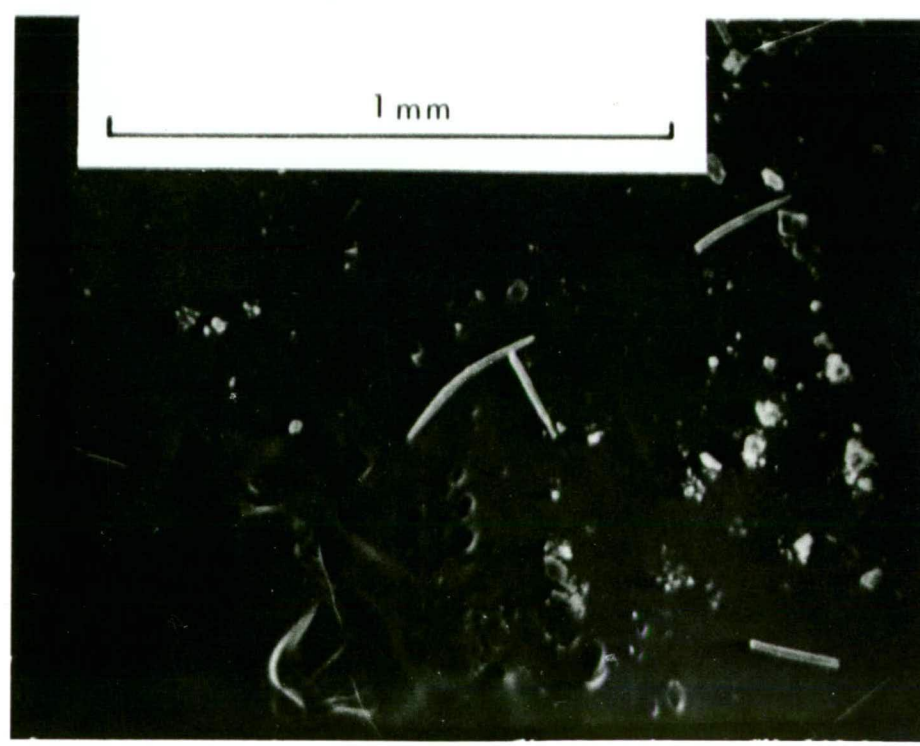

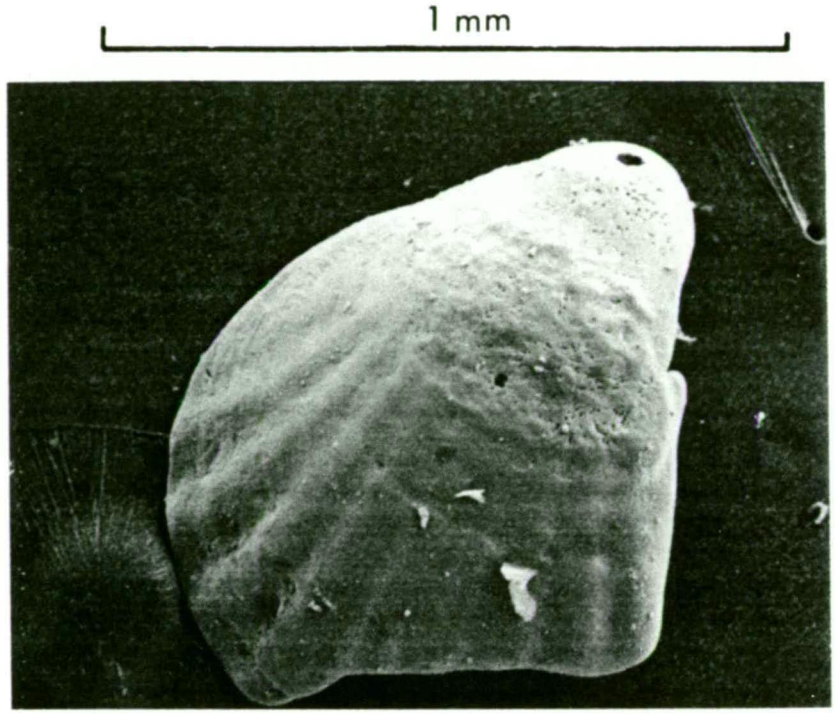

PLATE 22 Pelecypod from Stumpys Bay Sand at Tomahawk. (Bore 2, 4.53 m depth).

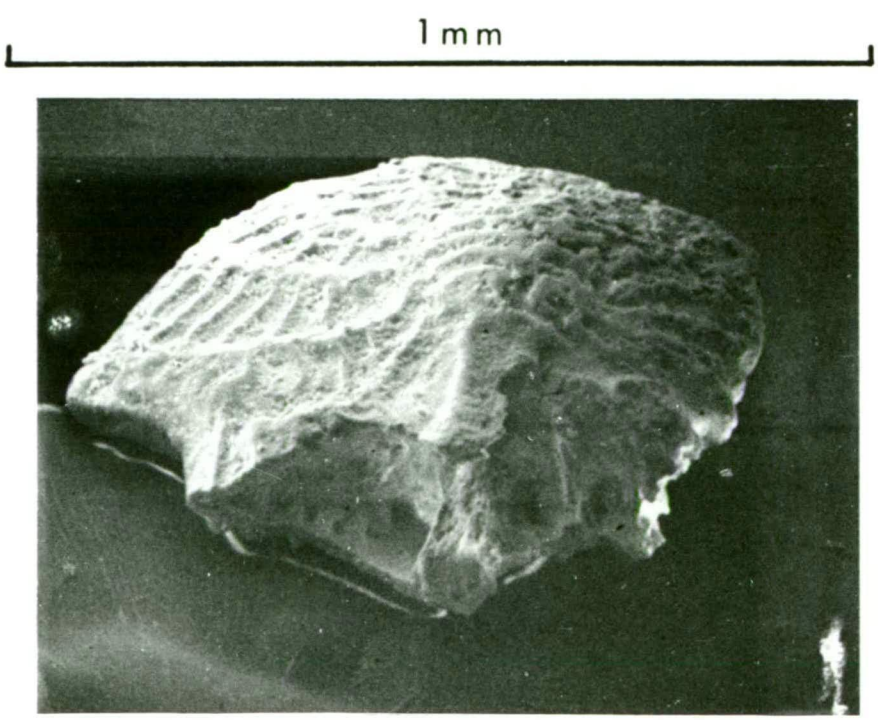

PLATE 23 Foraminifera fragment from Stumpys Bay Sand at Tomahawk. (Bore 2, 4.53 m depth).

factor is that the groundwater within the sands is usually acid, as low as pH 4.2 but average 6.1, and over a substantial period of time would be sufficiently chemically aggressive to leach the sand of its primary carbonate component. As at Stumpys Bay, all the characteristics of the sands at East Tomahawk point to a marine environment of deposition.

Six bores were drilled to the weathered granite basement, and samples were taken at 0.91 m intervals. The bores form a south to north transect across the plain, as shown by the location map (Figure 16) and cross profile (Figure 4). The samples were sieved using a 0.25 ϕ sieve interval and facies interpretations were performed in accordance with the procedures discussed on pages 59 to 70. Figure 18 is a plot of the facies proportions for the six bores. Several features are apparent on this diagram.

With the exception of the most inland bore hole, Bore 5, all the sequences show that the basal one third to one half of the deposits contains a continuous occurrence of lagoonal facies that decreases sharply in proportion towards the surface. These lagoonal sediments are overlain by beach and dune sands, often with a slight increase in beach facies towards the top. Minor variation occurs within some bores but the general sequence shows a definite trend. This is similar to the trend at Stumpys Bay and reflects a single marine transgression followed by regression. However, the beach facies of the regression are not as well shown at Tomahawk, largely because there has been a degree of post-depositional aeolian deflation of the upper sequence. Another factor which could explain the relative lack of surficial beach sands is that if the beach sands were fine grained (which could well occur in a shallow, protected embayment with a northerly aspect such as Tomahawk must

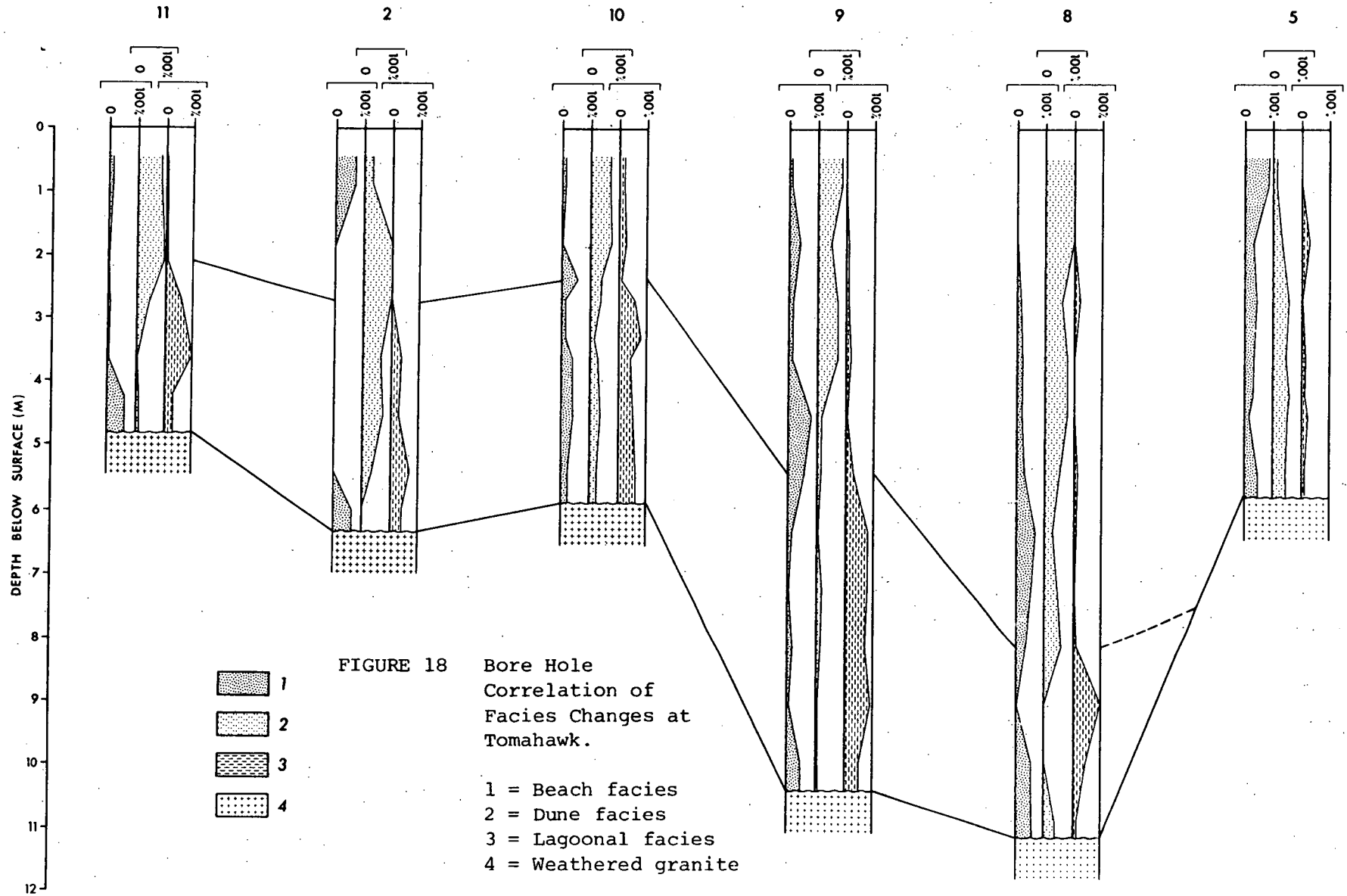

FIGURE 18 Bore Hole Correlation of Facies Changes at Tomahawk.

1 = Beach facies
2 = Dune facies
3 = Lagoonal facies
4 = Weathered granite

Figure 16 shows the bore hole location.

have been) then material which has been interpreted as dune sand could be partly of beach origin.

Although the broad depositional sequences at both Stumpys Bay and Tomahawk are similar, the Tomahawk sequences display more variation within the section. This is probably related to the slope of the surface over which the sea transgressed and therefore the sensitivity of the sedimentary record (see page 76) as Stumpys Bay has a higher surface slope (12.5 m/km) than Tomahawk (8 m/km). At Tomahawk, small term variations in depositional conditions would have a better chance of preservation in the sedimentary record than at Stumpys Bay which was probably not as sensitive to minor oscillations.

Bore 5 does not show the same sequence, but contains similar proportions of beach, dune and lagoonal facies which are represented throughout the sequence. An exception is the top 1 m or so which is dominated by beach sand. This bore is located close to the upper limit of marine transgression and was very close to the shore position during deposition. Therefore, a high degree of facies variation is less likely at this site than at sites further from the old shoreline. The absence of major peat horizons within the formation or any other evidence of buried subaerial weathering surfaces indicates that the sands were all deposited during a single transgression and subsequent regression. The same conclusions were drawn for the sequence at Stumpys Bay, which is 40 km east of Tomahawk. Although beach ridges are not preserved at Tomahawk, there is one fairly distinct morphologic similarity with the well preserved surface at Stumpys Bay. In both cases the plains are marked by an appreciable rise in the surface at an elevation of approximately 10 m. This minor break of slope could indicate the

same sea level event, or the change from one event to another, during the regression from 32 m in both areas. This similarity between the two areas provides some evidence that the original Tomahawk Plain has not been completely remodelled by deflation and probably no more than the top metre has been eroded from, or redistributed over, the surface.

2.2.1.3 Age

All of the arguments which have been used to infer a Last Interglacial age of the Stumpys Bay Sand at Stumpys Bay (pages 72 to 73) are valid for the Tomahawk area. In addition, the degree of sponge spicule surface solution provides a line of evidence which supports the conclusion that the sand plains at Tomahawk and Stumpys Bay are of approximately the same age. A hint of the degree of sponge spicules surface weathering with age was obtained by Scanning Electron Microscope examination of the spicule morphology of samples of increasing age. To this end, scanning electron micrographs were taken at 1000 magnifications of spicules from the present beach at Tomahawk (Plate 24), and from sands of Holocene age which are probably 3000 to 6000 years old (see pages 34 to 40 and Plate 25). Micrographs were also taken of spicules from the Stumpys Bay Sand at Tomahawk (Plate 26) and from Stumpys Bay (Plate 27). The surfaces shown depict a typical surface form sequence due to solutional etching and the samples were selected by inspection of at least 5 spicules. It is important to note that very little difference in surface morphology was detected within each sample or between samples from the same depositional unit but that strong contrasts occurred between units.

PLATE 24 Megasclere surface morphology of spicule from the present Tomahawk Beach.

PLATE 25 Megasclere surface morphology of spicule from the Holocene age Barnbougle Sand.

PLATE 27 Megasclere surface morphology of spicule from Stumpys Bay Sand at Stumpys Bay.

PLATE 26 Megasclere surface morphology of spicule from Stumpys Bay Sand at Tomahawk.

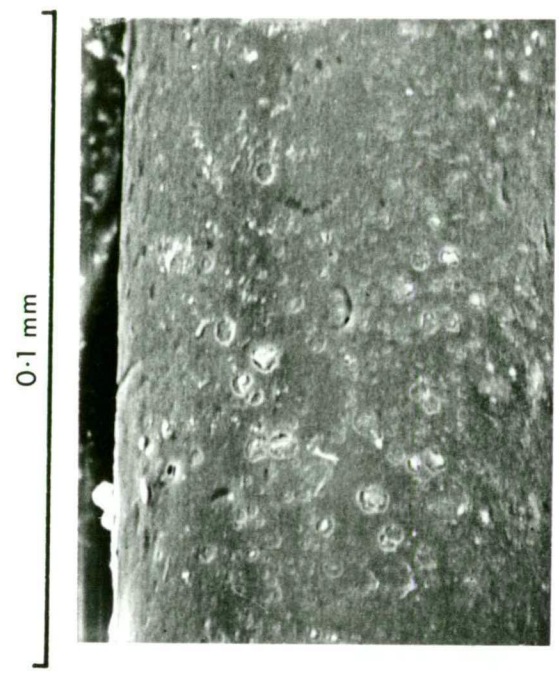
0·1 mm

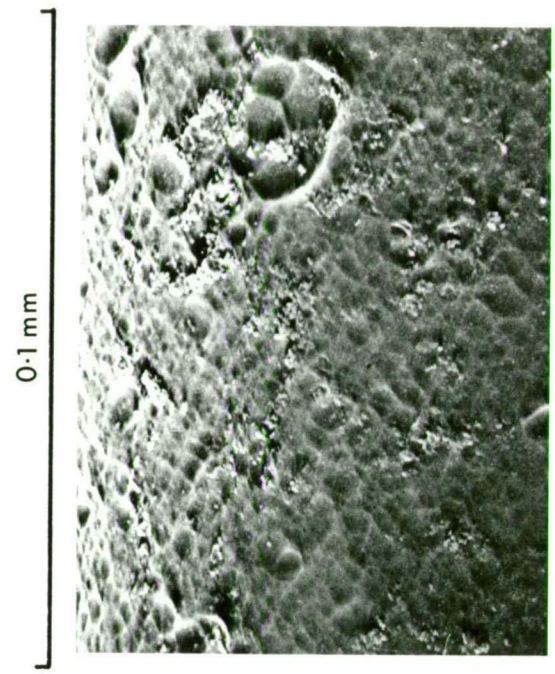
0·1 mm

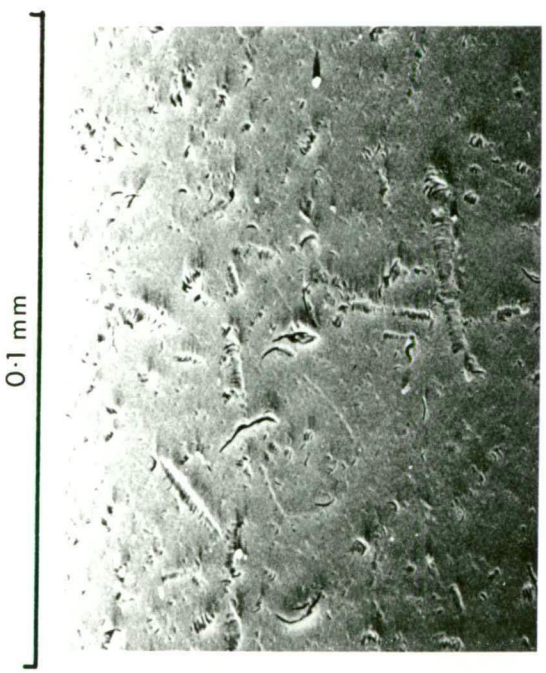
0·1 mm

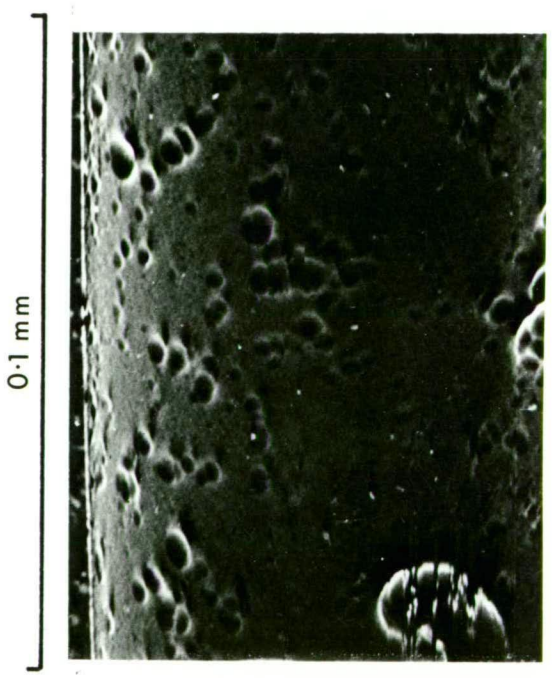
0·1 mm

The surface of the spicule from the present beach (Plate 24) still retains most of the original spicule surface but it is in the process of being modified by solution processes. Shallow crescentic solution crevasses (Krinsley & Doornkamp, 1973) are present and many solution crevasses are arranged in an *en echelon* pattern. The crescentic solution crevasses are on average 3.0 to 5.0 µm long but extend to a length of 10 µm, and are 0.5 to 1.0 µm wide. The *en echelon* solution crevasses occur as bands up to 30 µm long, but most are approximately 10 µm, and are 1.0 µm to 3.0 µm in width.

The Holocene spicule surfaces by comparison are more corroded (Plate 25). A much lower proportion of the original spicule surface remains and small, shallow solution pits 1 µm to 4 µm in diameter have formed on the surface.

Spicule surfaces from Tomahawk, which are probably around 125 ka (thousand years) old (see page 136) show an even greater degree of solution. In this case (Plate 26) the original spicule surface has been corroded away entirely and the solution pits have been enlarged and deepened considerably, to form a "raindrop impact" impression on the surface. This morphology is characteristic of most surfaces examined from Tomahawk samples.

The increasing degree of sponge spicule surface solution with increasing age is very marked in the above example. However, this approach is only intended for use as a guide to the relative age of the sands for northeastern Tasmania and differences might occur if spicules were buried in deposits with markedly different groundwater or oxidation conditions. It is justifiable to use the method as a comparative index of age in the present context because the spicules were all derived from siliceous deposits below the water table.

A comparison of spicules from Tomahawk and Stumpys Bay (Plates 26 and 27) shows that they are very similar in the degree of surface solution and could not be separated in age on these grounds. This provides support for the hypothesis that both sand bodies are of similar age.

The remaining western embayments have been studied by field traverses and some drilling has been carried out, but East Tomahawk received the most comprehensive coverage. The other embayments will now be described in order to further demonstrate the nature and distribution of the Stumpys Bay Sand. They are all considered to be of the same age as the Tomahawk plain because they have analogous topographic settings and relationships to Holocene deposits and the longitudinal dunes of Ainslie Sand.

2.2.2 *Other Embayments*

2.2.2.1 Tuckers Creek area

The Stumpys Bay Sand covers approximately 7 km^2 in the Tuckers Creek area, 6 km southeast of Bridport (Figure 1). The plain, as shown in Figure 7, is situated between lower, younger river terraces (Forester Gravel) of the Great Forester River to the northeast, and more elevated areas underlain by Tertiary age sediments (Figure 2) to the southwest. The surface of the sand plain is crossed by several longitudinal dunes of the Ainslie Sand and deflation hollows are bordered by low lunette ridges on their eastern margins. The surface has also been slightly modified by fluvial dissection.

Figure 6 is a surveyed profile from the coastal plain formed by Barnbougle Sand across the river terrace to the upper limit of the Stumpys Bay Sand at 32.2 m above HWM.

One borehole (number 47) was drilled to a depth of 10 m and sampled at 0.91 m intervals. The samples were sieved at 0.25 ϕ mesh intervals and the facies were interpreted as previously (pages 64-70). The bore log is shown in Figure 19 and consists predominantly of beach and dune sands with low proportions of lagoonal facies to a depth of 8.45 m.

Marine sponge spicules, both megascleres and microscleres were fairly common in this sequence. The predominance of beach facies also indicates that it is of marine origin. The uniformity of facies throughout this sequence and the generally low proportions of lagoonal facies indicates that the deposits were laid down in a much more open, or higher energy wave environment than the sequence at either Tomahawk or Stumpys Bay.

Peat was encountered between 8.45 m to 9.51 m depth and consists of up to 71% organic matter, as determined by weight loss on ignition to 450°C for 2 hours. A pollen sample from the peat at a depth of 9.36 m was prepared for cursory examination in order to determine whether it was of Tertiary or Quaternary age and to suggest at an exploratory level some environmental conditions during peat deposition.

Dr. E.A. Colhoun examined a pollen sample and regarded it as being of Quaternary age because *Eucalyptus* pollen was the most abundant and *Eucalyptus* species are not abundant in the known Tertiary deposits in Tasmania. In addition there was an absence of ancient *Nothofagus* pollen which is typical of the Tertiary flora (Stover & Partridge, 1973). He also considered that the pollen

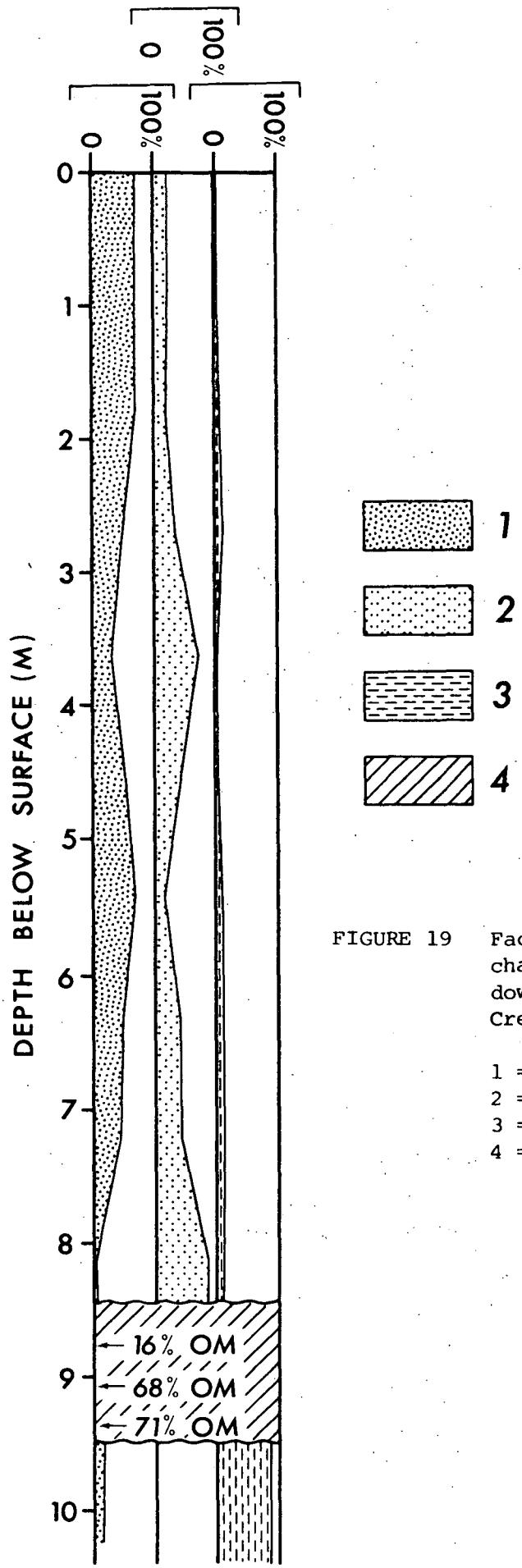

FIGURE 19 Facies proportion changes with depth down Bore 47, Tuckers Creek area.

1 = Beach facies
2 = Dune facies
3 = Lagoonal facies
4 = Peat

assemblage was typical of spectra in the Quaternary record elsewhere in Tasmania.

Pollen samples would need to be taken from more closely spaced and better controlled levels within the peat deposit, and detailed pollen analysis would be needed before a full evaluation could be obtained. However, the examination of the reconnaissance pollen sample showed that *Eucalyptus* pollen was almost twice as common as *Melaleuca* and three times more numerous than the grasses, which were also common. Other genera in the spectrum included Restionaceae, *Pomaderris* sp., Compositae, Cyperaceae, Liliaceae (probably *Xanthorhoea* sp.) and *Leptospermum* sp. This assemblage suggests that the area was vegetated by a dry sclerophyll forest or woodland with a reasonably dense grass understorey. The environment was apparently not that of a coastal lagoon or saltmarsh, as shown by the absence of Chenopodiaceae. Thus the pollen data indicate that the peat is of Quaternary rather than Tertiary age and contains elements that suggest a dry sclerophyll *Eucalyptus* forest/woodland vegetation. For these reasons, the peat is thought to represent a period of subaerial conditions prior to the marine transgression during which the overlying Stumpys Bay Sand accumulated.

The deposit beneath the peat consists of about 85% lagoonal silt and 15% beach sand and the two megascleres which were found in the sample point strongly towards a marine mode of deposition.

Thus the sequence at Tuckers Creek penetrated by Bore 47 indicates that a period of marine deposition was followed by a period which promoted the deposition of peat in a freshwater swamp environment and that later marine transgression, during the Last

Interglacial, was responsible for deposition of the Stumpys Bay Sand to an elevation of 32.2 metres above HWM.

2.2.2.2 Toddys Plain

Toddys Plain is about 10 km to the northeast of the Tuckers Creek area and is most likely the northeastern extension of the Tuckers Creek plain. The two areas have since been dissected and separated by the Great Forester River. Toddys Plain today covers an area of approximately 20 km^2 and is bounded by low hills composed of Mathinna Beds to the north and east, by the Great Forester River to the south, and is overlain by Holocene transverse and parabolic dunes at its seaward margin to the east.

In keeping with the other coastal plains of the region, Toddys Plain has low longitudinal dunes, deflation hollows and associated lunettes dispersed across its surface. The upper limit of sands at Toddys Plain has not been determined by survey, but map contour information and field checking indicates that the plain terminates at an elevation of approximately 30 m. A bore hole (number 49) was drilled 500 m northeast of Forester Lodge Homestead and penetrated 14 m without reaching the base of the Stumpys Bay Sand. Figure 20 is a log of Bore 49 and shows that the sequence, like the Stumpys Bay Sand at Tuckers Creek, consists predominantly of beach and dune sand facies throughout, with no systematic variation. This further supports the idea that the sand deposits of the Toddys Plain and the Tuckers Creek area, which have a westerly aspect and are closely associated, were laid down in an active wave environment. This was a more active wave environment than the relatively sheltered and restricted embayments

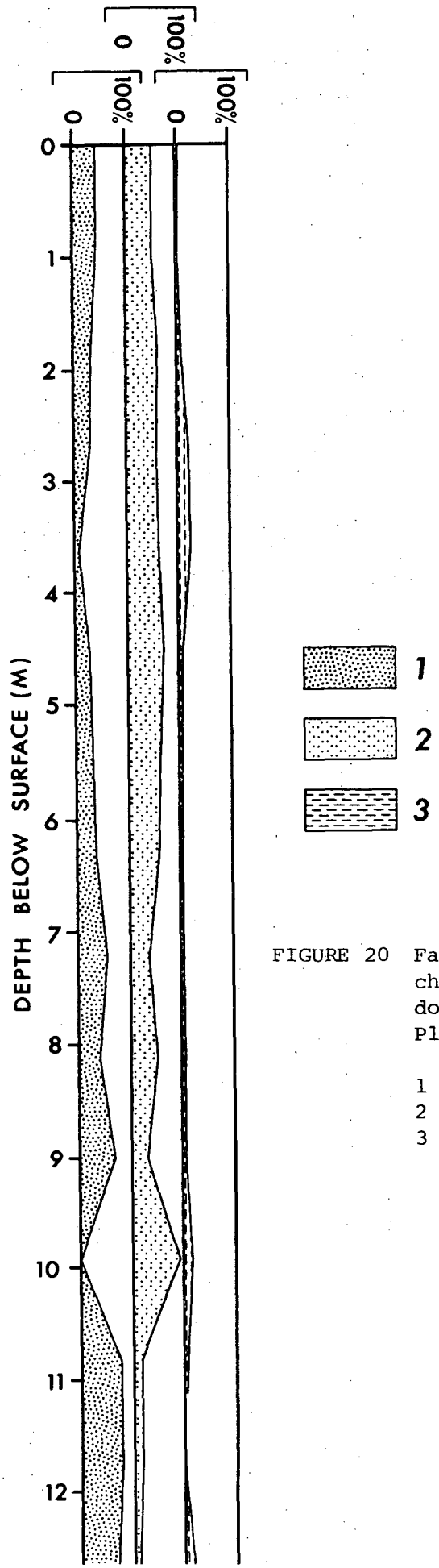

FIGURE 20 Facies proportion changes with depth down Bore 49, Toddys Plain.

1 = Beach facies
2 = Dune facies
3 = Lagoonal facies

of Tomahawk, which are exposed to the NNE, and Stumpys Bay, which is exposed to the NE.

2.2.2.3 Barooga

A small area of Stumpys Bay Sand covers about 5 km^2 at Barooga (Figure 1). Near the coast the formation is over-ridden by Holocene parabolic dunes and active transverse dunes. It is bounded on all other sides by low hills composed of slates and siltstones of the Mathinna Beds. The surface of the plain is inclined at about 7 m/km in a northwesterly direction and is traversed by several longitudinal dunes. Field sections and a drill hole show that the sand is up to about 7 m thick, thins towards the margins, and is underlain by Mathinna Beds and thin, discontinuous deposits of alluvial gravels which are probably of Tertiary age. The upper limit of the Stumpys Bay Sand is difficult to define accurately due to the absence of a marked landward break of slope. However, hand augering and sections near the upper limit indicate that it occurs at approximately 30 m above HWM.

Samples from a bore at the site have not been subjected to sieve analysis but the bore penetrated 5.43 m of medium to medium-coarse grained sand, with marine sponge spicules which overlies 0.91 m of organic silt. A quartzite gravel lag deposit up to 15 cm thick lies beneath the organic silt and overlies Mathinna Beds. A field section 30 m east of the bore showed 3 m of medium-coarse sand with sub horizontal bedding and low angle cross-beds dipping seaward (Plate 28). This is underlain by 80 cm of peat with incorporated wood material (Plate 29), but 50 m further down the ditch the peat bed is absent and the sands directly overlie quartz gravel and Mathinna Beds (Plate 30). Hand augering through the peat showed that the basal 15 cm is sandy peat and that

PLATE 28 Cross bedding in Stumpys Bay Sand at Barooga.

PLATE 29 Peat and wood below Stumpys Bay Sand at Barooga.

PLATE 30 Contact of Stumpys Bay Sand with Mathinna Beds slates at Barooga.

this is underlain by 5 cm of silty sand, 15 cm of well rounded quartzite gravel, and greater than 55 cm of weathered Mathinna Beds, composed of white kaolinitic clay with angular bedrock fragments.

A pollen sample was prepared from the peat in an attempt to determine whether the peat is of Quaternary or Tertiary age. Dr. E.A. Colhoun examined the sample and concluded that the peat contains a Quaternary flora which does not include ancient elements. The pollen present is consistent with a dry sclerophyll light woodland vegetation. The regional vegetation is indicated by abundant *Eucalyptus* pollen and minor proportions of *Monotoca* sp., *Melaleuca* sp., *Acacia* sp., *Banksia* sp., grasses, Compositae and Liliaceae. A thin drift of rainforest pollen from higher ground is indicated by occasional *Nothofagus cunninghamii* pollen. The local vegetation was dominated by freshwater aquatics which comprised greater than 40% of the pollen in the sample. *Myriophyllum*, and species of Cyperaceae and Liliaceae were the most common. The absence of Chenopods indicates that the environment was probably not a salt marsh and the abundant timber in the deposit confirms this. Elements which reflect wet climatic conditions; such as substantial rainforest pollen, tree fern spores, and pollen from the usual understorey taxa of wet sclerophyll forest, were also noticeably absent from the pollen spectrum. The pollen assemblage indicates that while the local environment of deposition may have been different from the site at Tuckers Creek, the two sites show a similar regional vegetation. The freshwater swamp deposit at Barooga was probably formed early in the Last Interglacial and was buried by marine sands during the Last Interglacial marine transgression.

The marine sands at Barooga therefore have very similar stratigraphic relationships to the Stumpys Bay Sand at Tuckers Creek and were also deposited as part of a similar sequence of events.

2.2.2.4 Boobyalla Plains

These plains extend over an area of approximately 35 km^2 and their inland margin is formed by hills composed of granite and Mathinna Beds. As with the other western embayments, the northern margin of Boobyalla Plains is over-ridden by coastal dunes of Holocene age. The eastern margin of the plain is bounded by the Ringarooma River. Near the sea the sands of the plain overlie Jurassic dolerite, as shown by a Tasmanian Department of Mines water bore, but further inland they are underlain by granite and Mathinna Beds.

The Boobyalla River effectively divides the plain into two morphologic regions (Figure 1). The plains to the west of the river are traversed by a series of longitudinal dunes of Ainslie Sand. To the east of the river the plain has suffered marked aeolian deflation, as indicated by about 17 deflation hollows, many of which are bordered by lunette ridges on their eastern margins. The plain follows the 1-2 km wide valley of the Boobyalla River and forms two small arms extending inland from the Boobyalla River-Little Boobyalla River confluence. The upper limits of the sand plains occur at a fairly well defined break of slope at 30.9 m above HWM.

Drilling was not carried out on the plains but field sections near Dugards Creek, where the main road crosses the

Boobyalla River, and in the western inland extension of the plain near the Winnaleah road, all indicate that the sands have similar composition and sedimentary structures to the other western embayments. Thus, these plains are considered to be a product of a marine transgression to around 30-32 m during the Last Interglacial Stage.

2.3 Little Musselroe Basin

2.3.1 *Extent*

The area of Stumpys Bay Sand at Little Musselroe Basin lies in a very different topographic setting to the coastal embayments described in 2.1 and 2.2 above. In the Little Musselroe River area the formation partially occupies a valley which is 7 to 8 km from the coast. The relatively flat floored valley is 2-3 km wide, approximately 10 km long, and trends in a north-south direction. It slopes towards the north where it widens to 5-6 km. Low gaps between isolated dolerite hills at the northern and northeastern end of the valley provide the only natural outlets to the coast via the Little Musselroe River and Cuckoo Creek. The Little Musselroe basin is confined to the west by the dolerite of Ringarooma Tier, and to the east by the granites of The Ranges. A very low drainage divide in the vicinity of Mygunyah Farm, south of Rushy Lagoon, separates northward drainage through Rushy Lagoon from southeastward drainage into the Great Musselroe River.

The areal extent of the Stumpys Bay Sand in this area is shown by Figure 21. The boundary which runs through Rushy Lagoon is the upper limit of the Stumpys Bay Sand and occurs at an elevation of 32.29 m above HWM. A field section here clearly shows

FIGURE 21 Little Musselroe Basin – Quaternary Geology

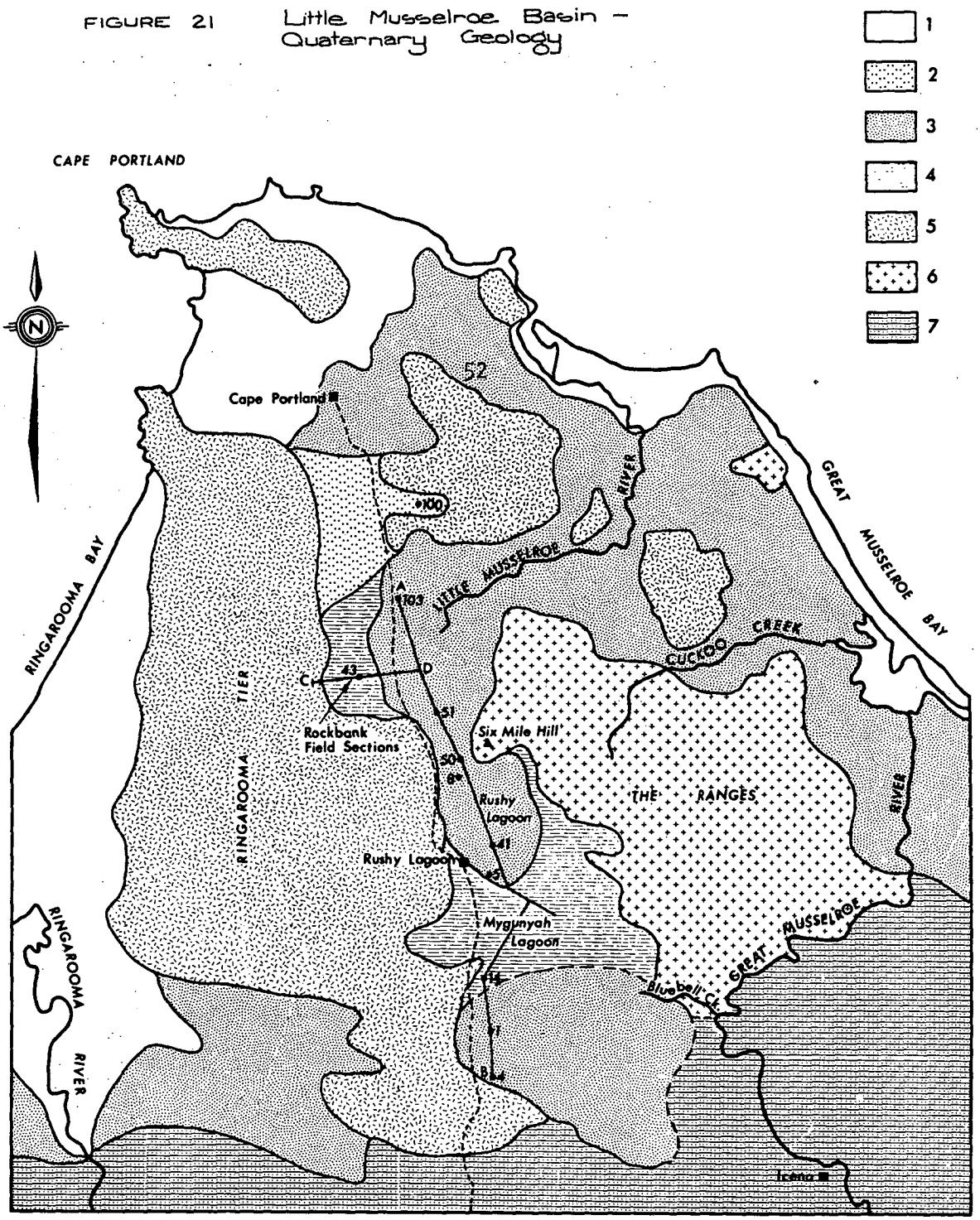

1 = Holocene beach and dune deposits
2 = Ainslie Sand
3 = Stumpys Bay Sand
4 = Older marine deposits
5 = Jurassic dolerite
6 = Granite
7 = Mathinna Beds

a very coarse, moderately bedded sand containing sparse marine sponge spicules which wedges out above older silts and clays (Plates 32 and 32) that also contain sponge spicules. The sands dip slightly (< 5°) towards the north, and are considered to be beach deposits of Last Interglacial age.

An alternative interpretation of the section however is that the sands represent a former beach of a Last Glacial age lake which formed the Rushy Lagoon lunettes (pages 186 to 197), and that the sponge spicules have been derived by reworking from the deposits below. This interpretation is not favoured because the beach is separated from the Rushy Lagoon lake by the lunette ridges which formed on its lee shore. Also, the coarse sands have been traced by augering and field sections and extend below the lake floor for a distance of at least 700 m from the lunette margins. This appears to be too wide for a beach developed by wave action in a lake with a fetch over water of around 1.5 km. A third objection to the lake beach interpretation is that the elevation of the beach is 1.5 m higher than the elevation of the highest point on the opposite shore. This elevation difference is probably too large to be wholly attributed to higher beach construction in the swash zone. In addition, the point where the beach deposit wedges out is 3-4 m higher than the base of the deposit beneath the lake floor. Again this elevation difference appears too great to have been formed in a relatively small inland lake with a short fetch, and the difference has been attributed to marine deposition during transgression to a sea level maximum.

The thickness of the formation in the Little Musselroe Basin is difficult to determine as the stratigraphy of the sediment fill in the valley is complex. Interpretation of samples from two

PLATE 31 Stumpys Bay Sand wedges out over older marine silts at Rushy Lagoon. The sands dip towards the north and the shovel is standing on the top of the older marine silts.

PLATE 32 Contact of Stumpys Bay Sand above older marine silts at Rushy Lagoon.

bore holes and from records, which were supplied by Mr. W.R. Moore, of six Mines Department water bores in the area suggests that the formation is probably not more than 6-7 m thick.

Figure 22 is a profile based on the drilling information from the Rushy Lagoon area. The stratigraphic sequences shown in the profile are tentative, mainly because the Mines Department bore results are from the driller's logs only, because the bore samples have been mislaid. Figure 22 shows that the Stumpys Bay Sand is thought to overlie older Quaternary marine deposits of clay, sand and gravel, which in turn overlie basalt of Tertiary age. Part of the profile (between Mines Department bore 103 and 51) infers that these older marine deposits are superimposed on alluvial clays and gravels which are usually found beneath the basalt. More detailed drilling and sample evaluation would be necessary to allow a more reliable interpretation.

2.3.2 *Environment of Deposition*

The composition of the Stumpys Bay Sand in the Little Musselroe Basin is a strong reflection of its depositional environment. Nearly all the samples from bores 50 and 51 contained sponge spicules which confirm a marine origin of the deposits. The spicules shown in Plates 33 and 34 are megascleres (triaenes) and are of the same type as those found in the Stumpys Bay Sand elsewhere.

Lagoonal marine deposition of the sequence is indicated by the abundance of silt and clay size particles compared with the sequences from the coastal embayments. The sequence in Figure 22 of supposed Last Interglacial age sediments in bores 50 and 51 shows a sequence from sand at the base, through a sandy clay, to

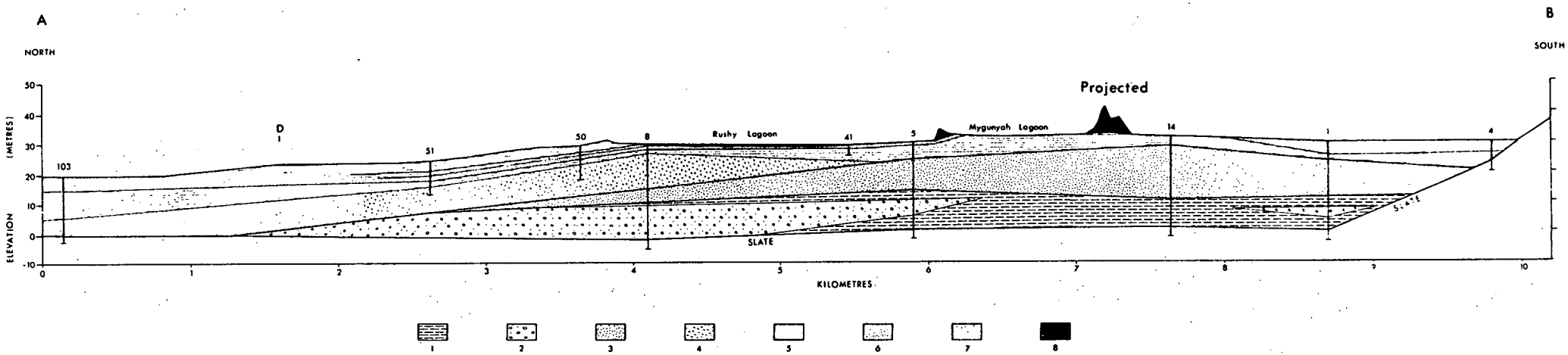

FIGURE 22 Drilling Section along Little Musselroe Basin.

All bores except 50, 51 and 41 were drilled by the Tasmanian Mines Department. The location of the profile is shown on Figure 21. VE = 20x. Elevations are metres above HWM.

1 = Tertiary alluvial clay
2 = Tertiary alluvial sand and gravel
3 = Tertiary basalt
4 = Quaternary marine sand and gravel (older than Stage 5?)
5 = Quaternary marine silt (older than Stage 5?)
6 = Quaternary marine sand (Stage 5)
7 = Quaternary lagoonal silt (Stage 5)
8 = Last Glacial age lake and dune deposits

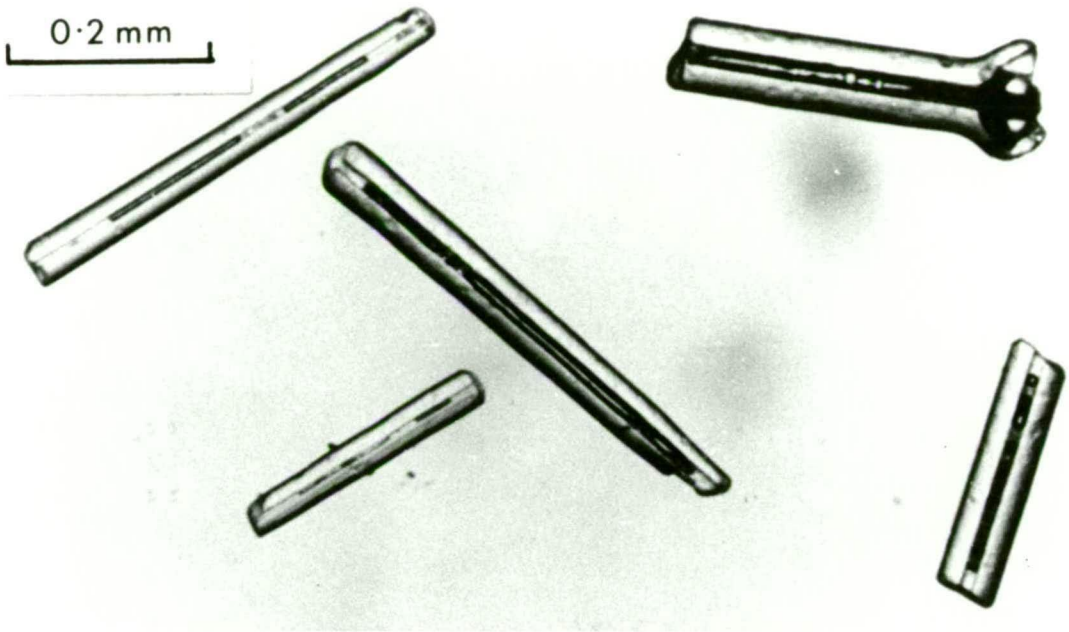

PLATE 33 Megascleres from Stumpys Bay Sand at Rushy Lagoon. Bore 51, 1.81 m depth. The central canal can clearly be seen in each specimen.

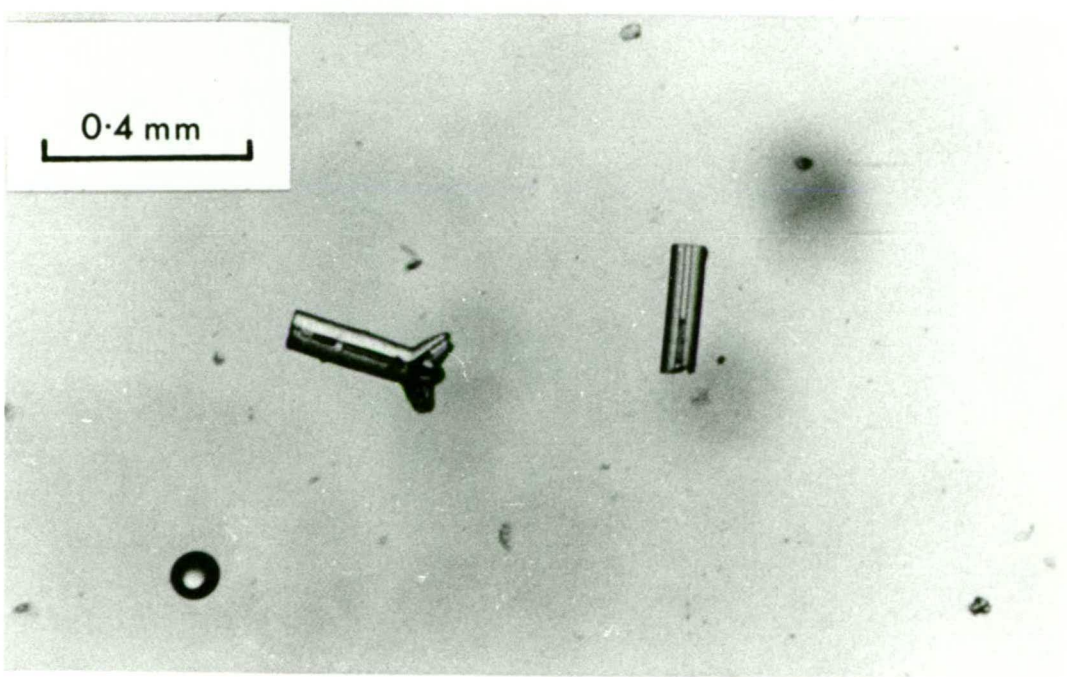

PLATE 34 Megascleres from Stumpys Bay Sand at Rushy Lagoon. Bore 50, 2.72 m depth.

clay deposits at the surface. As the deposits are of marine origin they reflect relatively quieter sedimentation conditions than the sands of the coastal embayments, in addition to a transition from beach sedimentation to more restricted lagoonal sedimentation. The basal sands were probably deposited during the initial stages of the marine transgression to ~ 32 m. The horizontal facies transition from sands in Mines Department bore 103 to the finer sediments further south (Figure 22) is coincident with marked basin restriction shown in Figure 21 in the vicinity of Six Mile Hill. Bore 52 was drilled outside the basin (Figure 21) at an elevation of approximately 30 m and penetrated 10 m of medium to medium coarse grained sands without reaching bedrock. Comparison of this bore, which is on the coastal plain to the north of the basin, with the marine sediments inside the basin demonstrates the degree to which partial enclosure of the marine environment caused the deposition of finer grained sediments.

The base of the Stumpys Bay Sand which is shown in Figure 22 has been placed at the contact with the underlying clay because the beach at the upper marine limit at Rushy Lagoon wedges out against the clay. Also, the decrease in thickness of the clay bed between Mines Department bore 103 and bore 51 may represent a degree of transgressive marine trimming of the clay, followed by beach deposition, which deposited the overlying sands, sandy clays, and clays. Furthermore, Quaternary marine deposits which are thought to be older than Last Interglacial age occur on the margin of the Little Musselroe Basin (pages 117-131). These deposits should extend beneath the Stumpys Bay Sand in the basin where they probably attained maximum thickness. The marine deposits above the Tertiary basalt and river deposits of Figure 22 are most likely the product

of several interglacial marine transgressions into the basin during the Quaternary Period.

More accurate definition of the number of marine transgressions into the basin should be possible by the implementation of coring in closely spaced bore holes. The information available to date is inadequate to permit confident stratigraphic analysis and the interpretation presented in Figure 22 is therefore tentative.

2.3.3 *Age*

The age of the marine deposits in the Little Musselroe Basin is not as readily established as for the deposits of the coastal embayments due to the more complex stratigraphy within the basin. However, a Last Interglacial age of the uppermost marine deposits is inferred because the surface is an extension of the coastal sand plains at Little Musselroe Bay and at the western end of Great Musselroe Bay. Using the same arguments as for the coastal embayments previously described these coastal plains are also considered to be of Last Interglacial age.

Spicule surface morphology is not likely to be a good indication of comparative age within the deposits of the floor of the Little Musselroe Basin because of the strong possibility of derivation from the lower marine deposits and their occurrence within clay beds. The degree of spicule surface corrosion may not be the same for spicules buried within clays and sands due to potential differences in the groundwater conditions. Clays, for example, do not allow passage of groundwater as freely as do sands. This may cause water within the clays to be more chemically aggressive due to lack of circulation and flushing and allow

consequent concentration of dissolved mineral salts. The greater turnover (even if only slow) of water within sand bodies might ensure that the mineral salts are constantly being flushed from the system. The nett effect of sediment type however, cannot be determined at this stage, but as the spicules from the sands and clays are not from comparable environments the degree of spicule surface solution cannot be used as an indicator of relative age.

Electron micrographs of spicules taken from all levels of bore 51 showed that the degree of spicule surface corrosion was very variable both within and between samples. This difference has been attributed mainly to reworking of older marine deposits which contained sponge spicules and partly to the differential solution processes as suggested above.

3. OLDER MARINE DEPOSITS

Two suites of marine deposits occur in the Rockbank area which is on the western margins of the Little Musselroe basin, under the lee of Ringarooma Tier. The Rockbank deposits can be separated from the Ringarooma deposits on the basis of lithology, stratigraphic relations, morphology, and upper limit elevations. A third probable marine deposit occurs at the Star Hill Mine, near Gladstone, and is higher than either of the deposits at Rockbank. These deposits are informally named as indicated for the purpose of this thesis.

3.1 Rockbank Deposits

Figure 21 shows the location of both deposits in the Rockbank-Ringarooma Tier area. The Rockbank deposits are exposed in two sections near the break of slope at the eastern foot of Ringarooma Tier. Figure 23a is a composite section of the Rockbank deposits and shows that they extend to an elevation of approximately 49 m above HWM, where they wedge out against clays. Bore 43 penetrated about 3.7 m of the deposit before encountering the basal clay, and the thickness of the Rockbank deposit probably does not exceed 4 m. The areal extent of the deposits is restricted to this small area at Rockbank. This site is one of the most favourable within the study area in terms of preservation of relatively old unconsolidated sediments because the Ringarooma Tier has provided protection from the powerful deflationary force of persistent westerly winds, both past and present. A concentrated drilling programme in this general area may prove the deposit to be more extensive than has been shown on Figure 21.

The Rockbank deposits consist of unconsolidated sands. The sands are almost entirely siliceous, are moderately well rounded and moderately sorted. They are uniformly and very well bedded in many cases and low angle cross-bedding, shown in Plate 35, is very common. Grainsize variation between adjacent beds is often marked, as shown in Plate 36. Thus, these deposits show many hallmarks of a beach environment of deposition. The siliceous sands cannot have been derived from the dolerite of Ringarooma Tier which they abut, and probably originated from granite source rocks which are common in northeastern Tasmania. A very minor input from the dolerite hinterland occurs as "ghost" dolerite pebbles, shown in Plate 37. The pebbles were originally fairly angular, are up

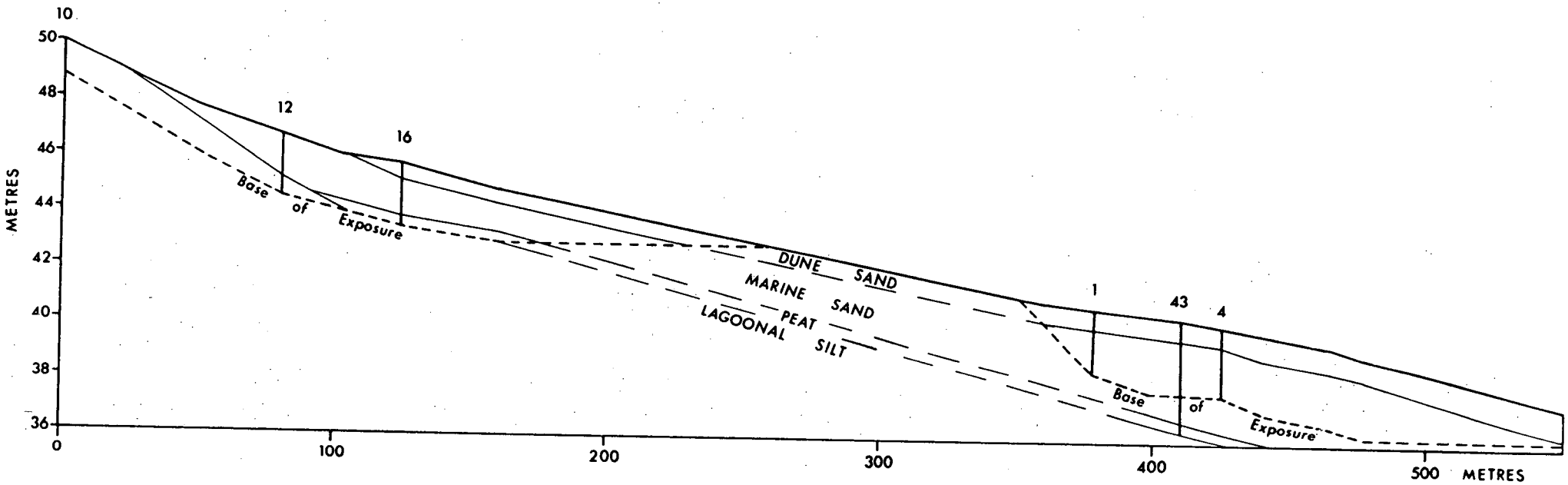

FIGURE 23(a) Stratigraphic section of the Rockbank area. VE = 10x.

Numbers refer to levelled sections within the exposure.
Number 43 is a bore hole.

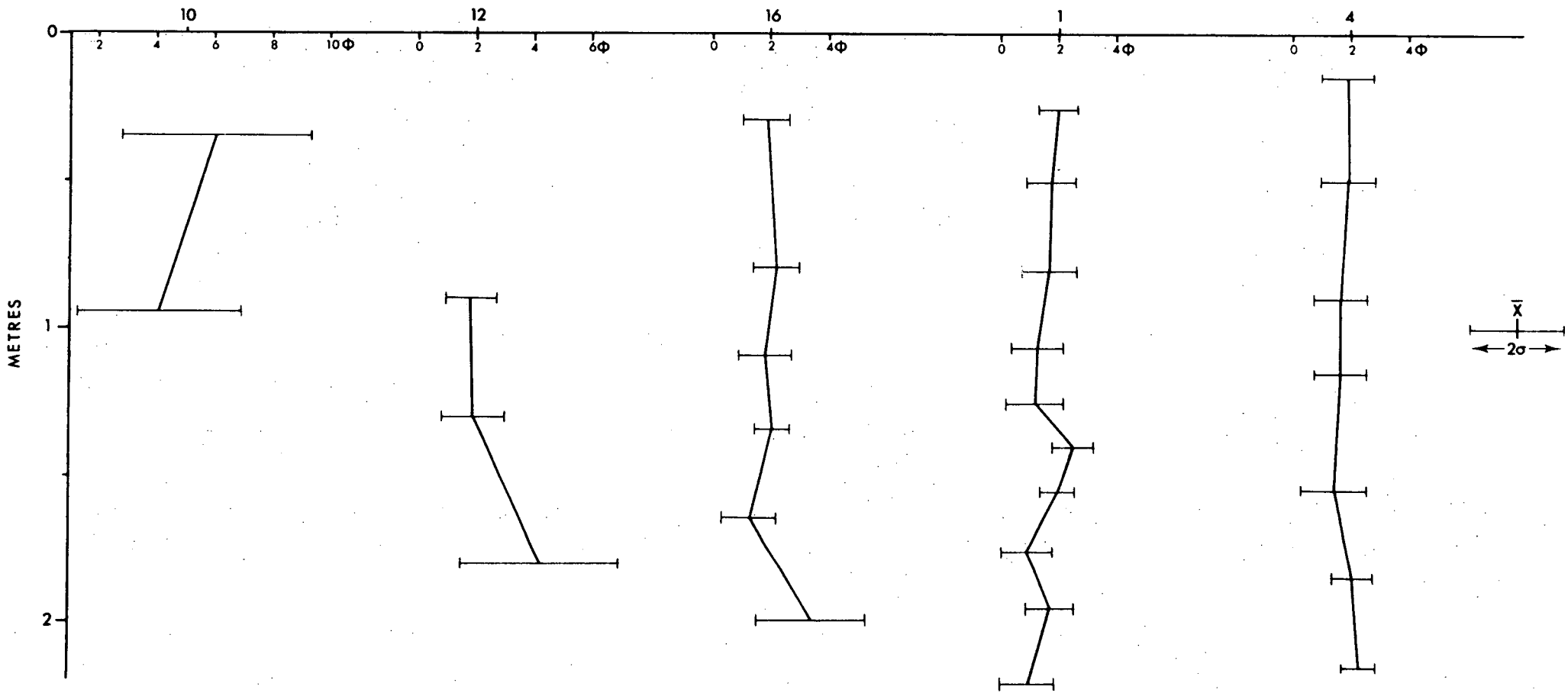

FIGURE 23(b) Grainsize characteristics of samples from the Rockbank and Ringarooma Deposits
Site numbers refer to the sections in Figure 23(a).

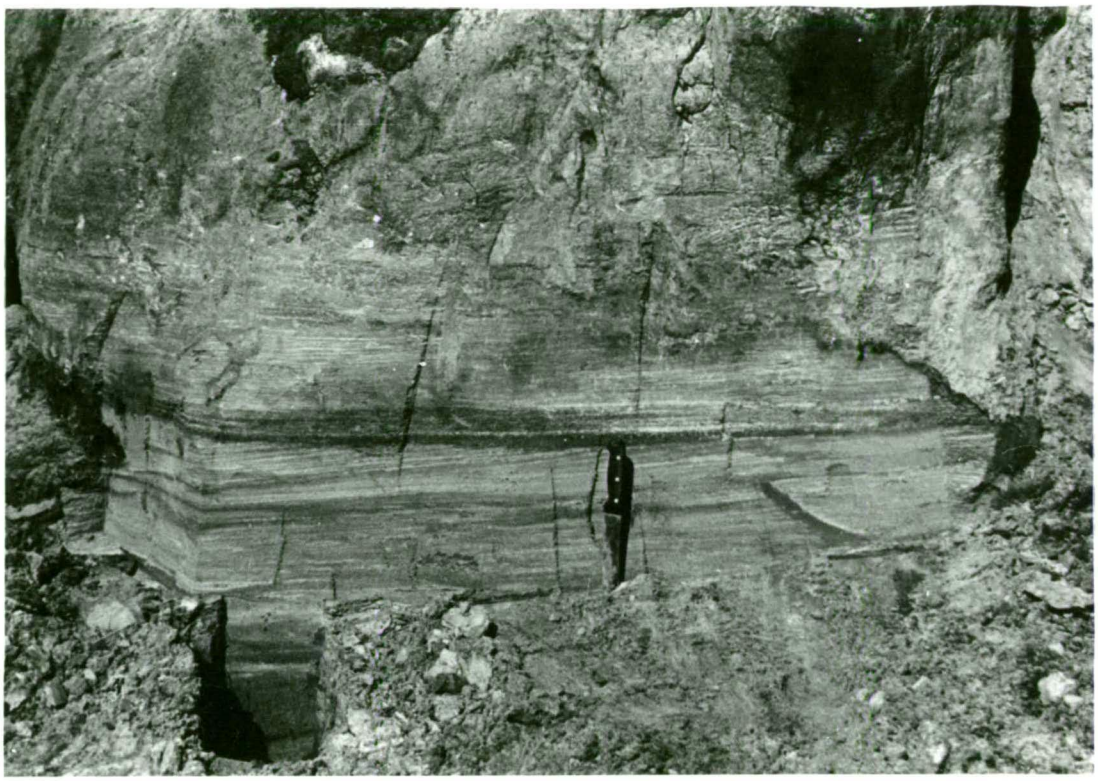

PLATE 35 Low angle cross bedding in Rockbank sands.

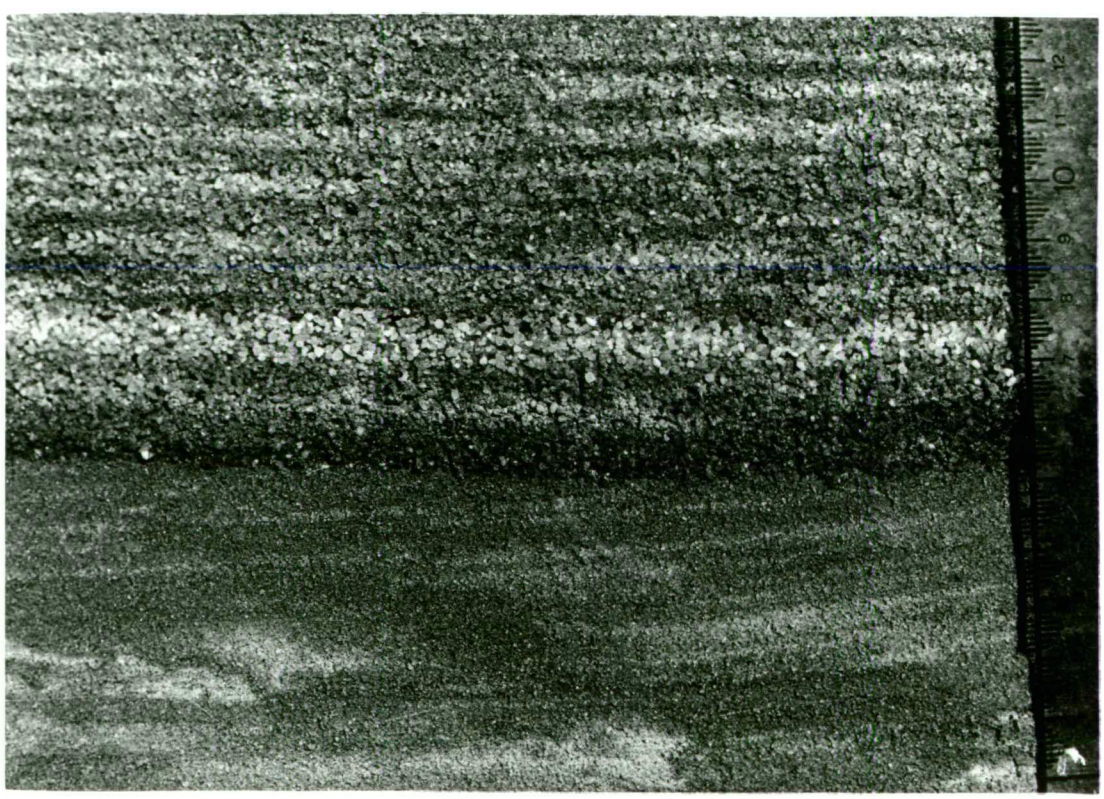

PLATE 36 Grain size variation between beds of the Rockbank deposits.

to 4 cm long but have since been weathered to clay and occur sporadically as discontinuous horizons within the sands.

Grainsize analysis was carried out at 0.25 ϕ sieve intervals on samples from four sections and the results are plotted on Figure 23b. The mean grainsize of the Rockbank deposits is 1.75 ϕ (standard deviation $\pm$ 0.42 ϕ, n = 22) and the average sorting coefficient is 0.84 ϕ (standard deviation $\pm$ 0.14 ϕ, n = 22). Figure 23b shows the degree of grainsize similarity within the Rockbank deposits, compared with, and in contrast to, the silty clays which they overlie.

Sponge spicules were found in most of the samples examined and are very similar to the spicules found within the marine sands of the Stumpys Bay Sand. Most of the spicules were megascleres, but some samples contained abundant microscleres (pointed diactines). The presence of the marine sponge spicules is convincing evidence that the deposits are of marine origin.

The possibility that the deposits are beach facies of a large inland lake can be discounted on the grounds that topographic closure is not possible.

The age of the Rockbank deposits is very difficult to ascertain but some conclusions can be drawn from their stratigraphic and topographic relations.

The higher elevation of the Rockbank deposits' upper marine limit ($\sim$ 49 m) compared with the Stumpys Bay Sand ($\sim$ 32 m) indicates that the Rockbank deposits are older. Although no sections are available of the contact between the Stumpys Bay Sand and the Rockbank deposits, the surface developed on the Rockbank deposits slopes at approximately 20-25 m/km and appears to pass below the surface formed by the Stumpys Bay Sand. This surface slopes at

PLATE 37 Weathered dolerite fragments (ghosts) within the Rockbank deposits marine sands.

PLATE 41 Exhumed soil horizon within the Rockbank deposits. The dark coloured exhumed $B_{2h,ir}$ horizon is approximately 80 cm below the surface and mantled by leached dune sand.

approximately 10-14 m/km and the indistinct break of slope between the two surfaces occurs at an elevation of around 30.5 m. The elevation of this break of slope is close to the upper limit of marine transgression during the Last Interglacial Stage.

The degree of spicule surface weathering can be compared between the Stumpys Bay Sand and the Rockbank deposits because both deposits have a similar composition. Plate 38 is a scanning electron micrograph at 1000 magnifications of a sponge spicule from bore 43 at a depth of 3.6 m. This surface is typical of the sponge spicules within the Rockbank sands. Comparison of Plate 38 with typical spicule surfaces from Tomahawk (Plate 26) shows that the "raindrop impact" solution features of the Tomahawk spicules are still apparent in Plate 38 but the surface has been much more weathered and deep solution pits have penetrated the surface. The great degree of spicule surface solution of the Rockbank deposits suggests that the Rockbank deposits are older than the Stumpys Bay Sand.

Remnants of an exhumed soil profile provide evidence that the sands are at least as old as the Last Interglacial. In both field sections (Figure 23), the surface metre or so consists of a strongly leached white sand which overlies an oxidized humic/iron horizon. This oxidized horizon, shown in Plate 41, has a very irregular upper surface which is heavily indurated, while the lower surface grades into an unoxidized $B_{2h,ir}$ groundwater podzol horizon. The horizon is probably all that remains of a former $B_{2h,ir}$ groundwater podzol soil horizon which has been exhumed and subjected to oxidation. The leached sand above the exhumed $B_{2h,ir}$ groundwater podzol horizon contains many fragments of iron oxide which are

PLATE 38 Megasclere surface morphology of spicule from the Rockbank deposits.

PLATE 39 Megasclere surface morphology of spicule from the Ringarooma deposits.

PLATE 40 Megasclere surface morphology of spicule from the Star Hill Mine.

0·1 mm

0·1 mm

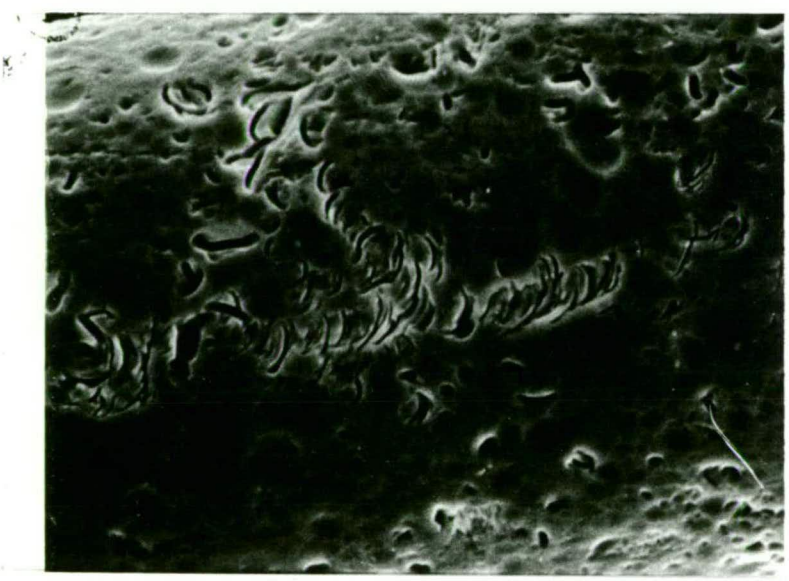

0·1 mm

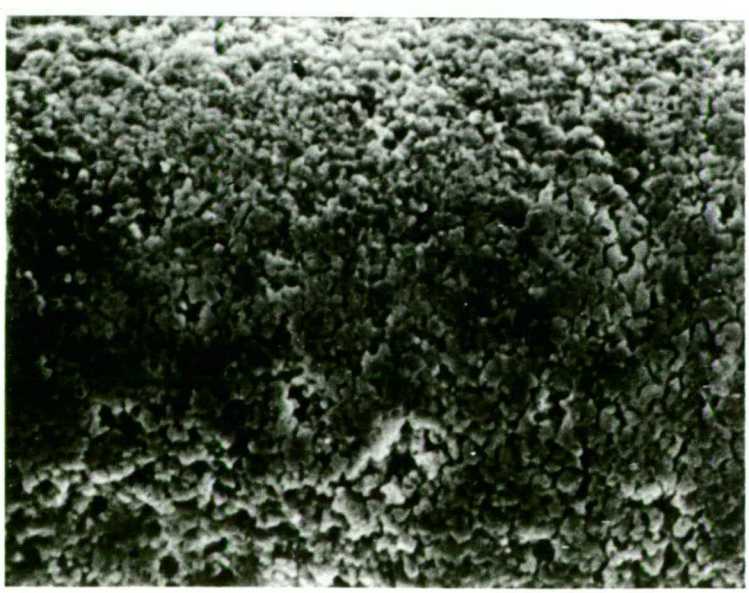

derived from the old soil layer. It is also fine grained and well sorted, characteristics which suggest aeolian deflation and redeposition of the original soil profile down to the $B_{2h,ir}$ horizon. The exhumed $B_{2h,ir}$ soil horizon has not been formed under today's conditions, as the present groundwater $B_{2h,ir}$ horizon is 1-2 m below it. The exhumed profile may have been formed during the Last Interglacial Stage when water tables may have been relatively high. During the Last Glacial Stage the increased aridity which produced lowered water table levels (pages 156 to 168) dried out the sandy surface and exposed it to aeolian reworking. At this time the leached sand, which may largely have been the original A_2 horizon of the soil profile, was deposited.

The Rockbank deposits and the underlying Ringarooma deposits are separated by a sandy peat layer. This layer is exposed in the section near the western end of the profile shown in Figure 23a. Also, an organic layer was penetrated by bore 43 at the contact between sands of the Rockbank deposits and the underlying clay. The organic layer appears to be truncated by the Rockbank sands at an elevation of approximately 44 m as it does not occur above this point in the section.

The peaty sand contains 9.3% organic matter, as determined by weight loss on ignition. Grainsize analysis of the inorganic fraction showed that this fraction is a silty-clayey sand (Shepard, 1954). This fraction is more closely akin to the underlying deposits than to the Rockbank deposits and is probably a thin swamp deposit developed on the surface of and largely derived from the underlying silty clays.

Dr. E.A. Colhoun examined a pollen slide prepared from the organic layer. Local aquatics were very highly represented, *Isoetes*

species being the most abundant. Prof. W. Jackson (Department of Botany, University of Tasmania) identified megaspores of *Selaginella uliginosa*. These spores indicate a freshwater/swamp environment. In addition grass and Compositae pollen were very common, but no certain pollen of tree species were found. Dr. Colhoun concluded that the pollen spectra was of Quaternary age, as no elements of a Tertiary flora were seen. Also the absence of trees and presence of grasses and composites indicates that the deposit has some affinities with glacial age terrestrial vegetation elsewhere in Tasmania.

This freshwater lake/swamp deposit which is probably of a glacial age occurs between the Rockbank marine deposits and the silty clays of the Ringarooma deposits (which are also marine, page 129) and indicates that the two interglacial deposits are probably of different ages and may be separated by a glacial stage. The swamp which formed the organic layer may have been created by waterlogging on the surface of the underlying poorly drained silty clays.

A summary of the above arguments suggests that the Rockbank deposits are of interglacial age, that they are older than the Last Interglacial, and that they may be a full interglacial stage younger than the deposits beneath them. The only estimate of maximum age is that they are not of Tertiary age. However, the deposits are not likely to be much older than the Last Interglacial stage because they are not likely to survive a long period of subaerial weathering due to their unconsolidated condition. Also, the degree of sponge spicule surface weathering, although more advanced than Last Interglacial age spicule surface weathering, still retains similar features to the spicule surfaces in younger

deposits. This indicates that they may be separated by a time period which has allowed the spicule surface weathering to go only one stage further. The minimum possible age of the Rockbank deposits is Second Last Interglacial (Stage 7 of Shackleton & Opdyke, 1973) and they have been tentatively assigned this age.

3.2 Ringarooma Deposits

One of the main problems of Quaternary research of land based studies is that evidence becomes more fragmented and conclusions less certain as the record becomes older. The climatic oscillations and consequent changing subaerial processes that have occurred during the late Quaternary are not generally conducive to preservation of older, unconsolidated deposits and landforms. However, like the Rockbank deposits, the Ringarooma deposits have been at least partially protected from deflation by Ringarooma Tier, against which they are banked.

The Ringarooma deposits extend as a surface which slopes eastward at 40 to 45 m per km and terminates against the Ringarooma Tier to the west, at an elevation of approximately 71 m above HWM. This upper limit of the deposits is marked by a conspicuous break of slope. The break of slope occurs at a fairly consistent elevation on the eastern flank of Ringarooma Tier. The lower limit of the surface occurs at a moderately well defined break of slope at the upper marine limit of the Rockbank deposits. However, field sections and one bore hole (bore 43) show that the Ringarooma deposits underlie the Rockbank deposits. The maximum thickness of the Quaternary deposits in the Rockbank area has not been determined.

The Ringarooma deposits are composed of silty, clayey sand. Grainsize analysis results of some samples from the deposit

are shown in Figure 23. The deposits contain abundant marine sponge spicules, both megascleres and microscleres, and therefore appear to be of marine origin. The fine grained composition of the deposits suggests that they represent a lagoonal facies.

Morphologic and stratigraphic evidence shows that the Ringarooma deposits are older than the Rockbank deposits. The sections at Rockbank show that the former underlie the latter and the Rockbank deposits wedge out forming a surface break of slope. Sponge spicule surface morphology also shows that the spicules in the Ringarooma deposits have been more heavily altered by solution processes than the Rockbank deposits. Plate 39 is a scanning electron micrograph, x 1000, of a typical spicule surface within the lagoonal deposits. The surfaces show much more strongly developed solution pitting than the spicules show in Plate 38. However, caution needs to be applied in this interpretation due to the possible differential solution rates in sediments of unlike composition (page 117).

The presence of the organic swamp deposit between the Rockbank and Ringarooma deposits also indicates that the two interglacial stages represented by the deposits may be separated by at least one glacial stage (pages 126-127). The minimum possible age of the Ringarooma deposits is therefore likely to be the Third Last Interglacial Stage (oxygen isotope Stage 9 of Shackleton & Opdyke, 1973). The deposit is considered here to be of Stage 9 age because there is no evidence which suggests an older age, and the present interpretation is based on the logic of working backwards through time.

Figure 24 is a profile which follows the marine surfaces from Ringarooma Tier to the centre of the Little Musselroe basin.

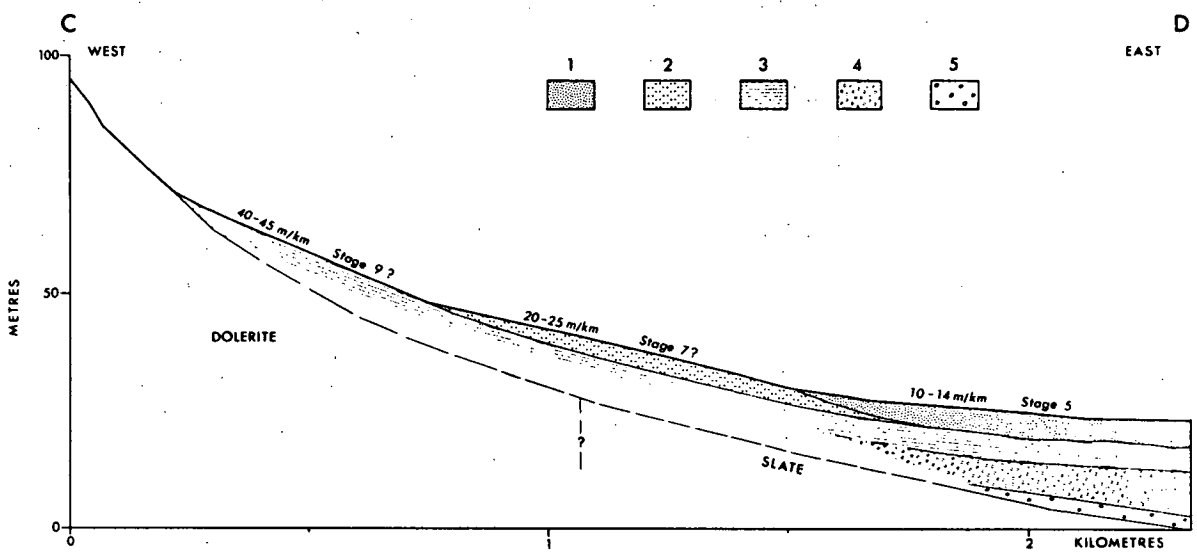

FIGURE 24 Profile showing surfaces of marine deposits at Rockbank. The location of the profile is shown on Figure 21. VE = 10x. The surface slopes are shown on the profile.

1 = Stumpys Bay Sand
2 = Rockbank deposits
3 = Ringarooma deposits
4 = Quaternary marine sand and gravel
5 = Tertiary age fluvial sand and gravel

Incorporated in the profile are the combined results from levelling, field sections and drilling. The sequence in the basin floor is determined by interpolation of the drill hole correlation of Figure 22. Figure 24 is therefore an interpretation only of the possible stratigraphic and morphologic relations between the Ringarooma deposits, the Rockbank deposits, and the Stumpys Bay Sand. The diagram portrays three interglacial marine deposits which have been successively superimposed at lower levels. The upper limits of each level are approximately 71 m, 49 m, and 32 m respectively.

3.3 Star Hill Mine Deposits

Star Hill Mine is located 3.5 km east of Gladstone (Figure 1). Alluvial tin mining operations have exposed highly leached, white, medium to coarse grained sands which lie beneath younger alluvial gravel. The sands in turn overlie Mathinna Beds and occur at an elevation of approximately 90 m above present sea level. The sand thickness has not been measured but is approximately 8 m. The sands are well bedded and frequently show low angle cross-bedding which is typical of beach deposition. Five sand samples from the mine all yielded rare, highly eolized, fragmented, sponge spicule megascleres. The fragmented spicules were not complete enough to determine whether they are of the same type as previously described. However their presence provides some support for a marine origin of the sands.

These sands are probably much older than any of the interglacial marine deposits discussed so far. The high degree of leaching indicates significantly greater antiquity. Also, scanning electron micrographs of the spicule surfaces (Plate 40) show that

the surfaces are very highly corroded; to a much greater degree than spicules in the other deposits. The spicule surfaces have been modified to such an extent that they are no longer transparent and are white in colour. It is impossible to place an estimate of age on the sands at the Star Hill mine, other than that they may be of Quaternary age.

The Star Hill sequence provides evidence that the sea in northeastern Tasmania probably attained an elevation of ~ 90 m at a time considerably earlier than oxygen isotope Stage 9. The sequence of alluvial gravels above the marine sand deposits may also be of Quaternary age and was probably deposited during a later glacial stage, when less forested and more unstable slopes in the catchment contributed to greater stream loads, a similar response to that which formed the alluvial terraces of Forester Gravel (page 32).

Study of the nature and occurrence of the Stumpys Bay Sand and the older marine deposits has provided a partial sea level curve for the Late Quaternary in northeastern Tasmania. This can now be compared with eustatic sea level records derived from elsewhere.

4. LATE QUATERNARY TECTONISM

This section considers the evidence for tectonic uplift in northeastern Tasmania since the Last Interglacial Stage by comparing the eustatic Last Interglacial Stage maximum sea level of known or presumed stable areas with the upper marine limits of Last Interglacial sea level in Tasmania. A comparison is then made of the elevation of older marine shorelines in northeastern Tasmania

with the deep sea oxygen isotope record to suggest a possible approximation of the nature of Late Quaternary uplift. The northeastern Tasmanian results are then compared with other areas within Tasmania and mainland Australia to assess whether differential uplift within the Australian region has occurred. Finally, possible reasons for Tasmania's relative instability are briefly considered.

4.1 Last Interglacial Eustatic Sea Levels

The Last Interglacial eustatic sea level in many stable areas has been determined by joint use of radiometric dating of corals and reef elevation.

Thurber *et al.* (1965) found that $^{230}Th/^{234}U$ determination of coral less than 12 m below the surface of Eniwetok Atoll, in the Pacific, showed that the coral was younger than 6000 years BP (6 ka). At depths from 12-21 m the coral yielded ages from 100 to 130 ka. They concluded that the hiatus in coral deposition was caused by a considerable lowering of ocean level between 5 and 100 ka. They also concluded that the sea level and climate of 120 ka resembled modern conditions due to the presence of coral-bearing horizons of this age in the lagoons. They also inferred that the period 100-130 ka may be the age of the Last Interglacial sea level maximum.

Veeh (1966) dated samples from emerged reefs on stable islands of similar height in the Pacific and Indian Oceans. His data from Hawaii, Tuamotu Islands, Society Islands, Samoa and Cook Islands in the Pacific and from Mauritius, the Seychelles and Western Australia in the Indian Ocean, consistently showed that at 120 ± 20 ka the sea level stood 2-9 m higher than now. He considered all of these areas to be stable and the levels to represent a eustatic sea level stand.

Later work in the Indian Ocean by Thomson & Walton (1972) showed that the age of the upper coral rich limestone which rises to approximately 8 m on Aldabra Atoll was 127 ± 9 ka.

Ku *et al.* (1974) dated extensive wave cut features (Waimanalo shoreline) at an elevation of 7.6 m on Oahu, Hawaii. The fossil corals associated with the Waimanalo shoreline were of 122 ± 7 ka age and they concluded that this was the last time during which the sea stood significantly higher than it does today. They also commented that the elevations from 1.5 to 10 m recorded by Veeh (1966) in the Pacific and Indian Oceans varied over this range because reefs are constructional features which descend progressively offshore, and felt that the Waimanalo stand at + 7.6 m was more reliable because it is marked by horizontal notches. Ku *et al.* also pointed out that although they had considered Oahu to be tectonically stable, Ward (1973) hypothesized that uplift of Oahu at a mean rate of 0.016 m/ka occurred since the Late Pliocene. On this basis the corrected eustatic sea level defined by the Waimanalo shoreline would be 5.7 ± 2 m above present sea level. However Ward's conclusions are based on dubious altitudinal correlations of shorelines of speculative age between South Carolina and Gippsland, and comparison of the Gippsland shorelines with the shorelines in Oahu. Ward's hypothesis of Hawaiian uplift must therefore be disregarded until more substantive evidence is produced.

$^{230}Th/^{234}U$ dates by Broecker and Thurber (1965) obtained from fossil coral and oolite on the Bahamas and Florida Keys clearly indicated marine limestone formation close to the present sea level at about 85 ka, 130 ka, and 190 ka. They also found no evidence of any submergence between 80 ka and 4 ka.

Also in the Bahamas, Neumann and Moore (1975) derived sixteen $^{230}Th/^{234}U$ dates from eight localities and described associated emergent coastal features. Using an erosional notch at 5.6 ± 0.3 m they concluded that a maximum sea level stand at 5.6 m occurred close to 125 ka. Lower level features were formed as sea level fell from the maximum position.

Land, Mackenzie and Gould (1967) dated limestone formation in Bermuda. They found no evidence for Pleistocene tectonism in Bermuda. Dates from the Devonshire Member indicated that at 130 ka the eustatic sea level was approximately 4.8 m above present mean sea level. Dates on the Spencer's Point Member indicated that at 110 ka the sea was 13.6 to 17.8 m above present level. However, Harmon, Schwartz and Ford (1978) collected more Bermudan coral samples, redetermined the age of the Spencer's Point sample collected by Land *et al.*, and dated speleothems. They considered that the Spencer's Point Member is storm deposited rubble that lies at least a few metres above a former sea level. Their subsequent eustatic sea level curve showed that sea level at approximately 125 ka was 4 to 6 m above the present elevation and at about 114 ka sea level became briefly stabilized at ~ 8 m.

In Australia, northern New South Wales is considered to be tectonically stable by Marshall & Thom (1976) because it is a continental coast far removed from plate boundaries. Lagoonal facies of the Inner Barrier at Newcastle and Evans Head reach elevations of 4-6 m above mean sea level. Corals collected from behind the Inner Barrier at Evans Head gave ages ranging from 112-127 ka and confirmed that the Inner Barrier was formed during the Last Interglacial. Marshall & Thom could not establish an interglacial sea level curve for eastern Australia but considered

there is enough evidence to "... point to a sea level during the final phase of the Last Interglacial ~ 4-6 m above present sea level." (page 120).

Table 3 is a summary of the key evidence for Last Interglacial eustatic sea levels derived from relatively stable areas.

TABLE 3 Stable Regions: Last Interglacial Eustatic Sea Levels

Area	Eustatic SL (m above present)	Radiometric Age (ka)
Bermuda	4 - 6	~ 125
Bahamas	5.6 ± 0.3	~ 125
Aldabra Atoll	~ 8	127 ± 9
Hawaii	7.6 ± 2	122 ± 7
Northern NSW	5 ± 1	118 - 125

The combined evidence is very strong that the maximum eustatic sea level during the Last Interglacial was approximately 6 ± 2 m and this elevation was attained approximately 125,000 years ago. This figure has become generally accepted and has been used to calibrate various tectono-eustatic models (e.g. Broecker *et al.*, 1968; Bloom *et al.*, 1974; Marshall & Launay, 1978; Konishi *et al.*, 1970).

4.2 Uplift in Northeastern Tasmania

The strong evidence in northeastern Tasmania of marine transgression during the Last Interglacial to approximately 32 m is patently at variance with the eustatic evidence from stable areas. It seems, therefore, that tectonic uplift in northeastern Tasmania has raised the Last Interglacial upper marine limit by approximately 26 m over the last 125 thousand years. This would be a rate of around 0.21 m/ka assuming uplift has been uniform over that period.

Table 4 places this calculated uplift rate in perspective by showing a comparison with some uplift rates derived from elsewhere.

TABLE 4 Unstable Regions: Comparison of Uplift Rates

Region	Uplift Rate (m/ka)	Source
Northeastern Tasmania	0.21	This thesis
Huon Peninsula, New Guinea	0.94 - 2.56	Bloom *et al.* (1974)
Indonesia and Malaysia	1.4 - 8.4	Tjia *et al.* (1972)
New Hebrides	0.6 - 0.8	Neef and Veeh (1977)
Loyalty Islands	0.15 - 0.18	Marshall and Launay (1978)
Ryukyu Islands	1 - 2	Konishi *et al.* (1970)
Macquarie Island	1.5 - 4.5	Colhoun and Goede (1973)
Barbados	0.23 - 0.38	Broecker *et al.* (1968)

Uplift rates in very active tectonic areas can apparently be up to forty times greater than the rate suggested for northeastern Tasmania and the Tasmanian rate is similar to the more moderate rates of the Loyalty Islands and Barbados.

A possible consequence of uplift since the Last Interglacial in northeastern Tasmania could be the occurrence of shore features above present sea level which were formed by brief minor transgressions during oxygen isotope Stages 5a and 5c (Emiliani, 1961 & Shackleton, 1969). The oxygen isotope record provided by Pacific Core V28-238 (Shackleton & Opdyke, 1973) is the longest and most reliable available to date (Shackleton & Opdyke, 1976). The independently derived glacio-eustatic sea level curve inferred from oceanic sediments (page 45, Shackleton & Opdyke, 1973) for the last 130 ka is in good agreement with eustatic sea level curves for that period which are derived from the tectonically active coastal areas of Barbados (Broecker *et al.*, 1968) and New Guinea (Veeh & Chappel, 1970). According to the oxygen isotope curve, eustatic sea level rose to about -10 m at approximately 100 ka (Stage 5c) and 80 ka (Stage 5a). This is slightly higher than the estimates of around -15 m to -13 m from Barbados and New Guinea raised reef sequences. The oxygen isotope sea level values are used for the present purposes due to the possibly doubtful assumption of constant uplift rates in Barbados (Stearns, 1976).

Assuming an uplift rate of 0.21 m/ka and eustatic sea levels of -10 m at 100 ka and 80 ka the expected elevations of shorelines formed in those times in northeastern Tasmania are 11.0 m and 6.8 m respectively. The east coast embayments show marked beach ridge development between 11.5 and 6.5 m compared with

relatively even surface slopes from about 12 m to the upper marine limit (Table 2, page 75). This is precisely within the altitude range expected for the Stage 5a and 5c shorelines. Although the crest of Beach Ridge 3 as shown in Table 2 is ~ 11.4 m and Beach Ridge 1 of the table is ~ 7.1 m, which correlate well with the predicted levels, they are separated by an intermediate beach ridge (Beach Ridge 2) which has an average ridge elevation of 9.4 m. A shoreline at this elevation is not indicated in the oxygen isotope sea level curve.

The generally close correlation of the beach ridge set with the expected shoreline elevations of the later Stage 5 sea levels only suggests that it is possible that the beach ridges are of this age. The level of resolution of the oxygen isotope curve is not sufficiently high to provide a eustatic sea level curve which can be applied with the accuracy required to confirm the correlation. In addition, no beach ridge dates are available and the assumption of uniform tectonic uplift may not be justified.

The presence in northeastern Tasmania of elevated interglacial marine deposits older than Stage 5 also implies tectonic uplift because the oxygen isotope record of Shackleton & Opdyke (1973) shows "... that sea level returned approximately to the same position, or slightly lower, during each succeeding interglacial over at least the past 700,000 yr." (Marshall & Thom, 1976, page 121).

The upper limit of the Rockbank deposits at ~ 49 m is interpreted to represent the Stage 7 sea level maximum and the respective elevation and age of the Ringarooma deposit is ~ 71 m and Stage 9. Shackleton & Opdyke (1973, page 50) considered that the Stage 7 sea level attained -10 m and the Stage 9 eustatic level

was very close to the present level. Interpolation of the absolute ages of Stage 7 and 9 sea level peaks from Shackleton & Opdyke (1973, page 48 & Figure 9) are 220 ka and 325 ka.

Figure 25 is a graph of present upper marine limit altitude minus eustatic sea level versus age, for the period to Stage 9. The resultant slopes are the uplift rates for the various intervals. The mean uplift rate over the last 325 ka is shown by this graph to have been ~ 0.22 m/ka. The graph also suggests that the rate of uplift may have risen from 0.11 m/ka during the interval between Stage 9 and Stage 7, to 0.35 m/ka from Stage 7 to Stage 5, and then dropped to 0.21 m/ka after Stage 5e.

The general uplift rate of 0.22 m/ka over the extended time interval agrees with that calculated for the better known last 125 ka and lends some support for the hypothesised ages of the Rockbank and Ringarooma deposits. However, the trend of the uplift rate curve, when extended further back, suggests that prior to about 500 ka the area may have been relatively more stable. If the trend is a real one it implies that Middle to Late Quaternary marine deposits are not likely to occur above about 80-90 m.

Although the occurrence of the Star Hill Mine deposits at ~ 90 m adds some support for the last conclusion above, they have not been used in the construction of Figure 25 because it has not been possible to even hazard a guess at their age.

The hypothesis that Quaternary shorelines did not exceed an elevation of ~ 90 m is supported in a minor way by the presence of a fairly obvious erosion surface in northeastern Tasmania at an elevation of approximately 90 m (Plate 42), which may have been formed by interglacial sea levels returning to similar elevations before uplift commenced ~ 500,000 years ago. Davies (1959) examined

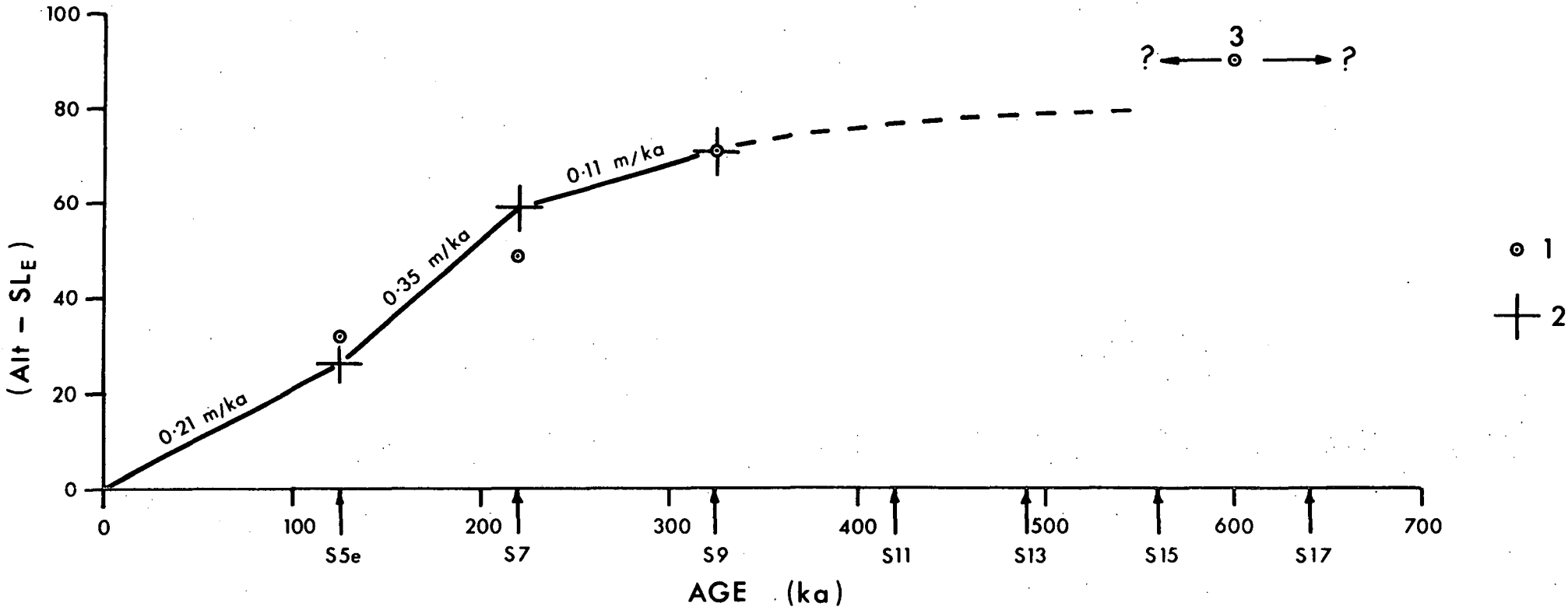

FIGURE 25 Upper marine limit altitude minus eustatic sea level compared with age.

Alt = Present altitude (m)
SL_E = Eustatic sea level (m)

1 = Present Altitude
2 = (Alt - SL_E)
3 = Altitude of Star Hill Mine deposits

Arrows indicate the major oxygen isotope interglacial sea level peaks.

PLATE 42 Erosion surface at ~ 90 m in northeastern Tasmania. Mount William (centre background) rises conspicuously above the plain.

erosion surfaces in Tasmania and concluded that the "lower coastal surface" at 300 to 900 feet (90-270 m) is an uplifted erosion surface which may be largely or even entirely of marine origin.

The above conclusions of the nature of tectonic activity in northeastern Tasmania are consistent with the field evidence. However, the whole argument would be strengthened if adequate time control of the shoreline features was available and if the Late Quaternary eustatic sea level record was more precisely known. While developments in oxygen isotope stratigraphy may largely eliminate the latter constraint, the former problem threatens to remain for a longer period unless new radiometric dating techniques can be applied to existing material within the deposits, or until discovery of new materials within the deposits which can be dated by methods currently available.

4.3 Last Interglacial Shorelines in Tasmania Compared with the Australian Mainland

4.3.1 *Tasmania*

Marine deposits of supposed Last Interglacial age attain maximum elevations of 20-22 m in several areas within Tasmania. van de Geer, Colhoun & Bowden (1979) summarized the evidence of these deposits. In northwestern Tasmania (van de Geer, pers. comm.; Colhoun, 1976 & Chick, 1971) marine deposits and shorelines extend to a well defined limit of 20-22 m. Similar observations have been made in western Tasmania at Strahan (Banks, Colhoun & Chick, 1977), and in east and southeast Tasmania (Colhoun, in van de Geer *et al.*, 1979). Davies (1960) interpreted features near Strahan at 50 m and 36 m as raised strandlines.

Jennings (1959, 1961) examined evidence for Pleistocene sea level change on King Island and found widespread evidence for a falling sequence of levels from approximately 20 m to the present level and considered them to be of Last Interglacial age. He also described slight indications of an older sea level stand at ~ 69 m and stronger evidence for one at ~ 37 to 46 m. These higher levels agree fairly well with the proposed Stage 9 and Stage 7 levels of northeastern Tasmania.

Dimmock (1957) recognized old coastal lagoon floors on the eastern coastal plain of Flinders Island which extend from ~ 24 m to ~ 8 m. He also described sandy flats, which he considered to be largely of fluvial origin, which fall gently from ~ 30 m to the coast. Sutherland & Kershaw (1971), Kershaw & Sutherland (1972) found evidence of possible Pleistocene sea levels at 60-75 m, 30-37 m, 18-21 m, and 7.5-9 m.

A summary of the Tasmanian evidence shows that the 20-22 m is well represented throughout the region and that higher sea levels may be present at Strahan and on King Island, Flinders Island, and in northeastern Tasmania. The level at ~ 60-75 m is represented in the three northern areas. The 50 m level occurs at Strahan and northeastern Tasmania. The level at 30-37 m which is found on Flinders Island is also found at Strahan and is strongly represented in northeastern Tasmania by an extensive upper marine limit at 32 m.

The evidence from the eastern embayments of northeastern Tasmania (pages 76-78) indicates that the Last Interglacial upper limit of ~ 20-22 m may be only an apparent limit on less sensitive coasts and that the real upper marine limit may lie at ~ 32 m. The Last Interglacial upper marine limits have not been studied in

sufficient detail in the rest of Tasmania to enable precise comparison and correlation on the basis of altitude alone is highly dangerous. However the available evidence suggests that there is a possibility that differential uplift within the Tasmanian region is unlikely and that the region may have responded fairly uniformly to tectonic forces.

4.3.2 *Australian Mainland*

The conclusion of late Quaternary tectonic uplift in Tasmania contrasts with the evidence from the mainland of Australia. Apart from special cases where uplift can be directly related to active Pleistocene volcanicity (Cook *et al.*, 1977), the continental mainland appears to be tectonically stable. Thom & Chappell (1975) have pointed out that the arguments for Holocene tectonic movement in Australia are unlikely to be readily solved because the probable uplifts are too small to be differentiated. They also state that "... Late Quaternary tectonism will not accurately be identified until the shoreline of 125,000 years ago is everywhere recognized." (page 92). Veeh (1966) dated *in situ* corals from Rottnest Island (+2 m) and Boundary Beach (+4 m) in Western Australia. Their ages fall in the range 100 ka to 140 ka which is consistent with the reef elevations from other stable areas. On the other side of the continent, Marshall & Thom (1976) dated corals of the age 118 ka to 127 ka in close association with the Last Interglacial age Inner Barrier at Evans Head, Northern New South Wales, thus demonstrating tectonic stability for the region. In western Victoria Gill & Amin (1975) dated molluscs of ~ 125 ka and ~ 108 ka age from marine terraces at 7.5 and 3-4 m. Although these results are of the correct order and imply tectonic stability

in the area, Marshall & Thom (1976) consider dates from molluscs unreliable. Thom (pers. comm.) has visited many sites in eastern Australia and has been unable to find conclusive evidence of Pleistocene marine deposition above approximately 8 m in the region.

Thus, while there is substantial evidence of general tectonic stability on mainland Australia there is also strong evidence for moderate rates of tectonic uplift of the Tasmanian region over at least the last 300 or so thousand years.

Detailed discussion of the possible causes of Tasmanian uplift is not within the scope of this thesis, but several observations suggest that relative tectonic instability of Tasmania compared with the mainland is probable.

4.4 Factors Leading to Tasmanian Instability

It is clear that Tasmania, which is a long distance from any plate boundary, does not have the same active tectonic framework usually associated with plate boundaries. Therefore a factor must exist which sets Tasmania slightly apart tectonically from most of the Australian plate.

A gravity map of southeast Australia (Bureau of Mineral Resources, 1976) shows a pronounced gravity low over Bass Strait, which separates the high gravity areas of mainland Australia and Tasmania. Interpretation of the map suggests that the continental crust is thinner beneath Bass Strait than beneath both mainland Australia and Tasmania. In terms of crustal thickness, Tasmania is therefore weakly attached to the mainland. In addition, the crust extends beneath Tasmania as a peninsula projecting southwards from the mainland continental crust.

The tectonic consequences of this crustal configuration may be that Tasmania is much more sensitive to application of tectonic forces from beneath the crust. For example, quite a large force applied to the Australian plate may not induce appreciable movement on mainland Australia because of its vast areal size and mass. The effect of this force on the Tasmanian crustal promontory however, may be to produce appreciable crustal movement beneath Tasmania, because the crust here is unsupported on three sides, and attached to the mainland by a relatively thin crustal layer which may facilitate flexure. Such forces could be exerted by processes operating continually beneath the crust or by migration of the Australian plate over a stationary convection plume. Convection plumes have now been recognized in many areas (Wilson, 1963(a), 1963(b); Morgan, 1971, 1972). Thom & Cull (pers. comm.) have postulated a stationary convection plume in the southeastern Australian region and have attributed the Tasmanian uplift as described here to consequent crustal expansion caused by the heating. Vertical crustal displacement could also be caused by relatively high velocity magma upwelling associated with convection plumes. This hypothesis is supported as a possibility by Tasmanian heat flow values which are anomalously high for the Australian region (Cull & Denham, 1979).

5. SUMMARY

The Stumpys Bay Sand is of Last Interglacial age and was deposited mainly in coastal embayments in response to a major single marine transgression to ~ 32 m. Its marine origin was established by the abundance of marine sponge spicules, the beach

ridge morphology of the eastern embayments, the sedimentary structures and grainsize characteristics of the deposits. Regression from the upper limit formed a declining series of beach ridges which may be partly related to minor transgressive or short term sea level stillstand phases. Conclusive proof of the age of the Stumpys Bay Sand will only be derived by radiometric dating, which to date is inapplicable for the sands. In the absence of such methods, a reasonably reliable age estimate has been derived from geomorphic and stratigraphic relationships within the area and by reference to the documented Last Interglacial sea level curve established from oceanic sediments and stable coastal areas.

Higher marine deposits in the area occur at maximum elevations of ~ 49 m and ~ 71 m, and are considered to be of oxygen isotope Stage 7 and Stage 9 ages respectively. Still older, higher, probable marine deposits occur to about 90 m.

Tectonic uplift since the Last Interglacial at a rate of approximately 0.21 m/ka has been inferred by comparison of the Stumpys Bay Sand upper marine limit elevation with the Last Interglacial eustatic sea level stand at ~ 6 m. Late Quaternary tectonic uplift may have commenced about 500,000 years ago and reached a peak between ~ 250,000-150,000 years ago. Tasmania appears to have undergone uplift independently of mainland Australia. Tasmanian activity is probably facilitated by relatively weak crustal attachment to the Australian plate. A stationary convection plume may be the principal driving force of the inferred Late Quaternary uplift.

PART II

Section 2

RELICT TERRESTRIAL DUNES: LEGACIES OF A FORMER CLIMATE

1. INTRODUCTION

This section analyses the distribution, morphology, and composition of the aeolian landforms and associated features in order to gain some insights into the climate of the Last Glacial Stage. The longitudinal dunes should hold some keys to the reconstruction of past air circulation patterns. Lunettes are lake shore features and fluctuations in lake level are often reflected in lunette morphology and stratigraphy. This aspect is studied so as to estimate palaeohydrologic conditions, particularly the changing relative importance of some components of the hydrologic cycle. Finally, the conclusions are compared with other areas in Tasmania, and on the Australian mainland, to see how the local evidence relates to existing knowledge of climates during the Last Glacial Stage.

2. LONGITUDINAL DUNES

2.1 Extent and Origin

Fields of longitudinal sand dunes occur over approximately 350 km^2 in coastal northeastern Tasmania (Figure 3b). Dune fields

occur on the sand plains at Tuckers Creek, Toddys Plain and Barooga. An extensive dune field extends almost without interruption from the Waterhouse area, through Tomahawk, to Boobyalla Plains. Suites of dunes extend from the western foot to the crest of Ringarooma Tier. Another large dune field in the north of the study area extends from Cape Portland and the northeastern flanks of Ringarooma Tier to the northwestern shores of Great Musselroe Bay. Suites of dunes extend eastwards from the Great Musselroe River in the Icena area. The most eastern dune field extends eastwards from the Great Musselroe River to Cape Naturaliste.

Most of the dune fields are found in close association with plains underlain by Stumpys Bay Sand. The dunes usually originate on the plains, extend up the flanks of the confining hills to the east of the plains and terminate near the hill crests.

The mean orientation of 89 well defined dune ridges is 099.6 ± 4.8° from True North. This WNW-ESE alignment is therefore very consistent over a wide area.

The average continuous dune ridge length is approximately 1 to 1.5 km but several ridges are up to 5 km long. The Ainslie Dune, which extends from Big Waterhouse Lake through Tomahawk, to the Boobyalla River is a linked set of dune ridges which can be traced continuously for 20 km. Ridge spacing is very variable but is commonly 300 to 500 m. The longitudinal dunes vary in height from 1-2 to about 10 m but the average dune height is around 5-6 m, and single ridges are often marked by peaks at dune convergences.

Field measurement of 18 representative, well defined dune ridges showed that strong asymmetry of dune flank slope angle occurs with the southern flanks always steeper than the northern flanks, and that lower dune ridges have lower slope angles. Figure 26 is a graph of northern flank angle versus southern flank angle. Linear correlation and regression analysis gave a correlation coefficient (r) of 0.969 and showed that $N = 1.53 + 0.5S$, where N = northern flank slope angle, in degrees, and S = southern flank slope angle, in degrees.

The distribution, morphology, and composition of the longitudinal dunes indicates an aeolian origin (pages 20-26). Their morphology also demonstrates (page 25) that they were a product of winds which blew mainly from the WNW.

2.2 Age

Due to the present lack of ^{14}C dates from the dunes the estimates of age which are given on pages 25-26 are based on their stratigraphy, morphology, and degree of soil development. These indicators all point strongly to a Last Glacial age for the longitudinal dunes.

Elsewhere in Tasmania there is evidence for dune formation during the Last Glacial Stage. Sigleo and Colhoun (1975) consider that aeolian erosion and deposition were widespread in southeastern Tasmania during the later part of the Last Glacial Stage. This is supported by morphologic, stratigraphic, palynologic and radiocarbon evidence. A radiocarbon date of 15,740 ± 700 BP (SUA-376) was obtained from charcoal in the siliceous sands of a dune at Malcolm's Hut Road, approximately 15 km northeast of Hobart.

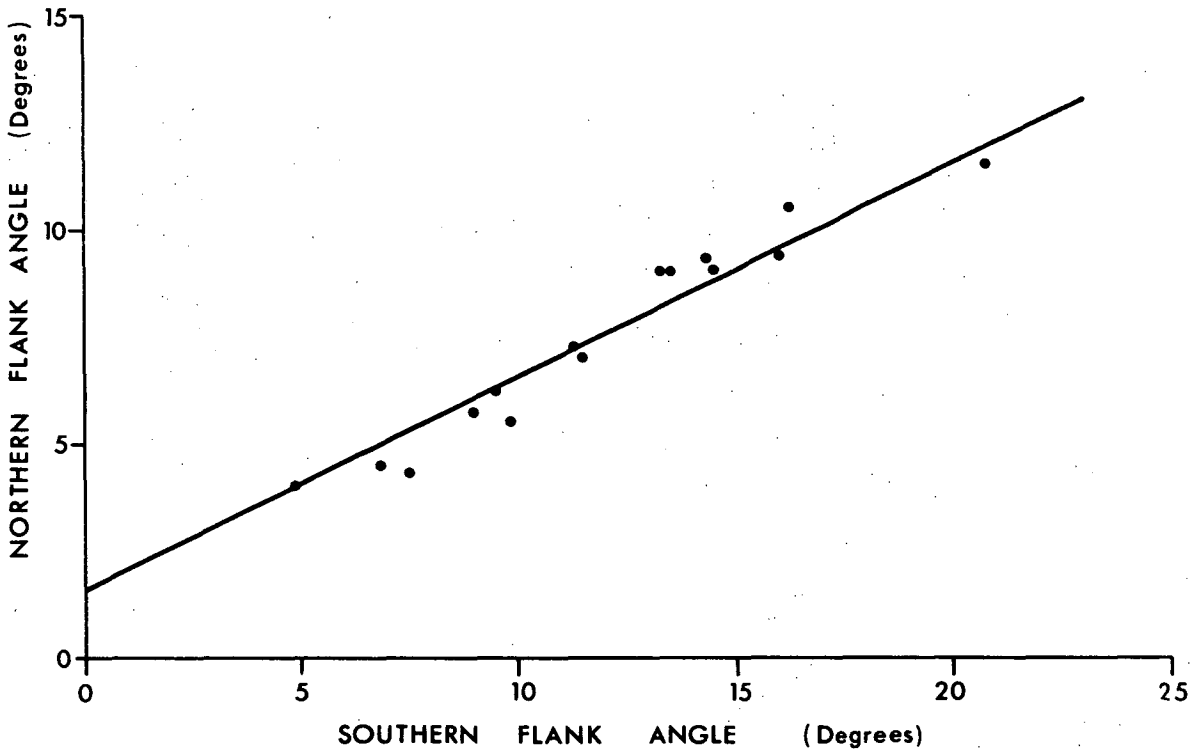

FIGURE 26 Relationship of north facing flank angle to the south facing flank angle of longitudinal dunes in northeastern Tasmania.

This age agrees with evidence from the Australian mainland which indicates that widespread dune formation took place between 22 ka and 14 ka (Bowler *et al.*, 1976).

Thus, the interpretation that the dunes of northeastern Tasmania are of late Last Glacial age fits well with the evidence of widespread aeolian activity from outside the region. This fact suggests that any estimates of climatic conditions during dune formation in northeastern Tasmania may be of value in determining broader scale circulation patterns.

2.3 Environmental Conditions During Longitudinal Dune Formation

The principal components of climate are temperature, precipitation, evaporation, and wind conditions. Given that the dunes are of Late Last Glacial age, it is possible to infer, from established work, the general climatic conditions during formation. It should also be possible to use direct evidence from the dunes and from contemporaneous deposits and features, to support and in some cases, to refine the climatic interpretations.

2.3.1 *Temperature*

Galloway (1965) concluded that the mean temperature of the warmest month during the height of the Last Glacial Stage in Tasmania was 5°C colder than the present. This estimate was based on changes in snowline elevation and changes in the elevation of the lower limit of solifluction. A figure of 8°C ± 2°C, derived from geomorphic and biogeographic evidence was considered by Bowden (1974) and Colhoun (1975) to represent the range of mean

annual temperature reduction during the latter part of the Last Glacial Stage in western Tasmania.

A reduction in mean annual temperature in northeastern Tasmania would have been one factor which contributed to longitudinal dune formation. Large plains of Last Interglacial age marine sand must have extended from their present coastal location onto the floor of Bass Strait, which was dry during the Last Glacial Stage due to the worldwide eustatic lowering of sea level. Vegetation cover may have been reduced in the lower temperature conditions and the potentially unstable sand plains were probably exposed to deflation.

The evidence for cold climate conditions during the deposition of the longitudinal dunes is outlined on page 25 but is expanded here. At Little Waterhouse Lake, which is bordered to the north by a steep dolerite hill, slope deposits are intermixed with dune sand. The slope deposits are up to 1.5 m thick and consist of very angular dolerite fragments up to 30 cm long, but most are 3 cm to 10 cm long (Plate 43). The dolerite particles are not enveloped by a thick weathering rind. The weathering rind is less than 2 mm thick and shows that post depositional weathering is not far advanced. A field section shows that the slope deposit contains more weathered dolerite fragments near the base, and fresher, more angular fragments near the top. This could indicate that the period of slope instability which removed the already weathered dolerite fragments was also responsible for some shattering and removal of the newly exposed fresh dolerite surface. This breakdown and removal has been mainly attributed to freeze-thaw action and the slope deposits are therefore considered to be the product of a cold climatic environment.

PLATE 43 Slope deposits on the southern flank of Hardwickes Hill near Little Waterhouse Lake.

The lower flanks of the hill are superimposed with dune sand which has the same moderately well developed podzol soil profile as the longitudinal dunes and they therefore seem to be of the same age. Many angular dolerite fragments are intermixed with the dune sand (Plate 44) and show that the slope deposits were being formed at the same time as the dune sand was accumulating.

Further intermixing of slope deposits and dune sand occurs at Three Mile Hill, near Cape Portland, in a very similar situation to that described above. Plate 45 shows the angular dolerite fragments mixed in the A_1 and A_2 horizons of the podzolized dune sand near Three Mile Hill.

The combined evidence is inconclusive but points towards colder conditions during formation of the longitudinal dunes. The surface instability which was partly induced by lower temperatures may have been one of the factors which combined to encourage remobilization of the sand plain surfaces to form the fields of longitudinal dunes.

2.3.2 *Precipitation*

Terrestrial linear dunes require arid or semi-arid climatic conditions for their formation. The presence of the longitudinal sand dunes alone provides some evidence of increased aridity during the Last Glacial Stage because decreased precipitation would be very effective in reducing the vegetation cover sufficiently for aeolian mobilization of the sand plains and dune formation. Therefore the dune fields may be considered the outcome of both reduced precipitation and temperature.

A feature which provides direct evidence of reduced rainfall is the presence of a groundwater podzol $B_{2h,ir}$ soil horizon,

PLATE 44 Slope deposits consisting of angular dolerite fragments intermixed with Last Glacial age dune sand near Little Waterhouse Lake (Hardwickes Hill).

PLATE 45 Angular dolerite (slope deposits) intermixed with Last Glacial age dune sand at Three Mile Hill (Cape Portland). The top of the $B_{2h,ir}$ soil horizon is 20 cm below the hand at left.

in the coastal sand plains, which is well below the groundwater level today, and hence has not been formed by the existing hydrologic regime. If this groundwater "level" can be demonstrated to be of Last Glacial age it should provide a key to the hydrologic conditions during that time.

Field records of 15 auger holes drilled through the Stumpys Bay Sand to the impermeable weathered granite basement at Tomahawk indicated the presence of a groundwater podzol $B_{2h,ir}$ horizon at depth. The average depth of the top of the horizon was 3.99 ± 0.73 m. Of the 18 remaining holes drilled, 12 were less than 4.5 m deep and were therefore too shallow for the horizon to occur, or to be sure that the groundwater level represented by the horizon was not influenced by proximity of the basement. Records from the six other holes did not show the presence of a well defined, deep $B_{2h,ir}$ horizon which was probably mainly due to its occurrence between the sampled depths. The sample interval was approximately 0.9 m. This horizon was also found in the three holes drilled at Stumpys Bay and the one hole drilled at Barooga.

The thickness of the deep $B_{2h,ir}$ horizon is difficult to estimate due to the interval sample method but where records were taken the thickness was from 0.3 to 0.6 m and it was always less than 1.0 m thick. The average thickness of the horizon is taken to be approximately 0.6 m.

This deep groundwater $B_{2h,ir}$ horizon may represent a period in the past when the groundwater level consistently fluctuated from a depth of approximately 4.0 m to 4.6 m. Under the present climatic conditions the water table fluctuates from

near ground level in the low areas to a depth of around 2 m. Thus, the deeper water table levels and the apparent decrease in amplitude of the groundwater fluctuations indicated by the fossil groundwater podzol $B_{2h,ir}$ horizon probably reflect a period when the water inputs to the system were lower than today.

Since the sand plain is of Last Interglacial age the fossil groundwater podzol must be of this age or younger. It is highly unlikely that the fossil $B_{2h,ir}$ horizon is of Last Interglacial age for the following reason. The climatic conditions during the Last Interglacial were probably very similar to those of today and groundwater which accumulated in the marine sand plains after the retreat of the sea from its maximum elevation probably also fluctuated within 2 m of the surface. Evidence of this older groundwater podzol has been found in many localities at Tomahawk. Small, discontinuous layers of heavily indurated and oxidized organic and ferruginous sand occur at or just below the surface of the plains. These are interpreted as the remains of the interglacial groundwater podzol $B_{2h,ir}$ soil horizon which has been exposed by deflation, and therefore oxidized, during the Last Glacial Stage. Similar features occur at Rockbank (page 124) and are also considered to be of Last Interglacial age. Thus, it is most likely that the groundwater levels of the late Last Interglacial Stage fluctuated near the surface of the sand plains.

Since the deep fossil groundwater podzol is therefore younger than the Last Interglacial and older than the Holocene during which formation of the current groundwater podzol near the surface has taken place, it must be of Last Glacial age. The question which now must be asked is: can the deep fossil groundwater podzol $B_{2h,ir}$ horizon provide evidence of the water balance,

particularly rainfall inputs, during the Last Glacial Stage? The following section will attempt to provide a first approximation to this question and is dependent on the principles of groundwater dynamics which were determined for the Tomahawk plain and which are defined in Part III.

Organic colloids and sesquioxides which are leached from above are deposited close to the water table under normal groundwater podzolization conditions to form the $B_{2h,ir}$ zone. The occurrence of the fossil groundwater podzol $B_{2h,ir}$ horizon between an average depth of 4.6 to 4.0 m indicates that the water table regularly fluctuated by 60 cm. As the present water table fluctuates by 1-2 m annually and has produced a groundwater podzol $B_{2h,ir}$ horizon 1-2 m thick it is reasonable to assume that the 60 cm thick $B_{2h,ir}$ of the fossil groundwater soil profile represents an annual water table fluctuation of approximately 60 cm.

The fossil groundwater podzol therefore reveals two pieces of information about the groundwater conditions during the Last Glacial Stage. These are: a) the water table was nearly always at or above 4.6 m depth, and b) the water table fluctuated annually by approximately 0.6 m. It is now possible to estimate the hydrological conditions needed to keep the water table at a depth of 4.6 m and to produce annual fluctuations of 60 cm.

During the Last Glacial Stage the East Tomahawk sand plain would have extended seaward of the present coast because sea level had drained Bass Strait. Therefore, the leakage from the aquifer which is now lost to the sea would not then occur. However, the Tomahawk River would have extended across the plain since the later part of the Last Interglacial Stage and was

therefore a pathway for leakage from the aquifer during the Last Glacial Stage. The weathered granite beneath the sands forms a very efficient aquiclude and therefore little or no water loss could occur through the base of the sands. The only other pathway for water loss was to the atmosphere due to evapotranspiration.

Water inputs to the aquifer could only have come from rainfall and runoff from the catchment. Rainfall is by far the most significant contributor to the aquifer system today. The low amount of runoff is readily absorbed at the margins of the sand plains but the excess water in the margins is very rapidly lost by evapotranspiration. Redistribution of this source of excess water by groundwater flow within the aquifer is a much slower process and evapotranspiration extracts the excess water faster than it can flow through the aquifer. Runoff therefore has very little influence on water level fluctuations away from the margins of the plain. Incident precipitation is considered also to have been the sole source of groundwater over most of the aquifer during the Last Glacial Stage.

Water table fluctuations during the Last Glacial Stage were therefore controlled by the interaction between direct precipitation inputs, and water losses by evapotranspiration and leakage to the Tomahawk River.

A balance between inputs and outputs must have occurred to maintain the water table at a depth above 4.6 m, but the total water inputs and outputs were lower to produce equilibrium conditions with a lower water table. It is now possible to calculate the conditions required to keep the water table above this depth by estimating the amount of rainfall which would be required to

keep pace with water loss to the Tomahawk River. From page 245 the amount of water lost (L_s) to the Tomahawk River per day is given by $L_s = Sp \times Th \times I \times P \ m^3/d$ .... (1)

where Sp = length of aquifer cut by river (m)

Th = sand thickness at the river (m)

I = the water table gradient

P = sand permeability ($m^3/d/m^2$)

$\therefore L_s = 5000 \times 4 \times 0.01 \times 4 \ (m^3/d)$

$= 800 \ m^3/d$

$= 800 \times 1000 \times 365$ l/year

$= 292 \times 10^6$ l/year

This represents a loss which is distributed over an aquifer area of $18.25 \times 10^6 \ m^2$.

Therefore, this is a loss of a layer of water over the whole area which is $\frac{292 \times 10^6}{18.25 \times 10^6}$ = mm thick

= 16.0 mm

Thus, 16.0 mm of rainfall was needed to reach the water table in order to keep pace with the annual loss through leakage to the Tomahawk River.

However, for water to reach the water table the sand above the water table must attain field capacity. If the sand is below field capacity then rainfall will be absorbed by the zone of aeration until field capacity is reached and water is able to drain freely to the water table (see pages 271-273, Part III). Over an annual period slow gravity drainage takes place which reduces the soil moisture content to below field capacity and further losses to the soil moisture occur through evapotranspiration.

Therefore the soil moisture must be restored to field capacity before any water can be added to the zone of saturation.

The usual minimum soil moisture content is determined by the pellicular limit, which is the proportion of the soil pore space which contains pellicular water. Pellicular water is held by strong adhesive forces and is therefore relatively immobile (page 253). By assuming that the soil moisture profile above the water table is reduced to the pellicular limit each year it is possible to calculate the amount of rainfall needed to restore the moisture profile to field capacity to allow water to enter the groundwater store.

In Figure 27 the area $\frac{R}{\phi}$ is the rainfall required to increase the soil moisture content from the pellicular limit to field capacity, which is expressed as a proportion of the porosity and is equal to DWT x (FC - PL).

$$\therefore \frac{R}{\phi} = DWT \times (FC - PL) \quad .... \quad (2)$$

where R = Rainfall (mm)

ϕ = Porosity of the sand

DWT = Depth to the water table (mm)

FC = Field Capacity (as a proportion of porosity)

PL = Pellicular limit (as a proportion of porosity)

The porosity and field capacity for clean sands have been determined at Tomahawk (page 260) and are approximately 40% and 35% respectively. The pellicular limit was not measured but is probably about 20% of the soil water for clean sands.

From equation (2)

$$R = 4600 \times (0.35 - 0.20) \times 0.40 \text{ (mm)}$$

$$= 276 \text{ mm}$$

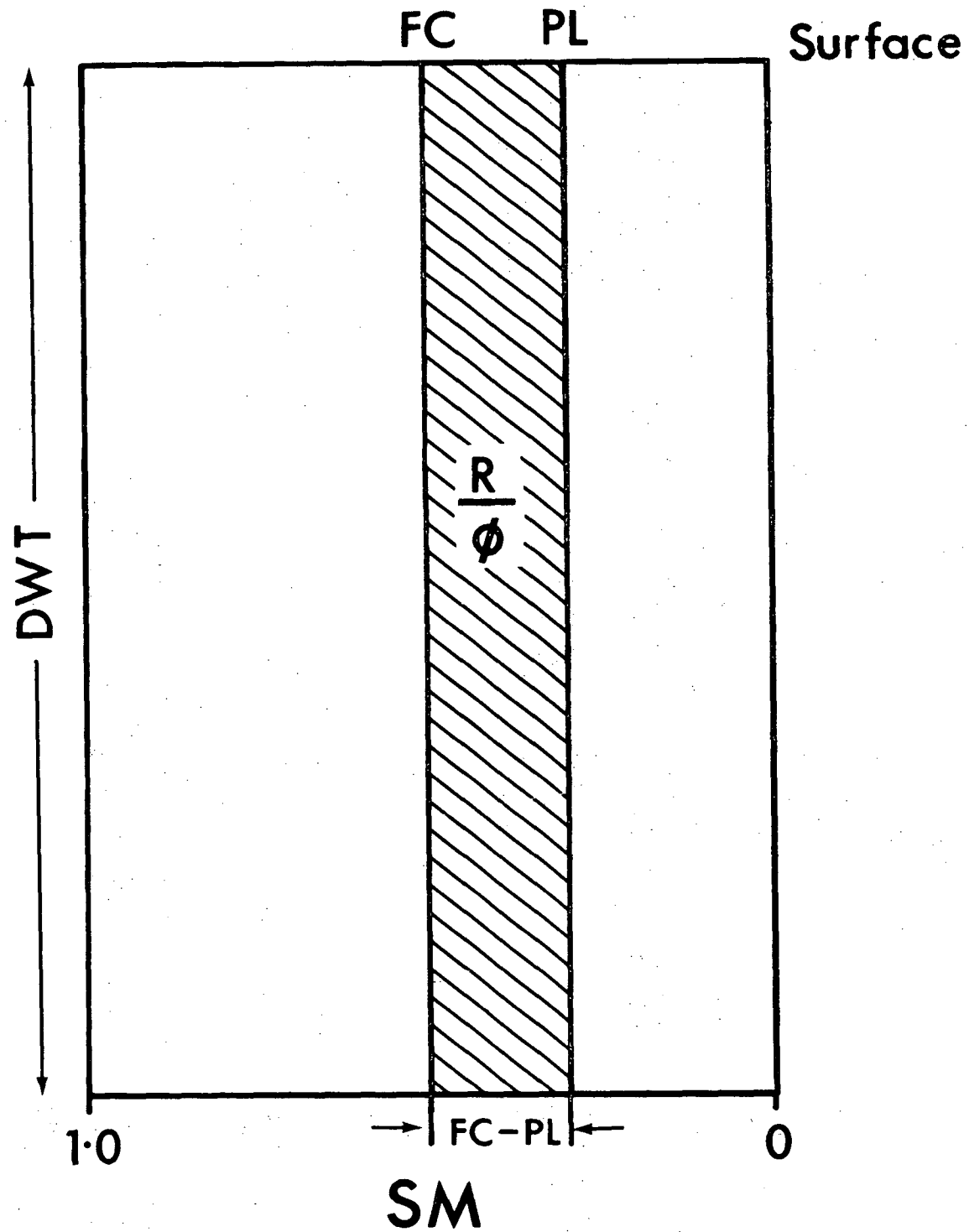

FIGURE 27 Soil moisture conditions at Tomahawk.

DWT = Depth to water table
SM = Soil moisture, expressed as a proportion of porosity
R = Rainfall
ϕ = Porosity
FC = Field capacity
PL = Pellicular limit

Therefore the total rainfall needed to maintain the water table at 4.6 m is 16 + 276 mm = 292 mm per year.

The amount of additional rainfall required to increase the water table level from -4.6 m to -4.0 m is given by the relationship shown in Figure 56 and is 135 mm. The annual rainfall therefore to maintain the water table above -4.6 m and to produce 60 cm fluctuation per year is 292 + 135 m = 427 mm.

Since the system is at equilibrium over a yearly period the losses from evapotranspiration would have been 427 - 16 mm = 411 mm.

This derivation of the mean annual rainfall is only a first approximation and is not considered to be a rigid value. Annual rainfall is innately a very variable quantity and areas which have low mean annual rainfall often show marked rainfall variability from year to year. In addition precipitation is likely to have varied considerably during the Last Glacial Stage.

One of the main assumptions, that the water table only moves once per year through the 60 cm fluctuation, does not take into account smaller range oscillations which may occur between the two water table limits and hence this is a potential source of under-estimation of the calculated rainfall. However, this assumption is supported by hydrographs of the water table response when the water table is low. Figures 43 and 49 show that when the water table is high, within 1 m of the surface, the water table shows large fluctuations over short periods but when it falls to more than 1 m below the surface the fluctuations become much more subdued and occur over a longer time period. This is because slow gravity drainage and evapotranspiration lower the soil moisture content during the dry conditions, and the zone of

aeration above the water table therefore acts as a buffer to short term surface inputs and outputs. This buffer effect would be more pronounced with the water table at 4-4.6 m and would smooth out the temporal water table fluctuations even more.

It is also recognized that rainfall which contributed only to the soil moisture profile when field capacity was not attained, and the subsequent extraction of that water by evapotranspiration would not have been manifested by changes in the water table level. This possibility has not been included in the estimate of annual rainfall. The omission may in part be balanced by the over-estimate of water needed to re-establish field capacity. This estimate is a maximum estimate based on the soil moisture being reduced to the pellicular limit throughout the 4.6 m soil profile. While this may have been true for the surface 2 m or so, due to its proximity to the surface and evapotranspiration forces, the lower portions of the profile may only have been slightly below field capacity because evapotranspiration becomes less effective with increased depth.

The Last Glacial age rainfall which has been derived is dependent on several assumptions which may not be entirely accurate. However, the perceived dynamics of the system are based on substantial field observation and are probably a fairly accurate representation of the groundwater hydrology. The estimate therefore is considered to be a reasonable first approximation of the rainfall at the time.

The present rainfall at Tomahawk is 790 mm per year and a Last Glacial rainfall of 427 mm is 54% of today's value. Present evapotranspiration at Tomahawk has been estimated as approximately 75% of pan evaporation (page 235) while

evapotranspiration during the Last Glacial Stage was about 33% (411 mm/year) of the potential evaporation (1240 mm). Potential evaporation during the Last Glacial Stage in northeastern Tasmania is considered by Nunez (In Prep.) to have been approximately the same as today. The lower amount of water loss through evapotranspiration during the Last Glacial Stage therefore seems almost certainly to have been a function of a reduction in vegetation cover which greatly reduced transpiration.

Several arguments can be put forward to explain increased aridity in northeastern Tasmania during the Last Glacial Stage.

Reduction of sea level during the Last Glacial Stage and consequent draining of Bass Strait would have increased the continentality of northeastern Tasmania. This would have caused a decrease in precipitation because the moist northwesterly circulation patterns which bring occasional rain to northeastern Tasmania derive moisture from the waters of Bass Strait. Drainage of Bass Strait to form a large continental plain (Figure 5) takes away the moisture source of these northwesterly winds. In addition, intense low pressure systems which currently move eastwards through Bass Strait and bring moisture to northeastern Tasmania would have been similarly affected by the presence of land in the Bass Strait area.

The more consistent zonal westerly air flow which is postulated for the Last Glacial Stage (Derbyshire, 1971; Galloway, 1965) would have formed a stronger barrier to the passage of easterlies which presently bring much rain to northeastern and eastern Tasmania. These systems were probably not as frequent in the area as they are today.

Cooler sea surface temperatures during the Last Glacial Stage would have reduced the moisture content of the westerly air streams due to decreased evaporation from the cooler ocean surfaces.

Figure 28 is a rainfall map of Tasmania which shows the strong decreasing rainfall gradient from west to east. The high west coast rainfall is due largely to orographic rainfall from moist westerly air streams. During the Last Glacial Stage when sea level was approximately 120 m lower than today, a larger proportion of this moisture may have been intercepted by the west coast mountains due to their increased elevation relative to sea level. Consequently, any increase in rainfall reception by the western regions would have had a stronger relative influence on the total rainfall received in the eastern areas. This would tend to increase the precipitation gradient.

Many workers believe that southeastern Australia during the Last Glacial Stage was more arid than the present. Galloway (1965) used a water balance approach to calculate the Last Glacial Stage rainfall at Lake George, which was little more than half the present long-term mean rainfall on the lake. Bowler *et al.* (1976) concluded from their review of research on the last decade that "throughout Australia cold periods seem generally associated with precipitation lower than today". (page 390). The evidence from northeastern Tasmania supports these views and points to cool, dry conditions.

2.3.3 *Wind*

Air circulation patterns during the Last Glacial Stage produced the large fields of longitudinal dunes. This section

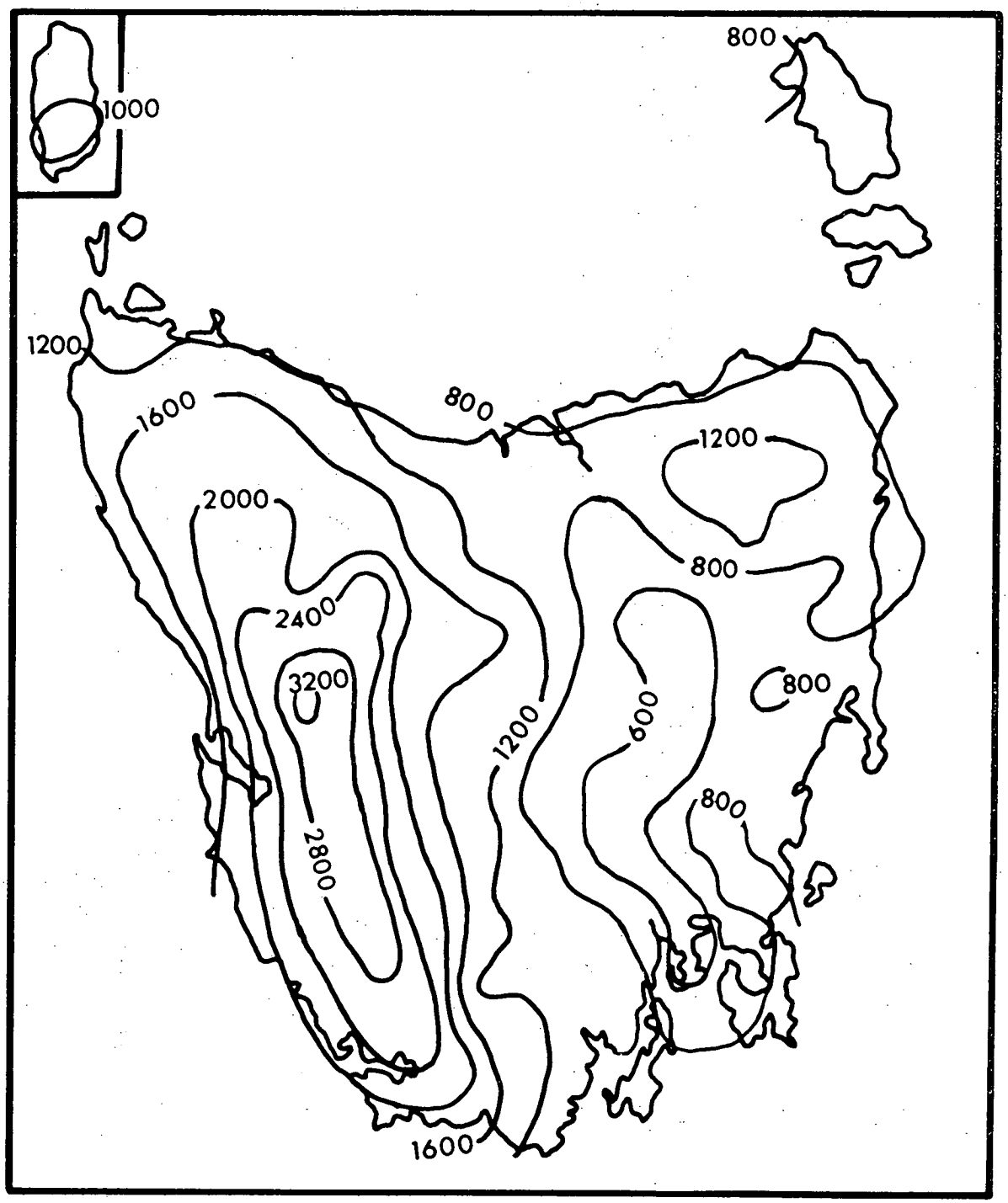

FIGURE 28 Mean Annual Rainfall of Tasmania.

(After Australian Bureau of Statistics, 1976, *Tasmanian Year Book* No. 10, p. 54).

Rainfall in mm.

attempts to examine the dunes and use evidence from them to estimate the wind direction and probable wind strength.

2.3.3.1 Wind Direction

The consistent linear arrangement of the longitudinal dunes as depicted in Figure 3b, is obviously very closely related to the direction of the winds at the time of their formation. Taylor (1930), Madigan (1936), King (1956, 1960) and Veevers & Wells (1961), concluded that alignment of longitudinal dunes was parallel to the prevailing wind and that dune asymmetry was due to infrequent cross-winds. Bagnold (1941), Mabbutt (1968) and Twidale (1972) considered that longitudinal dunes are the product of a bi-directional wind regime, and Mabbutt (1968) considered that cross-winds produced dune asymmetry. Brookfield (1970) measured wind regime over a short period, compared it with dune orientation and concluded that the main dune system neither correlates with nor diverges consistently from the mean wind direction. Mabbutt, Woodings and Jennings (1969) put forward arguments that dune asymmetry was due to a combination of turning of wind with height, unequal solar heating on the dune flanks, and a shift of the circulatory system. However Clarke & Priestley (1970) discounted the first mechanism on aerodynamic grounds and stated that asymmetry was caused by different seasonal synoptic conditions rather than climatic change and felt that this explanation was simpler than the theory of patterned thermal convection advanced by Mabbutt, Woodings & Jennings. Folk (1971) however, considered that the longitudinal dunes were the result of undirectional currents undergoing second order helical circulation. He also thought that the dune trend was parallel to the one predominant wind and that occasional cross-winds

produce crestal asymmetry, which is a view generally shared by the field workers. The prospect of more refined conclusions is best summed up by Mabbutt (1968) who said "... more detailed analysis of wind regime and of dune geometry are needed to establish the genetic relationship between the two ..." (page 147). This view was reiterated by Twidale (1972) when he wrote "A fundamental difficulty in evaluating these various suggestions ... is that there are no continuous and detailed observations of wind direction and strength from the desert proper ..." (page 81).

The longitudinal dunes of northeastern Tasmania bear a strong resemblance to the dunes of parts of central Australia and also consistently show crestal asymmetry; the southern flanks being steeper than the northern flanks (page 151). Following the general conclusions of the workers on the Australian mainland the Tasmanian dunes are probably the result of a predominant wind from the WNW (the mean dune orientation is towards 100 ± 5°) and the dune asymmetry could also be a product of occasional cross-winds from the northwest.

Detailed wind data are not available for coastal, northeastern Tasmania, and the problems pointed out by Mabbutt and Twidale have been recognized. Nevertheless, some comparison can be made of past with present wind conditions in northeastern Tasmania by utilizing a data source which is not available in central Australia.

Coastal parabolic dunes up to 2 km in length occur in close juxtaposition to the Last Glacial age longitudinal dunes and were formed under wind conditions of the last 6000 years (page 40). A comparison of the orientation and symmetry of the two sets of

dunes should provide some insights into the problem of whether dune forming wind directions have altered since the Last Glacial Stage.

Both sets of dune forms, although not of the same origin, are similar in that they consist of long, narrow, discrete dune ridges. Also, field observations show that the Holocene parabolic dunes have asymmetrical cross profiles with the southern flanks being steeper.

Measurement of the orientation of 86 parabolic dune ridges showed that the mean orientation is towards 097.9 ± 4.65° from True North. The mean orientation of 89 longitudinal dunes is towards 099.6 ± 4.76° from True North. Superficially, the two sets of dunes appear to have the same orientation. Application of a "Student's" t-test, which tests the probability that two sample means are from the same population, showed that there was less than a 2% chance that the samples were from the same population ($t = 2.367$, $v = 173$). Therefore there is a statistically significant difference between the mean orientation of the two sets of dunes, even though they are oriented in very similar directions.

The conclusion which has been drawn from the preceding evidence is that the dune forming winds, regardless of the actual relationships between wind regime and dune orientation, have shifted since the Last Glacial Stage. The Last Glacial circulation was from the WNW, but appears to have been from a slightly more northerly direction than the present.

2.3.3.2 Wind Strength

Dunes are direct products of the wind regimes in operation during dune formation. It is reasonable to expect therefore, that

the composition of a dune sand should partly reflect the intensity of the agent of deposition. For example, there should be a relationship between dune sand grainsize and wind velocity if a wide range of source material is available. A dune which is formed by strong winds should contain a larger proportion of coarser sand than a dune which was formed by light winds, because the lower velocity winds are not able to transport the coarser material. This is the underlying assumption of the first of the following two attempts to gain an impression of the wind intensity during formation of the longitudinal dunes. The second attempt, which is largely designed to provide a rough test of the first method, uses the problematical relationship between grainsize and threshold velocity to estimate wind speed of dune formation.

A sinuous grainsize pattern emerged from dune crest samples of the longest longitudinal dune in the study area. This dune, the Ainslie Dune, was sampled at a consistent depth of 0.5 m within the A_2 soil horizon and the samples were 450 to 500 metres apart.

The dune crest was selected as the sampling point to evaluate grainsize variation along the dune after analysis of samples taken from a transect across the dune. Figure 29(a) shows that the grainsize characteristics of samples taken across the dune at a uniform depth of 40-60 cm, and from within the A_2 horizon, are very similar. There is only approximately 0.3 ϕ variation of mean grainsize and 0.15 ϕ variation of the sorting co-efficient.

However, both the mean size and the coarsest percentile graphs show that the three samples from the crest of the dune are coarser than the sand on the flanks. The characteristics shown by this dune agree very well with the results of Folk (1971) who

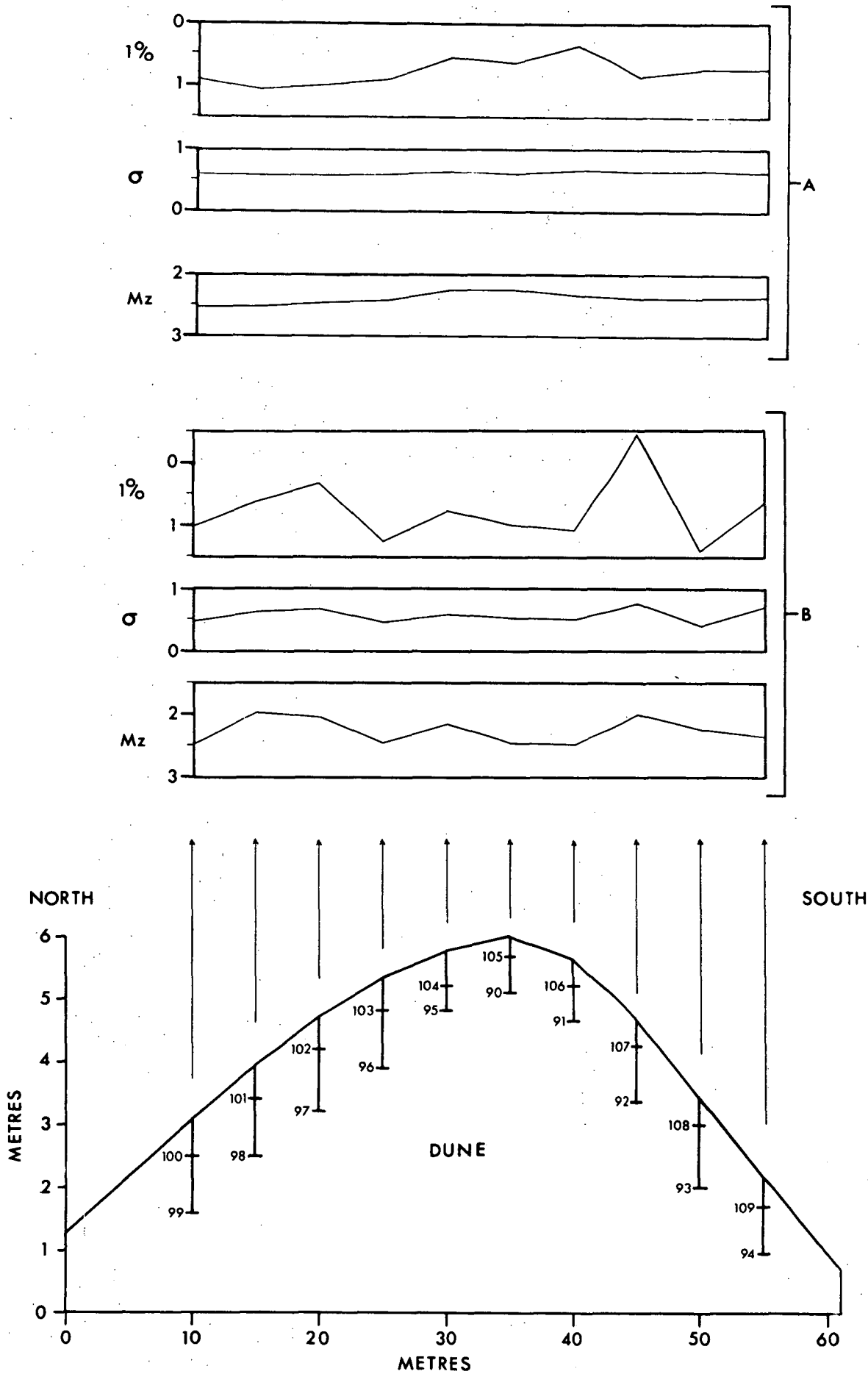

FIGURE 29 Grainsize characteristics of samples taken from a transect across Ainslie Dune.

A shows the values for the shallow samples, 100-109;
B shows the value for the deeper samples, 90-99.
1% is the size of coarsest 1% of the sample. σ is the sorting coefficient. Mz is the mean grainsize (measured in Phi units)

sampled longitudinal dunes in the Simpson Desert. Table 5 below compares the results from each region and shows that these minor grainsize differences across the Ainslie Dune are usual for Australian dunes of this type.

Sample points which are selected to test grainsize variation along a dune must therefore be located either on the windward flank, the lee flank or the crest. The dune crest can be accurately determined in the field as the highest point of the dune and therefore is the logical choice as the sample location.

The sample depth had to be near the surface because the near surface samples showed much more uniformity than samples from deeper within the dune. Figure 30 shows the mean size and sorting variations of samples from an auger hole through a dune at Carisbrooke. Figure 29(b) is a graph of the same parameters of samples taken from the B_2 horizon of the transect at variable depths between 1.5 and 2.5 m. These data show that the mean grainsize from a dune cross section may vary by up to 0.6 ϕ. This variation may be a composite product of slight lateral dune crest shift and intermittent, local erosional events during the period of dune formation.

The median grainsize, the sorting coefficient and the coarsest percentile of samples from the crest of the Ainslie Dune are plotted in Figure 31. The sampled dune length is 16.4 km. All of the parameters vary in a marked cyclic pattern which becomes apparent to the east of sample numbers 127 and 128. The pattern shown by the coarsest percentile has been used as the basis for the following interpretation but the other parameters closely follow the pattern. The coarsest percentile was used because it shows a greater range of variation than the other measures.

TABLE 5 Comparison of Grainsize Characteristics of Longitudinal Dunes of the Simpson Desert and Northeastern Tasmania

Area	Crests coarser than flanks	Mean crest size (ϕ)	Mean flank size (ϕ)	Difference between crests and flanks (ϕ)	Windward flank coarser than lee flank	Difference between windward and lee flanks (ϕ)
Simpson Desert (Folk, 1971)	YES	2.53	2.75	0.22	YES	0.14
Northeastern Tasmania (one transect only)	YES	2.27	2.43	0.16	YES	0.12

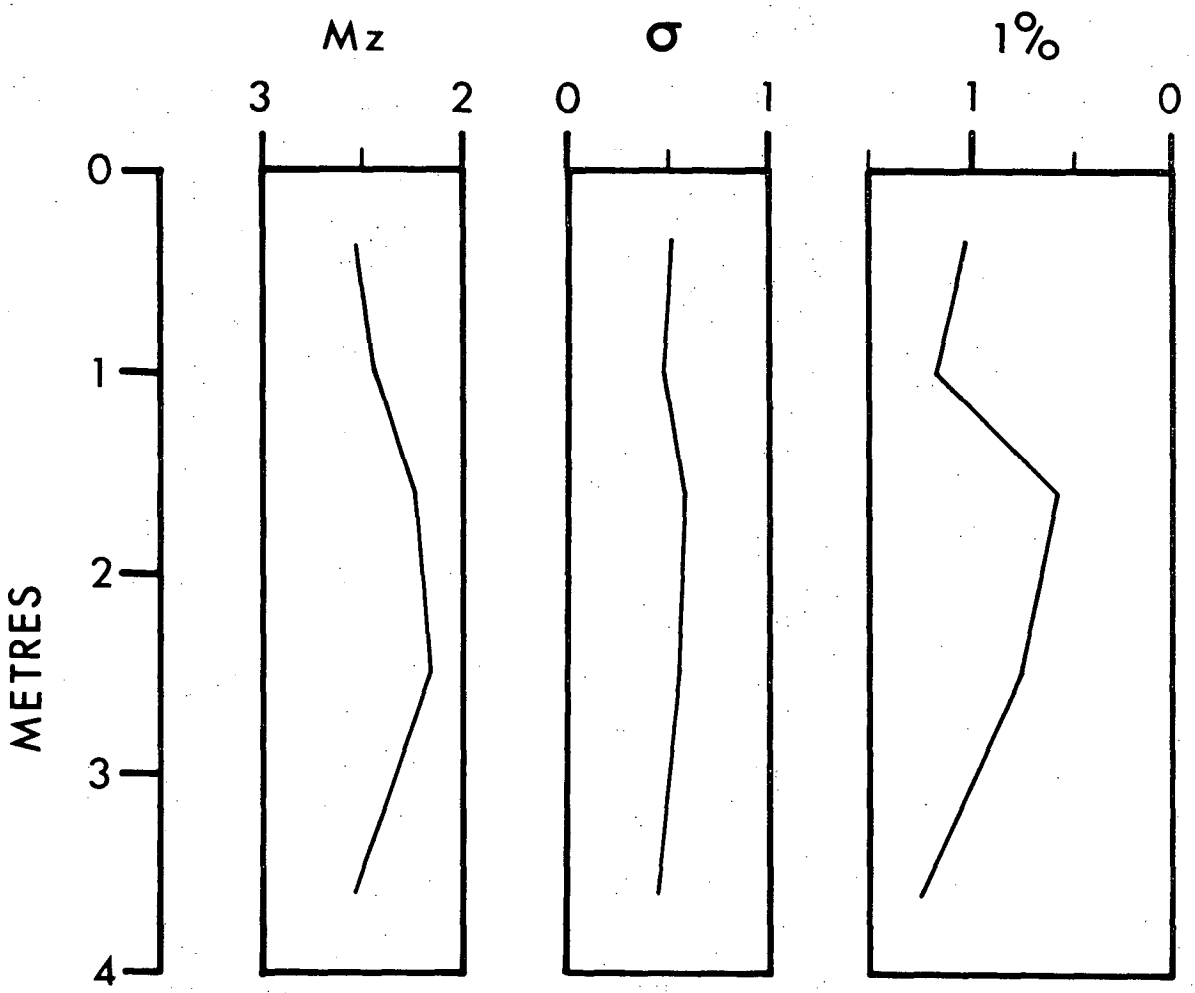

FIGURE 30 Grainsize characteristics taken from a profile through the Ainslie Dune.

Grainsize is measured in Phi units.

Mz = mean grainsize
σ = sorting coefficient
1% = the size of the coarsest 1% of the sample

FIGURE 31 Grainsize and threshold velocity variation along the Ainslie Dune.

σ = Sorting coefficient (ϕ)
Mdn = Median grainsize (ϕ)
1% = Grainsize of coarsest 1% of the sample (ϕ)

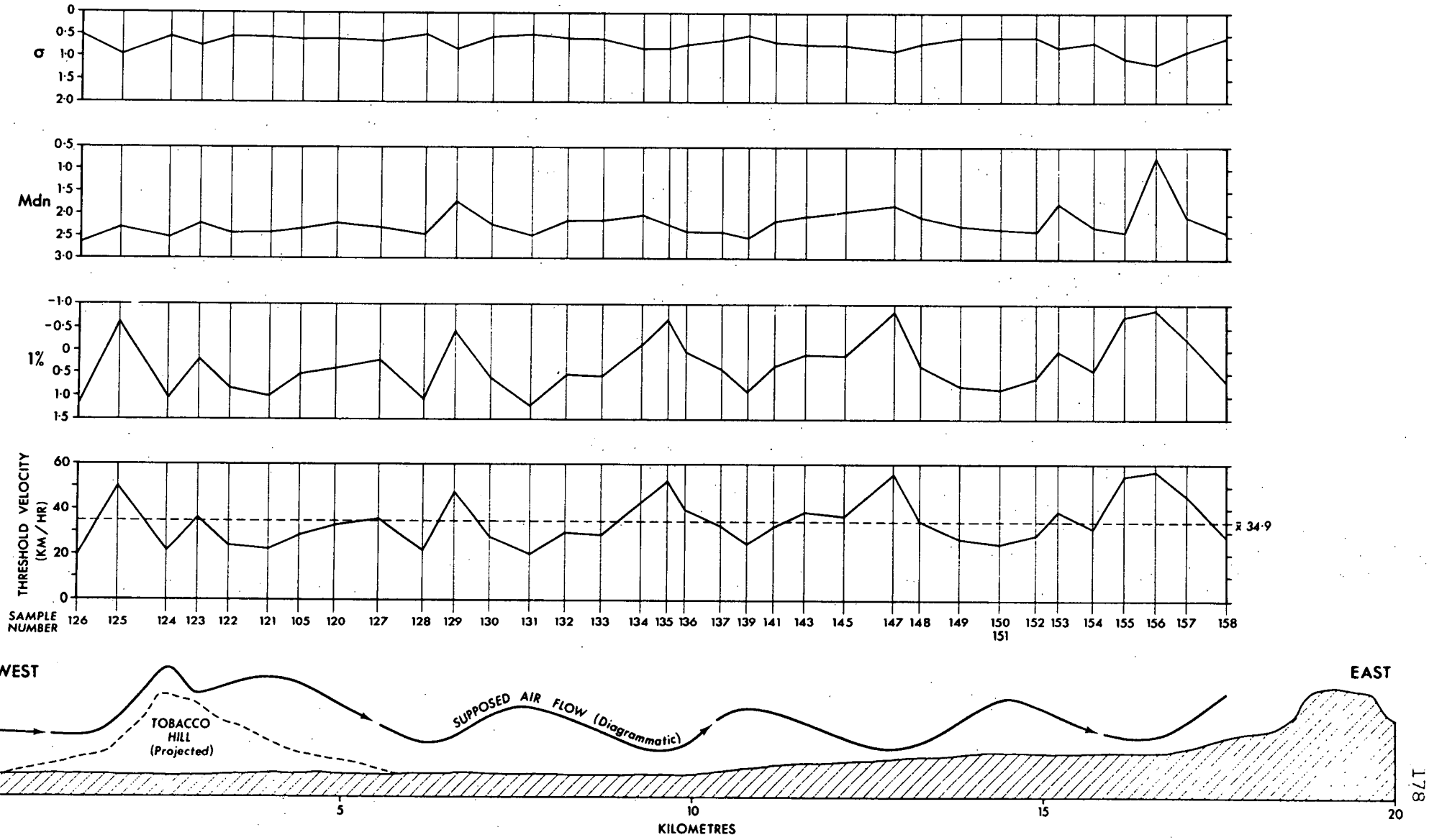
σ
0
0·5
1·0
1·5
2·0
Mdn
0·5
1·0
1·5
2·0
2·5
3·0
1%
-1·0
-0·5
0
0·5
1·0
1·5
THRESHOLD VELOCITY (KM/HR)
60
40
20
0
x̄ 34·9
SAMPLE NUMBER
126 125 124 123 122 121 105 120 127 128 129 130 131 132 133 134 135 136 137 139 141 143 145 147 148 149 150 151 152 153 154 155 156 157 158
WEST
EAST
ELEVATION (M)
60
40
20
0
TOBACCO HILL (Projected)
SUPPOSED AIR FLOW (Diagrammatic)
0
5
10
15
20
KILOMETRES

The cycles have grainsize peaks at sample localities 129, 135, 147 and 156, and troughs at sample localities 131, 139 and 150. The mean wavelength of the cycles is 3.35 km. The only genetic interpretation which has been placed on the cyclic variation of grainsize characteristics is that the depositional wind varied in its ability to transport sand along the direction of travel. Areas of larger grainsize correspond to areas where the wind was relatively stronger and the finer sand relates to areas where the wind was less intense. The cyclic pattern indicates that the variation of wind intensity was not random and that the repetition distance was about 3.35 km.

A commonly occurring and well documented air flow pattern best explains the cyclic variation in wind strength. Scorer (1948, 1961) and Holton (1972) describe the lee wave principle of laminar air flow. According to these authors, lee waves are very common and consist of a vertical wave motion of an airstream which is initiated by an obstacle, such as a hill, on a generally even surface. Lee waves are formed downwind of the obstacle and the wind velocity is twice as strong below the trough of the lee wave than below the crest. Scorer (1961) also showed that there is a direct relationship between lee wave length and wind speed.

The sand plain on which the Ainslie Dune is formed has an even surface and the dune lies at an elevation of about 20 m. Tobacco Hill, which lies 1 km north of the dune, is well positioned to initiate lee wave motion. This hill is 65 to 70 m high, and approximately 4 km wide in an east-west direction. The projected termination of Tobacco Hill onto the Ainslie Dune is approximately level with sample localities 127 and 128. Figure 31 shows the location of Tobacco Hill with respect to the Ainslie Dune.

Figure 31 also diagramatically shows the supposed air flow over the dune which is based on the location of peaks and troughs as determined from the grainsize maxima and minima.

There is a reasonable body of evidence which suggests that lee wave air flow may have been largely responsible for the grainsize variation along the Ainslie Dune. This allows an estimate to be made of the air flow velocity.

Scorer (1961) defined the relationship between wind velocity and wave length of lee waves as

$$\bar{u} = \frac{S^{\frac{1}{2}}}{\frac{2\pi}{\lambda}} \quad \ldots \quad (3)$$

where $\bar{u}$ = wind velocity (m/sec)

λ = wave length (m)

and S is a stability parameter

and $= \frac{g \times \Gamma}{To}$

where g = acceleration of gravity m/sec^2

Γ = atmospheric lapse value $^{\circ}K/m$

To = surface temperature ($^{\circ}K$)

As the flow is within an altitude of 100 m a lapse rate of 10°C/km has been used. The surface temperature has been taken as the mean annual temperature minus 6°C because the dunes were formed during the Last Glacial Stage (page 26). The Bridport mean annual temperature today is ~ 13°C, therefore the Last Glacial surface temperature for this calculation has been estimated at 7°C.

The air flow speed

$$\bar{u} = \frac{\left(\frac{9.8 \times 0.01}{280}\right)^{\frac{1}{2}}}{\frac{6.282}{3.35 \times 10^3}} \text{ m/sec.}$$

$$= 9.98 \text{ m/sec.}$$

$$= 35.92 \text{ km/hr}$$

Thus the wind speed required to produce lee waves with a wavelength of 3.35 km during the Last Glacial Stage in northeastern Tasmania is approximately 36 km/hr.

A method of testing whether this figure is of the right order of magnitude is to apply published relationships of wind threshold velocity to grain diameter. Two major methodological problems arise when using the technique to estimate wind speeds from the grainsize of dune sand. The first is to decide which part of the sample size spectrum to use. For example, is the mean size, the modal size or some other fraction best suited for the purpose? The second problem is related to the validity of the relationships between grainsize and threshold velocity and how the relationships can be applied to specific problems.

As the main concern is to determine the most frequently occurring wind velocity, consideration must be given to the relationship between dune sand size distribution and wind frequency. Folk (1971) pointed out that as early as 1898, Udden showed that the mean size of the dune crests was 2 to 3 ϕ, regardless of locality, because the dynamic properties of the wind tended to select that size. Therefore in any dune the 2-3 ϕ range will be strongly represented regardless of the wind regime during deposition.

Added to, and probably part of, this process the coarser grains which are moved by the more frequent, stronger winds will be greatly under-represented in a dune due to finer particle fallout as the wind subsides. The degree to which the coarse fraction related to the most frequently occurring winds is under-represented cannot be determined but the coarse fraction is a very much more sensitive indicator of high frequency winds than its relative proportions within a dune sand would suggest.

The selection of the coarsest percentile for determination of the frequently occurring wind speed was necessarily arbitrary and the coarsest five percent may have been more appropriate as it covers a higher proportion of the coarse tail of the grainsize frequency distribution. The difference in the results obtained by choosing between these two cut-off points is considered as part of the final assessment (page 185).

The second major methodological problem inherent in this analysis concerns the relationship between threshold wind velocity and particle size. The only way this can be overcome without entering the complex field of boundary layer aerodynamics, as described by Bagnold (1941), is to use published data on the relationship and at the same time, to be aware of their limitations when assessing the potential error of the application.

Zenkovitch (1967) summarized the findings of Petrov (1948) who found that "... particles with a diameter of 0.12 mm are set in motion when wind speed on the ground is 1.5 m/sec. The corresponding speeds for grain diameters of 0.32, 0.60 and 1.04 mm are 4.0, 7.4 and 11.4 m/sec." (Zenkovitch, 1967, page 586). These points have been plotted on Figure 32. Extension of the relationship into the coarser grainsize zone on Figure 32 has been done by extrapolation and is a potential additional error source.

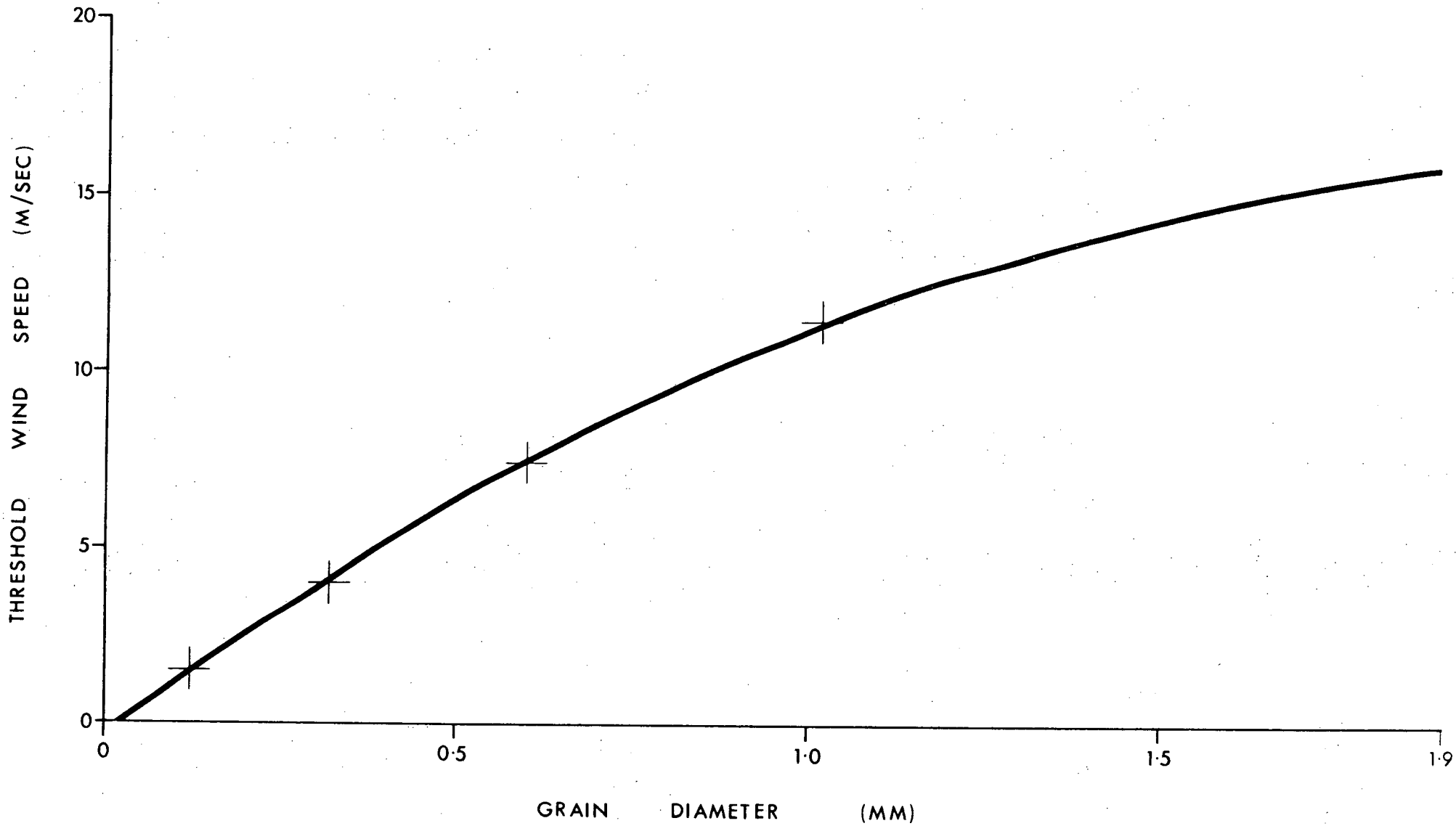

FIGURE 32 Wind Threshold Velocity versus Grain Diameter.

The major problem in applying this relationship is that wind speed on the ground is theoretically negligible due to the increasing effect of friction (Bagnold, 1941) and the measurements therefore must have been taken near the ground. Zenkovitch states that "... meteorological observations need adjustment, because wind speed is greatly reduced at ground level." (page 586). However, since dune deposition occurs near the ground the relationship should be reasonably valid for the present purpose.

Petrov's relationship was applied to the size of the coarsest percentile for all the samples along the Ainslie Dune. Figure 31 shows a plot of the resulting threshold wind velocity along the dune and shows that the maximum wind speed peaks at sample localities 129, 135, 147 and 156 average 53.6 km/hr. In addition, the mean threshold wind velocity for all data points is 34.9 km/hr.

The high level of agreement between the wind speed estimate of 35.9 km/hr derived from the lee wave calculation and the independent estimate of 34.9 km/hr derived from threshold velocities of the samples is perhaps a little unfortunate because it arouses a level of suspicion considering the imprecise nature of the inputs. However, the lee wave estimates are further supported by the threshold velocity calculations which show that the wind velocity beneath the lee wave crests is approximately 44% of the velocity beneath the lee wave troughs. This is in fair agreement with Scorer (1961) who stated that the wind velocity is twice as strong below the trough of the lee wave than below the crest.

The threshold velocity estimates can be loosely tested by estimating threshold wind velocities for samples from a Holocene

parabolic dune and comparing them with the present westerly wind strength. Seven samples spaced at 200 m intervals were taken from a depth of 0.5 m on the crest of the Holocene parabolic dune at Waterhouse. The grainsize parameters did not show any cyclic variation and the average threshold velocity derived from the coarsest one percent of the samples was 25.1 km/hr.

Bridport is the closest meteorological station but it is strongly sheltered from the westerly winds which have a long fetch in the Waterhouse area. Low Head, which is ~ 60 km west of the area is exposed to the westerly winds and probably most closely approximates the wind regime from this direction at Waterhouse. The Low Head wind data are based on 15 years of records and the average wind speed of westerly winds is 26.8 km/hr. For the Holocene dunes then, the threshold velocity derived from the coarsest one percent of dune sands approximates the meteorological average velocity of the westerly winds.

It seems therefore that the two major potential sources of error in the threshold velocity calculations compensate for each other. On the one hand the coarsest percentile probably represents a higher velocity wind than the mean wind speed and the coarsest 5 percent would probably be more appropriate. On the other hand the threshold velocity to particle size relationships has been taken at a level near the ground, where wind speed is greatly reduced, and the meteorological wind speeds are necessarily higher. The grainsize of the coarsest percentile of dune sand therefore appears to be quite a good indicator of the mean meteorological wind speed in this area, which allows more confidence to be placed in the mean wind speed estimates derived from the longitudinal dunes.

Thus, the mean wind speed of longitudinal dune formation during the Last Glacial Stage was approximately 35 to 36 km/hr, and has been derived from two independent sources of evidence. This speed is about 9-10 km/hr greater than the present mean westerly wind speed.

3. RUSHY LAGOON LUNETTES

The lunettes at Rushy Lagoon are the largest in the area and their morphology, stratigraphy and composition are examined in this section to define the stages of lunette development. As lunettes are fundamentally lake shore deposits, changes in the development of lunettes probably reflect changes in lake level which in turn are a reflection of changing relative effectiveness of the various components of the hydrologic cycle.

3.1 Origin

The physical setting of the old lakes, Rushy Lagoon and Mygunyah Lagoon, with their associated lunettes is shown in Figure 33. This map shows that the lakes are set in a broad depression which is filled with marine sands, silts and clays. The western boundary of the depression is formed by the dolerite bedrock of Ringarooma Tier while the lower granite hills of The Ranges enclose the depression to the east. A very low drainage divide passes through the area of Mygunyah Farm and through a low ridge of Mathinna Beds to the south. Another very low divide runs across the valley, tangential to the northern edge of Rushy Lagoon.

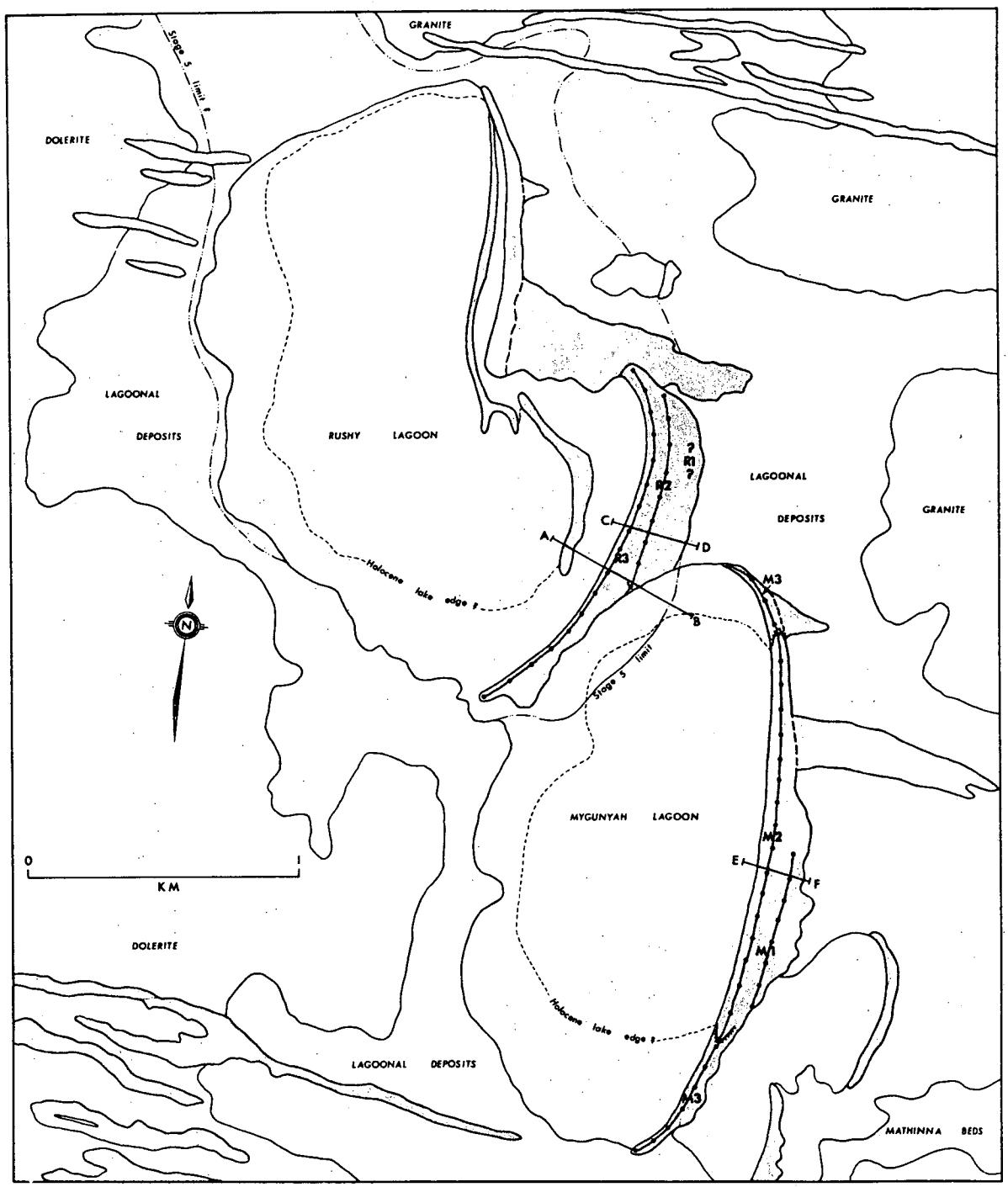

FIGURE 33 Rushy Lagoon Lake System and Lunettes.

Stippled areas are dune sands of the longitudinal dunes and lunettes.

Artificial ditches now drain Mygunyah Lagoon and Rushy Lagoon, and exit through the northern end of Rushy Lagoon. There is no evidence of natural surface drainage from the double lake system, but an outlet from Mygunyah Lagoon, which is 2.6 m higher than Rushy Lagoon, flowed into the southernmost corner of Rushy Lagoon, to form a very low angle distributary deposit.

The lakes probably originated as deflation hollows in the marine deposits. Lunette ridges bordering the eastern lake shores were developed under the influence of westerly winds, as lunettes occur on the lee shores of lakes (page 27).

A feature of Figure 33 is the occurrence of multiple lunette crests on the eastern shores of both lakes. Figure 34 shows surveyed profiles across both sets of lunette ridges with their morphology and simplified stratigraphy. The highest lunette in each set of ridges was augered and both showed a very similar sedimentary sequence.

The basal sedimentary unit of both lunettes is characterized by a medium to coarse sand which has been interpreted as a lake beach deposit. The relatively high elevation of this deposit 1-2 m above the lake levels, which are indicated by the break of slope at the lake edge of the innermost lunette, must be the result of wave action in the swash zone of the exposed lee shore, forming a beach above the quiet lake level. The basal unit does not represent a high lake level at Rushy Lagoon because there is no opposite shore at the northern end to contain the lake at that level.

In both ridges, the sequence above the beach sediments is marked by medium to fine grained sand beds 0.5 to 1.5 m thick separated by units of interbedded clay and medium-fine sand. The

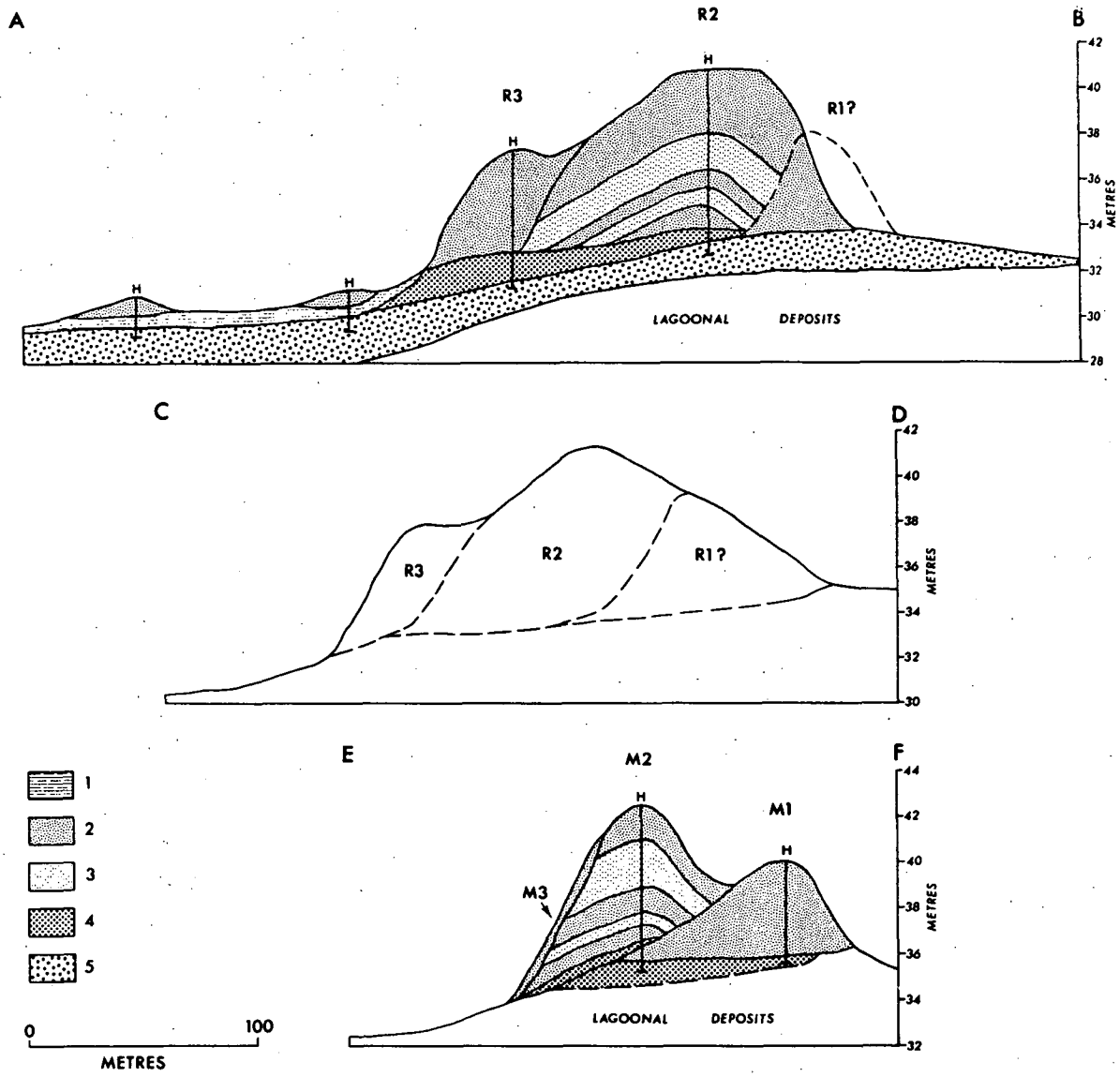

FIGURE 34 Profiles across the lunettes in the Rushy Lagoon area. VE = 20x.

The location of the profiles is shown in Figure 33.

1 = Lunette lake peat and clay
2 = Lunette sand
3 = Interbedded clay and sand
4 = Lake beach sand
5 = Stumpys Bay Sand
H = Location of auger hole

maximum thickness of these units is approximately 2 m. A section through the lunette ridge at Mygunyah Lagoon (Plate 46) shows the upper unit of interbedded clay and sand which is overlain by 1-2 m of medium-fine sand. The dark layer at the top of the cliff is the $B_{2h,ir}$ soil horizon from which the A_1 and A_2 horizons have been eroded. The top 1.5 m or so of the lunette is mantled in each case by medium-fine sand.

Field evidence suggests that three lunettes have formed at each locality, and have since been either partly buried or eroded, and that the two highest ridges are equivalent. Three lunette ridges occur on the eastern shores of Mygunyah Lagoon. A lunette ridge (M1) (Figures 33 and 34), composed entirely of sand lies behind the main lunette ridge (M2) and is therefore older. This ridge has been partly buried by the M2 ridge and is only topographically distinct for approximately one third of the length of the M2 ridge. A third ridge, M3, which is much lower than the M2 crest occurs as extensions to each abruptly terminating horn of the M2 lunette (Figure 33 and Plate 47). This extension of the lake shore indicates that the lake level was slightly higher during formation of the M3 lunette. This is also indicated by the lake proximal flank of the M2 lunette which appears to have been oversteepened by wave trimming. A thin veneer of sand approximately 50 cm thick was seen in small erosion gullies to truncate the clay beds on this windward lunette flank. This veneer is considered to be part of the M3 deposition.

Two lunette ridges are plainly evident on the eastern shore of Rushy Lagoon. The highest ridge R2, which has been equated with M2 on the grounds of stratigraphic similarities is separated from the lake shore by the R3 ridge, which is equivalent to M3 at

PLATE 46 Section at Mygunyah Lunette.

The interbedded clays and sands occur low down in the section and are overlain by sand.

PLATE 47 View from Rushy Lagoon lunette crest looking east towards Mygunyah Lagoon Lunette.

The flat lake floor of Mygunyah Lagoon is in the middle ground. The terminations of the M_2 lunette can be discerned towards each end of the lunette and are marked by sharp decreases in lunette height. The section through Mygunyah Lagoon Lunette (Plate 46) is to the centre-right of the ridge.

Mygunyah Lagoon. The profile AB of Figure 34 clearly shows that the back of the lunette sequence has been undercut by wave action on Mygunyah Lagoon. This has destroyed the morphology of the M1 equivalent at Rushy Lagoon. However, the profile EF, which has not formed part of the Mygunyah Lagoon lake shore, shows a faint convexity on the eastern dune flank. This suggests that a third lunette ridge, equivalent to M1, has been almost completely buried by the R2 lunette sediments.

Therefore the lunette sequence at Rushy Lagoon and Mygunyah Lagoon show three major stages of lunette formation. The recognition of multiple lunette ridges is used later (pages 204-211) as evidence of lake level fluctuation when reconstructing the environmental conditions during lunette formation.

3.2 Age

A wood fragment which was extracted from a section near the toe of the Rushy Lagoon lunettes in the drainage ditch which cuts through the Rushy Lagoon lunettes was submitted to Teledyne Isotopes, New Jersey, for radiocarbon analysis.

Analyses of the wood and humic acid extracts were reported as being 8,570 ± 135 BP (Isotopes Number I-11,448-A) and 8,435 ± 185 BP (Isotopes Number I-11,448-B) respectively. The Libby half-life of 5,568 years was used for the age calculation and no correction was made for variation in the atmospheric ^{14}C. The close age correlation of the two fractions demonstrates that the age determinations are reliable.

The stratigraphic position of the dated sample is shown in Figure 35. The section is close to the windward flank of the Rushy Lagoon lunette and the sand, peaty sand, and wood layer could

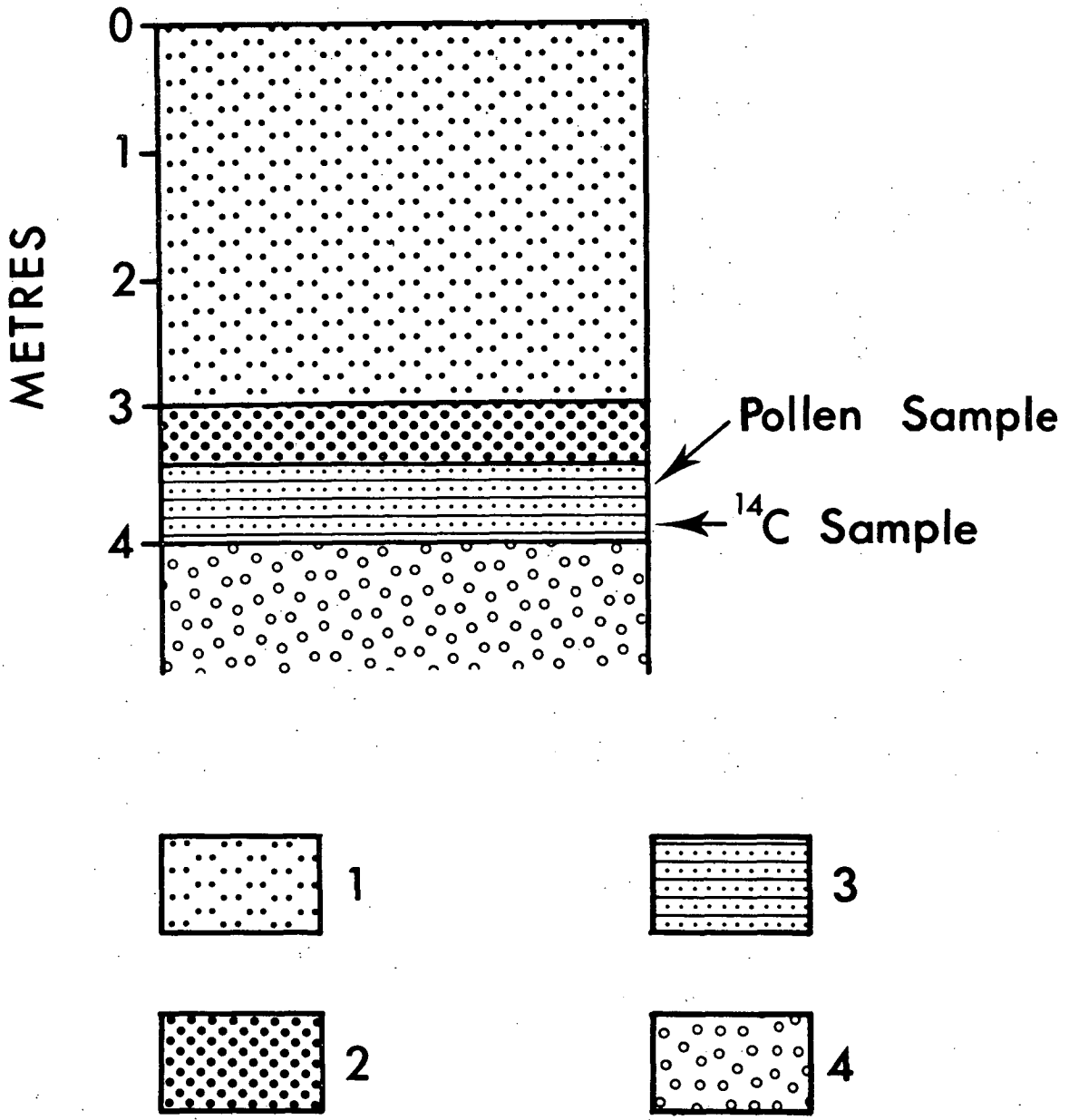

FIGURE 35 Section at Rushy Lagoon lunette old bridge site showing location of ^{14}C and pollen samples.

1 = Medium sand with charcoal
2 = Coarse sand
3 = Coarse sand, peaty sand and wood
4 = Coarse sand (Stumpys Bay Sand)

be interpreted as a swamp deposit which lies on the Stumpys Bay Sand and which is beneath lunette beach and dune facies of the innermost lunette (R3 lunette ridge). This strongly suggests that the two outer lunettes are of Pleistocene age and that the innermost lunette is of Holocene age.

There are several factors which detract from the strength of such an interpretation and these are as follows:

1) The section is located beneath a former bridge site and a substantial part of the upper section may be directly attributed to bridgeworks. Therefore it cannot be demonstrated beyond doubt that the upper layer is undisturbed lunette sand.
2) Charcoal has not been found within the lunettes, either elsewhere in the Rushy Lagoon lunette or in other lunettes. The coincidence of charcoal occurrence with possible human disturbance strengthens the case against the upper sand being undisturbed lunette sand.
3) Wood and peat has only been found in the banks of the drainage ditch and has not been encountered during hand boring, or in other field sections. This suggests that the organic material and sand could have been deposited by drainage water flowing in the ditch.
4) The wood and peat are buried with coarse sands which indicates that the entire sediment may have been laid down under relatively high energy sedimentation conditions and therefore the wood and peat may not be *in situ*.

This suggests an alternative interpretation to the one made previously. The alternative is that the coarse sand, sandy peat and wood may be all derived from elsewhere and have been deposited during times of high channel discharge or during disturbance resulting directly from the excavation of the ditch. Under these

circumstances the wood and peat could readily have been derived from the bed of the swamp which was present in Mygunyah Lagoon and which is drained by the ditch. The sand would have been eroded from the areas where the drainage ditch cuts through the Stumpys Bay Sand to the rear of the Rushy Lagoon lunette. The swamp deposits in Mygunyah Lagoon would therefore have been deposited since at least 8,500 years ago and be of early Holocene age which is consistent with the alternative explanation. This would imply that the lunettes are older, probably at least of late Last Glacial age, and that the vegetation was returning to the lakes by the early Holocene.

Soil profiles on the lunettes indicate that they are of similar age to the moderately developed podzols on the longitudinal dunes which are probably of late Last Glacial age. The podzol profile developed on the lunettes consists of a grey A_1 horizon, is usually up to 20 cm thick and is underlain by a greyish-white leached A_2 horizon which varies from 20 to 60 cm in thickness. The contact of the A_2 horizon with the dark brown $B_{2h,ir}$ horizon below is sharp and frequently characterized by pipes of leached sand extending into the $B_{2h,ir}$ horizon. The top 20-30 cm of the $B_{2h,ir}$ horizon is uniformly dark brown in colour but the sands become mottled and lighter coloured with depth, and the horizon grades slowly into the C horizon.

A comparison of the orientation of the lunettes and the longitudinal dunes also indicates that they may be of similar age. The orientation of a line normal to the ridges of 15 lunettes in the study area showed that they were oriented towards $100.5° \pm 5.4°$. A "student's" t-test showed that there was no significant difference between the orientation of the lunette normals and the longitudinal dunes ($t = 0.61$, $v = 102$, $p > 0.2$). When applied to

the Holocene parabolic dunes, the same test showed that it was unlikely that the lunettes and the parabolic dunes are oriented in the same direction ($t = 1.74$, $v = 99$, $0.05 < p < 0.1$) and therefore unlikely that they are of the same age. Thus the orientation of the lunette normals and the longitudinal dunes cannot be differentiated which supports the suggestion that they may have been formed contemporaneously in response to the same wind regime.

The relationship of the longitudinal dunes to the lakes provides some evidence of their relative ages. There are no cases where a longitudinal dune extends past the shoreline of a lake which means that the longitudinal dunes cannot be younger. However, at Rushy Lagoon, Rockbank, Leedway and Musselroe Bay, longitudinal dunes terminate near the windward lake shores. The dune ends do not appear to have been trimmed by later lake shores, as might be the case if the lakes were younger than the longitudinal dunes, because the terminations are fairly gradual and do not end abruptly at the very clearly defined lake edges.

On the basis of the evidence and the single ^{14}C date presented above, the two outer lunettes are considered to be of late Last Glacial age while the third, innermost lunette is probably of early Holocene age. More radiocarbon dates from undisputed, *in situ* locations are required before the lunette ages can be fully substantiated.

3.3 Environmental Conditions During Lunette Formation

3.3.1 *The Long Term Hydrologic Cycle*

The lunettes and associated lake basins can provide clues to the nature of the hydrologic cycle during the late Last Glacial

Stage. As the lakes are closed systems it should be possible to perform water balance calculations to estimate the relative importance of the inputs and outputs. Also, the sequence of lunette deposition should provide some information on the fluctuation of lake levels, which may have climatic implications.

Water balance calculations of the present lake system in the Rushy Lagoon area enable comparisons to be made with the Last Glacial Stage, as well as providing insights into the hydrologic cycle in operation today.

Prior to artificial drainage, Rushy Lagoon was a reed filled swamp approximately 0.6-1.0 m deep. Written records are unobtainable but residents of the area do not recall that the lagoon ever dried out. Geomorphic evidence does not indicate a natural surface drainage outlet from the swamp.

The sequence of lagoonal clays in the deposits below the lake floor precludes the possibility of large quantities of lake water leaking to the groundwater store below. Horizontal leakage may occur through the thin bed of coarse, beach sand shown in the profile of Figure 22. The bed is 1.0 to 1.5 m thick and overlies the clays. Near the northern shores of Rushy Lagoon this deposit grades laterally into sands and clays which are most likely of low permeability. Leakage from this source would occur within the flats between Six Mile Hill and Ringarooma Tier which are approximately 1 km wide.

Water lost through this groundwater sink can be estimated by equation (1) of page 162.

$$\therefore \quad Ls = Sp \times Th \times I \times P \quad m^3/d$$

where Sp = length of aquifer at northern end of the lagoon (m)

Th = Thickness of the aquifer (m)

I = Hydraulic gradient

P = Permeability of the aquifer at sink ($m^3/d/m^2$)

The permeability of the aquifer would not be as high as the sands at Tomahawk (Figure 39) and a value of 4 $m^3/d/m^2$ is probably an overestimate of the aquifer permeability at Rushy Lagoon. The sand thickness for the calculation is taken as 2 m, which again is a slight overestimate. Also, the hydraulic gradient is probably not as steep as 1:100. Use of these figures therefore gives a likely maximum estimate of the groundwater leakage from the lake system. In equation (1), Sp = 1000 m, Th = 2.0 m, I = 0.01 and P = 4 $m^3/d/m^2$.

$$\therefore \quad Ls = 1000 \times 2.0 \times 0.01 \times 4.0 \times 265 \ m^3/yr$$

$$= 21.2 \times 10^3 \ m^3/yr$$

$$= 21.2 \times 10^6 \ l/yr$$

Since the lake area is 5 km^2, this loss would be represented by a 4.24 mm drop in lake level per year. The mean annual rainfall over the last 11 years at Rushy Lagoon is 767 mm. The groundwater leakage from the lake system is only 0.6% of the rainfall which falls directly on the lake and is therefore not a significant loss in terms of the annual water budget.

The principal loss from the lake system occurs through direct evaporation from the water surface.

Nunez (in prep.) estimated the present lake evaporation at Rushy Lagoon as 1115 mm/yr. This estimate is based on an energy balance model which uses standard climatic data as inputs. The model calculated the present day evaporation if a lake was present at the site. Pan evaporation measurements were not considered satisfactory because Hoy and Stephens (1977) found that pan evaporation measurements overestimated the evaporation from shallow lakes by a factor of 1.1 to 1.4, depending on pan construction.

Water inputs to the lake system can only be supplied by direct precipitation on the lakes and by runoff from the surrounding catchment area.

The hydrologic conditions required to keep the lakes filled but not overflowing, as they were before drainage, requires a condition of equilibrium between the water inputs and outputs. The equilibrium can be represented by the water balance equation.

Gains		Losses		
(R + Ro)	=	(E + Ls)	...	(4)

where R = Rainfall on lakes (mm)

Ro = Runoff from catchment (mm)

E = Evaporation from lakes (mm)

Ls = Groundwater leakage (mm)

Groundwater leakage (Ls) can be neglected because it is much smaller than the error margin of the estimate for lake evaporation. By substitution of the above estimated inputs and outputs into equation (4)

$$767 + Ro = 1115$$

$$\therefore \quad Ro = 348 \text{ mm}$$

Thus runoff comes from a catchment area which is 4.6 times larger than the lake area. Therefore the runoff from each equivalent lake area of catchment = $\frac{348}{4.6}$ mm = 76 mm. The present runoff therefore = $\frac{75.7}{767}$ x 100 = 9.9 percent of the rainfall to the catchment. This appears to be a reasonable estimate as there are no permanent streams in the entire catchment area and runoff occurs only during very wet periods. This is probably due to the *Eucalyptus* and *Casuarina* forests with scrubby understoreys on the sandy catchment hills. This vegetation lowers the soil moisture content

to the extent that most incident rainfall is absorbed by the soil.

The presence of the large lunettes in the Rushy Lagoon area show that during the late Last Glacial Stage the lakes contained water for considerable periods. During these periods the hydrologic system must also have been in equilibrium because surface overflow from the lakes did not occur. A water budget calculation similar to the one above can be applied to the system during the late Last Glacial Stage.

The annual rainfall during the Last Glacial Stage has been estimated at Tomahawk as about 54% of the present rainfall (pages 161 to 166). Application of this figure to the present rainfall at Rushy Lagoon derives a late Last Glacial rainfall of 414 mm/yr. According to Nunez (in prep.) lake evaporation in northeastern Tasmania during the Last Glacial Stage was very similar to today and probably not more than 10% lower. Therefore evaporation from the lake surfaces probably approximated 1004 mm. Groundwater leakage would have been the same as today and can be disregarded as being too small to be meaningfully applied in the water budget calculations.

Following the same procedure as on page 200, equation (4) can be applied to the water budget of the lakes during the Last Glacial Stage.

Hence $R + Ro = E$

$\therefore \quad Ro = E - R$

$= 1004 - 414$ mm

$\therefore$ Runoff from the total catchment = 590 mm

$= 2950 \times 10^6$ l/yr

The runoff from each equivalent lake area of catchment = $\frac{590}{4.6}$ = 128 mm

= 31.0% of

the rainfall to the catchment.

The runoff during the Last Glacial Stage expressed as a percentage of the rainfall was 3.1 times greater than the present run-off. The principal contributor to increased runoff would have been decreased vegetation cover in response to the drier, colder conditions (pages 156-168). A decrease in vegetation cover increases runoff because more water is available to the soil moisture store during wet periods due to decreased plant transpiration. Therefore, when rain is added to the soil, less water is required to saturate the soil and runoff occurs sooner.

Examination of the present and past water budgets for the catchment area may provide a crude estimate of the degree of vegetation reduction which occurred during the late Last Glacial Stage.

For the present catchment area the water budget can be defined by

$$R = Ro + ET + \Delta Ws \quad \ldots \quad (5)$$

where R = Rainfall,

Ro = Runoff

ET = Water loss through evapotranspiration

and ΔWs = Change in groundwater storage

Seepage of surface water through the soil profile into the granite and dolerite bedrock of the catchment area is negligible and over an annual cycle there is no significant change to the water stored in the soil, therefore $\Delta Ws = 0$.

From equation (5) the present evapotranspiration from the catchment, ET = R - Ro

= 767 - 76 (mm)

= 691 mm

The present evapotranspiration is therefore 62.0% of the lake evaporation. This is a realistic figure for the area as most of the species of the catchment show marked xerophytic features.

Following the same argument, the estimated evapotranspiration from the vegetation of the catchment during the Last Glacial Stage was 414 - 128 (mm) = 286 mm which is only 28.5% of the lake evaporation.

Evapotranspiration consists of two components, evaporation and transpiration. Any decrease in vegetation cover is likely to increase the relative proportion of evaporation due to greater exposure of the soil to direct solar radiation. In order to make a conservative comparison between Last Glacial age and present vegetation densities the two previous ET calculations are considered to be entirely due to plant transpiration.

The above estimates indicate that compared with today, the vegetation appears to have been less than half (46.0%) as efficient as transpiring water to the atmosphere. As the relationship between biomass and transpiration is roughly linear, it would not be too unrealistic to assume that this decrease of about 50% in transpiration was concomitant with a similar reduction in biomass.

These results can be compared with the Last Glacial age evapotranspiration estimate from Tomahawk (page 167), which was

derived from a different theoretical base. Considering the imprecise nature of the data, the close correspondence between the Tomahawk evapotranspiration which was 33% of potential evaporation and Rushy Lagoon (29% of lake evaporation) provides some confirmation that the estimates may be of the right magnitude.

So far the lake basins associated with the lunettes in the Rushy Lagoon area have provided evidence of the water budgets during the Last Glacial Stage. The discussion will now turn to the lunettes themselves to see whether they indicate a sequence of hydrologic variations during the late Last Glacial Stage.

3.3.2 *Short Term Water Balance Fluctuations*

It has long been recognized that lunette composition is a potentially valuable pointer to their mode of origin and to the hydrology of the adjacent lakes at the time of lunette deposition. Hills (1940) gave lunettes their name and attributed the silty clay composition of the lunettes on the plains of northern Victoria to the capture of atmospheric dust by spray droplets derived from the lakes during "... the relatively wet, late Recent epoch ..." (page 18). Stephens & Crocker (1946) analyzed the distribution and composition of lunettes in the southern Australian region and considered Hills' hypothesis inadequate. They considered that both silty-clay and sandy lunettes were formed by aeolian transportation of material derived almost entirely from adjacent dry lake floors. They took the view that the fine grained lunettes were built up by aggregated silt and clay particles which behaved like sand grains under the influence of wind. This view was originally put forward by Coffey (1909) to explain the formation of clay dunes bordering lagoons

in South Texas. Twidale (1968, 1972) thought that salt crystallization in many areas helped to break up and roughen the surface of the clay lake bed. He also concluded, as did Campbell (1968), Bowler & Harford (1966) and Bowler (1968, 1971, 1976), that wave action causing longshore drift formed lee shore beaches from which the lunette foredune was derived.

Bowler & Harford (1966) recognized three successively younger phases of lunette formation in the Echuca area and attributed their occurrence to hydrologic response to climatic change. Bowler (1971, 1973, 1976) and Bowler *et al.* (1976) used lunette stratigraphy to develop detailed palaeohydrologic interpretations. The key concepts on which the reconstructions are based are (i) deposition of quartz sand in lunettes corresponds to aeolian accumulation of beach derived material during high water level in the lake; (ii) argillaceous deposition in lunettes corresponds to periods of lake fluctuation when pelletal clays, formed by desiccation and salt efflorescence, were blown to the lee shore; (iii) no lunette formation is possible when the water table and capillary fringe fall below the lake floor. "Thus a stratigraphic transition from well-sorted quartz to saline, clay-rich sediments provides clear evidence of a change in the hydrologic regime of the basin ...", and "In this way these aeolian facies provide a method of reconstructing past arid-humid oscillations." (Bowler, 1976, page 290). These principles are applied in the following palaeohydrologic evaluation of the lunette sequences in the Rushy Lagoon area.

The arguments for markedly increased aridity, increased wind speeds, and significant temperature reduction have been presented in the preceding pages of this chapter. The onset of all of these

factors would have been sufficient to cause a substantial reduction in vegetation cover which led to initial deflation of the pre-lunette surface. Deflation would have been most pronounced during the summer periods when dry surfaces were more susceptible to wind erosion. Incident precipitation and increased runoff into the depressions created the lakes associated with the lunettes.

The first phase of lunette formation is best represented at Mygunyah Lagoon. The M1 lunette consists of medium-fine sands which overlie a beach deposit of medium to coarse sand. Following the principles outlined on page 205 the sandy composition of the lunette indicates a substantial period when the lakes were consistently full and the lunette was formed as a source bordering foredune.

A sample which was considered typical of the sand within the lunettes was moderately well sorted (sorting coefficient 0.54 ϕ) and fine grained (mean grainsize 2.43 ϕ). The principal supply of this sand to the lake systems is thought to have been as aeolian material which was blown into the lakes. There is strong evidence that aeolian activity was widespread in northeastern Tasmania during lunette formation (pages 186-197). It is envisaged that the material derived in this way was concentrated in lee-shore beaches as a result of wave action and accompanying longshore drift, and subsequently winnowed by the wind from the beach.

Generally lower lake levels followed the initial period of high lake levels. Lunettes composed of interbedded sand and clay were formed during the second lunette phase and form the highest ridge at Mygunyah Lagoon (M2) and Rushy Lagoon (R2). Both

dunes show a very similar stratigraphy. The basal beach facies is overlain by aeolian sand layers which are separated by two argillaceous units (Figure 34).

The argillaceous units consist of clay beds up to 20 cm thick which are interbedded with thin sand beds up to 10-15 cm thick. Hygrometer analysis of the clay beds showed that approximately 50% of the sample weight is finer than 9 ϕ and that smaller modes occur in the size range 2.5 ϕ to 3.5 ϕ. This is a similar grainsize distribution curve to the top 4.5 m of Bore 50 which consists of Last Interglacial age lagoonal deposits with a minor aeolian input. The lagoonal sediments which were deposited prior to the Last Interglacial Stage and which form the floor of Mygunyah Lagoon have not been analyzed but field observations suggest that they also have a very high clay component. Again following the guidelines described on page 205, the clay components in the lunettes are interpreted as having originated by aeolian deflation of clay pelletal aggregates from seasonally dry lake floors. The lake floors were either composed of interglacial lagoon sediments or of lake sediments which were directly derived from interglacial lagoon deposits.

Production of clay pellets from seasonally dry lake floors in the Rushy Lagoon area appears to have been through the principal agency of wetting and drying because there is no evidence of salt deposition either in the lunettes or on the lake floors. Groundwater leakage from the system, which was only of a very low order on an annual basis (page 199), was probably a significant factor in maintaining salinities at relatively low levels compared with salt lakes.

The maximum possible salinity of the lake system can be calculated by equating salinity inputs with outputs. Dissolved salts are carried into the system almost entirely by runoff water from the catchment and leave the system by groundwater flow. Maximum salinity of the lake system is achieved when the quantity of salts entering the system equals the quantity lost from the system. The amount of salt entering the system = Ro x Qr,

where Ro = volume of runoff water (l/day)

Qr = concentration of salts in runoff water (mg/l).

Similarly, the quantity of salt leaving the system = C x Qx,

where C = the volume of water lost through leakage (l/yr)

Qx = the concentration of salts in lake water (mg/l).

The present concentration of salts in the Tomahawk River is 190-210 mg/l. This may be comparable to the maximum runoff concentration during the Last Glacial Stage because the Tomahawk River catchment and the lake catchment areas are of similar lithology. The runoff to and groundwater leakage from the system have been previously estimated (pages 201 and 199) and were 2950×10^6 l/yr and 21.2×10^6 l/yr respectively.

When the salt lost from the system is equivalent to the salts gained:

$$Ro \times Qr = C \times Qx \quad \ldots \quad (6)$$

Therefore $$Qx = \frac{2950 \times 10^6 \times 200}{21.2 \times 10^6} \text{ mg/l}$$

$$= 27830 \text{ mg/l}$$

This estimate provides a rough guide to the possible salinity levels in the lake system. The calculated value is about 80% of the concentration of sea water, but is well below the

concentration levels of Australian hypersaline salt lakes (Bowler, 1971). The estimated lake concentrations may have been sufficiently high to permit salt crystallization to assist formation of pelletal clay on the floor of the intermittently dry lake bed, but may not have been enough to cause significant salt deposition, on the lake floor, which could be incorporated into the lee-side dunes.

The lunette facies of the M2 and R2 lunettes have been used as hydrologic indicators in the manner suggested by Bowler (1976). The general changes from argillaceous to siliceous units within the second stage lunettes demonstrate that there were three main periods when the lakes contained water throughout the year which were separated by two, probably similar, periods when the lakes were frequently dry, and perhaps seasonally dry. The close association between the sand and clay units in the dunes also suggests that while the lakes contained water for periods of sufficient length to form the sand units, the lake levels were oscillating and generally low during the formation of the second stage lunettes.

The third lunette building phase was marked by a return to higher lake levels. This is indicated by the sandy composition of the R3 lunette at Rushy Lagoon and by the undercutting of the M2 lunette by the water levels which obtained during formation of the M3 ridge (page 190).

Little evidence can be found which reveals the lake system's response to the transition to present climatic conditions. Restoration of a much more complete vegetation cover was probably the most critical factor in the termination of lunette construction by stabilizing the lunettes and lake beaches. Also, invasion of the lake shores by aquatic plants such as rushes and reeds, would

severely reduce the longshore drift of sediment which was necessary to nourish the beaches. Slight contraction of lake level is indicated by two very low ridges, which are shown in the profile on Figure 34. These ridges were formed after the main period of lunette formation and probably represent shorelines of the lakes during Holocene times. If this is the case then the lakes contracted slightly in area from their late Last Glacial extent. Contraction may have been caused by the decreased contribution to the system by runoff from the catchment area.

An important deduction from the preceding analysis of lake level fluctuations during the late Last Glacial Stage and comparison with the present hydrology of the system is that the hydrology of the present system is much less dynamic than that of the past. The changing relative importance of the factors controlling lake hydrology explains this phenomenon.

Present lake levels (i.e. before drainage) were controlled mainly by the balance between evaporation from, and incident precipitation into, the lake system, with runoff from the catchment contributing very little to the system. The additions to the lake were relatively slow, as even heavy rainfalls could only raise the lake levels by a few centimetres. Likewise, evaporation from the lake system was a slow process. Thus, with low rates of input and output, the system was at a very low level of dynamic equilibrium.

By contrast, the relative importance of surface runoff during the late Last Glacial was considerably increased. The effect of wet periods at this time would have been to raise the lake water levels significantly because in addition to the incident precipitation input, a large volume of water was supplied by runoff from the catchment. Also the reduced mean annual rainfall

during the Last Glacial Stage was probably accompanied by a large decrease in reliability of rainfall, as is the case in semi-arid areas today (Critchfield, 1966). Under these circumstances there would be a greater tendency for drought periods to cause substantial lowering of lake levels and for wet periods to cause marked lake level rises. Thus the hydrology of the lake systems during lunette formation was dynamically much more active due to the higher proportions of water added by runoff and to probable greater variation of rainfall about an annual mean.

Figure 36 is a diagrammatic interpretation of the possible palaeohydrologic changes which may be implied from the lunette sequences in the Rushy Lagoon area.

4. CLIMATE OF THE LAST GLACIAL STAGE

This section summarizes the climatic and environmental inferences which have been drawn from the occurrence, morphology and composition of longitudinal dunes and lunettes, and their relationships with closely associated landforms, deposits and soils. In order to place the conclusions from northeastern Tasmania in perspective, comparisons will be made with other findings in Tasmania and mainland Australia.

4.1 Northeastern Tasmania

Direct evidence in northeastern Tasmania of temperature decline during the Last Glacial Stage is meagre, namely the occurrence of slope deposits, probably derived under cold climate conditions,

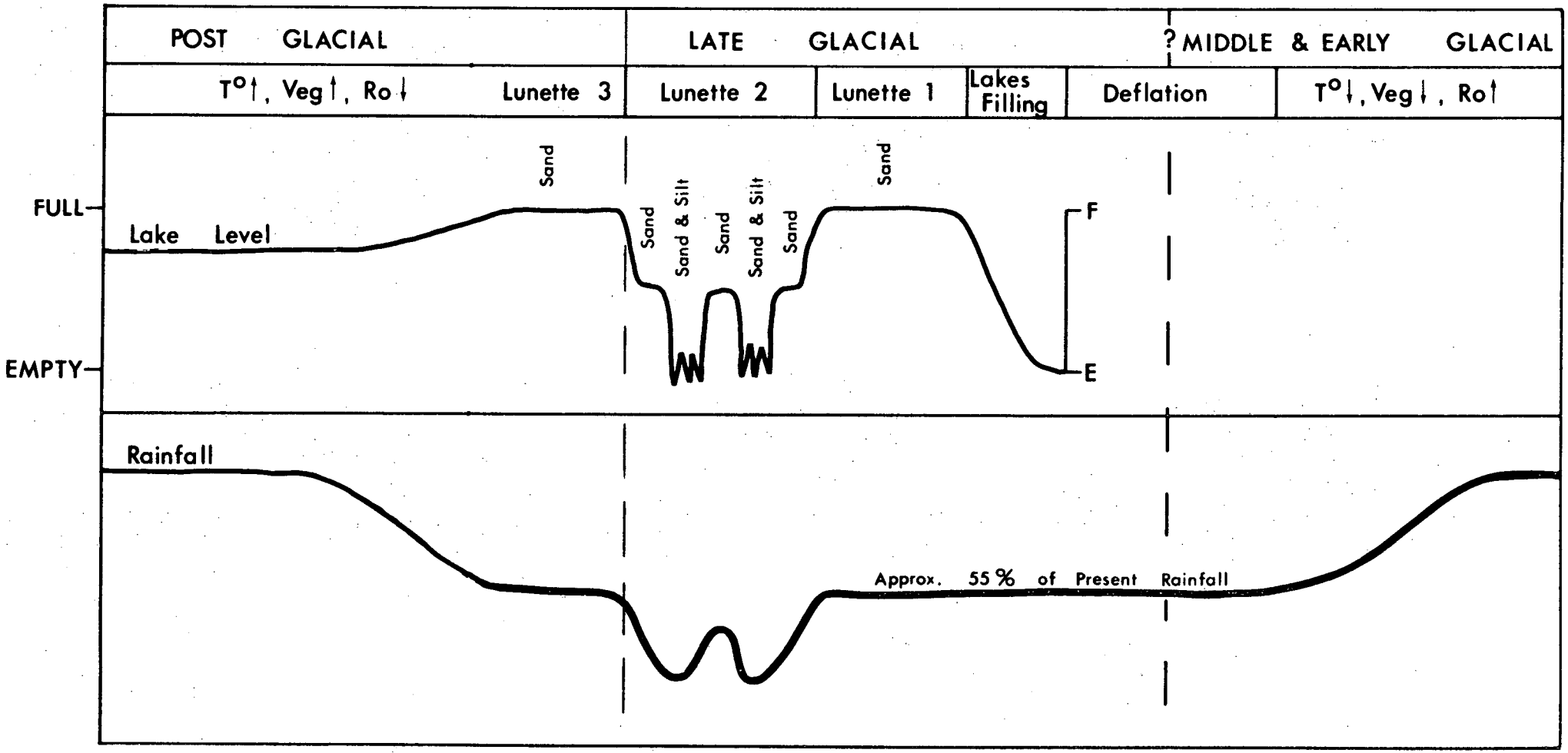

FIGURE 36 Possible Palaeohydrology of Rushy Lagoon Lake System.

which are contemporaneous with longitudinal dune activity. Widespread aeolian activity was probably partly induced by temperature lowering which aided reduced vegetation cover on the deflation sensitive coastal sand plains. Glacial and periglacial activity in the Tasmanian Highlands must also have influenced northeastern Tasmania and almost certainly indicates a regional temperature reduction.

A large reduction in precipitation (approximately 45 to 55% of the present rainfall) is suggested by the difference in water table level depicted by a fossil groundwater podzol within the coastal sand plains. Lunette sequences suggest that the rainfall was much more variable during the late Last Glacial Stage than it is today. Factors which could account for the marked rainfall reduction are an increased rainshadow effect of the western highlands, increased continentality produced by the drainage of Bass Strait, the blocking of intense low pressure systems which now pass through Bass Strait, and cooler sea surface temperatures which reduced the atmospheric humidity.

The strongest and most frequent winds during the Last Glacial Stage were from the west, as they are today, but comparison of Glacial and Holocene linear dunes indicates that the glacial age winds were from a slightly more northerly direction. Both sets of dunes show marked transverse asymmetry which has been interpreted as due to a secondary northwesterly wind component. The slightly more northerly wind direction shift could be due to expansion of the Australian continental high pressure cell which would tend to force a more northwesterly circulation over northern Tasmania.

The average westerly wind strength during the Last Glacial Stage is thought to have been around 35 to 36 km/hr, which is 9-10 km/hr greater than the present average westerly wind speed. Glacial wind speeds were derived by the analysis of grainsize threshold velocity and lee wave wavelength; methods which have independent theoretical bases. The mean wind speed associated with the formation of Holocene linear dunes was estimated by the threshold velocity-grainsize relationship and approximated the present mean westerly wind speed at Low Head. During the Last Glacial Stage a combination of expansion of the Australian continental anticyclone and northward extension of the Antarctic Convergence probably created steeper pressure gradients in the Tasmanian region which induced stronger wind activity.

The principal combined effect of these climatic conditions was to reduce the vegetation cover. This had a marked influence on the relative importance of runoff in the hydrologic cycle. Analysis of the Rushy Lagoon lake system indicates that runoff during the late Last Glacial Stage was approximately three times greater, as a percentage of incident rainfall, than it is today. Runoff estimates from the catchment area of the lake system were used to calculate evapotranspiration. Evapotranspiration, as a ratio of potential evaporation, was only 40-45% of the present ratio. This also points to a greatly reduced vegetation cover during the Last Glacial Stage.

The combined conditions of increased aridity, lower temperatures, and increased windiness which were in operation during the Last Glacial Stage favoured stronger aeolian activity. Due to the sensitivity of the coastal sand plains of northeastern

Tasmania to aeolian processes, these conditions favoured substantial modification of the landscape in the form of extensive fields of longitudinal dunes and the development of lunettes.

4.2 The Tasmanian Region

Terrestrial dunes and aeolian deposits of probable Last Glacial age are being increasingly recognized from other areas within Tasmania.

Nicolls (1957, 1958) mapped sand sheets which originated from flood plains under a prevailing westerly wind regime, and considered that they were probably deposited during the latest glacial phase. Davies (1967) described the occurrence of fixed inland dunes (valley dunes and lunettes) with strongly podzolized soils as occurring in areas with less than 755 mm precipitation. He left the question of age open, but concluded that common environmental factors for their formation are low rainfall, exposed location to strong winds, and a sandy surface which would aid initial deflation.

Jennings (1959) considered that the "Old Dunes" on King Island were mostly siliceous, parabolic dunes with podzol profiles and with an approximate west to east orientation. These dune ridges extend across the northern half of King Island. However he placed calcareous "Old Dunes" and "Old Dunes" with a "giant podzol" in the same group and considered them all to be of Last Interglacial age.

Sutherland & Kershaw (1971) and Kershaw & Sutherland (1972) mapped extensive areas of linear dunes, with a westerly orientation on Flinders Island. They stated that the dune systems reflect the influence of westerly winds, which were particularly severe

during glacials. They also considered that the dunes represented a continuum of dune formation over a time scale covering several interglacial stages. Field work on Flinders Island by the author confirmed the presence of longitudinal dune fields which were indistinguishable in form, occurrence, and soil profile development from the longitudinal dunes in northeastern Tasmania.

Similar longitudinal dunes with podzol profiles have been observed by van de Geer at Woolnorth Estate in the far northwest (Colhoun, 1978a) and south of Smithton (Colhoun, 1975), and by Chick at Badger Beach in northwestern Tasmania (Colhoun, 1975), and near the Henty River on the west coast (Banks, Colhoun & Chick, 1976).

The widespread Tasmanian distribution of aeolian landforms with similar levels of soil profile development indicates that they were mostly formed during the same period of aeolian activity. Three dated sites from Tasmania are available which shed light on their possible age. Charcoal from a sand dune with a podzol soil profile at Malcolms Hut Road, in southern Tasmania, yielded a late Last Glacial age (15,740 ± 700 BP) for the dune (Sigleo & Colhoun, 1975; Colhoun, 1978a). At Pipe Clay Lagoon in southern Tasmania, Colhoun (1977) dated freshwater pond deposits beneath aeolian sands with a podzol profile and concluded that the aeolian sands accumulated after 22,000 BP. At Lake Tiberias, in the Midlands, Goede (pers. comm.) obtained a date of 9550 ± 500 BP from basal peat sitting on lake floor shelly sand and clays which are closely associated with the lunette at Lake Tiberias. This indicates a minimum age of late Last Glacial Stage for the Lake Tiberias lunette.

Thus the dated evidence from Tasmania points strongly towards widespread aeolian activity between 22 ka and 10 ka, during the late Last Glacial Stage. Colhoun (1975, 1978a, 1978b) concluded that the climatic implications which can be drawn from the widespread Tasmanian occurrence of the aeolian landforms are that precipitation was significantly reduced over the whole region during the waning hemicycle of glaciation. This statement is in complete accordance with the conclusions derived from northeastern Tasmania.

4.3 Australia

Bowler *et al.* (1976) have produced a comprehensive account of current opinion and recent developments in studies of late Quaternary climates of Australia and New Guinea. Many of the recent findings are based on well documented field evidence combined with radiocarbon dating and are starting to allow finer detail at a continental scale to become apparent. One of their conclusions was that major aridity which caused the "... drying of lakes, construction of lunettes, and widespread extension of desert dunes ..." (page 389) occurred between 20 ka and 15 ka and was most marked around 17 ka. The evidence from Tasmania, particularly from the northeast, is that extension of desert dunes was not confined to mainland Australia but extended through the dry Bass Strait region to form major dune fields on King and Flinders Islands and in northeastern Tasmania.

Bowler *et al.* also concluded that "... throughout Australia reduced rainfall is associated with cold phases", and that "... high lake levels during colder phases were the consequence of reduced or unchanged, rather than increased precipitation ..."

(page 389). This conclusion is supported by evidence from northeastern Tasmania where estimates of precipitation during the late Last Glacial Stage are about half the present value. However in northeastern Tasmania the high lake levels during the period of generally reduced precipitation are explained by increased catchment runoff due to significant vegetation cover reduction, rather than to decreased evaporation rates.

PART III

GROUNDWATER HYDROLOGY

1. INTRODUCTION

Many coastal areas of Australia are fringed by plains of unconsolidated sand. These sand bodies should contain abundant groundwater because precipitation is able to drain freely through the sand into the groundwater store. Accumulation of this water creates unconfined aquifer conditions provided that excessive quantities of water do not escape from the margins or base of the sand body. Unless traversed by exogenous streams, these areas are often characterised by a lack of permanent surface water. Therefore water is often a scarce resource.

Although Tasmania is generally more humid than the continent of Australia much of eastern Tasmania is subject to summer drought and severe soil water deficits. Thus groundwater may be utilised to enable higher production and crop diversification. At Greens Beach, near the mouth of the Tamar River, the Tasmanian Department of Mines is currently assessing the potential of Holocene marine sands as a source of town water supply (Cromer, in press). Many holiday home owners in coastal areas of Tasmania require water in small quantities for domestic purposes and use of water from water table aquifers is on the increase.

Hydrologic testing of some unconsolidated coastal sand deposits in Tasmania has been carried out by the Tasmanian Department of Mines on an *ad hoc* basis (Stevenson, 1969, 1970, 1973; Moore, 1968, 1975; Leaman, 1970a, 1970b, 1971a, 1971b; Matthews, 1966, 1972, 1975; Matthews and Cromer, 1973; Cromer, 1972, 1974a, 1974b; Cromer & Sloane, 1976), but since the overall relationships of the various deposits were not well known, the results could only be applied to the immediate areas from which the data were obtained. No assessment of the aquifers as systems has been attempted.

Mapping and description of landforms and deposits has provided the basis for a systematic study of aquifer characteristics since each of the sediment bodies has been identified as a separate unit.

The preliminary evaluation, which is presented below, of the shallow groundwater potential of the Quaternary deposits of the northeast coast of Tasmania is based mainly on the assessment of their extent and composition as defined in Part I. Criteria of origin and age have aided in their definition and mapping. Most of these deposits contain unconfined groundwater, except in isolated cases within the Stumpys Bay Sand where minor silt beds occur, and within the Rushy Lagoon Sand where alternating beds of sand and clay act to confine portions of the groundwater.

1.1 Aquifer Potential

1.1.1 *Stumpys Bay Sand*

The geomorphic study has revealed that on the basis of their wide extent and sandy nature, the marine sands have considerable groundwater potential and should be studied in more

detail in order to appreciate the dynamics of the aquifer system and to estimate the quantities of water available for extraction. The results are presented in later sections.

1.1.2 *Ainslie Sand*

The Ainslie Sand consists of unconsolidated sand which is highly porous and permeable, but shows little aquifer potential. Although widely distributed, the Ainslie Sand forms narrow, isolated ridges, which preclude the accumulation of substantial amounts of groundwater. The main limiting factor is the lack of lateral confinement of precipitation which enters the dunes. Thus, although water freely enters the dune ridges, it is also free to drain from the base and lower flanks. In winter groundwater seepage is common from the lower flanks of the larger dunes and indicates that they do not effectively store large quantities of groundwater. Several dunes have been augered and found to be dry.

The Ainslie Sand may form small aquifer systems where it occurs as undulating sand sheets. Although these sand sheets also stand above their surroundings, and confinement of lateral groundwater seepage is absent, the ratio of their area to their perimeter is much higher than in the longitudinal dunes. The resulting lower leakage rates therefore provide a greater possibility of precipitation storage in the sand sheets. The development of small intermittent lakes on some sand sheets supports this view. Also, the development of sand sheets on the surface of the interglacial marine sands adds to the combined thickness of the two deposits and enhances the groundwater storage potential of the area.

1.1.3 *Rushy Lagoon Sand*

The lunettes are not regarded as promising aquifers due to their restricted areal extent, their high clay component, and the absence of a barrier to lateral seepage. However, the persistent occurrence of seepage lines on the flanks and near the bases of the larger lunettes may provide small local water supplies.

1.1.4 *Croppies Marl*

The Croppies Marl has no groundwater potential due to its very restricted lateral and vertical extent and to its composition.

1.1.5 *Forester Gravel*

The extent and thickness of the Forester Gravel indicates that it should form significant aquifers. The terrace material is probably moderately permeable and highly porous and should readily absorb precipitation. Drilling near the front of a terrace has shown that the water table is not maintained at a level close to the ground surface and there are relatively large volumes of water emanating from the bases of the terraces. If higher groundwater levels occur towards the centre and rear of the terraces where the effect of high lateral leakage is less pronounced the Forester Gravel should form a good aquifer.

1.1.6 *Barnbougle Sand*

These young marine deposits could form significant aquifers since they cover a wide area, and attain thicknesses of at least 11 m in some localities. Open water table conditions prevail within

the deposits, and the sands are likely to be highly porous and permeable. Since the sands extend to below present high water mark in many areas, salt water intrusion could be a problem if high rates of groundwater withdrawal were to occur near the coast.

1.1.7 *Waterhouse Sand*

Several auger holes in the parabolic dunes failed to encounter saturated sand. The small dimensions of the dunes and the absence of lateral confinement are severe limitations to their potential as groundwater aquifers.

1.1.8 *Bowlers Lagoon Sand*

The transverse dunes are unlikely to contain significant amounts of groundwater because their flanks are unconfined. One auger hole in the dunes encountered dry sand to its final depth of 9 m.

Table 6 summarizes the shallow groundwater potential of these formations.

Of these landforms and deposits the Stumpys Bay Sand is the most extensive, contains a continuous, open water table system over a wide area and is readily mapped. It therefore lends itself to a close study of the nature and dynamics of open groundwater systems. Also detailed study of the dynamics and characteristics of the Stumpys Bay Sand aquifer should yield results which may be partly applied to the other main aquifer of the area, the Barnbougle Sand. Detailed study of a small, representative area of the Stumpys Bay Sand was undertaken to establish the nature of

TABLE 6 Shallow Groundwater Potential of Quaternary Deposits

Aquifer	Landform Type	Composition	Area (km^2)	Average Thickness (m)	Permeability	Porosity	Likely Groundwater Potential
Stumpys Bay Sand	coastal plains	medium sand	118	7	high	high	good
Ainslie Sand	longitudinal dunes and sand sheets	fine sand	too scattered		high	very high	moderate to poor
Rushy Lagoon Sand	lunettes	fine sand and clay	too scattered		low	moderate	poor
Croppies Marl	inland lake	marl and clay	0.01	2	low	moderate	poor
Forester Gravel	river terraces	coarse sand and gravel	4	7	high	high	moderate
Barnbougle Sand	coastal plains	medium sand	91	13	high	high	good
Waterhouse Sand	parabolic dunes	fine sand	too scattered		high	very high	poor
Bowlers Lagoon Sand	transverse dunes	fine sand	16	10	high	very high	poor

groundwater conditions. Study of the less promising aquifers was less detailed and was designed only to establish some of their basic groundwater properties.

2. GROUNDWATER DYNAMICS WITHIN THE STUMPYS BAY SAND

2.1 Introduction

The coastal sand plain east of the Tomahawk River (Figure 1) was chosen for study because:

(i) It is a clearly defined, self-contained system bounded on the south and east by granite hills, on the north by the coast, and on the west by the river (Figure 17). This sand embayment extends to the west of the river but it was not considered necessary to examine the entire embayment in detail as the river effectively divides the groundwater system. The river bed has been cut into the underlying aquiclude of weathered granite, and the river acts as a drainage sink for both portions of the embayment. In addition, the entire embayment is too large for close study and the western boundaries of the embayment are not as clearly defined as the eastern boundaries.

(ii) Although small enough for detailed study, the selected area is large enough (24 km^2) to display areal variations of aquifer and water table characteristics.

(iii) The sands in the area form a relatively continuous cover of moderate thickness over an aquiclude of weathered granite.

(iv) Preliminary investigations showed that the aquifer in the area was of the water table type (unconfined) and was continuous except for several small, isolated granite hills which protrude through the aquifer (Figure 17).

(v) The sands of the area extend from sea level to an altitude of around 32 m, which covers the entire altitudinal range of the known occurrence of the Stumpys Bay Sand.

(vi) The area is easily accessible and rainfall records for the immediate area have been kept since 1965.

2.2 Physical Properties of the Aquifer

As indicated above, and in Figure 17, the boundaries of the Tomahawk Formation in this area are well defined. The granite hills which form the southern and eastern boundaries rise from the sand plains over a marked break of slope and extend to an altitude of about 85 m. The northern boundary of the area is formed by the coast where the present coastal processes have eroded the sand embayment. A narrow strip of sand of Holocene age is present between the shore and the Stumpys Bay Sand in places, but there is a sharp discontinuity where the Holocene sands have been deposited against the steep, eroded slope of the Stumpys Bay Sand. The eastern boundary, formed by the Tomahawk River, is clearly defined. The area enclosed within these boundaries is 24 km^2, the southern hills being an average of 4.5 km from the coast, and the east-west width being 5 km. Figure 16 shows the surface of the plain which rises fairly evenly from the coast to an altitude of 32 m at the southern margins.

The average thickness of the Stumpys Bay Sand in the East Tomahawk area, as determined from 33 drill holes (Figure 16), is 6 m and varies from less than 2 m to 11 m thick. As shown by Figure 15 the thickness decreases towards the inland boundaries where the sand wedges out at the break of slope. Some isolated granite hills protrude through the surface of the plain but have not been incorporated into Figure 15. These small hills are the tops of residual granite tors. The basement surface also rises from the coast, where it is commonly exposed to the marked inland break of slope. The basement, or basal aquiclude consists of granite which has a strongly weathered upper layer with a high clay content. Although the weathered granite has not been deeply penetrated, drilling and field sections in the area indicate that it is at least 2 m thick in places, and results of seismic refraction work indicate that it may attain a thickness of 8 m.

The sands of the East Tomahawk area are moderately sorted, moderately rounded, and are generally of medium grainsize. Figure 37 shows the relationship of mean grainsize and sorting with depth for the six bores from which samples have been sieved at 0.25 ϕ intervals. Some field sections show that the sands may range from coarse to fine grained over vertical distances of less than one metre and are sub-horizontally bedded. Drilling indicates that although the sediments locally show this range of variation, for practical purposes the aquifer sand as a whole can be considered almost homogeneous. This assumption is valid for the purposes of the groundwater study because although variation of sand size over short vertical distances is known, it is nevertheless relatively rare. Clay horizons, which, if widespread, would exert profound influences on the permeability of the sediments, have not been encountered.

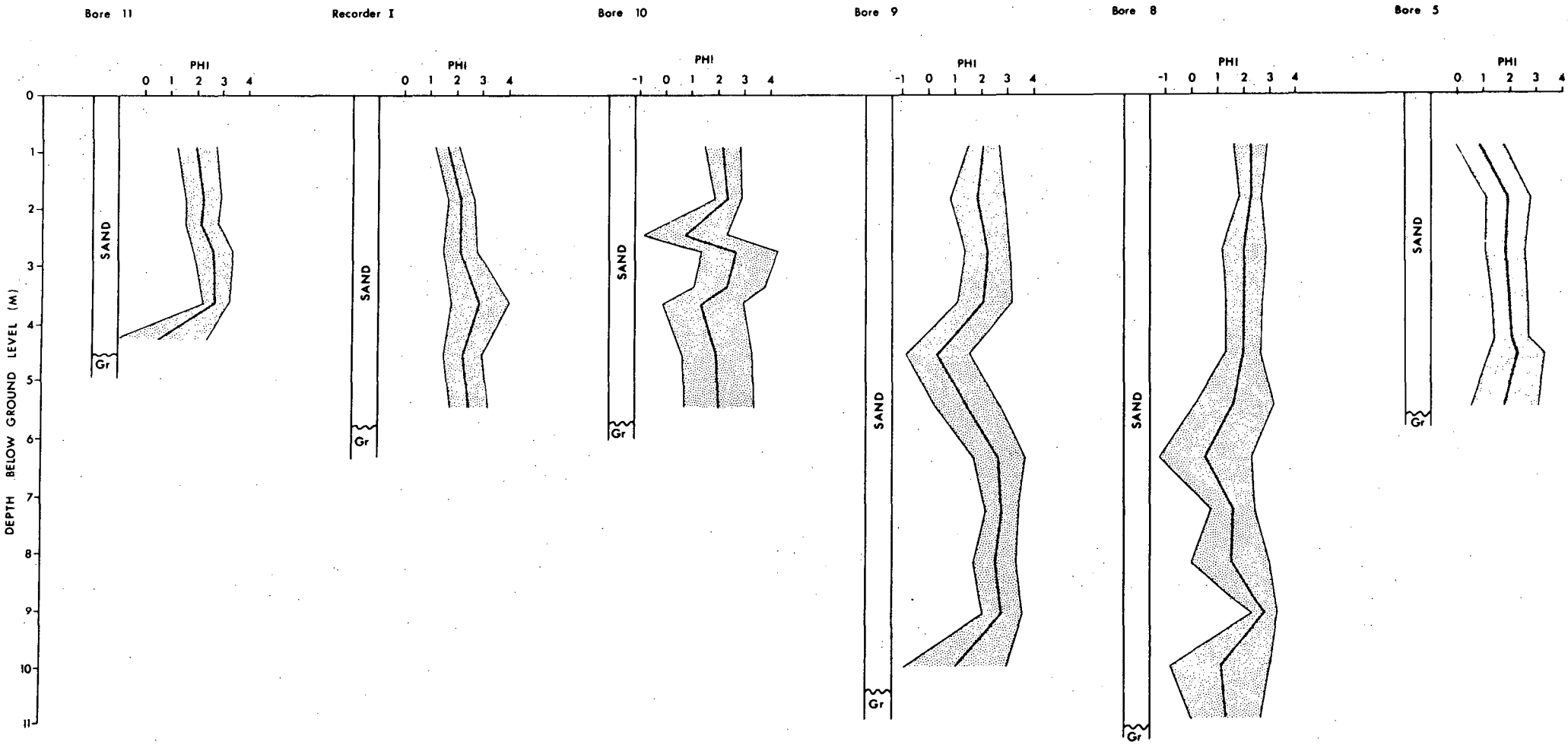

FIGURE 37 Selected Bore Logs from East Tomahawk.

The heavy line indicates the mean grainsize. The shaded portion represents the range from -1 to +1 standard deviation about the mean; that is, the range within which it may be expected that approximately two thirds of the sample will lie.

The transmissivity of the Stumpys Bay Sand was determined by the application of the Theiss Recovery Test method (Ferris *et al.*, 1962; Kruseman & De Ridder, 1970). This method was necessary due to the difficulty of measuring drawdowns in a small diameter hole during pumping. Well screens 5 cm in diameter were jetted to the base of the sands. The hole was usually pumped for 1-4 hours at rates of up to 1800 l/h. After a brief initial period of several minutes the pumping rate usually stabilized to the rate at which the aquifer could yield groundwater. The rate of water level recovery was measured after pumping had stopped. Residual drawdowns (s') was plotted on semilogarithmic graph paper against t/t', where t = time since pumping started and t' = time since pumping stopped. As the value of t' became larger the relationship usually fell on a straight line. According to Kruseman and De Ridder (1970, page 67), the slope of this line gives the value of the quantity $\log_{10}$ (t/t'/s') in the equation

$$s' = \frac{2.3Q}{4\pi kD} \log_{10} \frac{t}{t'} \quad \ldots\ldots \quad (7)$$

where kD = Transmissivity $m^3/d/m^2$

Q = Discharge m^3/d

The value of t/t' was chosen over one log cycle because its logarithm is unity. This reduced equation (7) to

$$kD = \frac{2.3}{4\pi \Delta s'} \quad \ldots\ldots \quad (8)$$

where $\Delta s'$ = the change in residual drawdown per log cycle of time

The permeability of the aquifer was calculated by dividing the transmissivity by the saturated aquifer thickness. Table 7 summarizes the pump test results from the East Tomahawk area and shows that the permeability of the Stumpys Bay Sand varies from ~ 0.4 to 20 $m^3/d/m^2$. This wide range of results may be due partly to limitations of the Theiss Recovery Test method which are discussed in Ferris *et al.* (1962) as well as to the variation in permeability of the sands. However, Figure 38 shows that a general pattern of permeability variation can be discerned when test data are mapped.

The collection of sand samples of known volume has permitted calculation of their porosity. Although the porosity values vary from 32 to 56 percent by volume, the average is around 40 percent.

2.3 The Hydrologic Cycle

Any groundwater system which evolves within unconsolidated sands, as at East Tomahawk, can be considered in terms of the hydrologic cycle. Water enters such systems through precipitation, surface runoff and groundwater flow. These last two mechanisms, as well as evapotranspiration, may also act to remove water from the aquifer. Initial soil moisture conditions combined with these sources and sinks result in specific water table changes. The difference between the inputs and outputs of the groundwater system over any period is represented by the change in water table level. If the inputs to and outputs from the system can be measured or estimated, and compared with the water level change

TABLE 7 Pump Test Results - East Tomahawk

Bore Hole Location (see Fig. 16)	Saturated Formation Thickness (Th) (m)	Transmissivity (kD)[1] ($m^3/d/m$)	Permeability (P) $P = \frac{T}{Th}$ ($m^3/d/m^2$)
21	4.87	3.52	0.72
RI	4.27	18.46	4.32
19	5.23	53.59	10.25
20	5.28	2.99	0.57
9	4.00	3.37	0.84
16	2.11	6.19	2.93
15	5.52	14.29	2.59
RII	3.00	1.96	0.65
12	6.50	6.00	0.92
13	5.59	7.27	1.30
14	2.96	57.83	19.54
7	3.75	17.31	4.62
6	2.77	3.87	1.40
RIII	2.55	1.06	0.41
28	2.76	22.86	8.28
30	1.85	5.72	3.09
RIV	2.70	19.03	7.05
5	4.31	34.79	8.07

[1] Transmissivity data is from pump tests. The screens were 5 cm in diameter and the screen aperture was 0.18 mm.

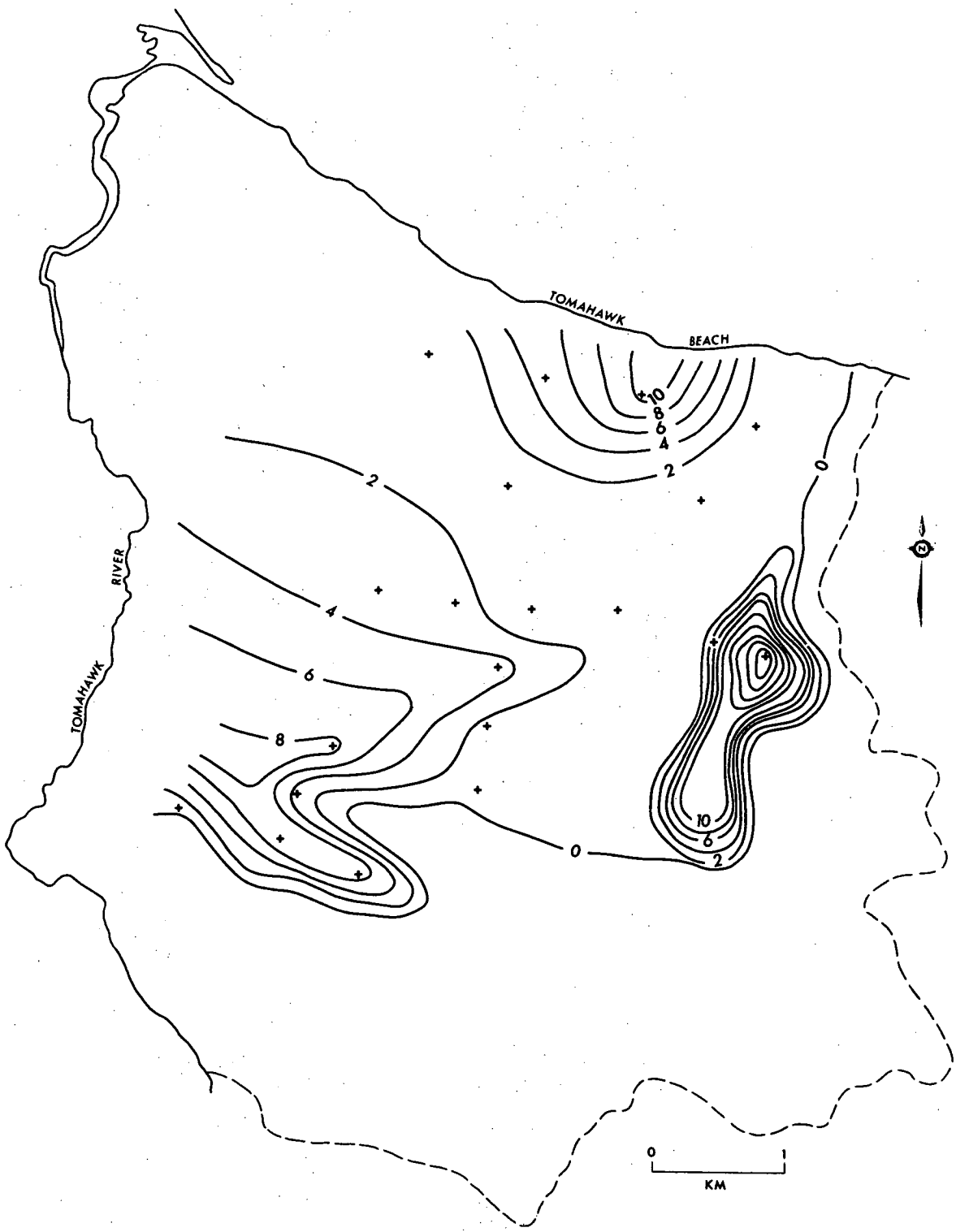

FIGURE 38 Sand Permeability - East Tomahawk.

Contour interval = 2 $m^3/day/m^2$
Crosses indicate pump test locations.

The high permeability zone on the eastern margin coincides with a sand sheet (Ainslie Sand).

within the system, then insights into the exchanges of liquid water can be gained and prediction may follow. A positive (negative) water table change represents a net gain (loss) by the system.

Precipitation and evapotranspiration are therefore important components of the system which need to be estimated before an analysis of the water budget is possible. Tables 8 and 9, and Figure 39, show precipitation data for Tomahawk and pan evaporation data for Scottsdale.

TABLE 8 Mean Monthly Precipitation, 1965-76, Tomahawk

(mm)

J	F	M	A	M	J	J	A	S	O	N	D	Year
31	29	49	70	84	65	97	99	72	61	70	63	790

TABLE 9 Mean Monthly Pan Evaporation, 1971-77, Scottsdale

J	F	M	A	M	J	J	A	S	O	N	D	Year
150	129	101	58	37	28	30	41	60	80	101	140	955

A daily record of the rainfall for the East Tomahawk area is available, but a complete set of daily pan evaporation measurements does not exist. Daily pan evaporation records are available for Scottsdale, which is 35 km inland. Since it was felt that the pan evaporation at Tomahawk is likely to be higher than the pan evaporation at Scottsdale, due to the increased exposure

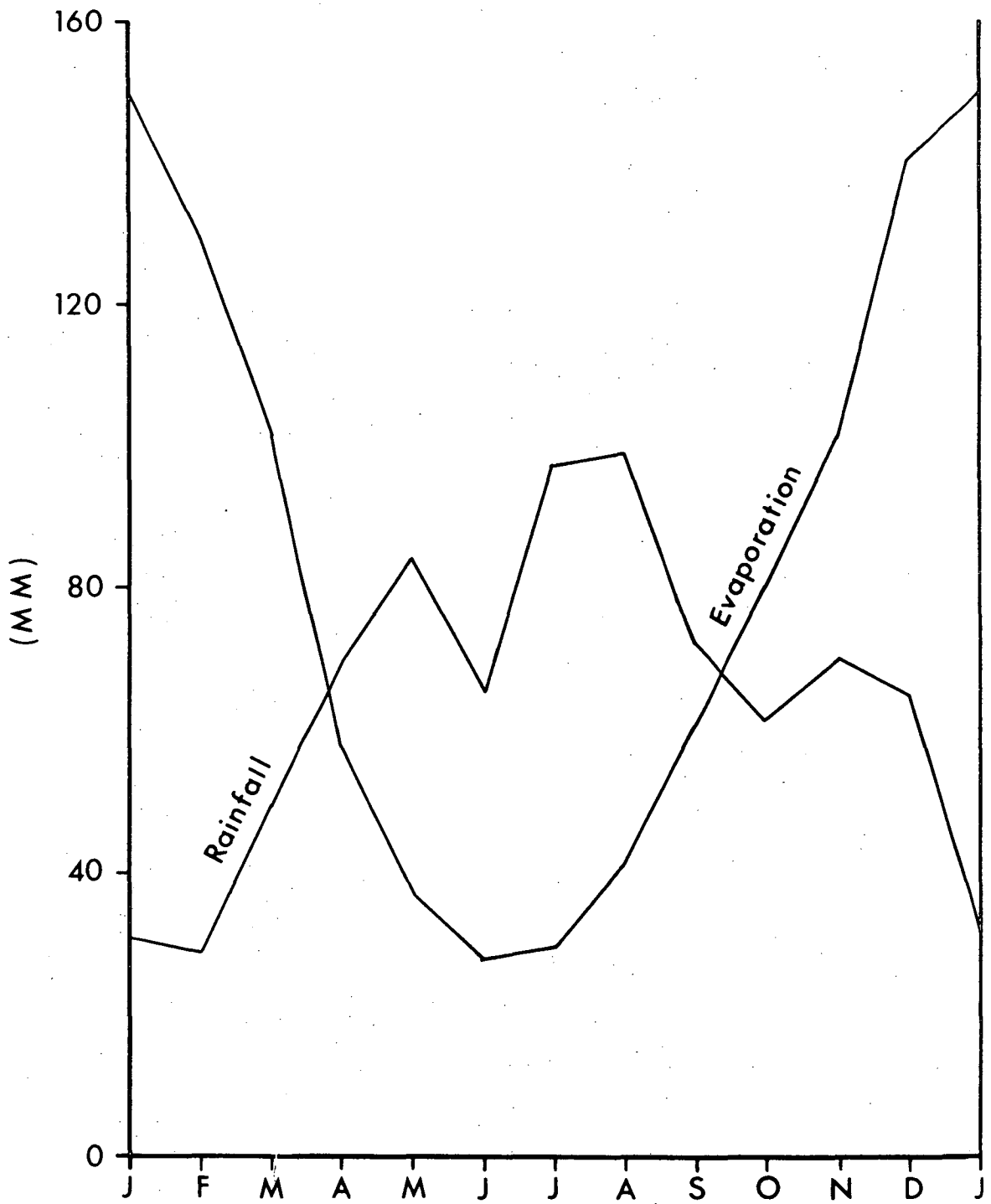

FIGURE 39 Mean Monthly Rainfall and Evaporation.

Rainfall data from Tomahawk
Evaporation data from Scottsdale

to wind and the probable higher insolation of the Tomahawk sand plains, a temporary evaporation pan was established at Tomahawk for comparison with the Scottsdale data. The relationship between the daily pan evaporation figures was examined using linear regression analysis. The high correlation coefficient of $r = 0.92$ indicates that the measurements are of the same derivation, but the line of best fit indicates that evaporation at Tomahawk is 1.3 times greater than at Scottsdale (Figure 40). Therefore, pan evaporation at Scottsdale is approximately 77 percent of that at Tomahawk, and as evapotranspiration in Tasmanian conditions is estimated to be between 70 percent and 80 percent of pan evaporation (Bureau of Meteorology) the figures for Scottsdale can be used as an approximation for Tomahawk.

2.4 Nature of the Water Table

Continuous results from three water level recorders provide evidence of the nature and magnitude of the water table fluctuations. The records show that the water table responds quickly, within four hours, to most showers of rain and Figure 41(a) is a typical response. The 15 month record displayed by Figure 42 shows that the water table rarely exceeds a depth of 2 m in the driest period of the year, and may rise to the surface after continuous, heavy rain during wet periods. In addition, there is a very pronounced diurnal water level variation. On dry days, for example Figure 41(b), all of the recorders show the greatest rate of water table decline between 11 a.m. and 9 p.m. with little decline overnight. The factor which best explains the regular diurnal variation in groundwater level is evapotranspiration. The period of greatest loss is during the day when solar radiation is

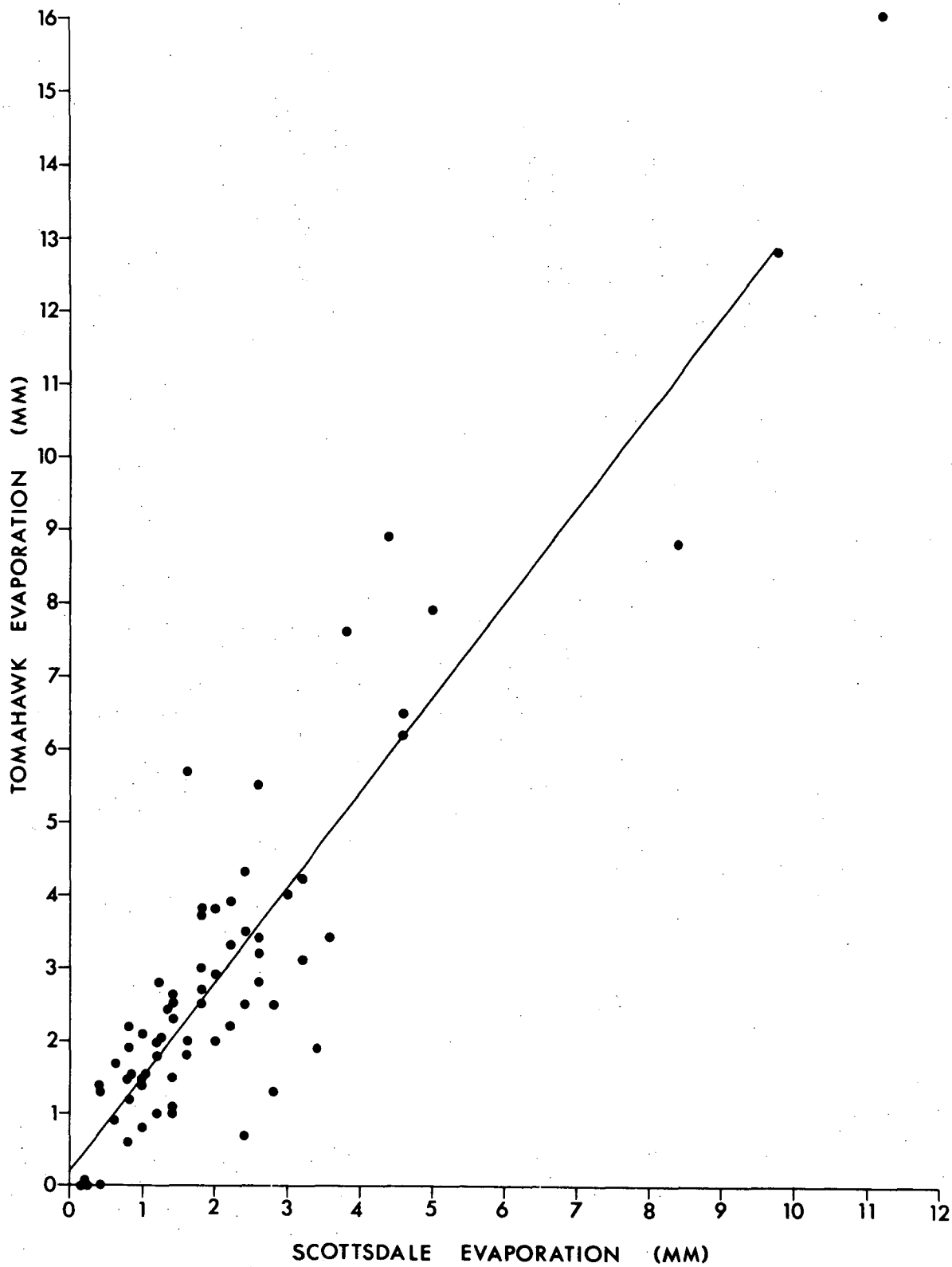

FIGURE 40 Relationship between pan evaporation at Tomahawk and Scottsdale.

Where necessary the Scottsdale data have been grouped for periods of several days to conform with grouped readings of several days from Tomahawk. Pearson's $r = 0.92$, $y = 0.23 + 1.29x$.

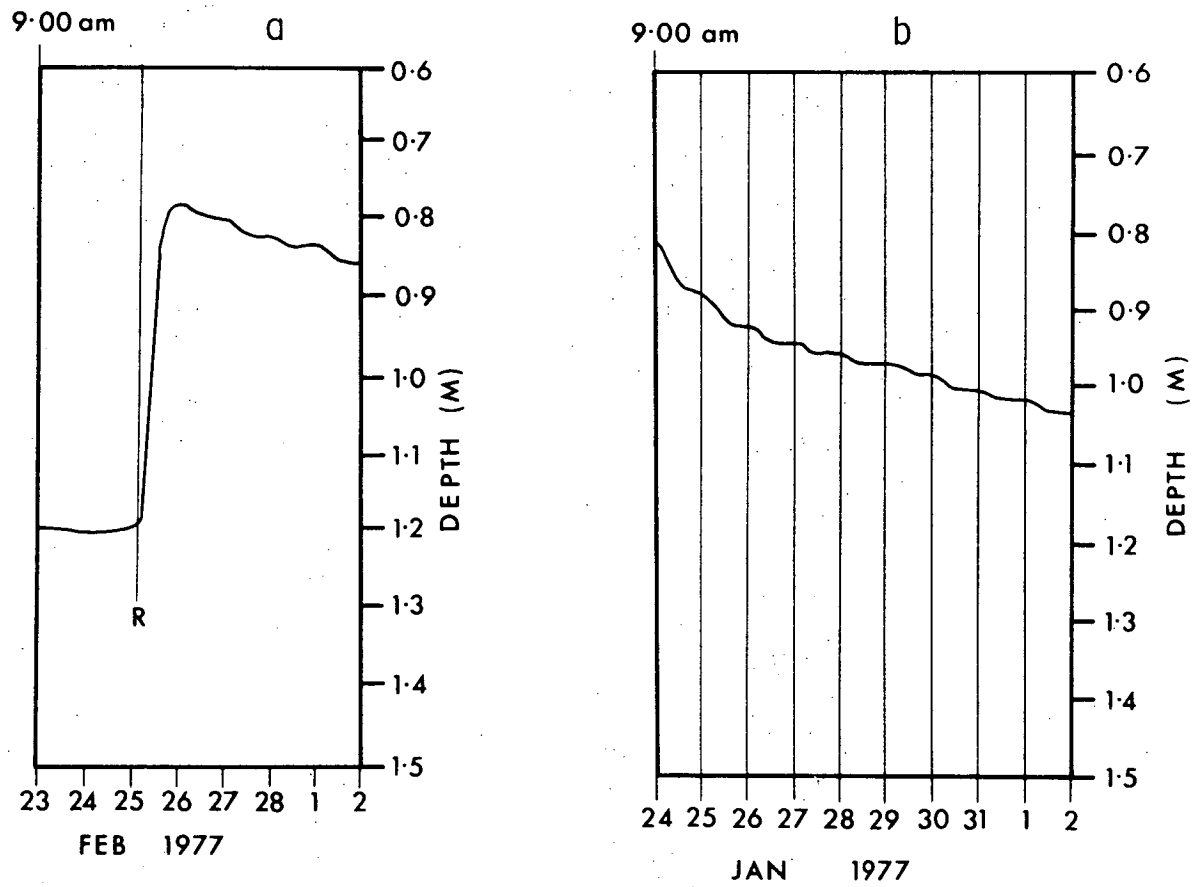

FIGURE 41 Groundwater Responses to Rainfall and Evapotranspiration.

(a) Rapid response of water table at Recorder I to rainfall. R indicates commencement of rain.

(b) Regular diurnal water table fluctuations due to evapotranspiration at Recorder I. The water table commences the daytime decline at approximately 9.00 a.m. Stabilization of the water table level occurs overnight.

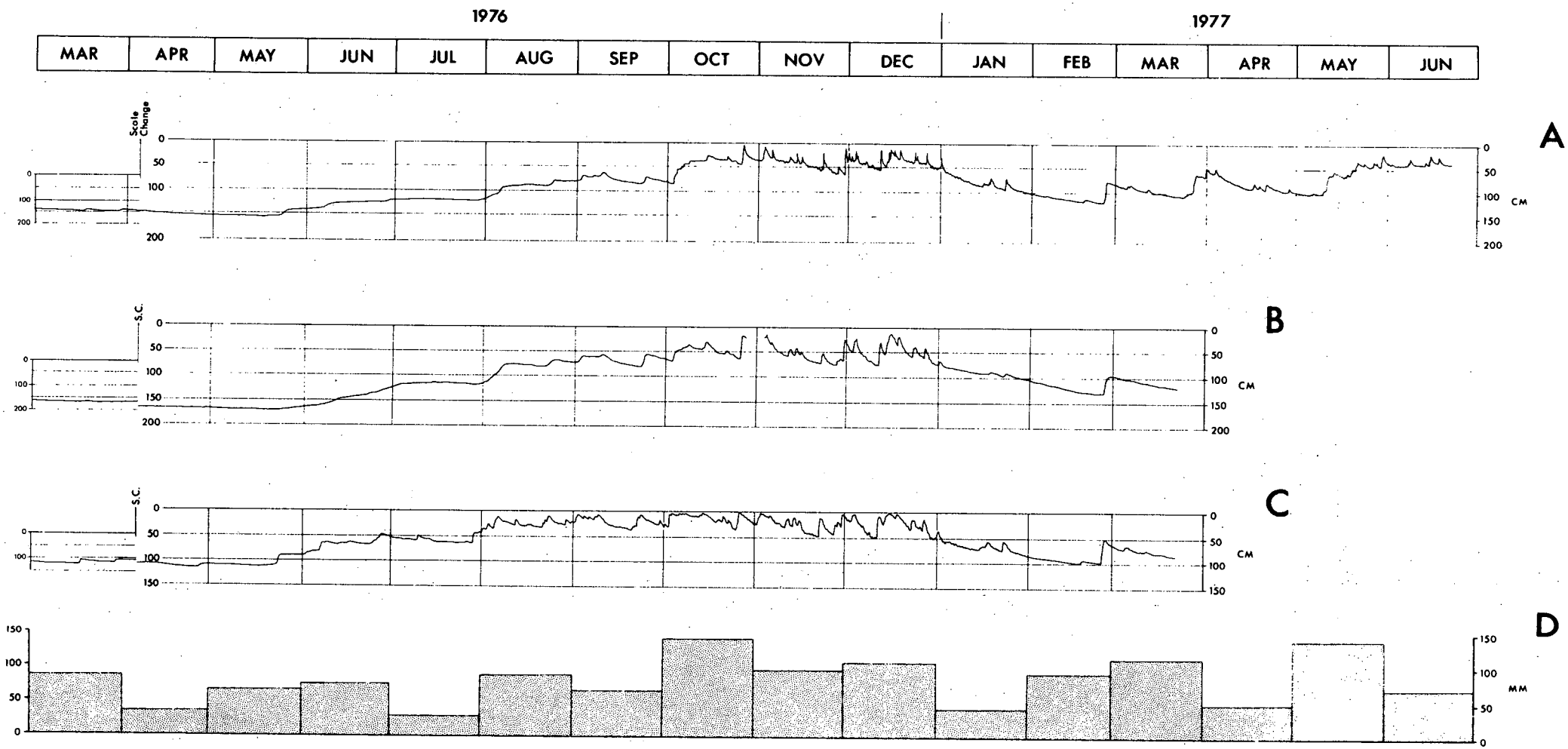

FIGURE 42 Water Table Records from March 1976 to June 1977

A, B and C show the records for Recorders I, III and IV respectively. Graph D shows the monthly rainfall for the period.

highest. The effects of evapotranspiration will be further discussed in the section on groundwater dynamics. The variation is not a response to ocean tides because the time of commencement of the cycles is consistent and there is only one cycle per day. The variation is not due to changes in atmospheric pressure because, unlike confined aquifers, changes in atmospheric pressure have no effect on open water tables (Todd, 1959).

Thirty three observation holes, which consist of open PVC tubes inserted through the sands to 2 m below the water table, were installed on the East Tomahawk plain to determine the configuration of the water table. The location of these holes is shown in Figure 16, and they were sited along several intersecting transects which covered the general water table conditions for the area. The holes were visited nine times between 26th March and 13th September 1976, and the depth to the water table was measured for every hole within a three hour period. This procedure enabled the elevation of the water table to be mapped and contoured for the days on which the measurements were taken. Figure 43 shows a typical water table elevation map.

Water table depth maps, such as Figure 44, show that the water table rarely exceeded a depth of 2 m below the ground surface and that it closely followed the topography of the land surface. The topographic contours of Figure 45 are drawn from data at the observation hole locations only, and correspond closely to the groundwater contours of Figure 43. Groundwater flow diagrams such as Figure 46, which are constructed from the water table maps purport to show the direction of groundwater movement as determined by differences in hydraulic head. However, the horizontal component of groundwater flow in the East Tomahawk

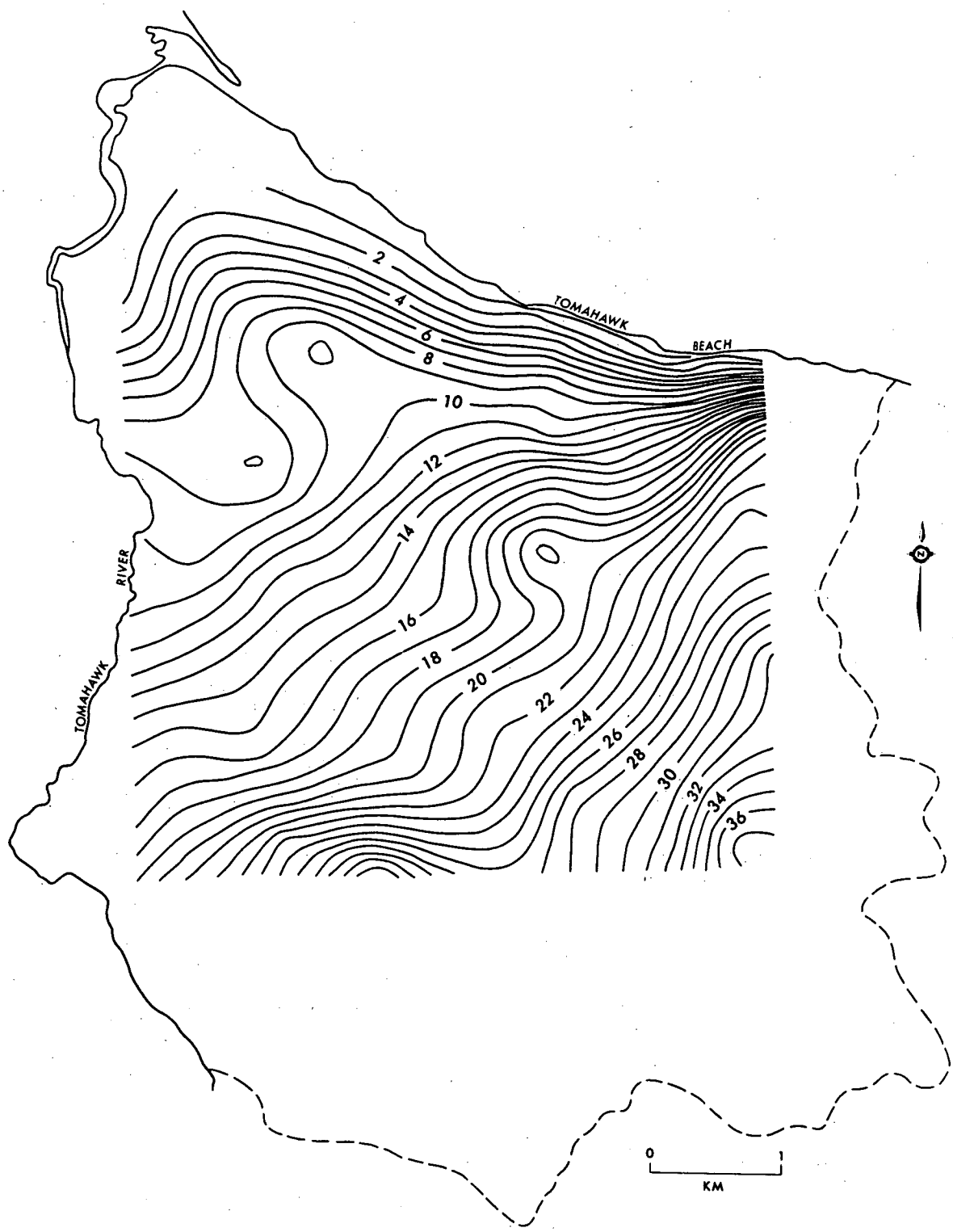

FIGURE 43 Water Table Elevation 26 March, 1976 - East Tomahawk.

Contour interval = 1 metre.
The altitudes are above State Datum.

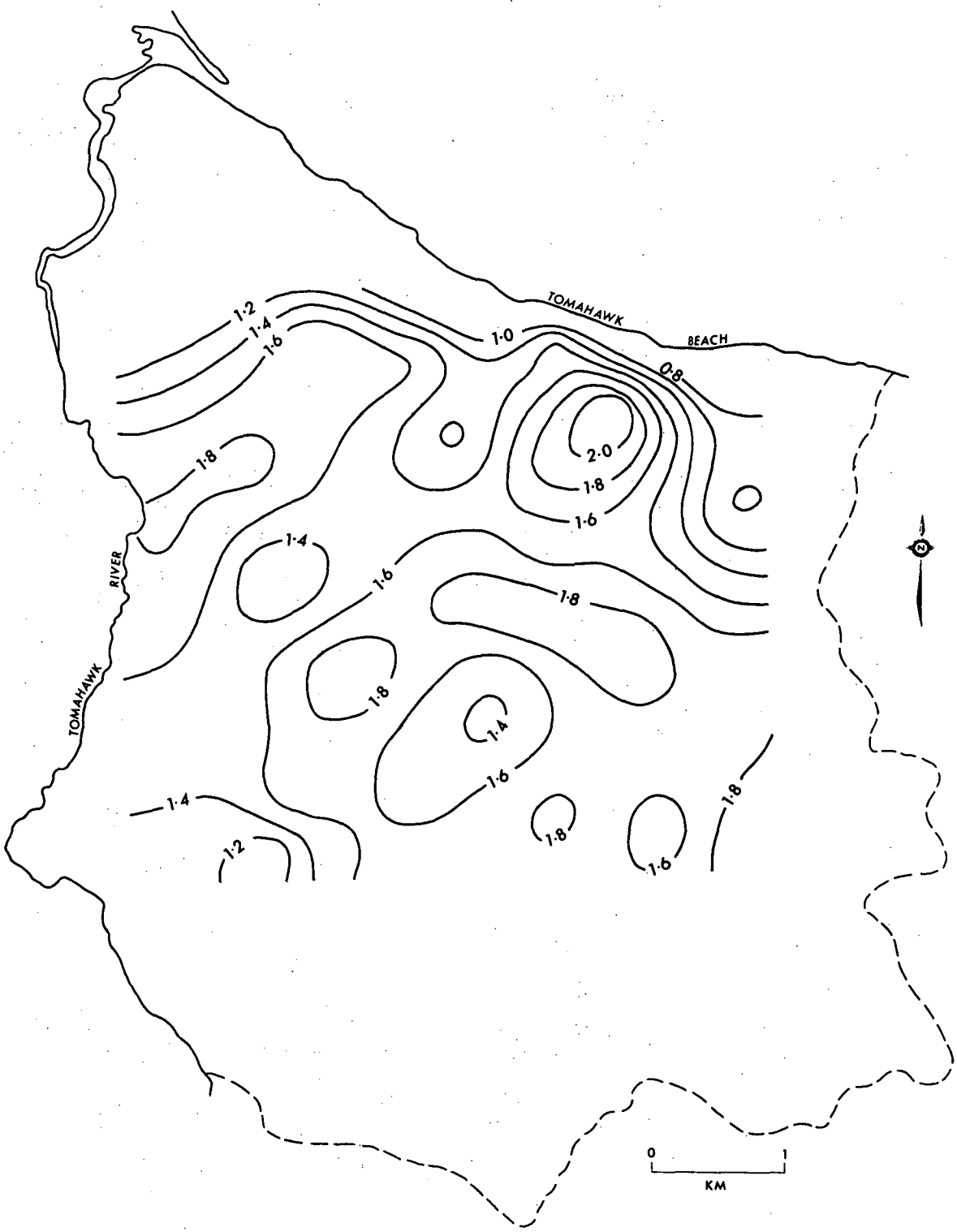

FIGURE 44 Depth to Water Table 26 March, 1976 - East Tomahawk.

Contour interval = 0.20 metres.

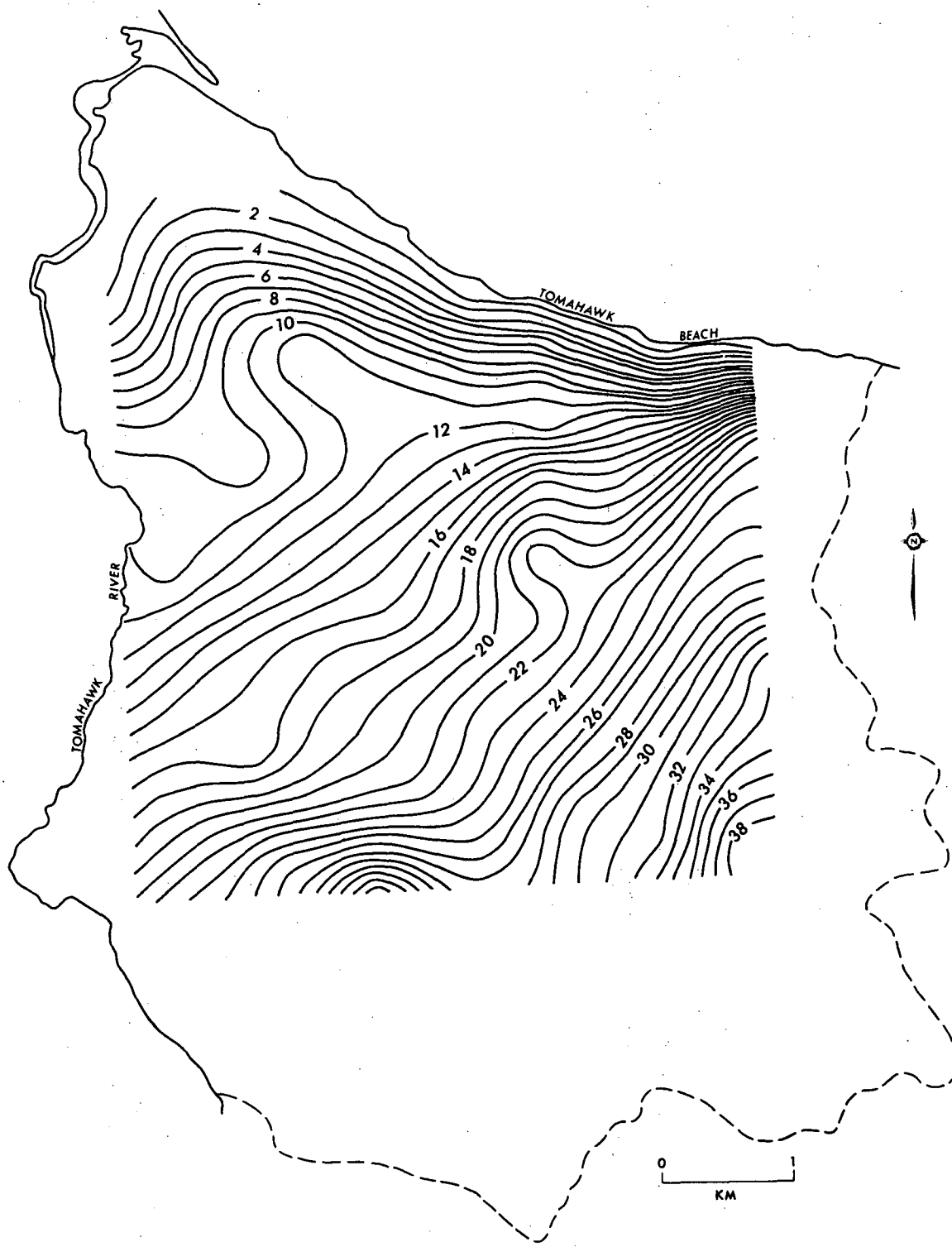

FIGURE 45 Topography - East Tomahawk.

Contour interval = 1 metre.
The altitudes are above State Datum.

The contours are based on the altitude of the observation hole locations only. Comparison with Figure 43 demonstrates the close correlation between the water table surface and the topography when plotted using the same data points.

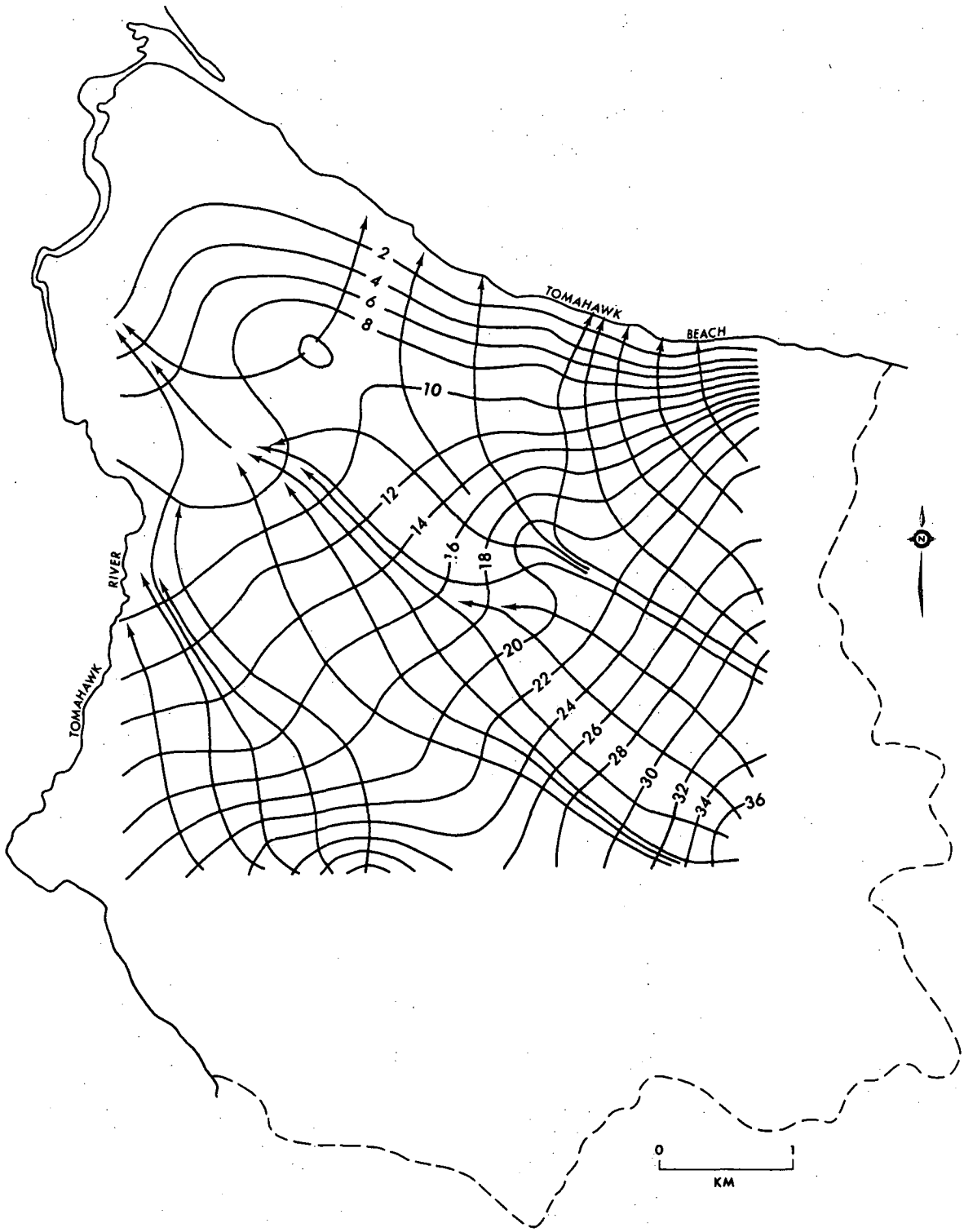

FIGURE 46 Groundwater Flow Lines 26 March, 1976 - East Tomahawk. Water table contour interval = 2 metres.

area is negligible compared with other forces which create the water table configuration and the usefulness of this type of map is limited.

2.5 Sources for the Aquifer System

There are only two ways in which water can enter the groundwater system in this area; through incident precipitation and surface runoff from surrounding bedrock slopes. Water cannot enter from the Tomahawk River or from the sea since both are below the level of the aquiclude. Horizontal groundwater flow into the aquifer is not possible as the aquifer wedges out against largely impermeable granite bedrock, as shown by Figure 4. Surface runoff from the granite areas within the East Tomahawk catchment contributes some water to the aquifer, particularly near the margins of the sands. The groundwater level records demonstrate that the dominant input to the system is through incident precipitation. Water levels respond rapidly to rainfall but it is not possible to draw a direct, simple relationship between a given input of rainfall and water table change.

2.6 Sinks from the Aquifer System

There are three ways in which water can be lost from the system. Discharge occurs to the sea, to the Tomahawk River, and to the atmosphere through evapotranspiration. Water loss through the base of the sands is negligible as the weathered granite is largely impermeable. Consequently water is lost either to the river or the sea where the aquifer is truncated, or to the

atmosphere from the surface. The length of exposure of the aquifer to the lateral sinks is not extensive, and since the hydraulic gradients are consistent over time, the rates of loss are considered to be constant.

The aquifer leakage to the sea is calculated by:

$$\text{Leakage} = P \times Th \times I \times Sp \quad \ldots\ (1)$$

where P = permeability of sand = 4 $m^3/d/m^2$ (Figure 38)

Th = thickness of saturated sand = 4 m (Figure 15)

I = hydraulic gradient = 0.016 (Figure 43)

Sp = length of coastal spring line = 4000 m (Figure 15)

Leakage to the sea = 1,024 m^3/d

Using the same data sources, the aquifer leakage to the Tomahawk River, where P = 3 $m^3/d/m^2$ $1/d/m^2$, Th = 3 m, I = 0.006, Sp = 5,000 m, is 270 m^3/day. Combined, the total leakage at the edges of the aquifer is 1,294 m^3/d (approximately 1.3×10^6 1/d). Since the area of continuous aquifer is 18.25 km^2, and if a low porosity of 20 per cent is assumed, then the water table decline over the entire area is

$$\frac{1.3 \times 10^6}{18.25 \times 10^6 \times 0.20} = 0.36 \text{ mm per day}$$

This rate of decline (0.036 cm/d), is only 0.24 percent of the loss indicated by the water level recorder charts, for example those of Figure 47, on which losses of up to 15 cm per day have been recorded.

FIGURE 47 Rapid Rates of Water Table Decline.

Chart from Recorder III showing water table decline of up to 15 cm/day.

FIGURE 48 Water Table Response to Increasing Length of a Dry Period.

Chart from Recorder IV showing the decreased rate of water table decline as the length of a dry period increases. R indicates rainfall incidence.

FIGURE 49 Rates of Water Table Decline soon after Rainfall.

Chart from Recorder I showing a rapid decline of the water table after the cessation of rain. R indicates rainfall incidence.

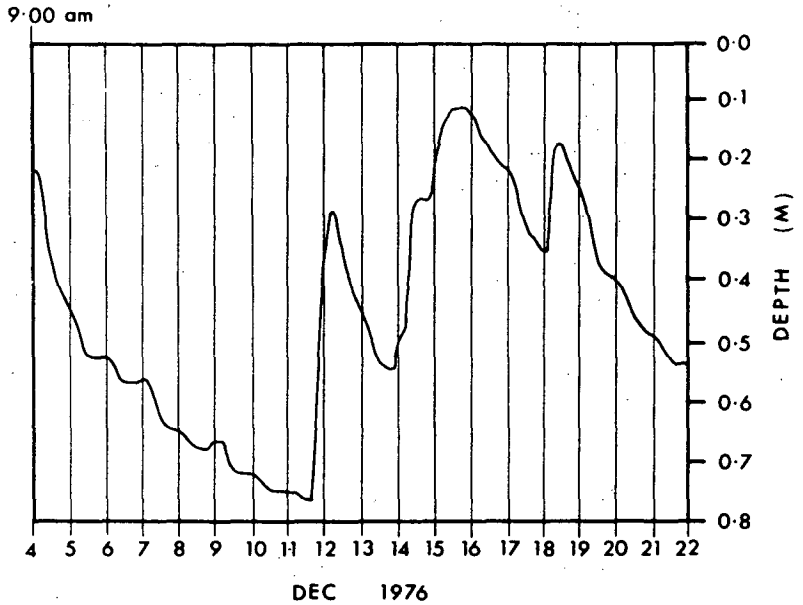
9·00 am
0·0
0·1
0·2
0·3
0·4
0·5
0·6
0·7
0·8
DEPTH (M)
4 5 6 7 8 9 10 11 12 13 14 15 16 17 18 19 20 21 22
DEC 1976

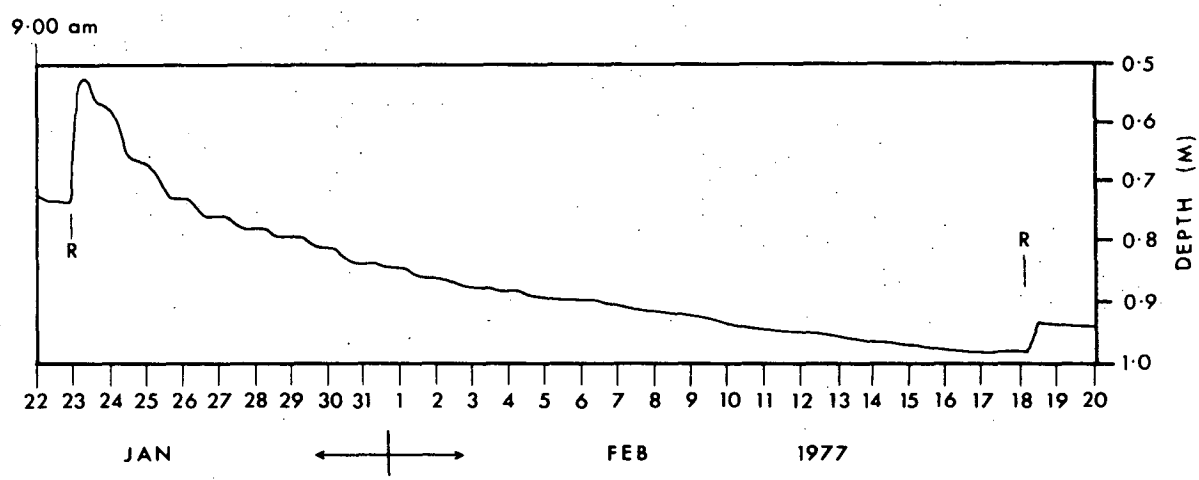
9·00 am
0·5
0·6
0·7
0·8
0·9
1·0
DEPTH (M)
R
R
22 23 24 25 26 27 28 29 30 31 1 2 3 4 5 6 7 8 9 10 11 12 13 14 15 16 17 18 19 20
JAN
FEB
1977

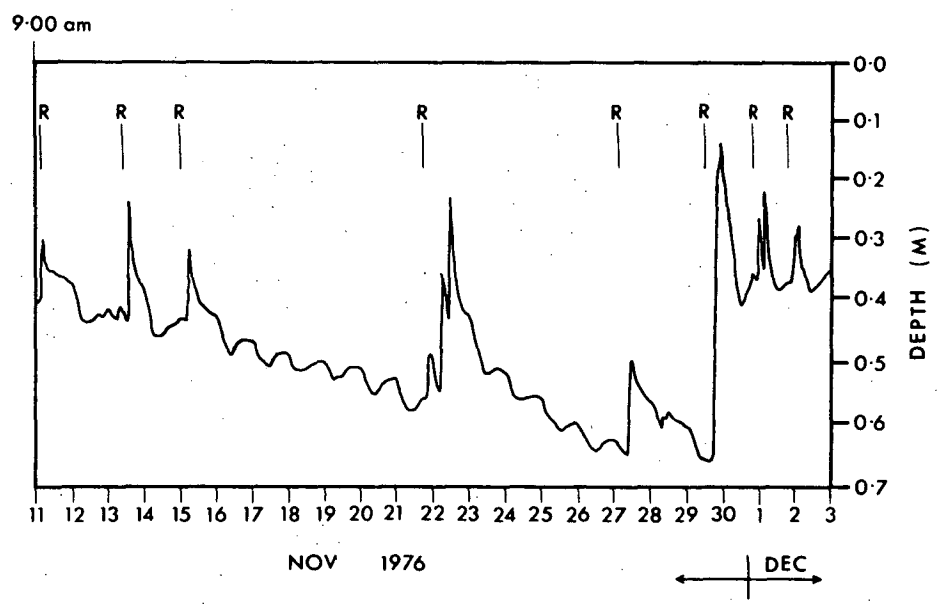
9·00 am
0·0
0·1
0·2
0·3
0·4
0·5
0·6
0·7
DEPTH (M)
R R R R R R R R
11 12 13 14 15 16 17 18 19 20 21 22 23 24 25 26 27 28 29 30 1 2 3
NOV 1976
DEC

As outlined on page 235 evapotranspiration is the most important process of removal of groundwater from the system. Study of losses during a continuous dry spell such as shown in Figure 48, indicates that losses due to evapotranspiration decrease as the dry period is prolonged. This is a function of increased protection of the water table from evaporation by an increased thickness of sand as the water table declines and of the effect of increased dryness (Davies & Allen, 1973). In addition, as the level declines, the water table falls below the root levels of the grasses, and the ability of the vegetation to transpire water derived directly from the water table is restricted.

2.7 Water Table Response to Sources and Sinks

2.7.1 *The Problem of Direct Correlation*

Examination of the groundwater level recorder charts indicates that the relationships between water table increase and rainfall, and between pan evaporation and water table decline are not simple. Although the water table response is immediate, and thus is primarily controlled by rainfall, the amount of the increase does not directly correlate with rainfall amount. Usually the water table rise is greater than the precipitation input, even when the figure is adjusted for porosity. Also, when the water table level is high the increase is usually relatively greater for light rainfalls than for heavy falls, and *vice versa* when the water table level is low.

Similarly, pan evaporation does not correlate directly with water table losses. The losses indicated on the charts as being due to evapotranspiration often significantly exceed the pan

evaporation, which is the maximum potential loss from a free water surface. In Tasmania evapotranspiration ranges from 70 percent to 80 percent of pan evaporation values, depending on the nature of the vegetation cover (Bureau of Meteorology). In addition, there is consistently a rapid decline of the water table soon after rain has ceased (Figure 49). This cannot be explained by evaporative losses, particularly as many of the water level recession curves occur during the night.

There are two possible factors which could account for these effects. Firstly, it is possible that redistribution of water may occur within the aquifer due to differential physical composition and this may produce apparent losses and gains in different areas rather than actual losses and gains by the system. Secondly, the development of a capillary fringe through which water must travel could act as a buffer zone between the groundwater and the surface while water is extracted from the system by evapotranspiration or added to the system by precipitation. The effect of such a buffer zone could produce the observed water table responses. Both of these possibilities have been examined.

2.7.2 *Possible Redistribution of Water within the Aquifer*

The hypothesis that water may be redistributed within the aquifer after rain has fallen is based on the concept that there is uneven reception of the rain water and that the imbalance established is redressed by flows of groundwater from areas which have received more to areas which have received less. The two factors which could control this type of phenomenon would be permeability of the sand and the hydraulic gradients of the groundwater surface.

To explain the mechanisms which may operate under these conditions it is best to consider a hypothetical situation where two contiguous areas of equal elevation have markedly different coefficients of permeability. During a given rainstorm, the low permeability area cannot accept the total amount of rainfall which occurs because the permeability is less than the rainfall rate, and the surface therefore becomes a temporary barrier to percolation. However, the area with high permeability is able to receive all the incident precipitation plus the excess which could not be absorbed by the low permeability area and which is transferred by runoff to the area of high permeability. Initially, the water table of the high permeability area would show an additional rise in level equivalent to the amount of extra water received. Similarly, the area of low permeability would show less rise than would be expected for the rainfall amount since it could not accept all of the precipitation at the time. This would result in contiguous areas developing different water table levels during and following significant periods of rainfall input. The resulting head difference would enable groundwater, at a later time, to move from the area of high permeability and high water table level to the low permeability zone with the lower water table level, until the water table levels were equalized (Figure 50).

This simplified example is far removed from the complex conditions prevailing in the Tomahawk area. If a realistic estimate of the effect of this mechanism on the water table response is to be gained for comparison with observed water table response then many considerations have to be taken into account. The factors which can readily be included in such an estimate are variation in surface elevation, the initial position of the water table, the average porosity of the sands, the losses at the seaward

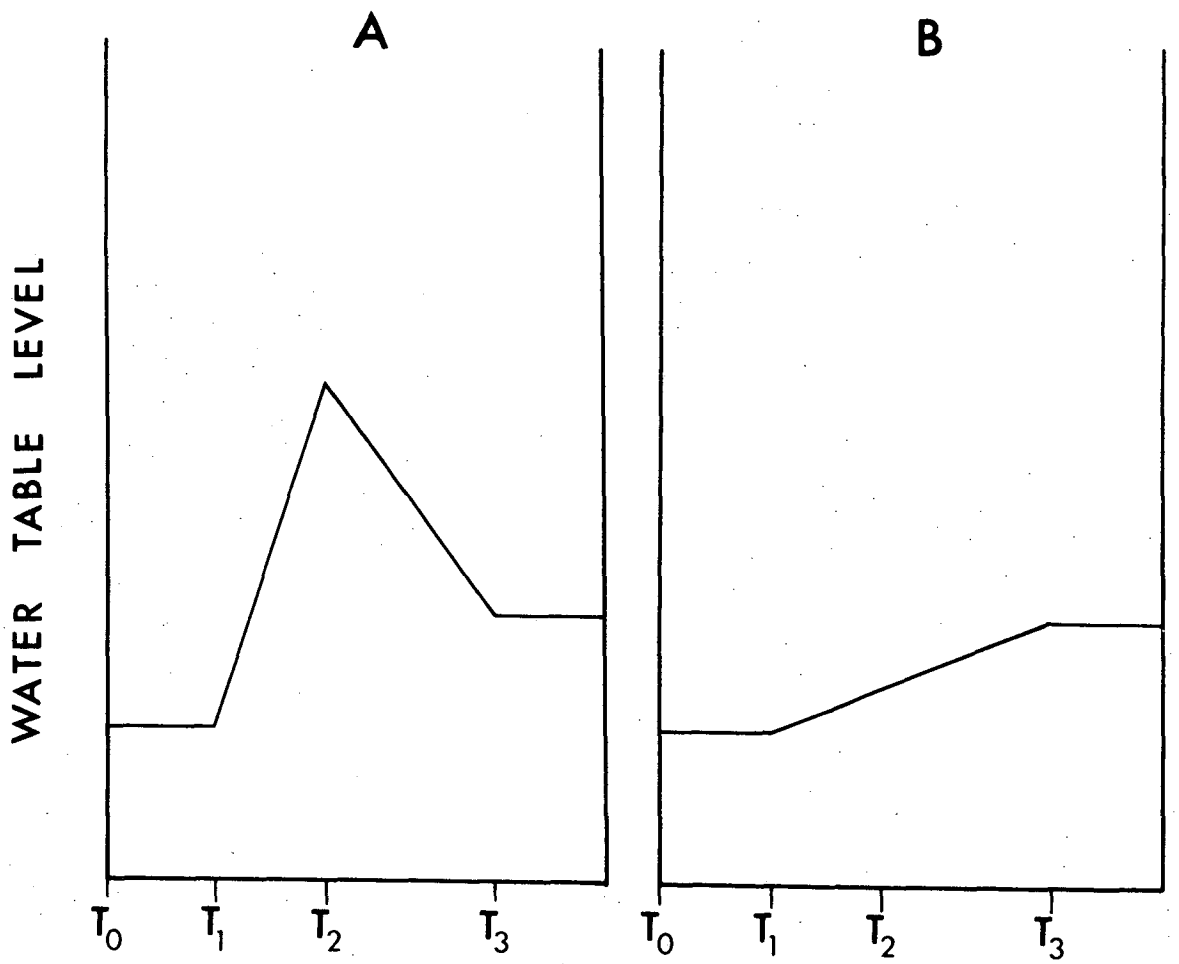

FIGURE 50 Hypothetical Water Table Response due to Redistribution of Water within a Heterogeneous Aquifer.

Chart A indicates the response within a highly permeable area

Chart B indicates the response within a low permeability area

T_0 = Initial groundwater level at equilibrium

T_1 = Time of rainfall

T_2 = Occurrence of maximum head difference between the two areas due to extra input to area A and reduced input to area B.

T_3 = Occurrence of equilibrium conditions due to groundwater flow from area A to area B. The difference in water table level between T_0 and T_3 is proportional to the rainfall.

and river margins, the inputs provided by runoff from the rainfall catchment area not mantled by the aquifer, and the variation in the permeability of the sands.

The easiest method of taking the above criteria into account on an areal basis is to compute the resultant flows. A computer program has been devised which includes the above criteria but it has some limitations related to the necessity to simplify a complex situation. The model is unable to deal adequately with details of the areal variation of rainfall, minor topographic variation, porosity variation, differences in horizontal and vertical permeability, and soil moisture conditions over the catchment. In addition, the measures which were used are derived from field and laboratory work and may not necessarily correspond to actual aquifer conditions. However, the model is useful because it allows an estimate of the relative importance of groundwater redistribution to water table response.

The model calculates the water input to each square of a 250 m grid placed over the study area, calculates the depth attained by the saturation front after set time intervals, and for grid squares where the front has reached the water table it calculates the horizontal flow as controlled by head differences and permeability. The period of observation can be set to any desired length. The groundwater level in all grid squares after each time interval, as well as the water loss to the sea and the Tomahawk River, is printed out. Appendix 1 is a computer printout of the computer program for the model.

The hypothesis which forms the basis of the model does not account for the observed water table responses. Although the model predicts the rapid water table rise, the amounts predicted

are not similar to the amounts observed on the recorder charts. An additional purpose of the calculation was to assess the extent to which the subsequent water table decline after rainfall could be attributed to differences in hydraulic head. Comparison of the calculated results and the water table level recorder shows for example, that the water table decline predicted by the model is only 17 percent of the actual decline in Recorder IV, and Recorder I showed an overall decline of 60 mm while the model predicted that the water table at this locality should have risen by 7 mm.

The model was designed to examine the possibility of groundwater flow from high permeability areas to low permeability areas as a major mechanism for redistribution of water within the aquifer. The flows calculated in this way only explain up to a maximum of 20 percent of the observed water table loss. Thus, it appears that the hydraulic gradients, combined with the various permeabilities of the aquifer, are too low to allow the observed water losses to be primarily attributed to redistribution within the aquifer. However, the use of the model has been valuable since groundwater redistribution can now be discounted as the principle source of observed water table fluctuation.

2.7.3 *The Effect of Soil Moisture on Groundwater Response*

Although the capillary fringe has been described as part of the zone of aeration (Meinzer, 1923; Tolman, 1937; Lambe, 1951; Todd, 1959; Davis & De Wiest, 1966) there are few references which describe the effect of the capillary fringe on water table response to precipitation input and evapotranspiration output

(White, 1932; Troxell, 1936). Here, the capillary fringe is considered as the active intermediary between the water table and these inputs and outputs, and to have a significant bearing on the water table response.

Water exists in three conditions within the zone of aeration (Briggs in Todd, 1959). Gravitational water drains freely to the water table. Capillary water, held by surface tension in the pore spaces, is moved by capillary action. Pellicular water which is held by strong adhesive forces, and is therefore not usually available to plants, is relatively immobile (Todd, 1959).

The capillary zone extends from the water table which is located by the static level of free water in supercapillary openings to the limit of capillary rise (Tolman, 1937). Within this capillary fringe there is a gradual decrease in moisture content with height above the water table. In the region just above the water table almost all pores contain capillary water. Higher in the profile only the smaller pores contain capillary water, and still higher only the smallest connected pores contain water which is linked to the water table. Figure 51 shows that the profile of moisture content above the water table decreases from 100 percent saturation of available pore space just above the water table to the moisture content of the pellicular water near the top of the capillary fringe (Todd, 1959). The openings in many fine grained, unconsolidated sediments allow a maximum capillary rise of 1 to 2 m. In sands the rise is between 0.1 and 1 m, and in gravels less than 0.1 m (Davis & De Wiest, 1966).

Short term water table fluctuations have been studied in detail by White (1932), who related many of them to transpiration from the capillary fringe. However, possibly due to the aridity

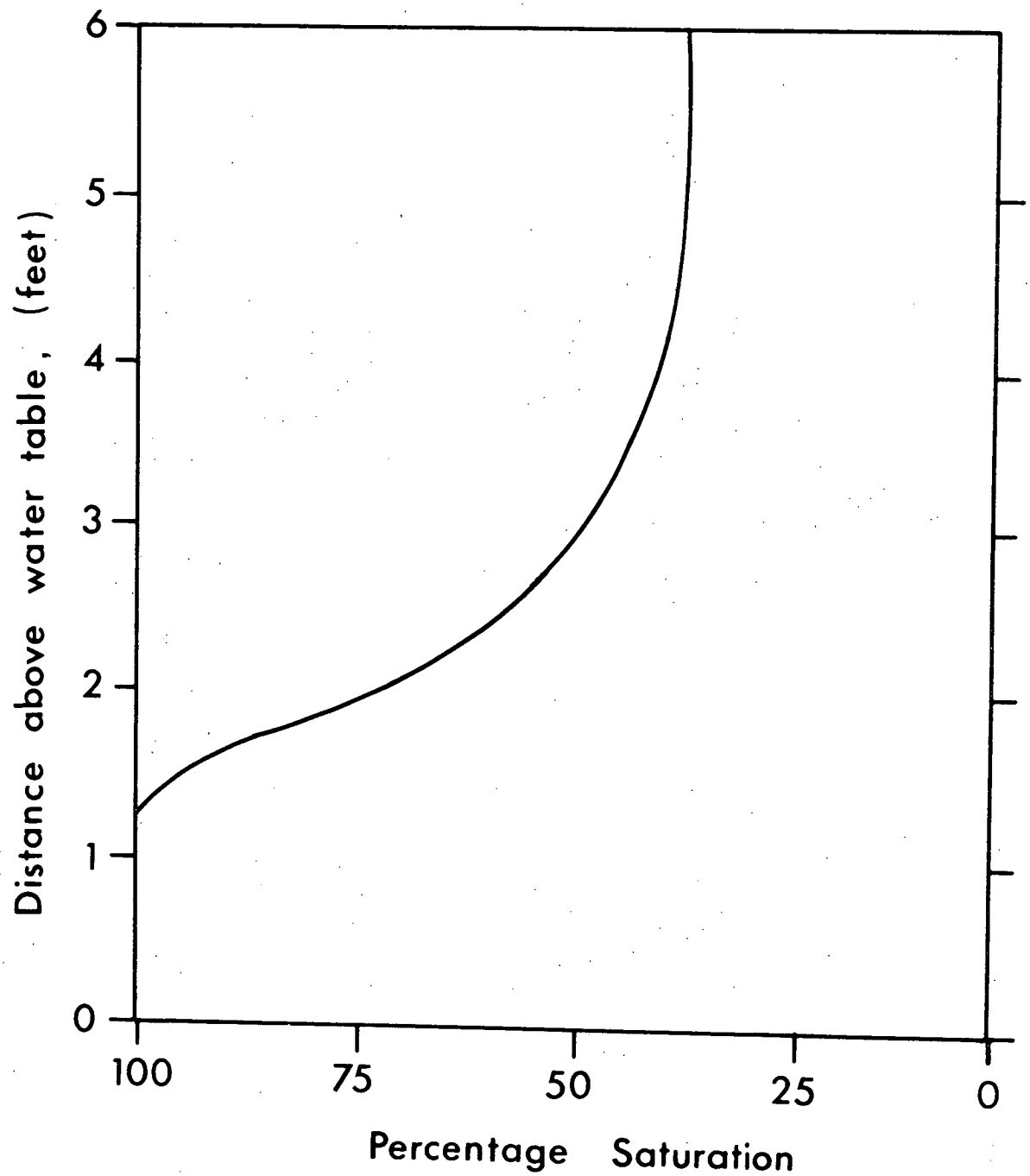

FIGURE 51 General Soil Moisture Conditions in the Zone of Aeration.

After Todd (1959)

of the Escalente Valley, Utah, which has a mean annual rainfall of around 300 mm, White paid little attention to the water table response to rainfall.

Since the capillary fringe is an integral part of the soil moisture conditions of areas where open water tables occur in sandy sediments, the soil moisture profile must be taken into account when considering water table response to rainfall and evapotranspiration.

If a hypothetical situation is considered in which the soil moisture content above the water table is zero, then provided no absorption of rainwater occurs in the soil, the water table will rise by an amount equal to the rainfall divided by the porosity of the sediment. However in reality, soil moisture occupies between 30 percent and 100 percent of the pore space above the water table and there is less downward moving water needed to saturate the sediment. Thus the water table will rise by a significantly greater amount than in the hypothetical case. A further implication of this phenomenon is that the gravitational water fills some of the vacant pore space within the capillary fringe and temporarily reduces the capillary fringe. Subsequently, when the supply of gravitational water becomes less than the rate of capillary rise, the capillary water rises from the water table and the capillary fringe reforms which lowers the water table. The net water table increase resulting from the precipitation is still in excess of the rise predicted in the hypothetical example because there is always some pellicular water present. Thus, the general response of the water table to rainfall should be to rise quickly to a maximum and recede more slowly at a rate determined by the capillary rise attainable under the soil conditions, to a

new level above the original water table level. This type of response to rainfall has been recorded frequently at Tomahawk as shown by Figure 49, and has been observed by White (1932, page 32).

If an approach similar to the problem of gains to the water table is adapted to the problems of losses due to evapotranspiration, then the effect of the soil moisture profile on the water table response can be ascertained. If the same example is taken where the water table lies beneath a zone of zero soil moisture content, then the water table level will decrease by the quantity of water lost through evapotranspiration divided by the porosity. In reality, the presence of soil moisture produces a decline which is apparently in excess of these amounts. The forces of evapotranspiration extract water from the zone of aeration, and since these forces extract water over relatively longer time periods than when water is added to the system, the capillary fringe is able to constantly readjust to the normal rates of loss. Since pellicular water in the soil moisture profile tends to remain constant, the water table drops by an amount equivalent to the moisture lost from the zone of aeration. This results in an apparently large water table decline, which is consistently observed at Tomahawk and Figure 49 provides a good example.

The pronounced diurnal fluctuations shown in Figure 52 and overnight recovery of the water level observed at Tomahawk and also by White (1932), is created by high evapotranspiration withdrawal from the capillary fringe. Under these conditions the plant cover draws water directly from the capillary fringe during the day and lowers the water table due to increased suction. In

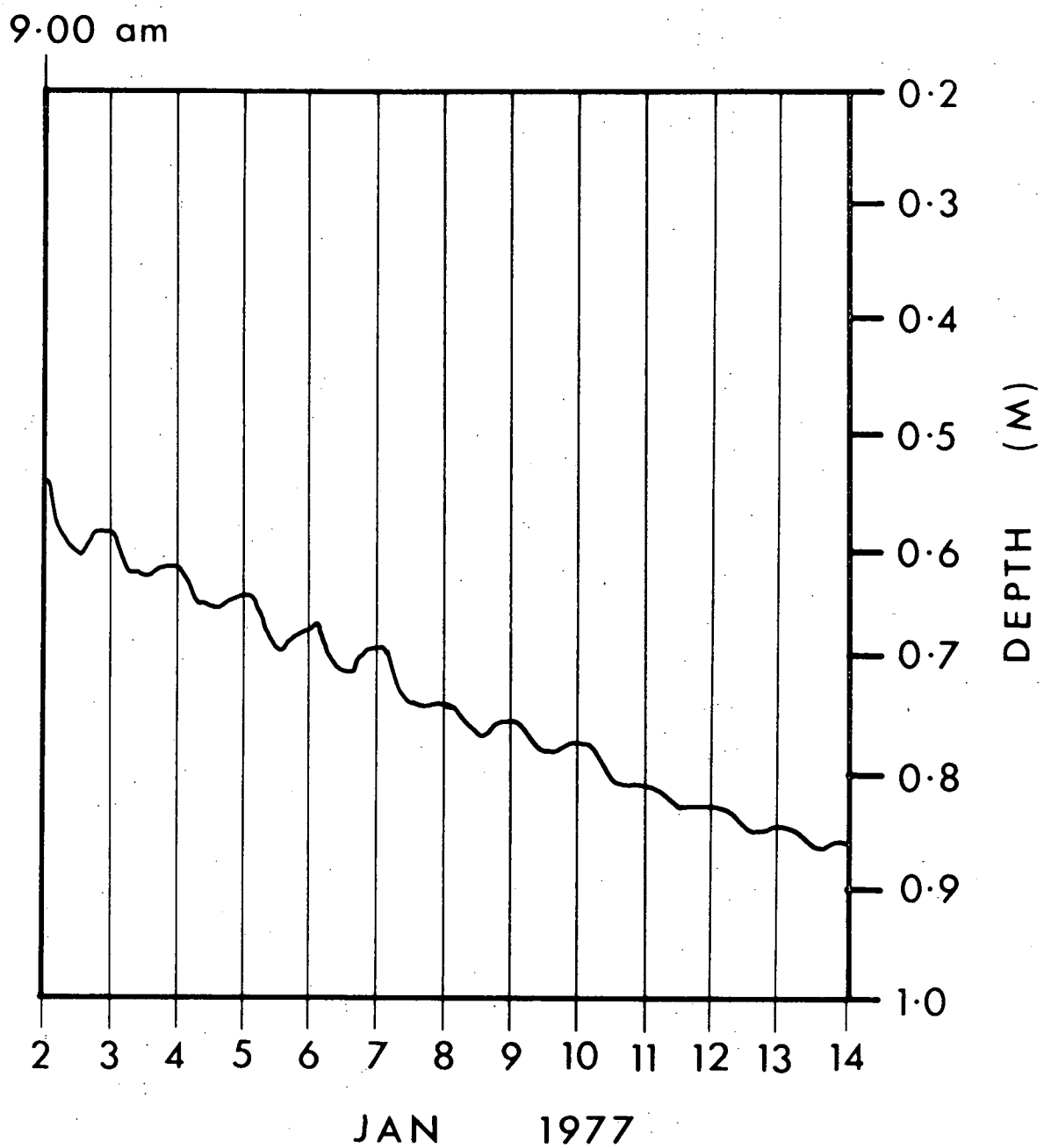

FIGURE 52 Water Table Rise Overnight.

Diurnal water table fluctuations with marked overnight recovery (Recorder I).

this case the added suction extends the length of the capillary tubes beyond the lifting capabilities of the capillary forces alone. However, during evening the rate of transpiration decreases and the suction exerted by the plants is less than the gravitational force required to maintain the column of water at the daytime height above the water table. As a result the water in the capillaries drops to the level of normal capillary lift which adds water to the zone of saturation and causes the water table to rise. White (1932) attributed the overnight rises entirely to recharge from artesian sources but at Tomahawk this can be discounted as artesian water does not enter the groundwater system, and they are probably explained by the above mechanism. The difference between the water table levels on successive mornings when the system is balanced is directly related to the amount of water lost.

Since precipitation is the major input, and evapotranspiration forms the principal loss from the Stumpys Bay Sand Aquifer, and as the soil moisture profile can be demonstrated theoretically to have a significant bearing on water table response to these inputs and outputs, it should be possible to quantify these relationships and develop a predictive model of groundwater response. The development of such a model here is not for prediction *per se*, but to assess the degree to which the parameters of the model account for the observed groundwater fluctuations. If the model proves to be capable of reasonable levels of prediction then the dynamics of the groundwater system can be demonstrated to be a function of the parameters of the model.

Since the proposed model was designed to simulate short term groundwater levels using only soil moisture, rainfall, and

evapotranspiration as the parameters it was necessary to determine the soil moisture characteristics for the Tomahawk area, and to obtain daily precipitation and evapotranspiration data.

Samples have been collected from five sites for determination of some soil moisture profile characteristics. Since they were taken during winter (May 25 and 26, 1977) more profiles need to be taken under summer conditions before the results can be applied to all situations.

The soil moisture determinations were carried out by the collection of soil samples of known volume with a 4.5 cm diameter sampling tube and subsequent calculation of moisture content by the measurement of weight loss after oven drying at 110°C. The samples were then ignited to 450°C for 2 hours and as there was a low proportion of fines in the soils the weight loss represented the weight of organic matter in the sample. The volume of organic matter was calculated by assuming a density of 1.3 for the organic matter. The porosity of each sample was calculated by subtraction of the volumes of sand and organic matter from the total volume of the sample. Lateral movement of the sample tube during collection caused a decrease in the volume of sample collected. This error can not be ascertained exactly but has been allowed for by subtraction of 10 percent from each calculated porosity. Soil moisture content was expressed as a percentage of the porosity. There are several sources of potential error inherent in the technique and the derived soil moisture profiles are therefore only approximate.

The profiles tested showed markedly different moisture characteristics. One group of profiles was taken from soils which consisted of a surface humic A horizon and clean sand below this

horizon. The other group was from soils which consisted of an organically enriched $B_{2h,ir}$ zone of a groundwater podzol to the level of the water table on the day the samples were taken. Since the two profiles represent the extremes of aquifer conditions near the ground surface they have been treated separately to determine the effect of each soil condition on the theoretical water table response to precipitation and evapotranspiration.

The soil moisture measurements were taken two days after heavy rain and the soil therefore was probably close to field capacity. Also, the water level recorder charts showed that the water table responded normally to the rainfall and therefore a major proportion of the precipitation reached the water table soon after the rain fell. The comparison shown in Figure 53 between the organically enriched sands and the cleaner sands, and between the humic surface horizons and the lower, non humic horizons of the cleaner sands, indicates that humic sands retain more water than clean sands. The simplified soil moisture profiles also shown in Figure 53 have been treated as compound straight line relationships to simplify calculation and have been taken to represent conditions within a clean sand profile without any marked organic enrichment and within a profile which has been markedly enriched by organic matter.

The water at field capacity in the organically enriched sands makes up approximately 72 percent of the soil water and is unavailable for rapid transfer through the profile under these conditions. On the other hand, 35 percent of the soil water is needed to establish conditions at field capacity for cleaner sands. The capillary fringe of the organically enriched sands extended

FIGURE 53 Soil Moisture Profiles at East Tomahawk.

(a) Plots of two profiles (o and x) from clean sands. o' and x' are samples with more than 2% organic matter.

(b) Plots of 3 profiles (o, x, and c) from organically enriched sands.

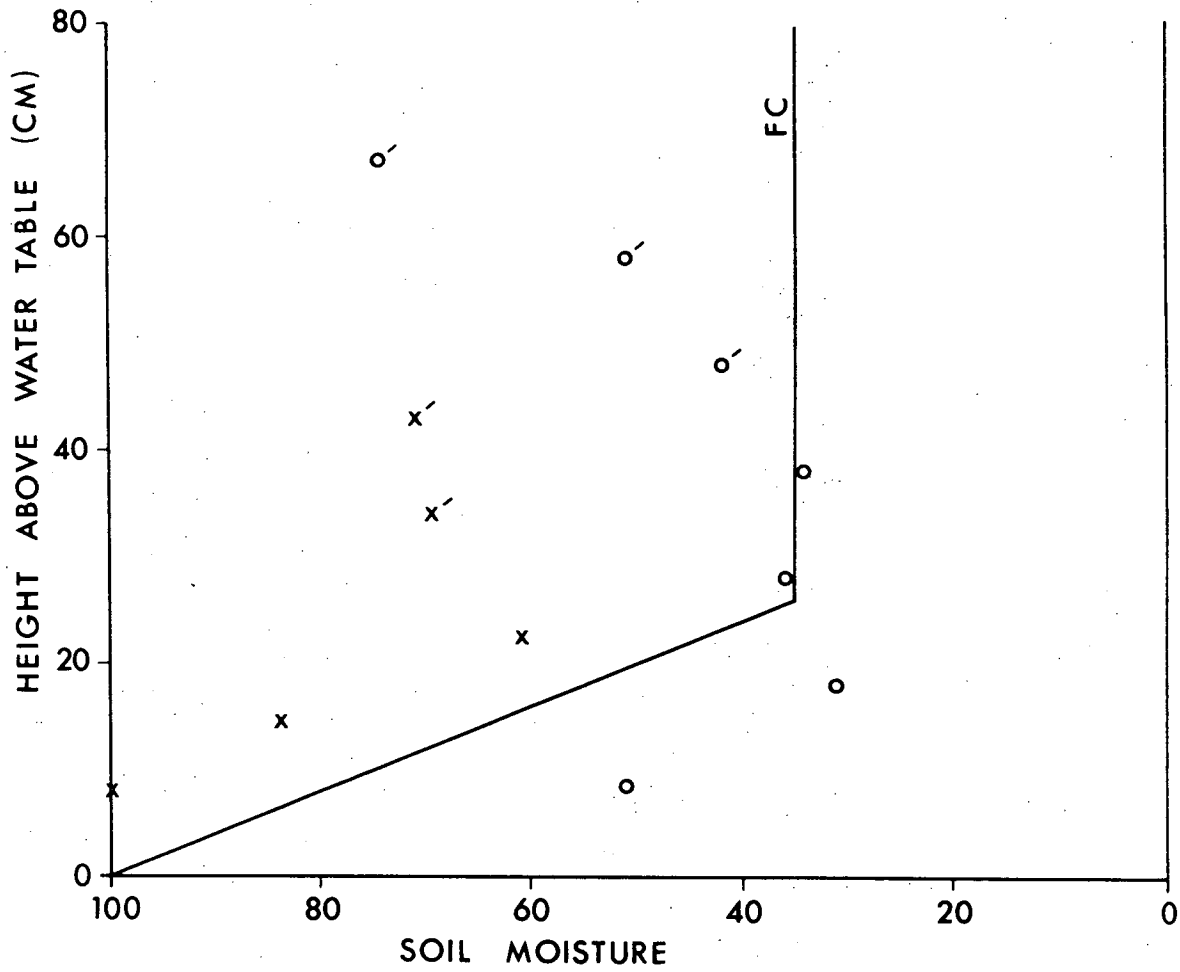
HEIGHT ABOVE WATER TABLE (CM)
80
60
40
20
0
FC
100
80
60
40
20
0
SOIL MOISTURE

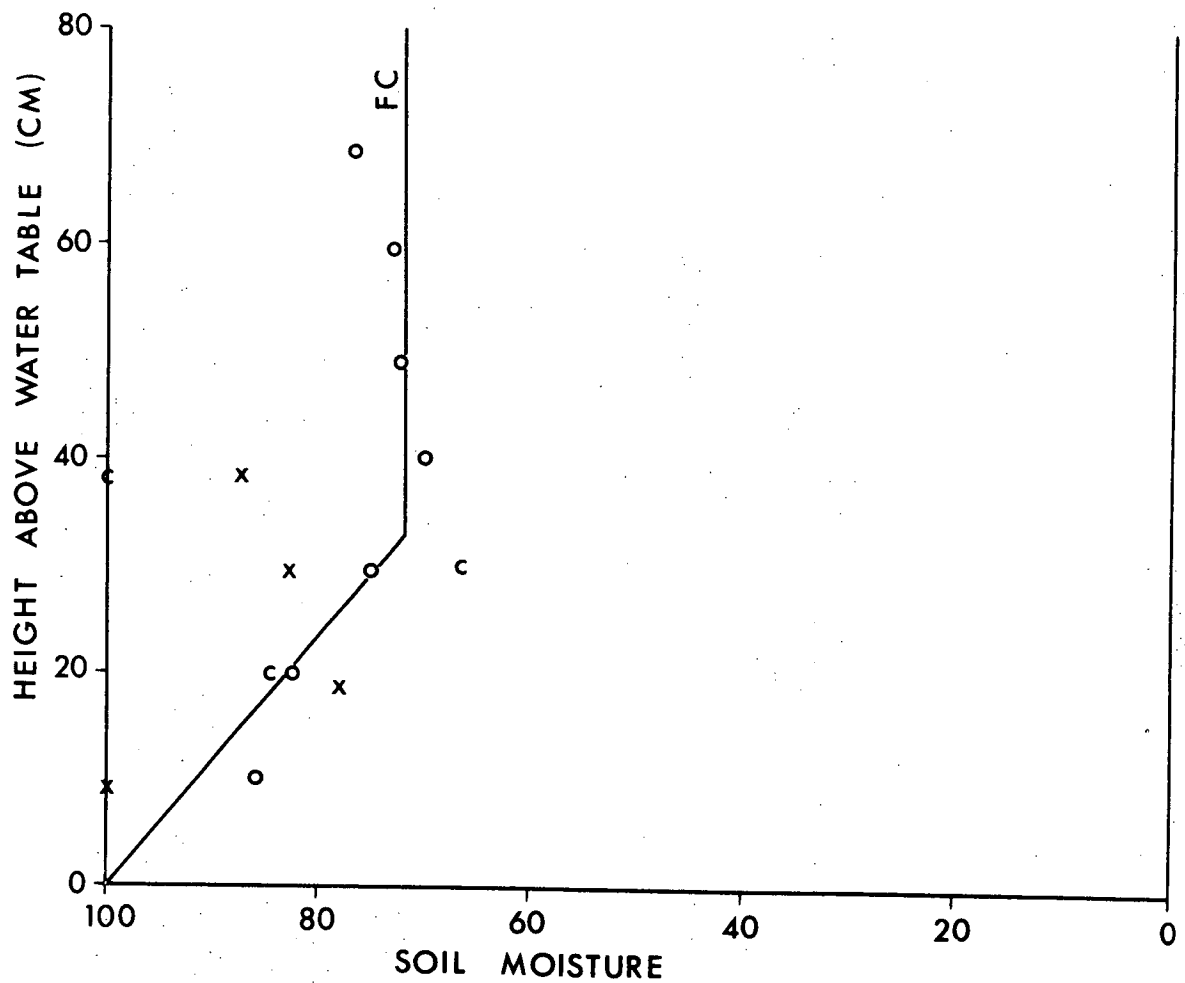
HEIGHT ABOVE WATER TABLE (CM)
80
60
40
20
0
FC
100
80
60
40
20
0
SOIL MOISTURE

to 33 cm above the water table while that of the cleaner sands only extended to 26 cm. Organic matter may increase capillarity of the sands by decreasing the pore diameter.

For each of the soil conditions the relationship between rainfall and initial water table rise was calculated. The assumption for this calculation was that the water which enters the soil fills the available pore space, shown in Figure 54(a), above the water table. Figure 54(b) shows the situation after rain when a portion of the capillary fringe water is temporarily included within the zone of saturation and a high initial water table rise follows. Decline of the water table then occurs until the capillary fringe is re-established. Figure 54(c) describes this equilibrium condition. This equilibrium relationship between water table response and rainfall input is linear for each soil profile. In Figure 54(c) the area $\frac{R}{\phi}$ multiplied by a unit length would give the volume of sand saturated by the rainfall R. This area can be written as:

$$\frac{R}{\phi} = \Delta WT \times (1 - FC)$$

$$\text{or} \quad \Delta WT = \frac{R}{\phi(1 - FC)} \text{ cm} \qquad \ldots\ (9)$$

where ΔWT = Water table change (cm)

R = Rainfall (cm)

FC = Soil moisture content at field capacity (expressed as a proportion of porosity)

ϕ = Porosity of the sand

Thus it is possible to predict the water table rise at equilibrium due to a given rainfall.

FIGURE 54 Theoretical Soil Moisture Changes.

Soil moisture (SM) is expressed as a proportion of porosity. H_0 = arbitrary datum.

(a) Equilibrium soil moisture profile at field capacity showing the amount of pore space which is available for occupation by rainwater.

(b) Disequilibrium soil moisture profile immediately after rain. The shaded area represents the water added by rainfall.

(c) Restoration of the capillary fringe causes the water table to decline until the new equilibrium moisture profile is established. Each shaded area represents the rainfall quantity.

(d) Basis for the calculation of the maximum water table level attained during the disequilibrium period. Calculation of the rainfall required to raise the water table to the two points S1 and S2 permits the construction of a graph which describes the disequilibrium water table rise due to a given rainfall.

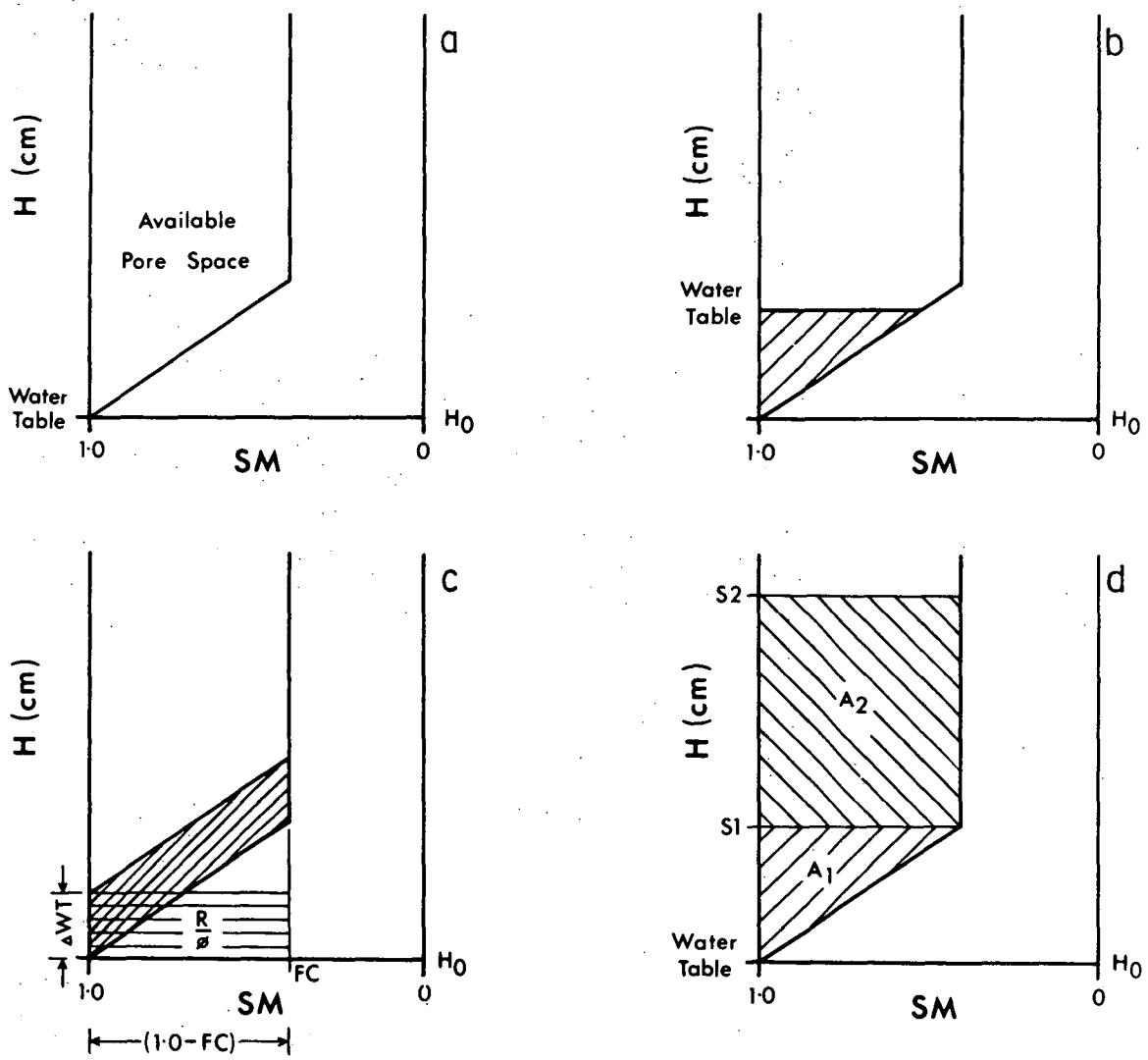
a
H (cm)
Available
Pore Space
Water
Table
H0
1·0
SM
0
b
H (cm)
Water
Table
H0
1·0
SM
0
c
H (cm)
ΔWT
R
ø
FC
H0
1·0
SM
0
(1·0-FC)
d
S2
H (cm)
A2
S1
A1
Water
Table
H0
1·0
SM
0

However, for the intervening disequilibrium period the calculation of the maximum water table rise is not quite as simple due to the change in gradient of the moisture profile. This relationship is determined by the calculation of the rainfall required to raise the water table to the point where the soil moisture profile alters slope. Therefore, in Figure 54(d), for a water table rise of S_1 cm, $(\frac{R}{\phi})$ equals the area of A_1.

$$\text{The area of } A_1 = \frac{(1 - FC) \times S_1}{2}$$

$$\text{since} \quad \frac{R}{\phi} = A_1$$

$$R = \frac{\phi(1 - FC) \times S_1}{2} \text{ cm} \quad \ldots\ldots \quad (10)$$

Similarly, for a water table rise of S_2 cm, the rainfall input $(\frac{R}{\phi})$ equals the area of A_1 plus the area of A_2. Thus,

$$A_2 = (S_2 - S_1)(1 - FC)$$

$$A_1 = \frac{(1 - FC)\ S_1}{2}$$

$$\text{and} \quad \frac{R}{\phi} = (A_1 + A_2)$$

$$R = \phi(1 - FC)(S_2 - \tfrac{1}{2}S_1) \text{ cm} \quad \ldots\ldots \quad (11)$$

These calculations were applied to each soil condition and Figure 55 shows the plotted relationships of water table response to rainfall.

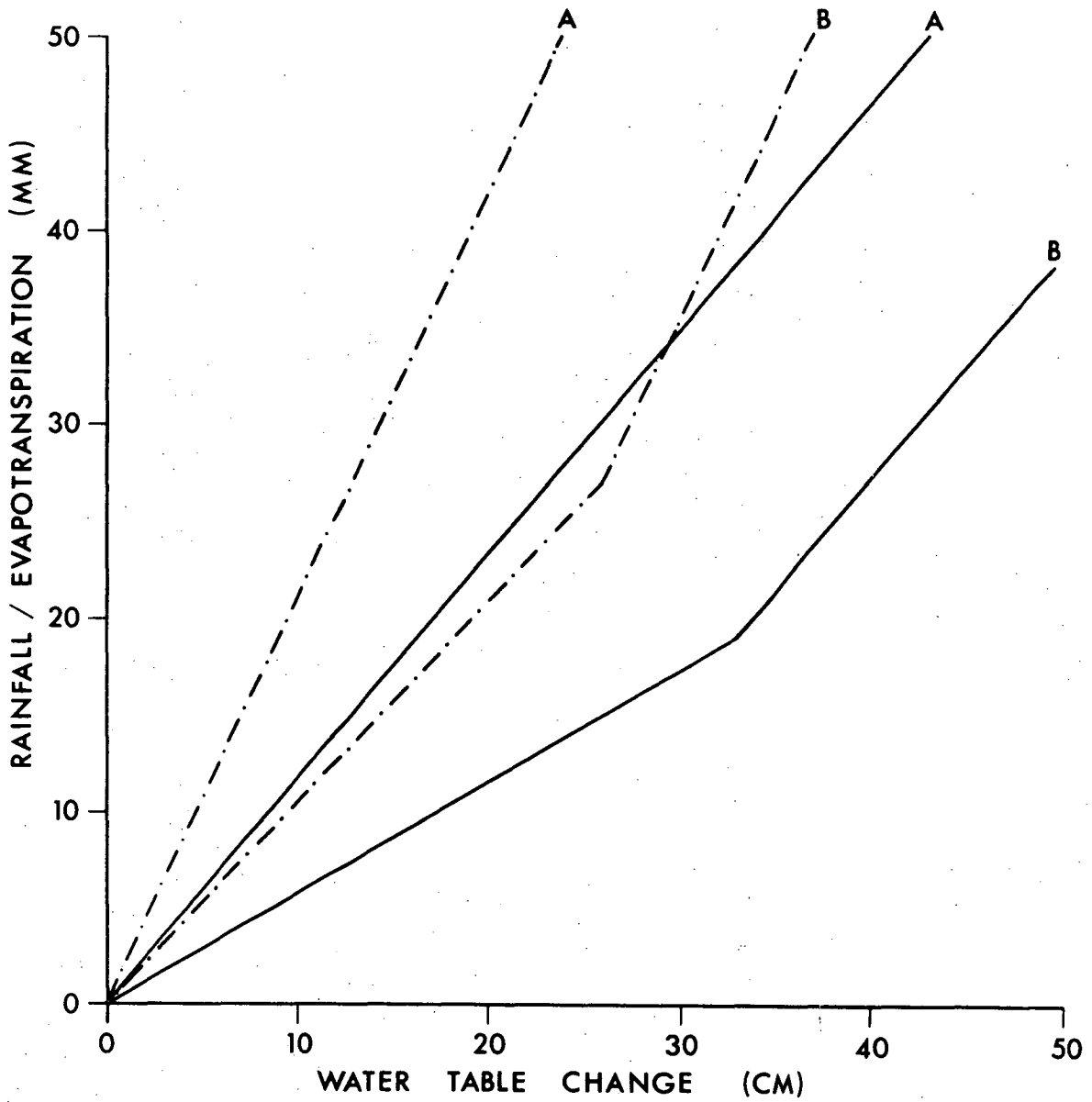

FIGURE 55 Relationships between Rainfall/Evapotranspiration and Water Table Rise/Fall for Two Types of Sand.

The broken lines represent the relationship for the cleaner sands and the continuous lines represent the relationship for the organically enriched sands. Equilibrium relationships are shown by the lines marked A, and disequilibrium relationships by the lines marked B.

The application of these relationships for any given rainfall when the soil is at field capacity enables the prediction of the initial increase in water table and of the subsequent drop to the equilibrium position after the capillary fringe has been re-established. Water loss through evapotranspiration occurs at such a rate that the capillary fringe is constantly able to adjust to the rates of these losses. Thus, if the evapotranspiration during a period is known, the resultant water table decline can be read directly from the equilibrium relationship.

A simulation was carried out for the 44 day period from 7 November to 22 December, 1976 and compared with the water table fluctuations in 3 recorded bore holes. This period was selected because the water table was within 1 m of the surface and the soil was probably close to field capacity for most of the time. As the time of commencement of rainfall is not known because the data is collected at 9 a.m. for the previous 24 hour period, it is assumed in the model that all rain recorded for that day fell at 9 a.m. This assumption produces obvious potential for discrepancies between the model and the observed water table response on rain days. In addition, the model assumes that the rainwater reached the water table within 4 hours and the initial disequilibrium water table level occurred at that time. This assumption is derived from water table records where the time of commencement of the rain was known. A further assumption is that the capillary fringe was re-established within 12 hours of the commencement of rain. Packard (in Tolman, 1937, pages 155-157) measured rates of capillary rise for various soil materials and found that sandy loam soils showed an initial rapid rate of rise of at least 46 cm per day. Since the height of the capillary

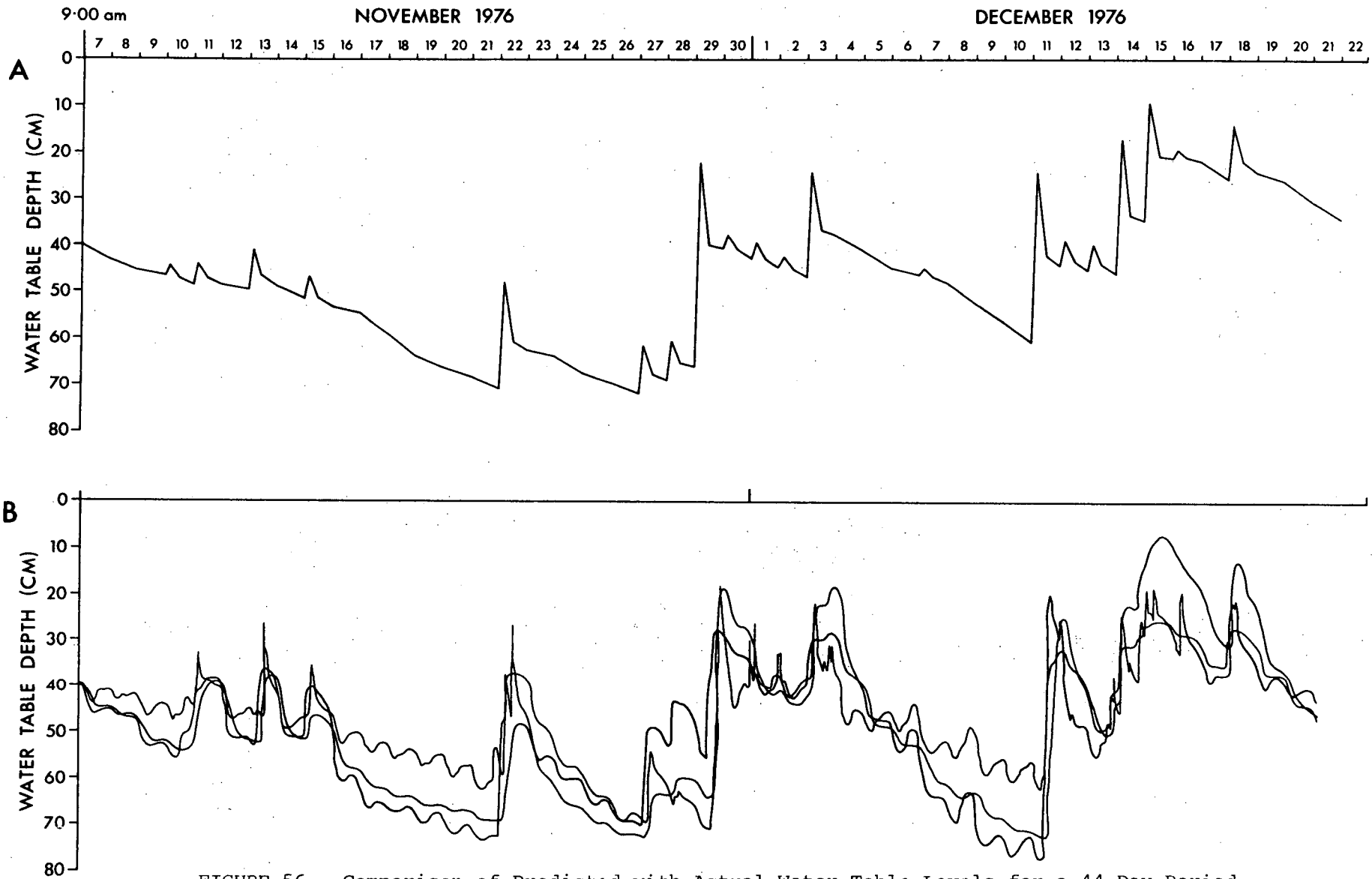

FIGURE 56 Comparison of Predicted with Actual Water Table Levels for a 44 Day Period.

Levels predicted by the model are shown by A. Graph B shows the levels observed at three recorder sites (I, III and IV).

fringe in the soils at Tomahawk appears to be a maximum of 40 cm this figure appears reasonable. Evapotranspiration losses from the model were assumed to have occurred evenly over the 24 hour period since this is the period of resolution of the model. In reality, the losses through this mechanism occur mainly during the afternoon. On days when rain fell, the equilibrium water table level of the model was calculated and one half of the daily evapotranspiration loss was subtracted from the equilibrium level for the initial 12 hour period. For the remaining 12 hour period the remainder of the evapotranspiration loss was subtracted from the water level.

The simulation was calculated for the organically enriched sands only, since this layer frequently forms the top 1 m of the sand, and the water table was within this zone in November and December 1976. Figure 56 shows a comparison between the model and the observed water table fluctuations in 3 recorded water level bore holes. The fairly wide range of response between the three recorded sites is almost certainly due to local variations in porosity, variation in rainfall inputs and evapotranspiration losses, and to variation of the configuration of the soil moisture profile.

A linear correlation and regression analysis of the predicted water table levels and an average of the three observed water table levels for 9 a.m. each day gave a correlation coefficient of 0.85 and showed that water levels predicted by the model were closely correlated with the observed levels (Figure 57). Scatter in the relationship is due to: (a) the model is based on only five soil moisture profiles, (b) the moisture profiles are considered as compound straight lines whereas they

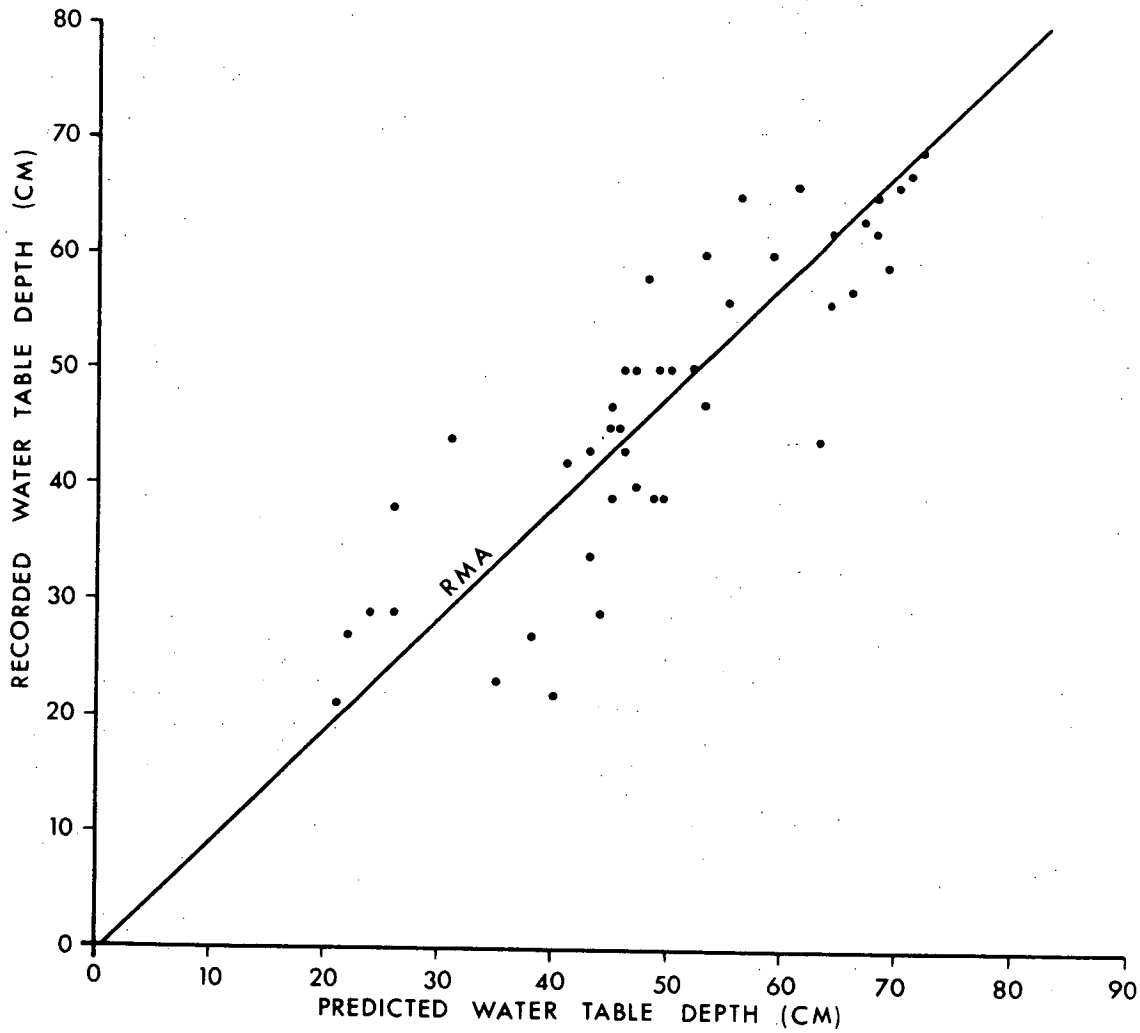

FIGURE 57 Relationship between Recorded Water Table Depth and Predicted Water Table Depth.

RMA = Reduced Major Axis line, (Till, 1973). Pearson's r = 0.85. The recorded water table depth is the mean depth for the three sites.

are almost certainly curves, (c) there is a lack of accurate synchronization of the rainfall events between the model and reality, (d) divergence between the model and reality occurs due to the compounding of errors as the time period is extended, (e) only one rain gauge is present in the area and some showers are very localized, (f) the evaporation data, although as reliable as possible, may not correspond precisely to the pan evaporation of the area, (g) the relationship between pan evaporation and evapotranspiration has not been accurately measured, and (h) the porosity value used in the model almost certainly is not representative of the whole area.

Given the above deficiencies, the high degree of correlation between predicted and observed water table levels indicates that the model accounts for 73 percent of the total variance. This suggests that for systems of this type the variables used in the model are the major determinants of groundwater levels.

The model discussed so far, provides insights into the mechanisms of water table response in times of high water table and humid meteorologic conditions. However, since the soil moisture profiles were measured under moist winter conditions there remains the problem of whether the fundamentals of the model apply to conditions when the water table is at greater depths below the surface and when the soils are much drier.

The recorder response under dry conditions differs from the response during high water tables and humid periods. During dry periods and low water table levels the water table rise due to a given rainfall is less than under moister conditions. Also, as Figure 42 shows, the response to rainfall is slower and there

is no subsequent rapid decline in water level due to the setting up of disequilibrium conditions. To evaluate the nature of this change the observed water table response under dry conditions has been compared with the response predicted by the model and plotted in Figure 58 against depth to the water table. Although only 12 events of significant rainfall were monitored, which produces scatter, there still exists a definite relationship. The graph indicates that, for Recorder I, as the depth of the water table from the surface increases, the water table rise due to precipitation decreases with respect to the response predicted by the model. Although measurements of soil moisture conditions during such dry conditions have not been made, this departure from the model can be explained in terms of the model.

Firstly, the model is based on water table fluctuations which occur in the top metre of sand which usually contains relatively high proportions of organic matter. The sand below 1 m is usually much cleaner and the water table response is therefore governed by the soil moisture characteristics of the clean sands when the water table is low. As shown in Figure 53, the field capacity of the clean sands is much lower than the field capacity of the organically enriched sands and the capillary fringe does not extend as high above the water table as in the organically enriched sands. Therefore the water table response to rainfall and evapotranspiration, as shown by Figure 42, will not be as pronounced in the clean sands.

Secondly, under humid conditions the soil is most often at field capacity (Rose, 1966) and the soil contains water which has not drained rapidly. With the extension of the period since the last rain, water continues to drain from the soil but at a

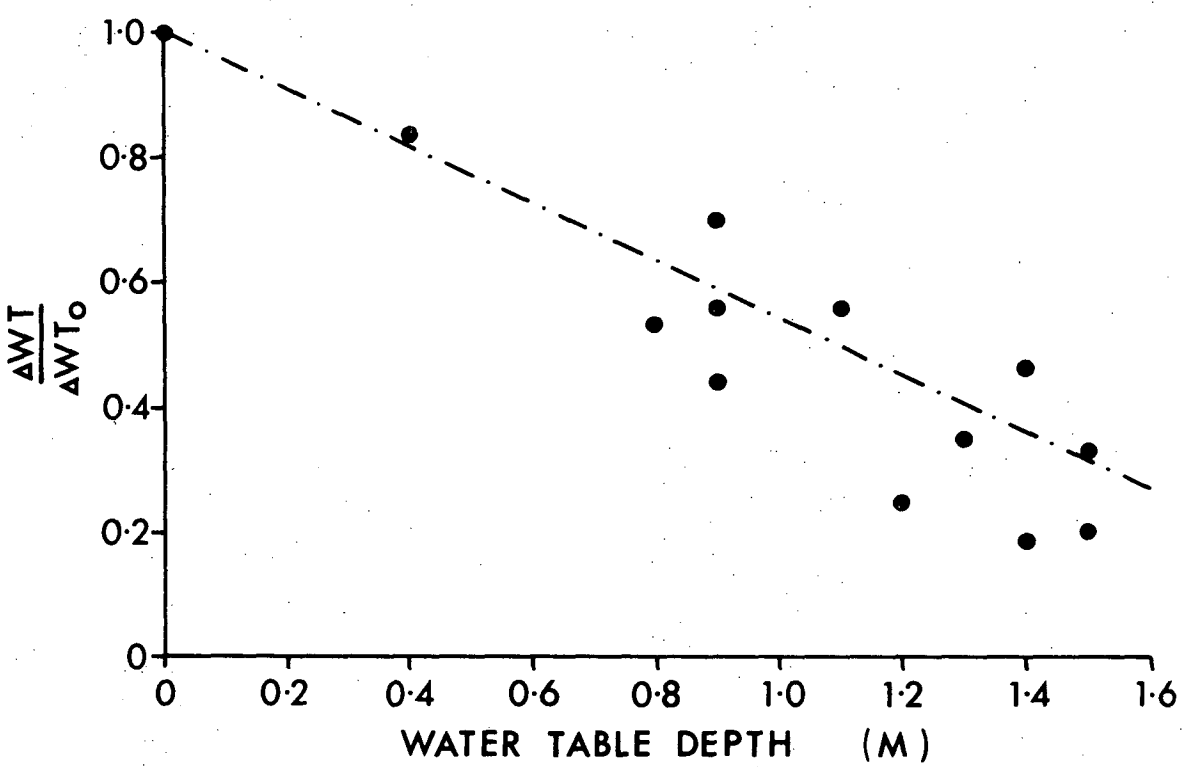

FIGURE 58 Relationship between Reliability of the Model and Water Table Depth.

ΔWT = Water table rise predicted by the model
ΔWT_o = Observed water table rise

much reduced rate. In addition, the plant cover exerts more stress on the moisture contained in the soil. The soil moisture content above the capillary fringe should therefore decrease with time, while the moisture of the capillary fringe remains relatively constant as its extent is determined by capillary conditions above the water table. This evacuation of pore space above the capillary fringe must leave more available space for later rainwater to enter (Figure 59). However, water can only percolate to the water table after the soil has attained field capacity and the excess gravitational water drains downwards. This means that small amounts of precipitation will not cause a rise in water table level until a limit is reached which is determined by the depth to the water table, the field capacity, and the initial soil moisture profile of the soil (Figure 59). A further effect of this set of conditions would be that the rate at which water penetrates the soil is lessened by the damping effect of these additional processes. This could account for the slower response of the water table to rain during these periods and could also account for the absence of the disequilibrium conditions soon after precipitation, because the water is being added to the water table at a rate which allows the capillary fringe to keep pace with the slow, constant rise of the water table.

Thirdly, losses induced by evapotranspiration can only be represented by water table losses if water is extracted directly from the capillary fringe or from the water table by the plant roots. Once the top of the capillary fringe is below the root zone then evapotranspiration can only extract water from the moisture profile above the capillary fringe. The quantity of water available to the plant cover under these conditions is governed by the field capacity, which determines the upper limit,

FIGURE 59 Soil Moisture Conditions after a Dry Period.

The broken line represents the soil moisture profile soon after rain, when the soil is at field capacity. As the dry period is extended the soil moisture profile takes the appearance of the continuous line. Any rain which falls at this time must exceed the quantity A_1 to restore the soil to field capacity before a water table rise can result. Soil moisture is expressed as a percentage of porosity.

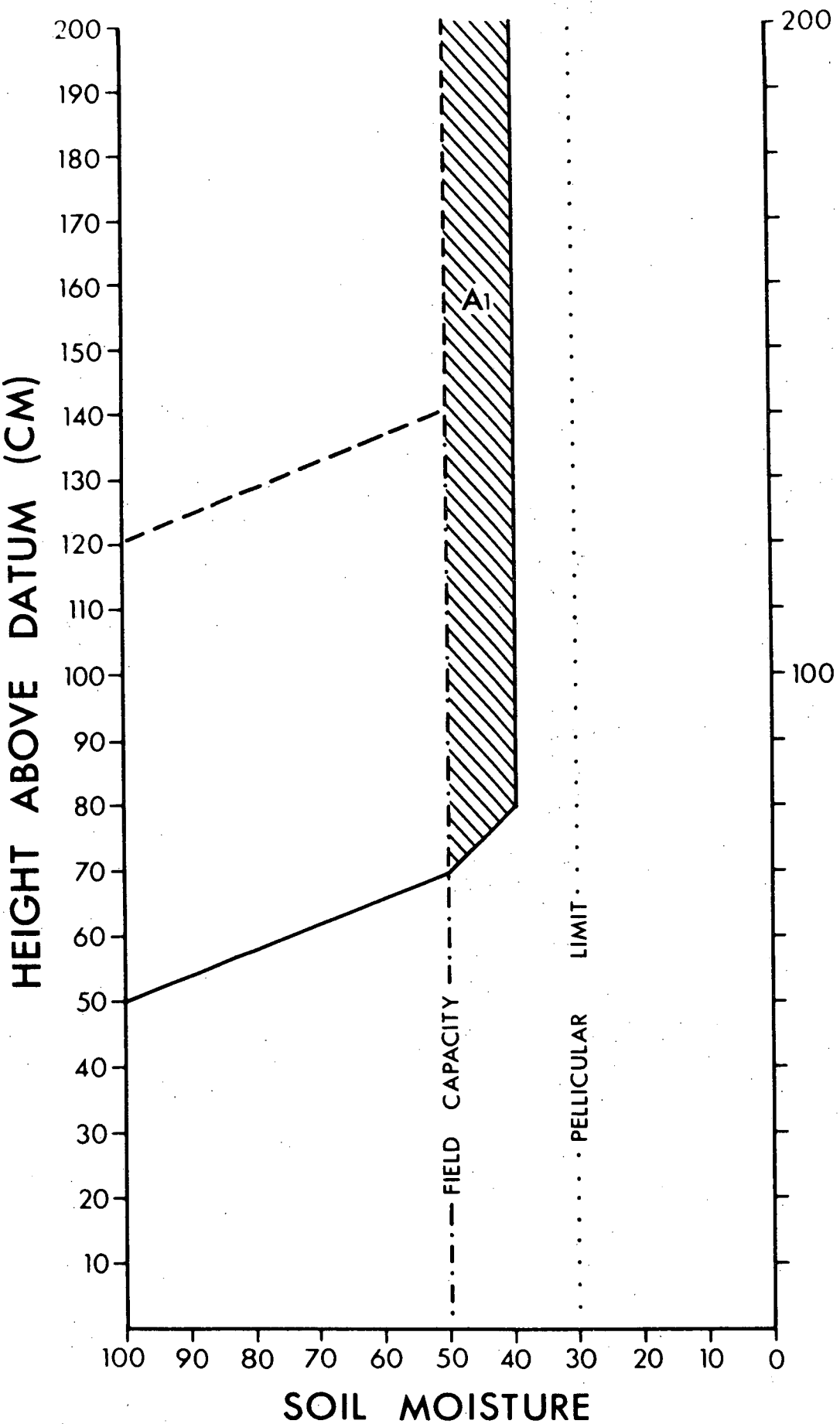
HEIGHT ABOVE DATUM (CM)
200
190
180
170
160
150
140
130
120
110
100
90
80
70
60
50
40
30
20
10
A1
FIELD CAPACITY
PELLICULAR LIMIT
100 90 80 70 60 50 40 30 20 10 0
SOIL MOISTURE
200
100

and the amount of pellicular water which determines the lower limit. The operation of these processes appears to explain the reduction in the effect of strong evaporative forces on the water table as its depth increases. In areas where root penetration depth is even the cut-off depth would be marked, but where uneven root penetration occurs a more gradual decrease of evapotranspiration effects is expected as the water table declines.

A feature observed in the groundwater level records is that the rate of water table decline due to evapotranspiration decreases as the period since the last rainfall increases (Figure 48). This indicates that as the soil moisture decreases the evaporation from the soil also decreases. Davies & Allen (1973) found that actual evaporation is related to surface soil moisture and that as this increases evaporation also increases.

2.8 Summary

Although a more precise determination of the relationships outlined above needs to be ascertained under drier soil moisture conditions and lower water table levels, it appears that the observed water table response to precipitation and evapotranspiration during dry periods can also be explained by soil moisture conditions. Thus, it is apparent that the total range of water table fluctuations under natural conditions is primarily dependent on the nature of the soil moisture profile, and that under differing soil moisture conditions a given rainfall will produce a different water table response.

3. GROUNDWATER POTENTIAL OF THE STUMPYS BAY SAND

3.1 Groundwater Storage

Table 10 summarizes the assessment of the groundwater storage in the Stumpys Bay Sand and is based on the aquifer characteristics in the East Tomahawk area. For this assessment, an aquifer porosity of 40 percent and an average field capacity of 50 percent are assumed. The theoretical recoverable water is therefore at least 50 percent of the groundwater in storage. The saturated thickness estimates are based on drilling data where possible. The extent of the aquifers shown in Figure 60 has been determined by field mapping and drilling and the boundaries are positioned where the sands attain sufficient thickness to allow sustained pumping from 5 cm diameter screens. The estimates in Table 6 are a guide to the possible groundwater reserves.

On the basis of these calculations of groundwater in storage, the Stumpys Bay Sand has good potential, particularly as very little surface water exists in these areas which form most of the agricultural land in the region.

3.2 Recharge Capacity

Although the water table response to rainfall and evaporation induced forces is dependent on the soil moisture profile, the depth to the water table, and the field capacity, a yearly water budget calculation allows estimation of the recharge capacity of the aquifers on a longer term basis.

At Tomahawk the average annual rainfall (1965 to 1976) is 790 mm. The rainfall for 1976 was 817 mm, slightly above the

TABLE 10 Groundwater Storage within the Stumpys Bay Sand

	Locality (Fig. 60)	Area (km^2)	Saturated Thickness (m)	*Groundwater Storage*	
				Megalitres	Depth of Water (cm)
1	Tuckers Creek	15	7	42,000	280
2	Melaleuka	4	7	11,000	280
3	Toddys Plain	18	7	50,000	280
4	Barooga	5	5	10,000	200
5	West Tomahawk	16	5	32,000	200
6	East Tomahawk	15	5	30,000	200
7	West Boobyalla Plains	4	4	6,000	160
8	East Boobyalla Plains	7	4	11,000	160
9	The Chimneys	6	5	12,000	200
10	Cape Portland	7	9	25,000	360
11	Rushy Lagoon	10	7	28,000	280
12	Stumpys Bay	11	6	26,000	240
		118		283,000	

annual average. The mean pan evaporation at Scottsdale is 955 mm. As pan evaporation at Scottsdale is ~ 77 percent of pan evaporation at Tomahawk the estimated mean pan evaporation at Tomahawk is 1240 mm. Thus the ratio of pan evaporation to precipitation at Tomahawk is ~ 1.57.

Since evapotranspiration is ~ 75 percent of pan evaporation and rainfall inputs are 74 percent of pan evaporation the annual precipitation is closely balanced by evapotranspiration under natural conditions. However, this balance is only valid

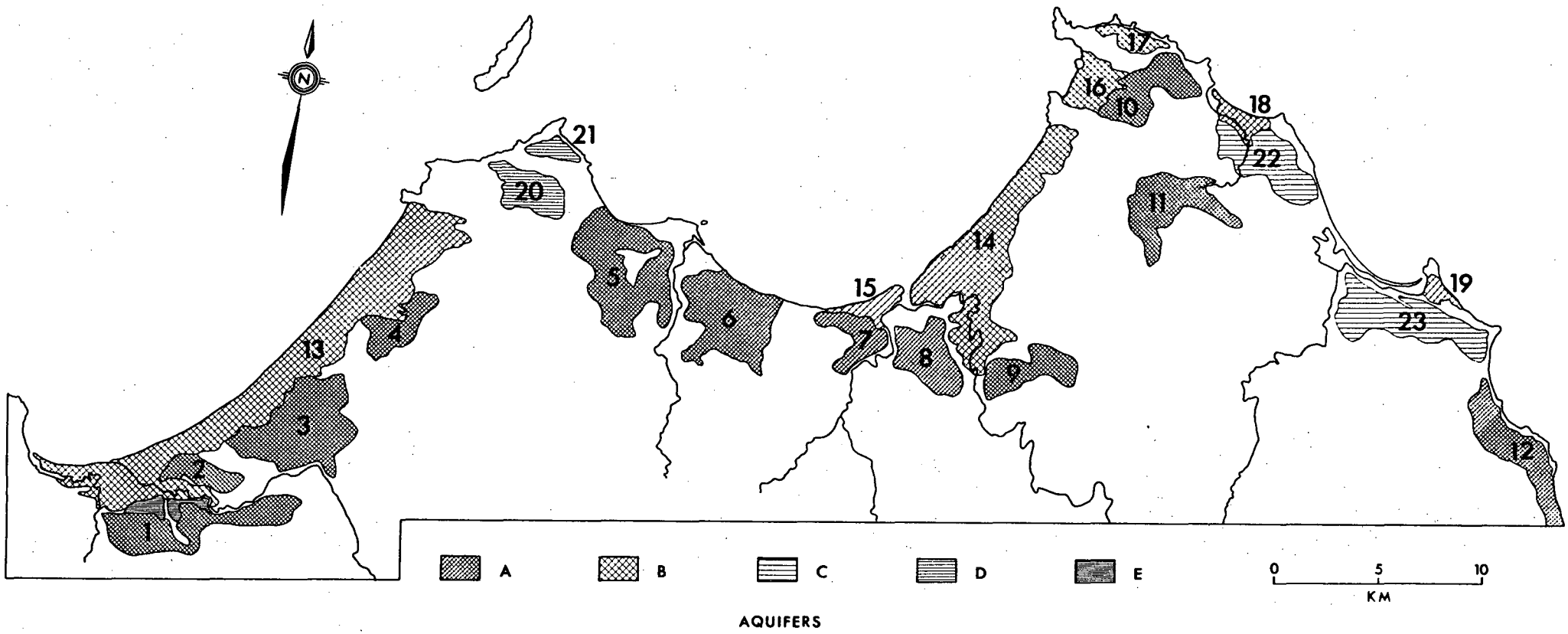

FIGURE 60 Principal Water Table Aquifers - Coastal Northeastern Tasmania.

A represents the aquifer formed by the Stumpys Bay Sand
B represents the aquifer formed by the Barnbougle Sand
C represents the aquifer formed by the Stumpys Bay Sand overlain by the Ainslie Sand
D represents the aquifer formed by sand sheets of the Ainslie Sand
E represents the aquifer formed by the Forester Gravel

The numbered areas refer to localities in Tables 11 and 13.

in terms of groundwater budget if the water table is consistently near the surface because as depth increases the effect of evapotranspiration decreases. Therefore the system should show a net gain over the yearly cycle as the water table is well below the surface during the period of highest pan evaporation which is from mid-summer to early winter.

3.3 Effects of Groundwater Withdrawal

The dynamics of the groundwater system become important when the possible effect of artificial discharge from the system is evaluated. Figure 42 demonstrates that during periods when the water table is within 50 cm of the surface water loss by evapotranspiration is high. Therefore, from a management point of view, it is desirable to keep the water table at a greater depth than 50 cm to conserve water. On the other hand, under natural conditions the amount of rainfall needed to raise the water table during periods of drought is considerably more than is required during moist periods.

Pumping usually occurs during periods of low water table level and is likely to modify the soil moisture profile. Pumping allows extension of the zone of aeration through gravity drainage and the moisture left in storage should be close to the field capacity (Figure 61). Thus, for the period when the zone of aeration is below field capacity the water table response should be the same as for normal low water table periods and rainfall will be absorbed in this zone until field capacity is attained. However, once the zone has attained field capacity any rainfall will raise the water table by the same amount as occurs during times of high water table level and soil moisture conditions, even

FIGURE 61 Soil Moisture Conditions after Pumping.

In this hypothetical example the soil moisture profile above the capillary fringe was below field capacity before pumping commenced. Pumping of a quantity of groundwater which is equivalent to the quantity shown by the less dense shading should produce the soil moisture profile represented by the continuous line. Subsequent rainfall must exceed the quantity shown by the more dense shading to allow any recovery of the water table level. Soil moisture is expressed as a percentage of porosity.

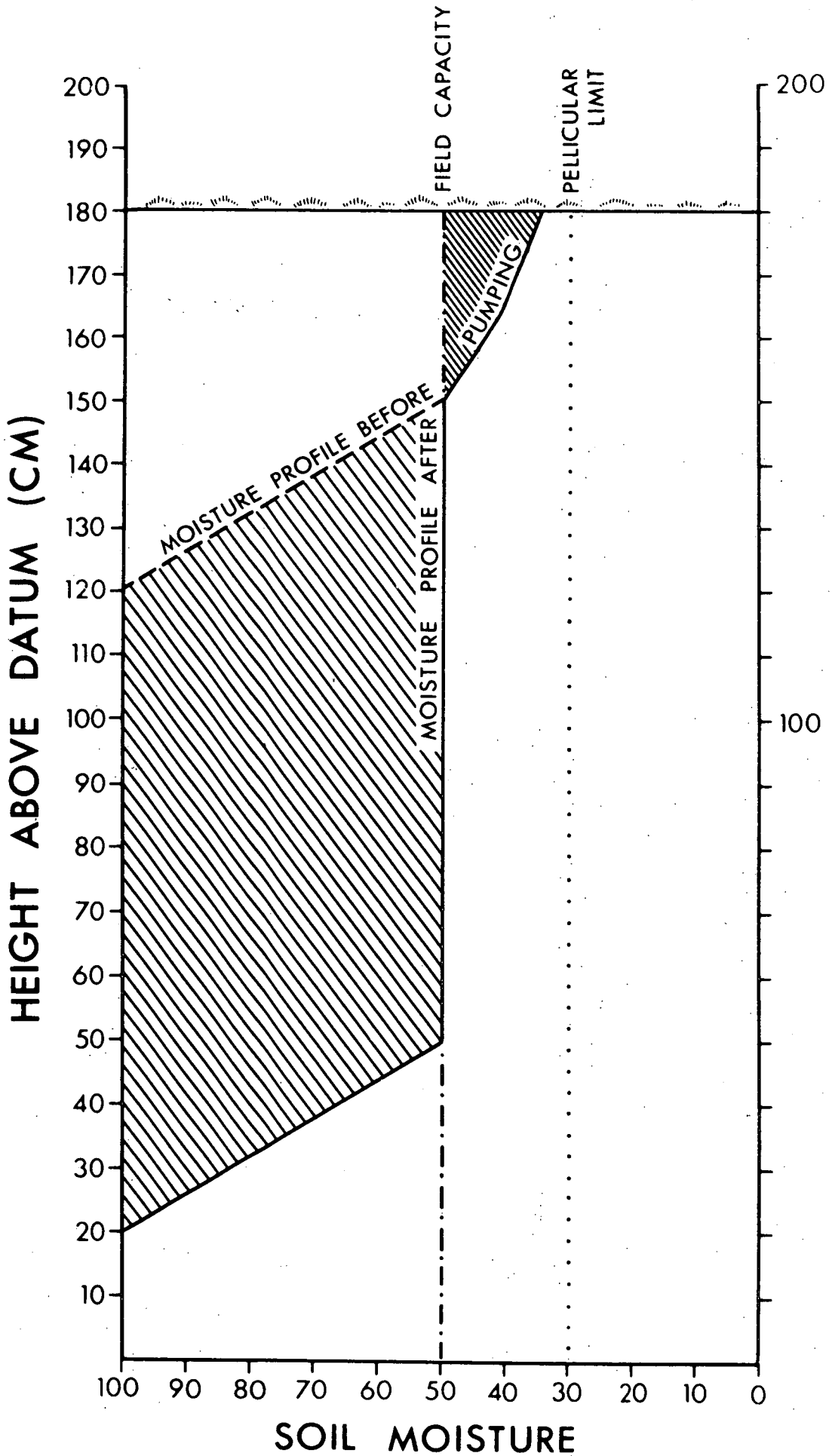
FIELD CAPACITY
PELLICULAR LIMIT
PUMPING
MOISTURE PROFILE BEFORE
MOISTURE PROFILE AFTER
HEIGHT ABOVE DATUM (CM)
SOIL MOISTURE
200
190
180
170
160
150
140
130
120
110
100
90
80
70
60
50
40
30
20
10
100 90 80 70 60 50 40 30 20 10 0

though the zone of aeration has been extended by pumping. As the water table level after summer pumping is much lower than under natural conditions, winter rainfall recharge should be much more effective because the water table level should be below 50 cm and therefore beyond the effects of excessive evapotranspiration losses.

Comparison of the three recorder charts (Figure 42) supports this view. From 1st May 1976 to 1st February 1977, Recorders I and III showed a gain of 57 and 61 cm respectively in water table height. Recorder IV, which shows that the water table is within about 50 cm of the surface for 5 months of that period compared with 3 months for Recorders I and III, gained only 26 cm. This indicates that a low initial water table allows the rainfall input to accumulate for a longer period when the effect of evapotranspiration is reduced by the greater water table depth.

Groundwater withdrawal therefore would have two principal consequences. Firstly, less water would be lost through evapotranspiration because the water level is frequently below 50 cm, and secondly, the problem of water-logging of the ground surface during winter should be reduced if sufficient groundwater is withdrawn. These factors suggest that some artificial dewatering of the aquifer allows the system to be more efficient than under natural conditions and alleviates water-logging. Although future work may enable quantification of the effects of broad-scale lowering of the water table, it is considered that if the water table was lowered by 1 m, providing a 200 mm irrigation capacity, there would be sufficient protection from evapotranspiration to reduce the losses by the 200 mm extracted from the system. This

would represent an increase in efficiency of 24 percent of present evapotranspiration losses and it may be that additional lowering of the water table would further increase the efficiency of the system.

Thus, it appears that not only is large scale dewatering of the aquifer possible in terms of recharge capacity, but that it is desirable, since the system would operate at a more efficient level.

3.4 Groundwater Yield

Pump tests through a 5.1 cm diameter screened bore carried out at Tomahawk indicate a relationship between the maximum rate of water withdrawal and the thickness of the aquifer (Figure 62). Although there is some scatter in the relationship, it appears that a thickness of less than 3 m will not yield a steady flow of water. However, once exceeded the aquifer yield increases at a rate of about 5000 litres per day for each additional metre of thickness. Although the general relationship is probably valid and yields were stable when tested, one should not place too much emphasis on its precision as the pump tests were of only 1 to 4 hours duration. In addition, yield is dependent on the permeability of the aquifer, a parameter which displays distinct spatial variation. However, the relationship is useful because it suggests the minimum thickness of sand required to extract adequate local water supplies from the aquifer and it indicates that the areas where the aquifer is thickest are likely to produce the highest yields.

The above rates of flow are from single bore holes and it should be possible to increase the yield substantially by

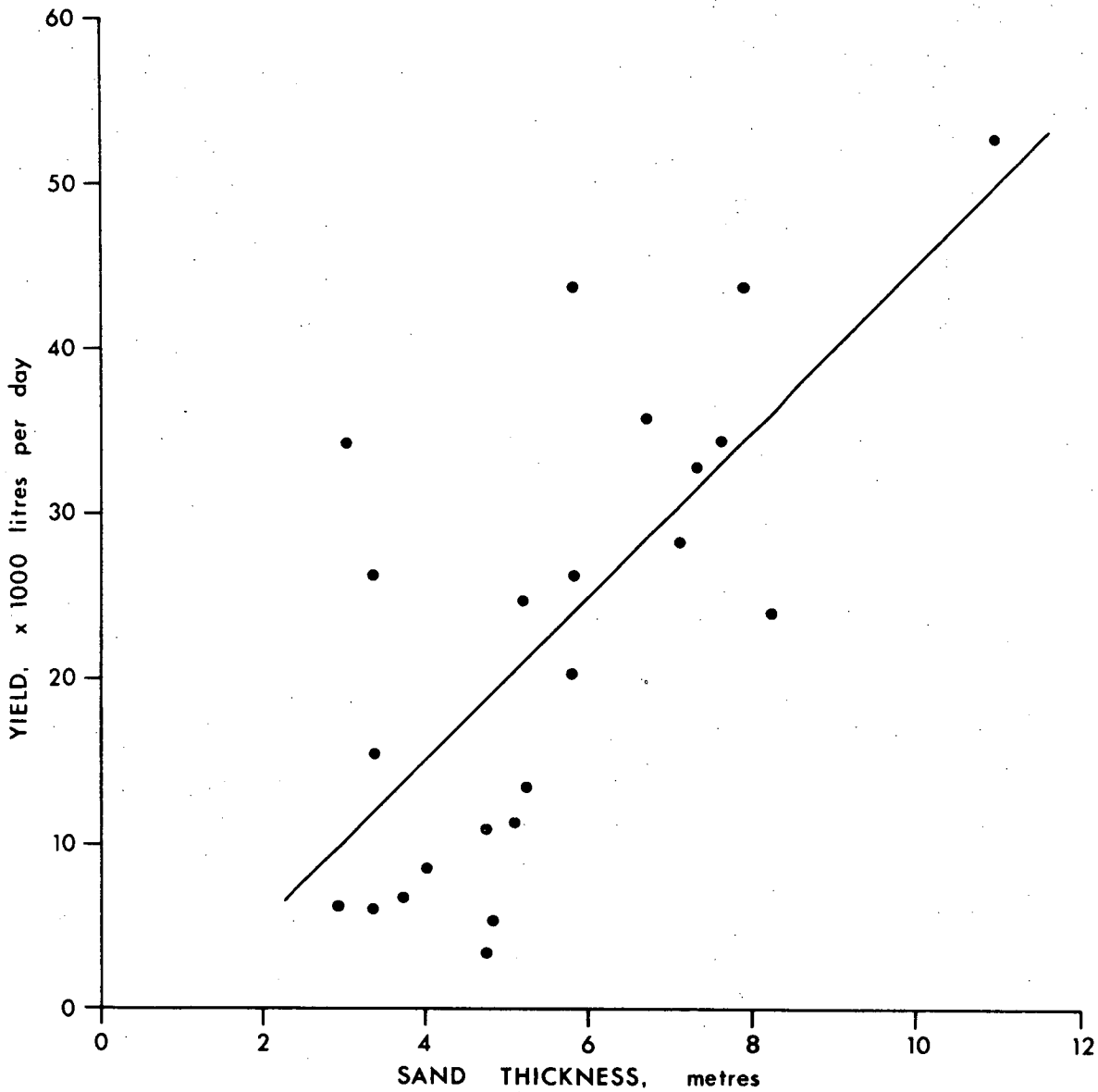

FIGURE 62 Relationship between Groundwater Yield and Aquifer Thickness.

Pearson's r = 0.705

either increasing the diameter of the bore or by installing an array of bore holes.

3.5 Water Quality

Water quality, as well as quantity, is an important factor in determining the suitability of water resources for various uses and chemical analyses have been undertaken to assist assessment of the groundwater potential of the interglacial marine sands.

Twenty four water samples were collected during pump testing of the Tomahawk Formation and analyses were carried out by the Tasmanian Department of Mines. Figure 63 is a location map of the samples taken from the East Tomahawk area. From these data the milli-equivalence per litre of the active cations and anions, the percent milli-equivalence per litre, the sodium absorption ratio (SAR), and the percent sodium were calculated, and are shown in Table 11.

4. GROUNDWATER POTENTIAL OF THE REMAINING AQUIFERS

4.1 Forester Gravel

Although the areal extent of the terraces of alluvial deposits is not large (Figure 60) one would expect that they would contain good groundwater supplies, as they form a continuous body of coarse, unconsolidated sediments which should be highly porous and permeable. An auger hole drilled near the seaward edge of the terrace did not encounter water until a depth of 4 m was reached, the level of the plain of Holocene marine sands which

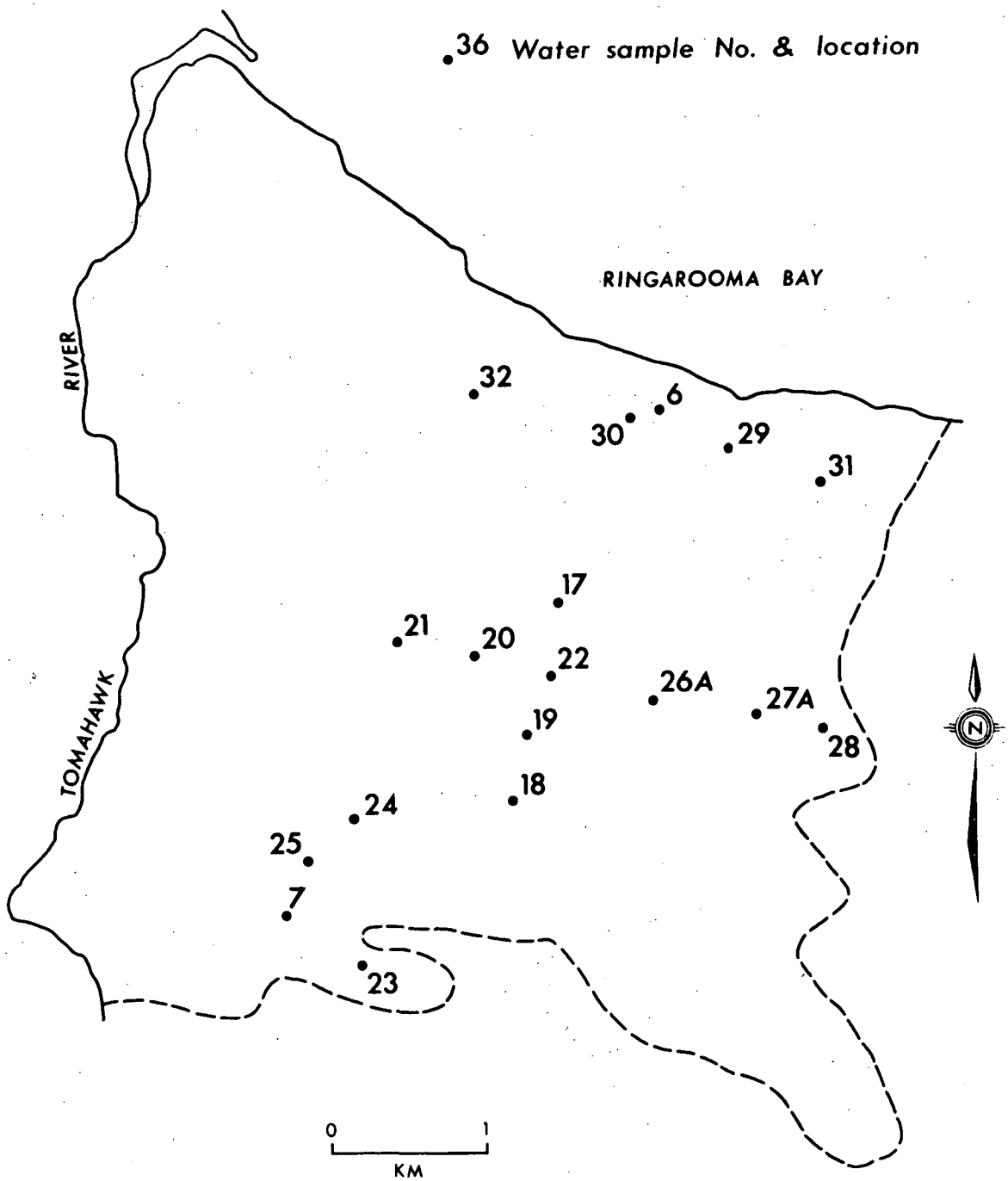

FIGURE 63 Location of Water Samples from Bores in the East Tomahawk Area.

TABLE 11 Water Quality - Coastal Northeastern Tasmania

Sample Number	6	7	17	18	19	20	21	22	23	24	25	26A
pH	6.2	6.1	5.5	5.8	5.4	5.7	6.2	6.2	5.5	6.1	6.2	6.0
CO_3 (mg/l)	0	0	0	0	0	0	0	0	0	0	0	0
HCO_3 "	110	40	25	35	25	50	50	35	35	120	85	51
Cl "	990	200	150	170	100	320	350	350	150	740	460	129
SO_4 "	5	5	14	<5	19	<5	<5	18	9	11	<5	8
SiO_2 "	40	18	30	35	10	30	35	35	30	<5	80	24
Ca "	28	4.3	4.4	12	9.6	8.6	7.4	7.4	4.3	15	10	6.1
Mg "	76	16	12	12	9.0	22	25	30	12	50	30	12.5
Fe "	7.7	7.7	1.8	4.2	2.0	3.0	2.0	5.3	4.5	2.0	7.5	8.7
Al "	13	1.8	<0.2	<0.2	<0.2	<0.2	1.5	1.5	<0.2	<0.2	7.5	3.8
K "	7.3	3.7	3.0	5.1	3.0	3.9	4.0	4.3	5.1	10	7.5	4.5
Na "	520	110	55	55	35	130	145	145	55	360	260	78
TDS	1950	450	380	390	260	670	780	770	390	1500	1200	345
Hardness as $CaCO_3$	380	77	60	79	60	110	120	140	60	240	150	67
Alkalinity as $CaCO_3$	93	33	20	30	20	40	40	30	30	100	70	42
HCO_3 (meq/l)	1.80	0.66	0.41	0.57	0.41	0.82	0.82	0.57	0.57	1.97	1.39	0.84
Cl "	27.92	5.64	4.23	4.79	2.82	9.02	9.87	9.87	4.23	20.87	12.97	3.64
SO_4 "	0.10	<0.10	0.29	<0.10	0.40	<0.10	<0.10	0.37	0.19	0.23	0.10	0.17
Ca "	1.40	0.21	0.22	0.60	0.48	0.43	0.37	0.37	0.21	0.75	0.50	0.30
Mg "	6.25	1.32	0.99	0.99	0.74	1.81	2.01	2.47	0.99	4.11	2.47	1.03
K "	0.19	0.09	0.08	0.13	0.08	0.10	0.10	0.11	0.13	0.26	0.19	0.12
Na "	22.62	4.79	2.39	2.39	1.52	5.65	6.31	6.31	2.39	15.66	11.31	3.39
Sum (meq/l)	60.28	12.81	8.61	9.57	6.45	17.94	19.58	20.07	8.71	43.85	28.93	9.49
SAR "	11.57	5.48	3.07	2.68	1.95	5.35	5.78	5.30	3.09	10.05	9.28	4.16
Percent Sodium	74.7	75.8	66.4	55.5	71.6	72.6	69.0	66.6	76.3	79.2	71.8	71.8
HCO_3 (% meq/l)	2.99	5.15	4.8	6.0	6.4	4.6	4.2	2.8	6.5	4.5	4.8	8.9
Cl "	46.32	44.03	49.1	50.1	43.7	50.3	50.4	49.2	48.6	47.6	44.8	38.4
SO_4 "	0.17	0.81	3.4	<1.0	6.2	<0.1	<0.5	1.8	2.2	0.5	<0.3	1.8
Ca "	2.32	1.68	2.6	6.3	7.4	2.4	1.9	1.8	2.4	1.7	1.7	3.2
Mg "	10.36	10.27	11.5	10.3	11.5	10.1	10.3	12.3	11.4	9.3	8.5	10.9
K "	0.31	0.74	0.1	1.4	1.2	0.1	0.5	0.5	1.5	0.6	0.7	1.3
Na "	37.53	37.36	27.8	25.0	23.6	31.5	32.2	31.4	27.4	35.7	39.1	35.7
Locality	EAST TOMAHAWK											
	200 m NE of Recorder I	Recorder IV	Bore 8	Bore 6	Bore 7	Bore 15	Bore 16	Recorder III	Bore 5	Bore 28	Bore 30	Bore 12

TABLE 11 (continued)

Sample Number	27A	28	29	30	31	32	8	9	10	11	13	15
pH	5.6	7.4	5.8	7.8	7.6	6.9	6.0	5.9	6.0	6.0	4.2	5.2
CO_3 (mg/l)	0	0	0	0	0	0	0	0	0	0	0	0
HCO_3 "	24	151	26	101	54	14	65	18	87	100	0	8
Cl "	118	118	198	1230	290	100	410	210	320	610	330	82
SO_4 "	6	13	21	<5	<5	<5	68	34	10	68	780	10
SiO_2 "	16	10.5	11	35	23	17	25	13	21	4	55	6
Ca "	3.7	47	5.5	61	12.6	5.4	16	7	15	40	50	2.5
Mg "	11	12	21	122	23.4	8.4	49	24	27	68	80	7.8
Fe "	2.1	1.1	1.5	0.3	2.1	0.9	7	2	11	5	130	0.1
Al "	5.1	3.8	5.1	<1.0	2.3	9.1	10	4	3	1	34	0.2
K "	3.9	3.8	5.0	9	7.8	4.8	11	6	7	12	8.4	2.3
Na "	66	68	110	600	180	64	220	110	190	420	240	39
TDS	287	392	496	2320	690	260	960	480	690	1530	1920	190
Hardness as $CaCO_3$	54	170	100	650	130	48	310	140	190	140	940	600
Alkalinity as $CaCO_3$	20	124	21	83	44	12	54	15	71	82	0	0
HCO_3 (meq/l)	0.39	2.48	0.43	1.66	0.89	0.23	1.07	0.30	1.43	1.64	0	0.13
Cl "	3.33	3.33	5.58	34.69	8.18	2.82	11.56	5.92	9.02	17.20	9.31	2.31
SO_4 "	0.12	0.27	0.44	<0.10	<0.10	<0.10	1.41	0.71	0.21	1.41	16.22	0.21
Ca "	0.18	2.35	0.27	3.04	0.63	0.27	0.80	0.35	0.75	2.00	2.50	0.12
Mg "	0.90	0.99	1.73	10.03	1.92	0.69	4.03	1.97	2.22	5.59	6.58	0.64
K "	0.10	0.10	0.13	0.23	0.20	0.12	0.28	0.15	0.18	0.31	0.22	0.06
Na "	2.87	2.96	4.79	26.1	7.83	2.78	9.57	4.79	8.27	18.27	10.44	1.70
Sum (meq/l)	7.89	12.48	13.37	75.85	19.75	7.01	28.72	14.19	22.07	46.42	45.26	5.17
SAR "	3.91	2.29	4.79	10.21	6.93	4.01	6.16	4.45	6.79	9.38	4.90	2.76
Percent Sodium	72.7	47.0	70.5	66.6	75.4	74.3	66.5	67.4	73.6	74.5	53.5	69.1
HCO_3 (% meq/l)	4.9	19.9	3.2	2.2	4.5	3.3	3.73	2.11	6.48	3.53	0	2.51
Cl "	42.2	26.7	41.7	45.7	41.4	40.2	40.26	41.75	40.89	37.06	20.56	44.70
SO_4 "	1.5	2.2	3.3	<0.1	<0.5	<1.4	4.92	4.99	0.94	3.05	35.85	4.02
Ca "	2.3	18.8	2.0	4.0	3.2	3.9	2.78	2.46	3.39	4.30	5.51	2.41
Mg "	11.4	7.9	12.9	13.2	9.7	9.8	14.02	13.91	10.06	12.04	14.53	12.39
K "	1.3	0.8	1.0	0.3	1.0	1.7	0.98	1.08	0.81	0.66	0.48	1.14
Na "	36.4	23.7	35.8	34.4	39.6	39.7	33.32	33.73	37.45	39.36	23.07	32.80
Locality	EAST TOMAHAWK						WEST TOMAHAWK					
	Bore 13	Bore 14	Bore 19	Recorder I	Bore 20	Bore 21	Leedway Homestead	4 km NNW of Leedway Homestead	5 km NNW of Leedway Homestead	Ainslie Homestead	0.5 km NW of Barooga Homestead	300 m behind beach at Stumpys Bay

truncates the terrace. This low water table near the terrace edge is due to the high permeability of the sands and gravels, which permits water to drain freely towards the lateral margins. Evidence of seepage from the base of the terrace can readily be seen on false colour infra-red aerial photographs and in the field.

However, between the middle portion of the fluvial terraces and the landward edge, where they truncate the higher terrace of the Tomahawk Formation sands the water table should be closer to the surface. The water table level should be higher due to the decreasing effect of lateral drainage with distance from the truncated terrace edge and to the drainage of groundwater from the higher terrace of interglacial marine sands.

Thus, although the saturated thickness of the aquifer is reduced towards the terrace margins, the high permeability of the sands should permit moderate groundwater yields. The terraces cover 4 km^2 and should contain 8,000 Ml of groundwater, if the sand thickness is 5 m and the porosity is 40 percent.

4.2 Rushy Lagoon Sand

Landforms of this type are not promising aquifers due to their restricted occurrence, small size, and composition. Lunettes occupy a very small proportion of the study area and are themselves relatively small landforms. The largest lunettes occur at Rushy Lagoon where they are up to 30 m high and 2.5 km long. These lunettes form closely spaced double ridges and are composed of alternate beds of sand and clay. The clay beds lower the storage capacity and permeability of the aquifer.

The lunettes derive their groundwater from incident precipitation only. Leakage of groundwater was found to occur low on the western flanks of the Rushy Lagoon lunettes. This indicates that some groundwater is contained in the dunes and that it is probably perched on the various clay beds. Potential utilization of groundwater from the lunettes, as with some of the longitudinal dunes, would be restricted to the collection of water which seeps from the dune flanks.

4.3 Ainslie Sand

Longitudinal sand dunes are widely distributed throughout the area (Figure 3b), and due to their limited height and width are generally devoid of recoverable water. Where small seepages occur at the base of the dunes there is a possibility that shallow excavations on the line of the seeps could be utilized for stock watering. However, where the dune sands form more extensive areas of sand sheets (Figure 60) they contain some groundwater. These sand bodies are highly porous (~ 50%), and moderately permeable. Pump tests carried out 1 km south of Tomahawk in a small (~ 0.5 km^2) sand sheet, which was 4.3 m thick, indicated that the aquifer permeability was 0.57 $m^3/d/m^2$.

Water inputs to these sand bodies are predominantly through incident precipitation but in areas where the sands are banked against bedrock hills a significant input through runoff probably occurs. Some loss from the dunes occurs through evapotranspiration, but field observation and false colour infra-red aerial photography indicate that large quantities of water are lost from the base of the unconfined lateral margins of the dunes.

A water sample taken from the dunes at Tomahawk contained 1,290 ppm TDS, which for this area is only of fair to poor quality.

As most occurrences of the dune sands are restricted in extent and thickness, the groundwater potential of the aeolian sands is very limited, unless they form continuous sheets which allow moderate groundwater yields. The two most extensive bodies occur at Waterhouse where they cover 8 km^2 and should contain ~ 16,000 Ml of groundwater (areas 20 and 21, Figure 60).

4.4 Croppies Marl

As stated on page 222 this member shows no promise as a groundwater source.

4.5 Bowlers Lagoon Sand

These transverse dunes cover areas of several km^2 but they allow water to pass freely through the sand to the underlying Barnbougle Sand. One auger hole failed to reach water after penetrating 9 m of sand. Infra-red photographs indicate some lateral seepage from the dunes after heavy winter rainfall.

4.6 Waterhouse Sand

Due to the limited size and extent of the siliceous parabolic dunes they do not appear to have promise as aquifer systems. The high, narrow discrete ridges of the dune material make the retention of groundwater unlikely. Where the dunes have been drilled they have been dry throughout.

4.7 Barnbougle Sand

The Barnbougle Sand which is composed of Holocene marine sediments, is extensive in the immediate coastal areas of northeast Tasmania. The principal occurrences of the Barnbougle Sand are near the mouth of the Great Forester River, adjacent to Anderson and Ringarooma Bays, at Tregaron Lagoons, and at Cape Portland (areas 13-19, Figure 60). The thickness of the sands exceeds 12 m but only one drill hole has been located in this aquifer.

The aquifer consists of medium to coarse grained sands with frequent shell material. Although the aquifer has not been pump tested, the nature of the sands indicates that it is likely to have similar hydrologic properties to the Stumpys Bay Sand.

The water table is often very near the surface and under natural conditions would respond to precipitation inputs and evapotranspiration outputs in a fashion similar to the Stumpys Bay Sand. However, the Barnbougle Sand aquifer differs from the Stumpys Bay Sand aquifer in two important ways. Firstly, the Barnbougle Sand, in the area around Barnbougle, is traversed by the Great Forester River which, although it does not cut completely through the aquifer, is nevertheless able to contribute water to it by seepage from the stream. Secondly, the Barnbougle Sand extends well below sea level, which almost certainly gives rise to a fresh-water/sea-water interface. This could pose problems of salt water intrusion if the aquifer were to be subjected to heavy artificial withdrawals in the immediate vicinity of the coast. Detailed aquifer testing would be required to estimate the effects of these two differences.

An initial estimate of the groundwater storage of the Barnbougle Sand has been calculated using an average thickness of 13 m, an average porosity of 40 percent, and an estimate of the areal extent of the aquifer in each locality. This calculation estimates that 472,000 megalitres of water are held in storage (Table 12).

Samples of the groundwater have not been collected, but the presence of the shell material in the sediments may have the effect of counteracting the development of acid conditions. At Greens Beach which is approximately 60 km to the west of Barnbougle, some water samples were taken daily during a 13 day pump test from an equivalent to the Barnbougle Sand (Cromer, W.C., in prep.). These samples had a mean pH of 7.4 and a mean salinity of 500 mg/l TDS.

The Barnbougle Sand therefore shows considerable promise as an aquifer and should contain abundant, good quality groundwater supplies.

5. CONCLUSIONS

The groundwater which is contained within the Stumpys Bay Sand is a potentially important resource as there is sufficient to supplement the relatively low rainfall during the summer. This water is near the surface and is therefore easily extracted for irrigation and stock watering. Water quality, rather than quantity, may be a limiting factor for domestic use. Similar deposits which should also contain plentiful shallow groundwater occur on

TABLE 12 Groundwater Storage within the Barnbougle Sand

	Locality (Fig. 60)	Area (km^2)	Saturated Thickness (m)	*Groundwater Storage*	
				Megalitres	Depth of Water (cm)
13	Anderson Bay	49	13	254,000	520
14	Ringarooma Bay	29	13	151,000	520
15	Boobyalla	3	13	16,000	520
16	Tregaron Lagoons	5	13	26,000	520
17	Cape Portland	2	13	10,000	520
18	Little Musselroe Bay	2	13	10,000	520
19	Musselroe Bay	1	13	5,000	520
		91		472,000	

Flinders Island, the northwest of Tasmania near Smithton, and as more isolated pockets on the east coast of Tasmania.

The Barnbougle Sand also contains abundant water of potentially higher quality than that of the Stumpys Bay Sand. This could be extracted for stock, irrigation, and possibly for domestic uses. Holocene deposits of predominantly marine origin are widespread in eastern Tasmania, Flinders Island, and northwestern Tasmania.

The remaining water bearing landforms and deposits which have been described are often too small and restricted in occurrence to form important groundwater sources. This is also generally true of similar landforms and deposits outside the study area.

In northeastern Tasmania the plains formed by the Stumpys Bay Sand and the Barnbougle Sand contain unconfined groundwater

which is usually within 1.5 to 2.0 m of the surface. Groundwater extraction is facilitated if 5 cm diameter wire wound screens are jetted into the sands and subsequently pumped. This method is an efficient way of utilizing the groundwater because it draws water from the entire thickness of the aquifer, as opposed to shallow basins excavated into the surface of the sands which are subject to drying out if the water table drops below the floor. In addition, if screens are utilized they can readily be removed to another location and re-used. It is considered that an array of screens in areas where the sands are greater than 4 m thick, each yielding 20,000 litres/day, would provide ample water for most local irrigation purposes, and that this supply would ensure that the intensity of land use could be substantially increased if desired. Large scale withdrawal of groundwater from these systems is desirable, since the widespread lowering of the water table provides added protection of the aquifer from evapotranspiration loss during the recharge periods. If large quantities of groundwater extraction is planned from the Holocene marine sands of the immediate coastal areas care would have to be taken to ensure that salt water intrusion of the aquifer did not occur.

For livestock watering, shallow excavations below the water table in the sand plain areas provide abundant water in most cases. However, if new sites are planned, it is recommended that the best time to carry out excavation is when the water table is very low, so that the floor of the excavation is below the water table during dry periods. Trenches cut along a line of seepage from areas where the aquifer margins have been eroded would

allow the water to be retained for stock watering. Similarly, excavations located on the lower flanks of longitudinal dunes and lunettes offer modest potential for collection of seepage water.

Since this project was of limited duration, further work is needed to establish more precisely, the nature of the groundwater dynamics and the potential of the Barnbougle Sand as an aquifer system. This should involve drilling, pump testing, collection of water samples, and assessment of the effect of the salt water-freshwater interface. Soil moisture profiles need to be determined for the duration of a year or more, so that soil moisture variation through the seasons can be monitored and compared with water table response to inputs and outputs.

If similar projects are to be undertaken elsewhere in Tasmania to determine shallow groundwater potential, then it is recommended that initial field mapping and test drilling is first carried out to determine the extent, thickness, and storage capacity of the aquifer. This should be followed by the installation of a water table level recorder in order to gauge the magnitude of water table fluctuations and their relationships to inputs and outputs. Detailed drilling and pump testing should then be carried out to determine the hydraulic characteristics of the aquifer.

PART IV

CONCLUSIONS

1. INTRODUCTION

As with many studies, more problems are raised here than solved. A large number of ideas have been put forward, much evidence has been cited and a number of conclusions have been drawn, some necessarily rather tentatively. Some of these could probably be more strongly stated with further research, but others may, by their very nature, be difficult to prove. Nevertheless, the conclusions summarized below represent the product of field observation and laboratory analysis carried out in the present study.

2. REGIONAL GEOMORPHOLOGY

Evidence presented in this study indicates that the major landforms and deposits of coastal northeastern Tasmania were produced principally by processes and conditions which have occurred since near the beginning of the Last Interglacial Stage. The changing relative importance of the main operative processes

were in general sympathy with major climatic changes that were at least sub-continental in scale.

Evolution of the present landscape probably commenced during middle Tertiary times. Marine transgression and regression was a common occurrence between the Late Oligocene and the Middle Miocene periods. Deposition of siliceous alluvial gravels occurred at intervals during the Tertiary period but their relationships to the marine sequence have not been determined. The interval from the Middle Miocene period to the Late Quaternary is not represented in the known deposits of the area. However marine transgression and regression may also have been a feature of the area then as appears also to have been the case during the Late Quaternary.

There is evidence to suggest that sea levels during the Second and Third Last Interglacial Stages reached approximately 49 and 71 metres respectively. Transgression during the Last Interglacial Stage to an elevation of 32 metres formed sand filled coastal embayments.

Terrestrial dune formation was the dominant process during the Last Glacial Stage. The dunes were formed mainly on the plains of marine deposits abandoned by the sea during its regression at the commencement of the Last Glacial Stage. Formation of the longitudinal sand dunes and lunettes was probably caused by a marked reduction in vegetation cover induced by increased aridity and cooler conditions. Reduced vegetation cover and slope instability in river catchments were probably also responsible for increased stream sediment loads and the formation of large alluvial floodplains which now comprise the Forester Gravel.

Amelioration of climate and the transgression of the sea to its present level was a feature of the Holocene stage. These conditions allowed the longitudinal dune systems and lunettes to stabilize and favoured the development of a coastal fringe of marine sands, parabolic dunes, and transverse dunes.

3. LATE QUATERNARY TECTONIC UPLIFT

The stable areas of the world indicate that sea level during the Last Interglacial reached a maximum of ~ 6 m ± 2 m. This conclusion is supported by deep sea oxygen isotope analysis which also indicates that the Last Interglacial sea levels were the highest since at least the Middle Quaternary.

The elevation difference between the Last Interglacial upper marine limit at ~ 32 m in northeastern Tasmania and the limit attained in stable areas appears to be explained by relative uplift of northeastern Tasmania. The calculated uplift rate of 0.21 m/km in northeastern Tasmania is up to forty times less than rates in very active tectonic areas and is similar to the more moderate rates of Barbados and the Loyalty Islands. If this uplift rate has been uniform over the last 120 ka the low sets of beach ridges in the eastern embayments may have been formed during minor, later transgressions during Stages 5a and 5c but this is hard to demonstrate unequivocally.

The presence of older, higher, interglacial marine deposits at Rockbank and Ringarooma Tier also suggests that tectonic uplift has occurred. Consideration of their present altitude and postulated age indicates that the mean uplift rate over the

last 325 ka may have been approximately 0.22 m/ka, and that the greatest uplift rate probably occurred between Stages 7 and 5. The trend of the uplift curve also indicates that prior to about 500 ka, the area may have been relatively stable.

Although there is strong evidence for Late Quaternary tectonic activity in northeastern Tasmania, the arguments would be much stronger if radiometric dates of the deposits were obtainable and if the Late Quaternary eustatic sea level curve were better known.

Evidence from the rest of Tasmania indicates that Last Interglacial sea levels higher than the eustatic level at ~ 6 m are widespread in Tasmania and offshore islands. Differential tectonic movement within Tasmania is not considered to be a strong possibility and some apparent differences in upper marine limits may be explained by different coastline sensitivities to marine modification. Tasmania is at variance with adjacent regions of mainland southeastern Australia, where there is strong evidence of general tectonic stability.

The possible reasons for Tasmanian instability may be related to the crustal configuration of the region as a peninsular extension of the continent with thinning beneath Bass Strait. The presence of a convection plume beneath Bass Strait may be one of the forces involved in producing Tasmanian uplift.

4. CLIMATIC CONDITIONS DURING THE LAST GLACIAL STAGE

The longitudinal sand dunes and lunettes which were active during the late Last Glacial Stage hold several keys to

the climatic conditions during their formation. The evidence has been obtained from study of the landforms themselves and from examination of their relationships to other elements in the landscape.

Decreased mean annual temperatures during the late Last Glacial Stage are fairly well documented from the Tasmanian region but the only evidence of temperature decline from northeastern Tasmania is the close relationship between dune sands and slope deposits which are probably of cold winter climate origin.

The prevailing winds during the late Last Glacial Stage were from the WNW, with occasional crosswinds from the northwest. The alignment of longitudinal dunes and Holocene parabolic dunes is statistically different and the late Last Glacial dune forming winds appear to have been from a slightly more northerly direction than the post glacial winds. Wind speeds during the late Last Glacial Stage may have been greater than today's values. Calculations of wind speed from the published relationship of wind speed to lee wave length indicates that the velocity of the air flow which produced the lee waves was around 36 km/hr. Estimates using the size of the coarsest one percent of the samples and comparison with published threshold velocity data gave mean threshold wind speed values of approximately 35 km/hr. This is in close agreement with the figure of 36 km/hr derived from the lee wave calculation. In addition, the threshold wind velocity calculation agrees fairly well with the lee wave theory as the calculated wind velocity was approximately twice as strong below the trough of the lee wave than below the crest.

The technique has been tested by estimating threshold wind velocities for samples from a Holocene parabolic dune and comparing them with the present westerly wind strength. The respective values so derived were 25 km/hr and 27 km/hr. This adds considerable support to the validity of the calculations of late Last Glacial wind speeds, which appear to have been 9-10 km/hr greater than today's.

Precipitation during the Last Glacial Stage was estimated by consideration of the water inputs and outputs required to produce groundwater fluctuations needed to produce a fossil groundwater podzol profile. The rainfall necessary to maintain such a system would be 427 mm/year, which is 54 percent of today's mean annual rainfall. Evapotranspiration losses from the system probably amounted to only 33 percent of the potential evaporation, as compared with a value of approximately 75 percent today.

The lunettes and associated lake basins provide key evidence for the nature of the water budget during the late Last Glacial Stage. The changing water levels of the lake basins are reflected in the stages of lunette formation and the changing composition of the lunette sediments.

The palaeohydrology of the lakes was controlled by the relationships between the inputs, rainfall and runoff, and the outputs, evaporation and groundwater flow. Runoff was found to have been a controlling variable in lake hydrology. During the late Last Glacial Stage runoff was around 31 percent of the rainfall to the catchment, as opposed to only 10 percent today. This vastly increased runoff is thought to be a direct product of

a considerably reduced vegetation cover at the time of lunette formation.

Calculation of the evapotranspiration from the catchment was approximately 29 percent of the lake evaporation, which agrees fairly well with the figure derived from the estimate based on fossil groundwater conditions. This decline in evapotranspiration during the late Last Glacial Stage which is about 42 percent of today's value, may reflect a decrease of 55-60 percent in vegetation density.

The lunette stratigraphy indicates that lake levels were generally higher and that the system was in a much more dynamic state of equilibrium during the late Last Glacial Stage than during the subsequent post glacial. These factors have been attributed to the greater proportion of water inputs through runoff and a much greater variability of annual precipitation.

Increased aridity was probably caused by the drainage of Bass Strait and the consequent increased continentality of the location compared with its present coastal position, by an increased rainshadow effect of the highlands in western Tasmania, and by cooler sea surface temperatures which would have reduced the atmospheric humidity.

Increased windiness may have been caused by a combination of expansion of the Australian continental high pressure systems and the northward extension of the Antarctic Convergence. These two events would have increased pressure gradients between the two regions with the creation of a stronger zonal air flow. The slightly more northerly wind direction may have been due to the stronger direct influence on northeastern Tasmania during the late Last Glacial Stage of the Australian continental anticyclone.

The events in northeastern Tasmania during the late Last Glacial Stage are very similar to those of mainland Australia and northeastern Tasmania probably defines the southernmost extension of the expanded semi-arid zone of mainland Australia.

5. GROUNDWATER HYDROLOGY

The regional study permitted selection of the aquifer best suited to an applied groundwater hydrology study. The classification of the landforms and deposits has highlighted the groundwater potential of the Stumpys Bay Sand and Barnbougle Sand on the basis of their wide extent, moderate thickness, and composition. Detailed study of the East Tomahawk area has revealed that the interglacial marine sands form unconfined aquifer systems which gain water from precipitation and lose water through evapotranspiration. Lateral groundwater flow, although present, is not responsible for significant water table fluctuations. The water table responds quickly to rainfall inputs and evapotranspiration losses, but the nature of the response is controlled by the soil moisture conditions in the zone of aeration. The presence of moisture in this zone reduces the pore space available for rainwater, and when precipitation occurs, causes large water table rises. If the moisture in the zone of aeration is below field capacity, rainfall inputs must raise the soil moisture level to field capacity before excess water is able to percolate to the water table. Thus, during dry periods when this zone is below field capacity, significantly more rainfall is needed to produce an equivalent rise of the water table than

is needed during moist periods. The capillary fringe component of the zone of aeration has a profound effect on the short term response of the water table to rainfall inputs. Where the capillary fringe is well developed, the water table rises sharply in response to precipitation, and the capillary fringe is temporarily destroyed by the downward moving water. The water table then declines until the capillary rise from the water table re-establishes the capillary fringe and equilibrium is again attained. The complex nature of these short term reactions to inputs precludes direct correlation between water table response and precipitation.

The above relationships which have been determined for the aquifer formed by the Stumpys Bay Sand probably also apply to the aquifer formed by the Barnbougle Sand, provided that the inputs from river water, where significant, are taken into consideration. The amount of groundwater estimated to be stored in the Stumpys Bay Sand is approximately 283,000 Ml. The Barnbougle Sand is estimated to contain 472,000 Ml. The estimated recoverable reserves for both of these aquifers is approximately 50 percent of the groundwater in storage, and they therefore show promise as valuable groundwater sources in an area of scarce surface water supplies. Water budget calculations indicate that the amount of water added to the aquifer system of the interglacial marine sands by precipitation is closely balanced by evapotranspiration losses. If water is pumped from the aquifer at a rate sufficient to lower water table levels over wide areas, then less water will be lost through evapotranspiration since the water table will be further from the surface. Also, as more rainfall is needed to raise the water table to the surface, under these conditions, there

is less likelihood of water-logging during winter. For an irrigation application of 200 mm of water, the general level of the water table would need to be lowered by only 1 m.

Measurements of rates of groundwater yield from bores in the Stumpys Bay Sand indicate that if the aquifer is less than 3 m thick, it will not generally yield a steady flow of water. However, once this minimum aquifer thickness is exceeded, the yield increases at a rate of approximately 5,000 l/day for each additional metre. The quality of the groundwater stored in the Stumpys Bay Sand is adequate for most irrigation and livestock purposes.

The Barnbougle Sand has not been studied in as much detail but is similar to the Stumpys Bay Sand, and comparisons indicate that the Barnbougle Sand is also a potentially good aquifer. The water potential of the other landforms and deposits which occur in the study area is severely restricted due to their limited extent, and in most cases their inability to arrest water.

REFERENCES

Australian Bureau of Statistics, 1976. *Tasmanian Year Book*, No. 10, Government Printer, Hobart, Tasmania.

Australian Code of Stratigraphic Nomenclature, 1973. *J. Geol. Soc. Aust.*, 20(1), 105-112.

Bagnold, R.A., 1941. *The Physics of Blown Sand and Desert Dunes*, Methuen, London, 265 pp.

Banks, M.R., Colhoun, E.A. and Chick, N.K., 1977. A reconnaissance of the geomorphology of central western Tasmania, in Banks, M.R. and Kirkpatrick, J.B. (eds.), *Landscape and Man*, Royal Society of Tasmania, Hobart, 29-54.

Bird, E.C.F., 1961. The coastal barriers of east Gippsland, Australia, *Geogr. J.*, 127, 460-468.

Bird, E.C.F., 1973. Australian coastal barriers, in Schwartz, M.L. (ed.), *Barrier Islands*, Dowden, Hutchinson and Ross, Stroudsburg, 410-426.

Bloom, A.L., Broecker, W.S., Chappell, J.H.A., Matthews, R.K. and Mesolella, K.J., 1974. Quaternary sea level fluctuations on a tectonic coast: New $^{230}Th/^{234}U$ dates from the Huon Peninsula, New Guinea, *Quat. Res.*, 4, 185-205.

Bowden, A.R., 1974. The glacial geomorphology of the Tyndall Mountains, Western Tasmania. B.Sc. Honours Thesis, Department of Geography, University of Tasmania.

Bowden, A.R., 1978. Geomorphic perspective on shallow groundwater potential, coastal northeastern Tasmania, *A.W.R.C. Tech. Pap.*, 36, 84 pp.

Bowler, J.M., 1968. Australian landform example No. 11: lunette, *Aust. Geogr.*, 10, 402-404.

Bowler, J.M., 1971. Pleistocene salinities and climatic change: evidence from lakes and lunettes in southeastern Australia, in Mulvaney, D.J. and Golson, J. (eds.), *Aboriginal Man and Environment in Australia*, ANU Press, Canberra, A.C.T., 47-65.

Bowler, J.M., 1973. Clay dunes: their occurrence, formation and environmental significance, *Earth Sci. Rev.*, 9, 315-338.

Bowler, J.M., 1976. Aridity in Australia: age, origins and expression in aeolian landforms and sediments, *Earth Sci. Rev.*, 12(213), 279-310.

Bowler, J.M. and Harford, L.B., 1966. Quaternary tectonics and the evolution of the Riverine Plain near Echuca, Victoria, *J. Geol. Soc. Aust.*, 13, 339-353.

Bowler, J.M., Hope, G.S., Jennings, J.N., Singh, G. and Walker, D., 1976. Late Quaternary climates of Australia and New Guinea, *Quat. Res.*, 6, 359-394.

Broecker, W.S. and Thurber, D.L., 1965. Uranium-series dating of corals and oolites from Bahaman and Florida Key Limestones, *Science*, 149, 58-60.

Broecker, W.S., Thurber, D.L., Goddard, J., Ku, T.L., Matthews, R.K. and Mesolella, K.J., 1968. Milankovitch Hypothesis supported by precise dating of coral reefs and deep-sea sediments, *Science*, 159, 297-300.

Brookfield, M., 1970. Dune trends and wind regimes in Central Australia, *Zeit. f. Geomorph. N.F. Suppl.*, 10, 121-153.

Bull, W.B., 1962. Relation of textural (CM) patterns to depositional environment of alluvial fan deposits, *J. Sed. Petrol.*, 32, 211-216.

Bureau of Mineral Resources, 1976. *Gravity Map of Australia*, 1:5,000,000, Department of National Resources, Geology and Geophysics.

Campbell, E.M., 1968. Lunettes in southern South Australia, *Trans. R. Soc. South Aust.*, 92, 85-109.

Chick, N.K., 1971. Fossil shorelines of the Ulverstone District, Tasmania, *Pap. Proc. R. Soc. Tasm.*, 105, 29-40.

Clarke, R.H. and Priestley, C.H.B., 1970. The asymmetry of Australian desert sand ridges, *Search*, 1(2), 77.

Coffey, G.N., 1909. Clay dunes, *J. Geol.*, 17, 754-755.

Colhoun, E.A., 1975. A Quaternary climatic curve for Tasmania, *R. met. Soc.*, Australasian Conference on Climate and Climatic Change, Monash University, Dec. 7-12.

Colhoun, E.A., 1976. The glaciation of the lower Forth Valley, northwestern Tasmania, *Aust. geogr. Stud.*, 14, 83-102.

Colhoun, E.A., 1977. A sequence of Late Quaternary deposits at Pipe Clay Lagoon, southeastern Tasmania, *Pap. Proc. R. Soc. Tasm.*, 111, 1-12.

Colhoun, E.A., 1978a. The late Quaternary environment of Tasmania as a backdrop to man's occupance, *Rec. Q. Vict. Mus., Launceston*, 61, 12 pp.

Colhoun, E.A., 1978b. Recent Quaternary and geomorphological studies in Tasmania, *Aust. Quat. Newsletter*, 12, 2-15.

Colhoun, E.A. and Goede, A., 1973. Fossil penguin bones, ^{14}C dates and the raised marine terrace of Macquarie Island: some comments, *Search*, 4, 11-12, 499-501.

Cook, P.J., Colwell, J.B., Firman, J.B., Lindsay, J.B., Schwebel, D.A. and Von der Borch, C.C., 1977. The late Cainozoic sequence of southeast South Australia and Pleistocene sea-level changes, *BMR J. of Aust. Geol. and Geophys.*, 2, 81-88.

Crespin, I., 1945. Middle Miocene limestone from Cape Barren Island, Furneaux Group, Bass Strait, *Proc. R. Soc. Tasm.*, for 1944, 13-14.

Critchfield, H.J., 1966. *General Climatology*, Prentice-Hall, New Jersey.

Cromer, W.C., 1972. Groundwater prospects, Nine Mile Beach, *Tech. Rep. Dep. Mines Tasm.*, 17, 157-159.

Cromer, W.C., 1974a. Groundwater prospects, Cape Sorell and Bradden Point, western Tasmania, *Tech. Rep. Dep. Mines Tasm.*, 19, 106-109.

Cromer, W.C., 1974b. Water in coastal sands, *Tech. Rep. Dep. Mines Tasm.*, 19, 128-135.

Cromer, W.C., 1979. Groundwater from coastal sands: Greens Beach, Northern Tasmania, *Geol. Surv. Bull. Tasm.*, 57.

Cromer, W.C. and Sloane, D.J., 1976. The hydrology of Seven Mile Beach, *Unpub. Rep. Dept. Mines Tasm.*, 1976/10.

Cull, J.P. and Denham, D., 1979. Regional variations in Australian heat flow, *BMR J. Aust. Geol. and Geophys.*, 4, 1-13.

Davies, J.L., 1959. High level erosion surfaces and landscape development in Tasmania, *Aust. Geogr.*, 7, 5, 193-203.

Davies, J.L., 1960. Quaternary strandlines in Tasmania, in Summary of the Report of the ANZAAS Sections C and P Committees, *Aust. J. Science*, 23, 75.

Davies, J.L., 1967. Tasmanian landforms and Quaternary climates, in Jennings, J.N. and Mabbutt, J.A. (eds.), *Landform Studies from Australia and New Guinea*, Cambridge University Press, Cambridge.

Davies, J.A. and Allen, C.D., 1973. Equilibrium, potential and actual evapotranspiration from cropped surfaces in southern Ontario, *J. appl. Meteorology*, 12(4), 649-657.

Davis, S.N. and De Wiest, R.J.M., 1966. *Hydrogeology*, Wiley, New York, 463 pp.

Derbyshire, E., 1971. A synoptic approach to the atmospheric circulation of the last glacial maximum in southeastern Australia, *Palaeogeog. Palaeoclimatol. Palaeoecol.*, 10, 103-124.

Dimmock, G.M., 1957. The soils of Flinders Island, Tasmania, *Soils and Land Use Series*, CSIRO, Melbourne, 23, 68 pp.

Emiliani, C., 1961. Cenozoic climatic changes as indicated by the stratigraphy and chronology of deep-sea cores of *Globigerina* facies, *Ann. N.Y. Acad. Science*, 95, 521-536.

Emiliani, C., 1966. Isotopic paleotemperatures, *Science*, 154, 851-857.

Emiliani, C. and Shackleton, N.J., 1974. The Brunhes epoch: isotopic paleotemperatures and geochronology, *Science*, 183, 511-514.

Ericson, D.B. and Wollin, G., 1968. Pleistocene climates and chronology in deep-sea sediments, *Science*, 162, 1227-1234.

Ferris, J.G., Knowles, D.B., Brown, R.H. and Stallman, R.W., 1962. Theory of aquifer tests, *U.S. geol. Surv. Wat. - Supply Pap.* 1536-E.

Flint, R.F., 1965. *Glacial and Quaternary Geology*, Wiley, London, 892 pp.

Folk, R.L., 1965. *Petrology of Sedimentary Rocks*, Hemphill's, Austin, Texas, 159 pp.

Folk, R.L., 1966. A review of grainsize parameters, *Sedimentology*, 6(2), 73-93.

Folk, R.L., 1971. Longitudinal dunes of the northwestern edge of the Simpson Desert, Northern Territory, Australia, 1. Geomorphology and grainsize relationships, *Sedimentology*, 16, 5-54.

Folk, R.L. and Ward, W.C., 1957. Brazos River bar: a study in the significance of grainsize parameters, *J. Sed. Petrol.*, 27(1), 3-26.

Friedman, G.M., 1961. Distinction between dune, beach and river sand from textural characteristics, *J. Sed. Petrol.*, 31, 514-529.

Galloway, R.W., 1965. Late Quaternary climates in Australia, *J. Geol.*, 73, 603-618.

Geological Survey of Tasmania, 1974. Launceston, Sheet SK55-4, *Tasm. Geol. Atlas Ser.*

Gill, E.D. and Amin, B.S., 1975. Interpretation of 7.5 and 4 metre Last Interglacial shore platforms in southeast Australia, *Search*, 6, 394-396.

Harmon, R.S., Schwarcz, H.P. and Ford, D.C., 1978. Late Pleistocene sea level history of Bermuda, *Quat. Res.*, 9, 205-218.

Hills, E.S., 1940. The lunette, a new landform of aeolian origin, *Aust. Geogr.*, 3, 15-21.

Holton, J.R., 1972. *An Introduction to Dynamic Meteorology*, Academic Press, New York, 319 pp.

Hoy, R.D. and Stephens, S.K., 1977. Field study of evaporation - analysis of data from Eucumbene, Cataract, Manton and Mundaring, *Aust. Wat. Res. Council Tech. Pap.*, 21.

Jennings, D.J. and McShane, R.F., 1971. Geology: Mt. William-Eddystone Point Area, *Dep. Mines Tasm.*

Jennings, J.N., 1959. The coastal geomorphology of King Island, Bass Strait, in relation to changes in the relative level of land and sea, *Rec. Q. Vict. Mus. Launceston*, N.S. 11, 1-39.

Jennings, J.N., 1961. Sea level changes in King Island, Bass Strait, *Zeits. f. Geomorph. Supplbd.*, 3, 80-84.

Jennings, J.N., 1971. Sea level changes and land links, in Mulvaney, D.J. and Golson, J. (eds.), *Aboriginal Man and Environment in Australia*, ANU Press, Canberra, 1-13.

Kershaw, R.C. and Sutherland, F.L., 1972. Quaternary geology of Flinders Island, *Rec. Q. Vic. Mus., Launceston*, 43, 28 pp.

King, D., 1956. The Quaternary stratigraphic record at Lake Eyre north and the evolution of existing topographic forms, *Trans. R. Soc. South Aust.*, 79, 93-103.

King, D., 1960. The sand ridge deserts of South Australia and related aeolian landforms of the arid cycles, *Trans. R. Soc. S. Aust.*, 89, 99-108.

Konishi, K., Schlanger, S.O. and Omura, A., 1970. Neotectonic rates in the Central Ryukyu Islands derived from $^{230}Th/^{234}U$ coral ages, *Marine Geology*, 9, 225-240.

Kruseman, G.P. and De Ridder, N.A., 1970. Analysis and evaluation of pumping test data, *International Institute for Land Reclamation and Improvement, Bulletin 11*, 200 pp.

Ku, T.L., Kimmel, M.A., Easton, W.H. and O'Neil, T.J., 1974. Eustatic sea level 120,000 years ago on Oahu, Hawaii, *Science*, 183, 959-962.

Krinsley, D.H. and Doornkamp, J.C., 1973. *Atlas of Quartz Sand Surface Textures*, Cambridge University Press, London, 91 pp.

Lagaaij, R. and Gautier, Y.V., 1965. Bryozoan assemblages from marine sediments of the Rhône delta, France, *Micropaleontology*, 11(1), 39-58.

Lahee, F.H., 1961. *Field Geology*, McGraw-Hill, New York, 926 pp.

Lambe, T.W., 1951. Capillary phenomena in cohesionless soils, *Trans. Am. Soc. civ. Engrs.*, 116, 401-432.

Land, L.S., Mackenzie, F.T. and Gould, S.J., 1967. Pleistocene history of Bermuda, *Geol. Soc. Am. Bull.*, 78, 993-1006.

Leaman, D.E., 1970a. Underground water resources, Arm End-Gellibrand Point, South Arm, *Tech. Rep. Dep. Mines Tasm.*, 15, 129-132.

Leaman, D.E., 1970b. Water prospects at Eaglehawk Neck, *Tech. Rep. Dep. Mines Tasm.*, 15, 134.

Leaman, D.E., 1971a. Underground water prospects from unconsolidated aquifers in the George Town area, *Tech. Rep. Dep. Mines Tasm.*, 16, 216-217.

Leaman, D.E., 1971b. The geology and groundwater resources of the Coal River Basin, *Undergr. Wat. Supply Pap. Tasm.*, 7.

Mabbutt, J.A., 1968. Aeolian landforms in central Australia, *Aust. geogr. Stud.*, 6(2), 139-150.

Mabbutt, J.A., Wooding, R.A. and Jennings, J.N., 1969. The asymmetry of Australian desert sand ridges, *Aust. J. Science*, 32 (4), 159-160.

Madigan, C.T., 1936. The Australian sand ridge deserts, *Geogr. Rev.*, 26, 205-227.

Marshall, J.F. and Lavnay, J., 1978. Uplift rates of the Loyalty Islands as determined by $^{230}Th/^{234}U$ dating of raised coral terraces, *Quat. Res.*, 9, 186-192.

Marshall, J.F. and Thom, B.G., 1976. The sea level in the Last Interglacial, *Nature*, 263, 120-121.

Mason, C.C. and Folk, R.L., 1958. Differentiation of beach, dune and aeolian flat environments by size analysis, Mustang Island, Texas, *J. Sed. Petrol.*, 28(2), 211-226.

Matthews, W.L., 1966. Underground water at proposed factory site, Deloraine, *Tech. Rep. Dep. Mines Tasm.*, 11, 119-120.

Matthews, W.L., 1972. Investigation of water supply, Currie, King Island, *Tech. Rep. Dep. Mines Tasm.*, 17, 144-157.

Matthews, W.L., 1975. Groundwater investigations, Flinders Island, *Tech. Rep. Dep. Mines Tasm.*, 20, 252-283.

Matthews, W.L. and Cromer, W.C., 1973. Groundwater investigations at Currie, King Island, *Tech. Rep. Dep. Mines Tasm.*, 18, 106-123.

Meinzer, O.E., 1923. The occurrence of groundwater in the United States, with a discussion of principles, *U.S. geol. Surv. Wat. Supply Pap. 489*, 321 pp.

Moore, W.R., 1968. Underground water investigation, Tomahawk, *Tech. Rep. Dep. Mines Tasm.*, 13, 125-128.

Moore, W.R., 1975. The groundwater potential of northeastern Tasmania, *Tech. Rep. Dep. Mines Tasm.*, 20, 249-252.

Morgan, W.J., 1971. Convection plumes in the lower mantle, *Nature*, 230, 42-43.

Morgan, W.J., 1972. Deep mantle convection plumes and plate motions, *Am. Assoc. Petr. Geol. Bull.*, 56, 203-213.

Neef, G. and Veeh, H.H., 1977. Uranium series ages and late Quaternary uplift in the New Hebrides, *Nature*, 269, 682-683.

Neumann, A.C. and Moore, W.S., 1975. Sea level events and Pleistocene coral ages in the Northern Bahamas, *Quat. Res.*, 5, 215-224.

Nicolls, K.D., 1957. Reconnaissance soil map of Tasmania - Sheet 47 - Longford, *CSIRO Australia Div. Soils, Divisional Rept. 14/57*, 1-17.

Nicolls, K.D., 1958. Aeolian deposits in river valleys in Tasmania, *Aust. J. Science*, 21, 50-51.

Nunez, M., in prep. A micro-climatic approach to Pleistocene evaporation: the case of northeastern Tasmania.

Passega, R., 1957. Texture as characteristic of clastic deposition, *Am. Assoc. Petr. Geol. Bull.*, 41, 1952-1984.

Petrov, M.P., 1948. The topography of dune sands and stages in its development, *Trudy Inst. Geogr. Akad. Nauk., SSSR*, 39.

Quilty, P.G., 1972. The biostratigraphy of the Tasmanian marine Tertiary, *Pap. Proc. R. Soc. Tasm.*, 106, 25-44.

Rose, C.W., 1966. *Agricultural Physics*, Pergamon.

Scorer, R.S., 1948. Theory of waves in the lee of mountains, *R. Met. Soc. Quarterly J.*, 75, 41-56.

Scorer, R.S., 1961. Lee waves in the atmosphere, *Scientific American*, 204(3), 124-134.

Shackleton, N.J., 1969. The last interglacial in the marine and terrestrial records, *Proc. R. Soc. Lond.*, B, 174, 135-154.

Shackleton, N.J. and Opdyke, N.D., 1973. Oxygen isotope and palaeomagnetic stratigraphy of Equatorial Pacific Core V28-238: oxygen isotope temperatures and ice volumes on a 10^5 year and 10^6 year scale, *J. Quat. Res.*, 3(1), 39-55.

Shackleton, N.J. and Opdyke, N.D., 1976. Oxygen isotope and palaeomagnetic stratigraphy of Pacific Core V28-239, Late Pliocene to latest Pleistocene, *Geol. Soc. Am. Mem.*, 145, 449-464.

Shepard, F.P., 1954. Nomenclature based on sand-silt-clay ratios, *J. Sed. Petr.*, 24, 151-158.

Sigleo, W.R. and Colhoun, E.A., 1975. Glacial age Man in southeastern Tasmania: evidence from the Old Beach site, *Search*, 6(7), 300-302.

Spry, A. and Banks, M.R. (eds.), 1962. The geology of Tasmania, *J. Geol. Soc. Austr.*, 9(2), 362 pp.

Stearns, C.E., 1976. Estimates of the position of sea level between 140,000 and 75,000 years ago, *Quat. Res.*, 6, 445-449.

Stephens, C.G. and Crocker, R.L., 1946. Composition and genesis of lunettes, *Trans. R. Soc. South Aust.*, 70(2), 302-314.

Stevenson, P.C., 1969. Groundwater prospects at Nine Mile Beach, *Unpub. Rep. Dep. Mines Tasm.*

Stevenson, P.C., 1970. Groundwater prospects at South Bruny Area School, Alonnah, *Tech. Rep. Dep. Mines Tasm.*, 15, 135.

Stevenson, P.C., 1973. Water in coastal sands, *Tasm. J. Agric.*, 44, 182-185.

Stover, L.E. and Partridge, A.D., 1973. Tertiary and Late Cretaceous spores and pollen from the Gippsland Basin, southeastern Australia, *Proc. R. Soc. Vict.*, 85(2), 237-286.

Sutherland, F.L. and Kershaw, R.C., 1971. The Cainozoic geology of Flinders Island, Bass Strait, *Pap. Proc. R. Soc. Tasm.*, 105, 151-175.

Taylor, T.G., 1930. Agricultural regions of Australia, *Econ. Geogr.*, 6, 109-134.

Thom, B.G. and Chappell, J., 1975. Holocene sea levels relative to Australia, *Search*, 6(3), 90-93.

Thom, B.G., Polach, H.A. and Bowman, G.M., 1978. Holocene age structure of coastal sand barriers in New South Wales, Australia, Unpubl. Manuscript. Department of Geography, Faculty of Military Studies, University of New South Wales.

Thompson, J. and Walton, A., 1972. Redetermination of chronology of Aldabra Atoll by $^{230}Th/^{234}U$ dating, *Nature*, 240, 145-146.

Thurber, D.L., Broecker, W.S., Blanchard, R.L. and Potratz, H.A., 1965. Uranium-series ages of Pacific Atoll Coral, *Science*, 149, 55-58.

Till, R., 1973. The use of linear regression in geomorphology, *Area*, 5(4), 303-308.

Tjia, H.D., Fujii, S., Kigoshi, K., Sugimura, A. and Zakaria, T., 1972. Radiocarbon dates of elevated shorelines, Indonesia and Malaysia. Part I, *Quat. Res.*, 2, 487-495.

Todd, D.K., 1959. *Groundwater Hydrology*, Wiley, New York, 336 pp.

Tolman, C.F., 1937. *Groundwater*, McGraw-Hill, New York, 593 pp.

Troxell, M.C., 1936. The diurnal fluctuations in the groundwater and flow of the Santa Anna River and its meaning, *Trans. Am. geophys. Un.*, 17(2), 496-504.

Twidale, C.R., 1968. *Geomorphology: with Special Reference to Australia*, Nelson, Melbourne, 406 pp.

Twidale, C.R., 1972. Evolution of sand dunes in the Simpson Desert, Central Australia, *Trans. Inst. Br. Geogr.*, 56, 77-110.

Udden, J.A., 1898. Mechanical composition of wind deposits, *Augustana Library Publication*, 1, 69 pp.

van de Geer, G., Colhoun, E.A. and Bowden, A.R., 1979. Evidence and problems of interglacial marine deposits in Tasmania, *Geol. en. Mijn.*, 58(1), 29-32.

Veeh, H.H., 1966. Th^{230}/U^{238} and U^{234}/U^{238} ages of Pleistocene high sea level stand, *J. Geophys. Res.*, 71(4), 3379-3386.

Veeh, H.H. and Chappell, J., 1970. Astronomical theory of climatic change: support from New Guinea, *Science*, 167, 862-865.

Veevers, J.J. and Wells, A.T., 1961. The geology of the Canning Basin, Western Australia, *Commonwealth of Australia, BMR Geol. Geophys. Bull.* 60, 323 pp.

Ward, W.T., 1973. Correlation of Pleistocene shorelines in Gippsland, Australia, and Oahu, Hawaii, *Geol. Soc. Am. Bull.*, 84, 3087-3092.

White, W.N., 1932. A method of estimating groundwater supplies based on discharge by plants and evaporation from soil: results of investigations in Escalente Valley, Utah, *U.S. geol. Surv. Wat.-Supply Pap. 659-A.*

Wilson, J.T., 1963a. Evidence from islands on the spreading of ocean floors, *Nature*, 197, 536-538.

Wilson, J.T., 1963b. A possible origin of the Hawaiin Islands, *Can. J. Phys.*, 41, 863.

Wyrwoll, K.H. and Milton, D., 1976. Widespread late Quaternary aridity in Western Australia, *Nature*, 264, 429-430.

Zenkovitch, V.P., 1967. *Processes of Coastal Development*, Oliver and Boyd, London. Edited by J.A. Steers.

APPENDIX

TOMAHAWK GROUNDWATER MODEL

COMPUTER PROGRAMME

```
      PROGRAM OSCA(INPUT,OUTPUT,TAPE5=INPUT,TAPE6=OUTPUT)
C
C     TOMAHAWK AREA 29X27 MATRIX  17 MARCH 1976  2 DAY INTERVAL  FOR  30 DAYS
C
C
C*****************************************************************************
C* VARIABLE LIST=                                                            *
C* ALT... GROUND LEVEL (METRES)                                              *
C* PERM... PERMIABILITY OF SAND (LIT/DAY/SQ.METRE)                           *
C*PTNR... PRECIPITATION RATE (MM)/DAY)                                       *
C*WTHT... ELEVATION OF WATER TABLE (METRES)                                  *
C* NBLOCK... BLOCKING SYSTEM WHICH ENABLES DIFFERENTIATION OF SEA,(NBLOCK=2), *
C*  SAND,NBLOCK=3), AND BEDROCK(NBLOCK=1), AREAS.                            *
C* SANDTH... SAND THICKNESS (METRES)                                         *
C* FLO... SURFACE WATER FLOW ADDED TO A CELL                                 *
C* EXES... PRECIPITATION OR FLOW UNABLE TO BE ABSORBED BY A CELL             *
C* DUR... DURATION OF RAINFALL (DAYS)                                        *
C* PTNRX... PRECIPITATION RATE (MM/DAY)                                      *
C* IROW... NUMBER OF ROWS IN MATRIX                                          *
C* KOL... NUMBER OF COLUMNS IN MATRIX                                        *
C* TINT... TIME INTERVAL BETWEEN STEPS(DAYS)                                 *
CC* PHI... POROSITY OF SAND                                                  *
C* MONITR... NUMBER OF DAYS OVER WHICH SIMULATION IS RUN                     *
C* ACRCY... MAXIMUM WATER TABLE HEIGHT DIFFERENCE BETWEEN CELLS WHICH ARE    *
C*   CONSIDERED TO BE EQUAL (METRES)                                         *
C* WTIN... AMOUNT OF WATER ADDED TO EACH SQUARE METRE OF A CELL (LITRES)     *
C* THWTIN... AMOUNT OF WATER ADDED TO WATER TABLE FROM PRECIPITATION (METRES)*
C* FRONT... DEPTH FROM GROUND SURFACE OF WATER FRONT FROM THE INPUTS         *
C* ARRIVE... CONDITION WHERE THE FRONT HAS REACHED THE WATER TABLE           *
C* HOZFLO... AMOUNT ADDED TO WATER TABLE FROM R                              *
C* HOZFLO... AMOUNT ADDED TO THE WATER TABLE FROM GROUNDWATER FLOW (METRES)  *
C* FLOLOS... AMOUNT LOST FROM WATER TABLE FROM GROUNDWATER FLOW (METRES)     *
C* CELLSZ... LENGTH OF SIDE OF EACH CELL (METRES)                            *
C*****************************************************************************
      REAL MONITR,NUALT
      DIMENSION ALT(40,40),PERM(40,40),PTNR(40,40),FLO(40,40),EXES(40,40
     ,),WTIN(40,40),ADDFLO(40,40),THWTIN(40,40),RUNOFF(40,40),DTOWT(40,4
     ,0),WTHT(40,40),FRONT(40,40),NBLOCK(40,40),NAME(20),ARRIVE(40,40),H
     ,OZFLO(40,40),FLOLOS(40,40),SANDTH(40,40)
      READ(5,500)(NAME(J),J=1,20)
  500 FORMAT(20A4)
      WRITE(6,501)(NAME(J),J=1,20)
  501 FORMAT(1H1,20X,20A4)
      READ(5,99)DUR,PTNRX,IROW,KOL,TINT,PHI,MONITR,ACRCY
   99 FORMAT(F5.3,F5.1,2I2,F6.2,F4.2,F6.2,F5.3)
      READ(5,86)CELLSZ
   86 FORMAT(F6.1)
      DO 60 I=1,IROW
   60 READ(5,100)(PERM(I,J),J=1,13)
      DO 61 I=1,IROW
   61 READ(5,100)(PERM(I,J),J=14,26)
      DO 62 I=1,IROW
   62 READ(5,101)PERM(I,KOL)
  100 FORMAT(1X,13F6.0)
  101 FORMAT(1X,F6.0)
      DO 70 I=1,IROW
   70 READ(5,200)(ALT(I,J),J=1,13)
```

```
      PROGRAM OSCA       76/76   OPT=1                    FTN 4.4+R401       14/12/76  11.03.1

                  DO 71 I=1,IROW
                71 READ(5,200)(ALT(I,J),J=14,26)
60                DO 72 I=1,IROW
                72 READ(5,201)ALT(I,KOL)
               200 FORMAT(1X,13F6.2)
               201 FORMAT(1X,F6.2)
                  DO 80 I=1,IROW
65                DO 80 J=1,KOL
                  FLO(I,J)=0.0
                80 PTNR(I,J)=PTNRX
                  DO 7010 I=1,IROW
              7010 READ(5,7000)(NBLOCK(I,J),J=1,KOL)
70            7000 FORMAT(1X,27I1)
                  DO 7030 I=1,IROW
              7030 READ(5,7020)(WTHT(I,J),J=1,15)
                  DO 7031 I=1,IROW
              7031 READ(5,7021)(WTHT(I,J),J=16,KOL)
75            7020 FORMAT(1X,15F5.2)
              7021 FORMAT(1X,12F5.2)
                  DO 7270 I=1,IROW
              7270 READ(5,7280)(SANDTH(I,J),J=1,19)
                  DO 7271 I=1,IROW
80            7271 READ(5,7281)(SANDTH(I,J),J=20,KOL)
              7280 FORMAT(1X,19F4.1)
              7281 FORMAT(1X,8F4.1)
                  WRITE(6,505)DUR,PTNRX,IROW,KOL,TINT,PHI,MONITR,ACRCY,CELLSZ
               505 FORMAT(1X,F5.3,F5.1,2I2,F6.2,F4.2,F6.2,F5.3,F6.1)
85                DO 507 I=1,IROW
                  WRITE(6,400)
               507 WRITE(6,506)(PERM(I,J),J=1,14)
               506 FORMAT(1X,14F7.0)
                  DO 607 I=1,IROW
90                WRITE(6,400)
               607 WRITE(6,606)(PERM(I,J),J=15,KOL)
               606 FORMAT(1X,13F7.0)
                  DO 508 I=1,IROW
                  WRITE(6,400)
95             508 WRITE(6,509)(ALT(I,J),J=1,14)
               509 FORMAT(1X,14F6.2)
                  DO 608 I=1,IROW
                  WRITE(6,400)
               608 WRITE(6,609)(ALT(I,J),J=15,KOL)
100            609 FORMAT(1X,13F6.2)
                  DO 510 I=1,IROW
                  WRITE(6,400)
               510 WRITE(6,511)(NBLOCK(I,J),J=1,KOL)
               511 FORMAT(1X,27I1)
105               DO 513 I=1,IROW
                  WRITE(6,400)
               513 WRITE(6,514)(WTHT(I,J),J=1,15)
               514 FORMAT(1X,15F5.2)
                  DO 613 I=1,IROW
110               WRITE(6,400)
               613 WRITE(6,614)(WTHT(I,J),J=16,KOL)
               614 FORMAT(1X,12F5.2)
                  DO 7180 I=1,IROW
                  WRITE(6,400)
```

```
      PROGRAM OSCA       76/76   OPT=1                    FTN 4.8+R401       14/12/76  11.03.1

115          7180 WRITE(6,7170)(SANDTH(I,J),J=1,19)
             7170 FORMAT(1X,19F4.1)
                  DO 7181 I=1,IROW
                  WRITE(6,400)
             7181 WRITE(6,7171)(SANDTH(I,J),J=20,KOL)
120          7171 FORMAT(1X,8F4.1)
                  II=IROW-1
                  JJ=KOL-1
                  KC=0
                  DO 13 I=2,II
125               DO 13 J=2,JJ
               C
               C     CALCULATES EXCESS IN INITIAL CYCLE
               C
                1 IF(PTNR(I,J).LE.PERM(I,J)) GO TO 13
130               DIV=0.
                  D1=0.
                  D2=0.
                  D3=0.
                  D4=0.
135               EXES(I,J)=PTNR(I,J)-PERM(I,J)
                  IF(ALT(I,J-1).GE.ALT(I,J)) GO TO 2
                  D1=1.0
                  GO TO 3
                2 D1=0.
140             3 IF(ALT(I,J+1).GE.ALT(I,J)) GO TO 4
                  D2=1.
                  GO TO 5
                4 D2=0.
                5 IF (ALT(I-1,J).GE.ALT(I,J)) GO TO 6
145               D3=1.
                  GO TO 7
                6 D3=0.
                7 IF(ALT(I+1,J).GE.ALT(I,J)) GO TO 8
                  D4=1.
150               GO TO 9
                8 D4=0.
                9 DIV=D1+D2+D3+D4
                  IF(ALT(I,J-1).GE.ALT(I,J)) GO TO 10
                  FLO(I,J-1)=(EXES(I,J)/DIV)+FLO(I,J-1)
155            10 IF(ALT(I,J+1).GE.ALT(I,J)) GO TO 11
                  FLO(I,J+1)=(EXES(I,J)/DIV)+FLO(I,J+1)
               11 IF(ALT(I+1,J).GE.ALT(I,J)) GO TO 12
                  FLO(I+1,J)=(EXES(I,J)/DIV)+FLO(I+1,J)
               12 IF(ALT(I-1,J).GE.ALT(I,J)) GO TO 121
160               FLO(I-1,J)=(EXES(I,J)/DIV)+FLO(I-1,J)
              121 PTNR(I,J)=PTNR(I,J)-EXES(I,J)
                  EXES(I,J)=0.
               13 CONTINUE
                  WRITE(6,7100)
165           7100 FORMAT(1X,* LOOP 13 COMPLETED *)
                  TPTNS=0.
               19 II=IROW-1
                  JJ=KOL-1
               45 KK=0
170               DO 35 I=2,II
                  DO 35 J=2,JJ
```

```
      PROGRAM OSCA       76/76   OPT=1                    FTN 4.4+R401       14/12/76  11.03.16

                  PTNR(I,J)=PTNR(I,J)+FLO(I,J)
                  FLO(I,J)=0.
                20 IF(PTNR(I,J).LE.PERM(I,J)) GO TO 35
175               DIV=0.
                  D1=0.
                  D2=0.
                  D3=0.
                  D4=0.
180               EXES(I,J)=PTNR(I,J)*PERM(I,J)
                15 PTNR(I,J)=PTNR(I,J)-EXES(I,J)
                21 IF(ALT(I,J-1).GE.ALT(I,J)) GO TO 22
                  D1=1.
                  GO TO 23
185             22 D1=0.
                23 IF(ALT(I,J+1).GE.ALT(I,J)) GO TO 24
                  D2=1.
                  GO TO 25
                24 D2=0.
190             25 IF(ALT(I-1,J).GE.ALT(I,J)) GO TO 26
                  D3=1.
                  GO TO 27
                26 D3=0.
                27 IF(ALT(I+1,J).GE.ALT(I,J)) GO TO 28
195               D4=1.
                  GO TO 29
                28 D4=0.
                29 DIV=D1+D2+D3+D4
                  IF(ALT(I,J-1).GE.ALT(I,J)) GO TO 30
200               FLO(I,J-1)=(EXES(I,J)/DIV)*FLO(I,J-1)
                30 IF(ALT(I,J+1).GE.ALT(I,J)) GO TO 31
                  FLO(I,J+1)=(EXES(I,J)/DIV)*FLO(I,J+1)
                31 IF(ALT(I+1,J).GE.ALT(I,J)) GO TO 32
                  FLO(I+1,J)=(EXES(I,J)/DIV)*FLO(I+1,J)
205             32 IF(ALT(I-1,J).GE.ALT(I,J)) GO TO 33
                  FLO(I-1,J)=(EXES(I,J)/DIV)*FLO(I-1,J)
                33 EXES(I,J)=0.
                35 CONTINUE
                  WRITE(6,7110)
210           7110 FORMAT(1X,* LOOP 35 COMPLETED *)
                  MATCEL=IROW*KOL
                  DO 75 I=1,IROW
                  DO 75 J=1,KOL
                  PTNR(I,J)=PTNR(I,J)+FLO(I,J)
215               FLO(I,J)=0.
                  IF(PTNR(I,J).LE.PERM(I,J))KK=KK+1
                75 CONTINUE
                  WRITE(6,7120)
220           7120 FORMAT(1X,* LOOP 75 COMPLETED *)
                  WRITE(6,7160)KK
              7160 FORMAT(I3)
                  IF(KK.NE.MATCEL) GO TO 45
                  DO 55 I=1,IROW
                  DO 55 J=1,KOL
225               WTIN(I,J)=PTNR(I,J)*DUR
                55 CONTINUE
                  WRITE(6,7130)
              7130 FORMAT(1X,* LOOP 55 COMPLETED *)
```

```
      PROGRAM OSCA       76/76   OPT=1                    FTN 4.4+R401       14/12/76  11.03.10

               C
230            C     THIS SECTION ADJUSTS FOR SITUATION WHERE THWTIN .GT.DTOWT
               C
                     DO 6000 I=1,IROW
                     DO 6000 J=1,KOL
                     IF(NBLOCK(I,J).LE.2) GO TO 6000
235                  DTOWT(I,J)=ALT(I,J)-WTHT(I,J)
                     THWTIN(I,J)=(WTIN(I,J)/PHI)+0.001
                6000 CONTINUE
               C
               C
240            C
               C
               C     PROGRAM WILD (SECOND STAGE TO GROUNDWATER FLOW)
               C
               C
245            C
                     DO 1000 I=1,IROW
                     DO 1000 J=1,KOL
                     THWTIN(I,J)=WTIN(I,J)/PHI+0.001
                     IF(NBLOCK(I,J).NE.2) GO TO 999
250                  RUNOFF(I,J)=WTIN(I,J)*CELLSZ**2/1000.
                     GO TO 1000
                 999 RUNOFF(I,J)=0.
                     ARRIVE(I,J)=0.
                1000 CONTINUE
255            C     THIS LOOP ENSURES RUNOFF TO SEA IS CUMULATIVE
                1500 DO 2001 I=1,IROW
                     DO 2001 J=1,KOL
                     FLOLOS(I,J)=0.
                     IF(NBLOCK(I,J).LE.2) GO TO 2001
260                  ADDFLO(I,J)=0.
                2001 CONTINUE
                     WRITE(6,7150)
                7150 FORMAT(1X,* LOOP 2001 COMPLETED *)
               C
265            C
               C
               C      THIS SECTION ADJUSTS GROUNDWATER FLOW IN ACTIVE AREAS AND CALC-
               C     ULATES FLOWS TO SEA.
               C
270            C
               C
                     DO 3000 I=2,II
                     DO 3000 J=2,JJ
                     IF(NBLOCK(I,J).LE.2) GO TO 3000
275                  IF(NBLOCK(I,J-1).EQ.1) GO TO 3010
                     IF(NBLOCK(I,J-1).EQ.2) GO TO 3015
                     WTHT(I,J-1)=WTHT(I,J-1)+ACRCY
                     IF(WTHT(I,J).GT.WTHT(I,J-1)) GO TO 3020
                     GO TO 3010
280                3015 HOZFLO(I,J-1)=PERM(I,J)*TINT*(WTHT(I,J)+WTHT(I,J-1))*(SANDTH(I,J)-
                    ,DTOWT(I,J))/PHI/CELLSZ**2/1000.
                     GO TO 3050
                3010 HOZFLO(I,J-1)=0
                     GO TO 3050
285                3020 IF(PERM(I,J).LE.PERM(I,J-1)) GO TO 3030
```

```
      PROGRAM OSCA       76/76   OPT=1                    FTN 4.4+R401       14/12/76  11.03.10

                  HOZFLO(I,J-1)=TINT*(WTHT(I,J)-WTHT(I,J-1))*((((SANDTH(I,J)-DTOWT(I
                 ,,J))+(SANDTH(I,J-1)-DTOWT(I,J-1)))/2)+(DTOWT(I,J)-DTOWT(I,J-1)))/C
                 ,ELLSZ**2/1000,/PHI*PERM(I,J-1)
                  GO TO 3050
290           3030 HOZFLO(I,J-1)=TINT*(WTHT(I,J)-WTHT(I,J-1))*((((SANDTH(I,J)-DTOWT(I
                 ,,J))+(SANDTH(I,J-1)-DTOWT(I,J-1)))/2)+(DTOWT(I,J)-DTOWT(I,J-1)))/C
                 ,ELLSZ**2/1000,/PHI*PERM(I,J)
              3050 IF(NBLOCK(I,J+1).EQ.1) GO TO 3110
                  IF(NBLOCK(I,J+1).EQ.2) GO TO 3115
295               WTHT(I,J+1)=WTHT(I,J+1)+ACRCY
                  IF(WTHT(I,J).GT.WTHT(I,J+1)) GO TO 3120
                  GO TO 3110
              3115 HOZFLO(I,J+1)=PERM(I,J)*TINT*(WTHT(I,J)-WTHT(I,J+1))*(SANDTH(I,J)-
                 ,DTOWT(I,J))/PHI/CELLSZ**2/1000.
300               GO TO 3150
              3110 HOZFLO(I,J+1)=0.
                  GO TO 3150
              3120 IF(PERM(I,J).LE.PERM(I,J+1)) GO TO 3130
                  HOZFLO(I,J+1)=TINT*(WTHT(I,J)-WTHT(I,J+1))*((((SANDTH(I,J)-DTOWT(I
305               ,,J))+(SANDTH(I,J+1)-DTOWT(I,J+1)))/2)+(DTOWT(I,J)-DTOWT(I,J+1)))/C
                 ,ELLSZ**2/1000,/PHI*PERM(I,J+1)
                  GO TO 3150
              3130 HOZFLO(I,J+1)=TINT*(WTHT(I,J)-WTHT(I,J+1))*((((SANDTH(I,J)-DTOWT(I
                 ,,J))+(SANDTH(I,J+1)-DTOWT(I,J+1)))/2)+(DTOWT(I,J)-DTOWT(I,J+1)))/C
310               ,ELLSZ**2/1000,/PHI*PERM(I,J)
              3150 IF(NBLOCK(I-1,J).EQ.1) GO TO 3210
                  IF(NBLOCK(I-1,J).EQ.2) GO TO 3215
                  WTHT(I-1,J)=WTHT(I-1,J)+ACRCY
                  IF(WTHT(I,J).GT.WTHT(I-1,J)) GO TO 3220
315               GO TO 3210
              3215 HOZFLO(I-1,J)=PERM(I,J)*TINT*(WTHT(I,J)-WTHT(I-1,J))*(SANDTH(I,J)-
                 ,DTOWT(I,J))/PHI/CELLSZ**2/1000.
                  GO TO 3250
              3210 HOZFLO(I-1,J)=0.
320               GO TO 3250
              3220 IF(PERM(I,J).LE.PERM(I-1,J)) GO TO 3230
                  HOZFLO(I-1,J)=TINT*(WTHT(I,J)-WTHT(I-1,J))*((((SANDTH(I,J)-DTOWT(I
                 ,,J))+(SANDTH(I-1,J)-DTOWT(I-1,J)))/2)+(DTOWT(I,J)-DTOWT(I-1,J)))/C
                 ,ELLSZ**2/1000,/PHI*PERM(I-1,J)
325               GO TO 3250
              3230 HOZFLO(I-1,J)=TINT*(WTHT(I,J)-WTHT(I-1,J))*((((SANDTH(I,J)-DTOWT(I
                 ,,J))+(SANDTH(I-1,J)-DTOWT(I-1,J)))/2)+(DTOWT(I,J)-DTOWT(I-1,J)))/C
                 ,ELLSZ**2/1000,/PHI*PERM(I,J)
              3250 IF(NBLOCK(I+1,J).EQ.1) GO TO 3310
330               IF(NBLOCK(I+1,J).EQ.2) GO TO 3315
                  WTHT(I+1,J)=WTHT(I+1,J)+ACRCY
                  IF(WTHT(I,J).GT.WTHT(I+1,J)) GO TO 3320
                  GO TO 3310
              3315 HOZFLO(I+1,J)=PERM(I,J)*TINT*(WTHT(I,J)-WTHT(I+1,J))*(SANDTH(I,J)-
335               ,DTOWT(I,J))/PHI/CELLSZ**2/1000.
                  GO TO 3350
              3310 HOZFLO(I+1,J)=0.
                  GO TO 3350
              3320 IF(PERM(I,J).LE.PERM(I+1,J)) GO TO 3330
340               HOZFLO(I+1,J)=TINT*(WTHT(I,J)-WTHT(I+1,J))*((((SANDTH(I,J)-DTOWT(I
                 ,,J))+(SANDTH(I+1,J)-DTOWT(I+1,J)))/2)+(DTOWT(I,J)-DTOWT(I+1,J)))/C
                 ,ELLSZ**2/1000,/PHI*PERM(I+1,J)
```

```
      PROGRAM OSCA       76/76   OPT=1                    FTN 4.4+R401       14/12/76  11.03.10

                 GO TO 3350
            3330 HOZFLO(I+1,J)=TINT*(WTHT(I,J)-WTHT(I+1,J))*((((SANDTH(I,J)-DTOWT(I
     345        ,,J))+(SANDTH(I+1,J)-DTOWT(I+1,J)))/2)+(DTOWT(I,J)-DTOWT(I+1,J)))/C
                ,ELLSZ**2/1000,/PHI*PERM(I,J)
            3350 FLOLOS(I,J)=HOZFLO(I,J-1)+HOZFLO(I,J+1)+HOZFLO(I-1,J)+HOZFLO(I+1,J
                ,)
                 THIS SECTION READJUSTS WATER LEVEL FOR ACRCY FACTOR
     350         C
                 IF(NBLOCK(I,J-1).LE.2) GO TO 1600
                 WTHT(I,J-1)=WTHT(I,J-1)*ACRCY
            1600 IF(NBLOCK(I,J+1).LE.2) GO TO 1610
                 WTHT(I,J+1)=WTHT(I,J+1)*ACRCY
     355    1610 IF(NBLOCK(I-1,J).LE.2) GO TO 1620
                 WTHT(I-1,J)=WTHT(I-1,J)*ACRCY
            1620 IF(NBLOCK(I+1,J).LE.2) GO TO 1630
                 WTHT(I+1,J)=WTHT(I+1,J)*ACRCY
                C
     360         C
            1630 ADDFLO(I,J-1)=ADDFLO(I,J-1)+HOZFLO(I,J-1)
                 ADDFLO(I,J+1)=ADDFLO(I,J+1)+HOZFLO(I,J+1)
                 ADDFLO(I-1,J)=ADDFLO(I-1,J)+HOZFLO(I-1,J)
                 ADDFLO(I+1,J)=ADDFLO(I+1,J)+HOZFLO(I+1,J)
     365    2995 HOZFLO(I,J-1)=0.
                 HOZFLO(I,J+1)=0.
                 HOZFLO(I-1,J)=0.
                 HOZFLO(I+1,J)=0.
            3000 CONTINUE
     370         WRITE(6,7140)
            7140 FORMAT(1X,* LOOP 3000 COMPLETED *)
                C
                C       THIS LOOP ADDS FLOWS TO THE WATER TABLE
                C
     375         TPTNS=TPTNS+TINT
                 DO 1672 I=1,IROW
                 DO 1672 J=1,KOL
                 IF(NBLOCK(I,J).EQ.1) GO TO 1672
                 IF(NBLOCK(I,J).EQ.2) GO TO 1675
     380         WTHT(I,J)=WTHT(I,J)+ADDFLO(I,J)-FLOLOS(I,J)
                 GO TO 1672
            1675 RUNOFF(I,J)=RUNOFF(I,J)+(ADDFLO(I,J)*PHI*CELLSZ**2)
                 ADDFLO(I,J)=0.
            1672 CONTINUE
     385         C
                 C       THIS SESTION CALCULATES POSITION OF FROMT AFTER EACH TIME INTERVAL
                 C
                 DO 2000 I=2,II
                 DO 2000 J=2,JJ
     390         IF(NBLOCK(I,J).LE.2) GO TO 2000
            2999 DTOWT(I,J)=ALT(I,J)-WTHT(I,J)
                 FRONT(I,J)=((PERM(I,J)*TPTNS)/PHI)*0.001
                 IF(FRONT(I,J).GE.DTOWT(I,J)) GO TO 2100
                 GO TO 2000
     395         2100 ARRIVE(I,J)=ARRIVE(I,J)+1
                 IF(ARRIVE(I,J).GE.2.) GO TO 2000
                 WTHT(I,J)=WTHT(I,J)+THWTIN(I,J)
            2000 CONTINUE
                C
```

```
      PROGRAM OSCA       76/76   OPT=1                    FTN 4.4+R401       14/12/76  11.03.10

400           C
              C
                    WRITE(6,400)
                    WRITE(6,4000)(TPTNS)
               4000 FORMAT(3X,*TPTNS= *,F6.2)
405                 WRITE(6,4101)
               4101 FORMAT(1H1,20X,*WTMT MATRIX.....METRES*)
                    DO 4100 I=1,IROW
                    WRITE(6,400)
               4100 WRITE(6,4200)(WTMT(I,J),J=1,15)
410            4200 FORMAT(1X,15F6.3)
                    DO 4102 I=1,IROW
                    WRITE(6,400)
               4102 WRITE(6,4201)(WTMT(I,J),J=16,KOL)
               4201 FORMAT(1X,12F6.3)
415                 WRITE(6,4301)
               4301 FORMAT(1H1,20X,*RUNOFF MATRIX.....CUBIC METRES*)
                    DO 4300 I=1,IROW
                    WRITE(6,400)
               4300 WRITE(6,4400)(RUNOFF(I,J),J=1,14)
420            4400 FORMAT(1X,14F6.0)
                    DO 4302 I=1,IROW
                    WRITE(6,400)
               4302 WRITE(6,4409)(RUNOFF(I,J),J=15,KOL)
               4409 FORMAT(1X,13F6.0)
425                 WRITE(6,8000)(TPTNS,MONITR)
               8000 FORMAT(2F5.2)
                    IF(TPTNS.GE.MONITR) GO TO 1009
                    GO TO 1500
               1009 WRITE(6,4401)
430            4401 FORMAT(1H1,20X,* WTIN MATRIX *)
                    DO 66 I=1,IROW
                    WRITE(6,400)
                 66 WRITE(6,300)(WTIN(I,J),J=1,15)
                300 FORMAT(1X,15F5.1)
435                 DO 67 I=1,IROW
                    WRITE(6,400)
                 67 WRITE(6,301)(WTIN(I,J),J=16,KOL)
                301 FORMAT(1X,12F5.1)
                400 FORMAT(1H )
440                 STOP
                    END
```